R-08-73

Meteorological, hydrological and hydrogeological monitoring data and near-surface hydro-geological properties data from Laxemar-Simpevarp

Site descriptive modelling SDM-Site Laxemar

Kent Werner, EmpTec

Johan Öhman, Golder Associates

Björn Holgersson, SWECO VIAK

Kristoffer Rönnback, Aqualog

Fredrick Marelius, WSP Sverige

December 2008

Svensk Kärnbränslehantering AB
Swedish Nuclear Fuel
and Waste Management Co

Box 250, SE-101 24 Stockholm
Phone +46 8 459 84 00

ISSN 1402-3091
SKB Rapport R-08-73

Meteorological, hydrological and hydrogeological monitoring data and near-surface hydro-geological properties data from Laxemar-Simpevarp

Site descriptive modelling SDM-Site Laxemar

Kent Werner, EmpTec

Johan Öhman, Golder Associates

Björn Holgersson, SWECO VIAK

Kristoffer Rönnback, Aqualog

Fredrick Marelius, WSP Sverige

December 2008

Summary

This report presents and analyses meteorological, hydrological and hydrogeological time-series data and near-surface hydrogeological properties data from the Laxemar-Simpevarp area (in the report referred to as the "Laxemar area"), available in SKB's Sicada database at time of the Laxemar 2.3 data freeze (Aug. 31, 2007). For some time-series parameters, the evaluation takes into account quality-controlled Sicada data for the period up to Dec. 31, 2007.

The meteorological data set includes data from two local stations, located on the island of Äspö and at Plittorp, located further inland. In addition, the data evaluation uses a longer-term data set from 7 surrounding stations, operated by SMHI. As part of this study, a time series is constructed of the water content of snow, using a combination of site-specific snow data, snow data from SMHI, snow data from SKB's snow monitoring in Forsmark, and a simplified degree-day method. According to the data evaluation, the site-average annual precipitation and potential evapotranspiration can be estimated to be on the order of 600 and c 535 mm, respectively. In particular, precipitation demonstrates a near-coastal gradient, with less precipitation at the coast compared to areas further inland.

The surface-water level data set includes data from 4 lake-level gauging stations and 3 sea-level gauging stations. All lakes are located above sea level, including the near-coastal Lake Sörå. Hence, no intrusion of sea water to lakes takes place. There is a strong co-variation among the monitored lake-water levels, typically with maxima during spring and minima during late summer and early autumn. Further, it is noted that the lake-water level amplitudes are relatively small, and that the variability pattern of Lake Sörå deviates from the other three lakes, most likely because it is a man-made storage pond, with no surface in- and outlets. Concerning the sea as a hydraulic boundary, the maximum and minimum sea levels (daily averages) during the site-investigation period (May 2004–Dec. 2007) were –0.52 and 0.71 metres above sea level, respectively, whereas the average sea level was 0.03 metres above sea level (RHB 70). The largest daily sea-level changes occurred on Nov. 1, 2006 (+0.26 m) and Dec. 22, 2004 (–0.23 m).

The data set on stream discharge, surface-water temperature and electrical conductivity includes data from 9 discharge-gauging stations in 7 streams. Based on the discharge data, the site-average specific discharge for the years 2005–2007 can be estimated to 165 $mm \cdot y^{-1}$, which is within the interval of the estimated long-term average. Most streams in the Laxemar area are affected by land improvement and drainage operations. Of the monitored streams, there is flow throughout the year in the streams Laxemarån, Kåreviksån downstream from Lake Friskjön and Kärrviksån. The stream Ekerumsån is dry during dry summers, whereas the other monitored small streams are dry during approximately half of the year.

Except from one gauging station (PSM000364, located in Laxemarån), the gauging stations are of two types, constructed V-notch weirs and natural critical sections. The weir design at PSM000364 consists of two rectangular notches, and is considered as a natural critical section when calculating the discharge. For the natural critical sections, there may be seasonal variations of the section geometry and the flow resistance, which may lead to erroneous interpretations of variations of the discharge. Overall, discharge-data errors are likely small. The exception is the natural critical section at the oulet from Lake Frisksjön (PSM000348), for which the accumulated discharge yields deviating values of the specific discharge.

The hydrogeological time-series data set includes data on groundwater levels measured in groundwater monitoring wells installed in the Quaternary deposits, and so called point-water heads (groundwater levels in systems of constant density) measured in borehole sections in percussion and core boreholes, drilled to various depths in the rock. Totally 92 groundwater monitoring wells have been installed as part of the site investigations in Laxemar, of which groundwater-level data are available from 76 wells; 62 wells were monitored at Aug. 31, 2007,

and 45 wells at Dec. 31, 2007. As part of the present study, activities that may affect groundwater levels and point-water heads are identified and the associated monitoring data periods excluded. The objective of this data screening is to obtain a better representation of natural (undisturbed) conditions, as a basis for data evaluation.

An attempt is also made to transform measured point-water heads to environmental-water heads (groundwater levels in systems of variable density) for a number of boreholes in the rock. The objective is to provide a better basis for interpretation of prevailing vertical hydraulic-head gradients in the variable-density groundwater flow system in the rock. Except for some deep borehole sections in boreholes at the coast, the density data show that density differences are small and hence have only minor effects on hydraulic-head gradients. The data evaluation show that groundwater levels in the Quaternary deposits are shallow. There is hence a close correlation between the ground-surface topography and groundwater levels in the Quaternary deposits, which in turn implies that topography has a strong influence on near-surface patterns of groundwater recharge and discharge. The correlation is found to be much smaller for point-water heads in the rock, indicating that point-water heads are affected also by other factors than the local topography.

The near-surface hydrogeological data set includes data obtained from particle-size distribution (PSD) curves, permeameter tests, slug tests and hydraulic single-hole and interference tests in groundwater monitoring wells. Sandy-gravelly till is overlying the rock in the whole area, also in most areas mapped as exposed/shallow rock. According to the data evaluation, the sandy-gravelly till is characterised by a relatively high hydraulic conductivity (c $4 \cdot 10^{-5}$ $m \cdot s^{-1}$). Furthermore, there are indications that the hydraulic conductivity of the Quaternary deposits overlying the rock in the deepest parts of the large (wide and deep) valleys is about one order of magnitude higher compared to till in other parts of the area. Permeameter tests on till indicate an anisotropic hydraulic conductivity, with an anisotropy ratio (K_h/K_v) that may be on the order of 15–30.

The findings from the hydrogeological properties data evaluation are summarised in a data table. This table is connected to a depth and stratigraphy model developed for the Laxemar area. The table can be used as a starting point for parameterisation of quantitative models (MIKE SHE, CONNECTFLOW) of water flow in Laxemar. In the data table, generic data are used to support the estimates of the hydrogeological properties for types of Quaternary deposits other than till.

Joint data evaluations are used to investigate interaction between groundwater in the Quaternary deposits and surface waters. Such evaluation of stream discharges and groundwater levels in the Quaternary deposits in the vicinity of the streams indicate that there is an (unconfined) groundwater level "threshold" for initiation of discharge, likely related to the local drainage depth (i.e. the depth to the bottom of the stream). Moreover, joint evaluation of lake-water levels and groundwater levels near and below lakes indicates that interaction between lake water and groundwater in the underlying Quaternary deposits is limited to near-shore areas.

Conceptually, groundwater flow in the deeper parts of the rock in Laxemar primarily occurs in a connected system of deformation zones, and the associated groundwater discharge takes place at locations where this system connects to zones that outcrop in the valleys. According to joint evaluation of groundwater levels in the Quaternary deposits and point-water heads in percussion and core boreholes, upward hydraulic-head gradients from the rock to the Quaternary deposits primarily prevail in connection to deformation zones in the rock. Hence, the topography in combination with the geometry and the hydrogeological properties of the deformation zones and their contact with the Quaternary deposits are likely important factors for groundwater discharge from rock to Quaternary deposits. At least in a qualitative sense, the interference tests summarised in this study indicate that there exist such hydraulic connections between outcropping deformation zones and Quaternary deposits.

Sammanfattning

Denna rapport presenterar och analyserar meteorologiska, hydrologiska och hydrogeologiska tidsseriedata och data gällande ytnära hydrogeologiska egenskaper från Laxemar-Simpevarpsområdet (i rapporten huvudsakligen benämnt (“Laxemarområdet” (the Laxemar area)), tillgängliga i SKBs databas Sicada vid tidpunkten för datafrys Laxemar 2.3 (31 aug. 2007). För några tidsserieparametrar inbegriper utvärdringen kvalitetskontrollerade Sicada-data för perioden till och med 31 dec. 2007.

Den meteorologiska datamängden inkluderar data från två lokala stationer, belägna på ön Äspö samt i Plittorp, beläget längre inåt land. I datautvärderingen används dessutom längre tidsserier från 7 omgivande stationer som drivs av SMHI. Som del av denna studie har en tidsserie konstruerats av snöns vatteninnehåll, genom en kombination av platsspecifika snödata, snödata från SMHI, snödata från SKBs monitering i Forsmark, samt en förenklad graddagar-metod. Som platsmedelvärde är enligt datautvärderingen den årliga nederbörden och den potentiella evapotranspirationen i storleksordningen 600 respektive 535 mm. Speciellt nederbörden uppvisar en kustnära gradient, med mindre nederbörd nära kusten jämfört med områden längre inåt land.

Datamängden på ytvattennivåer inkluderar data från 4 sjönivåstationer och 3 havsnivåstationer. Samtliga sjöar är belägna över havets nivå, inklusive den kustnära sjön Sörå. Detta innebär att det inte sker någon inträngning av havsvatten till sjöarna. Sjönivåerna uppvisar en stor samvariation, typiskt med högsta nivåer under vår och lägsta nivåer under sensommar och tidig höst. Noterbart är även att sjönivåernas amplitud är relativt liten, och att variationsmönstret för sjön Sörå avviker från de andra tre sjöarna, troligen beroende på att sjön är en konstgjord lagringsdamm, utan in- och utlopp. Beträffande havet som hydraulisk gräns, så var de högsta och lägsta havsvattennivåerna (som dygnsmedelvärde) under platsundersökningsperioden (maj 2004–dec. 2007) –0,52 respektive 0,71 meter över havet och den genomsnittliga havsnivån var 0,03 meter över havet (RHB 70). De högsta havsnivåförändringarna under ett dygn inträffade 1 nov. 2006 (+0,26 m) och 22 dec. 2004 (–0,23 m).

Datamängden på vattenföring, ytvattentemperatur och elektrisk konduktivitet inkluderar data från 9 vattenföringsstationer i 7 vattendrag. Enligt datautvärderingen kan den specifika avrinningen för åren 2005–2007 som platsmedelvärde skattas till 165 mm·år^{-1}, vilket är inom intervallet för skattat långtidsmedel. De flesta vattendragen i Laxemarområdet är påverkade av kulturtekniska åtgärder. Av de moniterade vattendragen är det flöde under hela året i Laxemarån, Kåreviksån nedströms Friskjön samt i Kärrviksån. Ekerumsån är torr under torra somrar, medan de andra moniterade små vattendragen är torra under ungefär halva året.

Förutom en station (PSM000364, belägen i Laxemarån) är vattenföringsstationerna av två typer, konstruerade V-formade överfall och naturliga kritiska sektioner. Överfallet vid PSM000364 består av två rektangulära skåror, och behandlas som en naturlig kritisk sektion vid beräkning av vattenföringen. Vad gäller de naturliga kritiska sektionerna, kan det råda säsongsvariationer i deras geometri och därmed flödesmotstånd, vilket kan leda till felaktiga tolkningar av variationer i vattenföringen. Felen i vattenföringsdata är troligen små. Undantaget är den naturliga kritiska sektionen vid Friskjöns utlopp (PSM000348), för vilken den ackumulerade vattenföringen ger avvikande värden på den specifika avrinningen.

Datamängden på hydrogeologiska tidsserier omfattar data på grundvattennivåer mätta i grundvattenrör (jordrör) installerade i kvartära avlagringar, och s. k. “point-water heads” (grundvattennivåer i system med konstant densitet) uppmätta i borrhålssektioner i hammar- och kärnborrhål borrade till olika djup i berget. Totalt har 92 grundvattenrör installerats inom platsundersökningarna i Laxemar, av vilka det finns grundvattennivådata från 76 rör; 62 rör moniterades 31 aug. 2007, och 45 rör 31 dec. 2007. Som del av denna studie har aktiviteter som kan påverka grundvattennivåer och “point-water heads” identifierats, och tillhörande perioder

med moniteringsdata har tagits bort. Syftet med denna datarensning är att erhålla en bättre representation av naturliga (påverkade) förhållanden, som grund för datautvärdering.

Ett försök har även gjorts att transformera uppmätta "point-water heads" till s. k. "environmental-water heads" (grundvattennivåer i system med varierande densitet) för ett antal borrhål i berg. Syftet är att erhålla en bättre grund för skattning av rådande vertikala hydrauliska gradienter i grundvattensystemet i berget med varierande densitet. Förutom några djupa borrhålssektioner i borrhål nära kusten, visar densitetsdata att densitetsskillnaderna är små och därmed endast har små effekter på de hydrauliska gradienterna. Datautvärderingen visar på ytnära grundvattenivåer i jord. Det råder därmed ett nära samband mellan markytans topografi och grundvattennivåerna i jord, vilket i sin tur innebär att topografin har en stor inverkan på mönstret för ytnära in- och utströmning av grundvatten. Detta samband visar sig vara mycket mindre vad gäller "point-water heads" i berget, vilket indikerar att "point-water heads" påverkas även av andra faktorer än den lokala topografin.

Datamängden på ytnära hydrogeologiska egenskaper inkluderar data från kornstorlekskurvor, permeametertester, slugtester samt hydrauliska enhåls- och interferenstester i grundvattenrör. Sandig-grusig morän överlagrar berget i hela området, även i de flesta områden karterade som blottat/ytnära berg. Enligt datautvärderingen karaktäriseras den sandiga-grusiga moränen av en relativt hög hydraulisk konduktivitet (ca $4 \cdot 10^{-5}$ m·s^{-1}). Det finns dessutom indikationer på att den hydrauliska konduktiviteten i de kvartära avlagringar som överlagrar berget i de djupaste delarna av de största (breda och djupa) dalgångarna är ungefär en storleksordning högre jämfört med moränen i andra delar av området. Permeametertester på morän indikerar en anisotrop hydraulisk konduktivitet, med en anisotropikvot (K_h/K_v) som kan vara i storleksordningen 15–30.

Slutsatserna från utvärderingen av de hydrogeologiska egenskaperna summeras i en datatabell. Denna tabell är kopplad till en modell för jordlagrens djup och stratigrafi, utvecklad för Laxemarområdet. Tabellen kan användas som utgångspunkt för parameterisering av kvantitativa vattenflödesmodeller (MIKE SHE, CONNECTFLOW) för Laxemar. I datatabellen används generiska data som stöd för skattningar av de hydrogeologiska egenskaperna för kvartära avlagringar av andra typer än morän.

Samutvärderingar används för att undersöka interaktion mellan grundvatten i jord och ytvatten. Samutvärdering av vattenföring och grundvattennivåer i jord nära vattendrag indikerar att det finns en "tröskel" (avseende öppna grundvattenförhållanden) för grundvattennivån för att vattenföring skall initieras, troligen relaterad till det lokala dräneringsdjupet (dvs. djupet till vattendragets botten). Samutvärdering av sjönivåer och grundvattennivåer nära och under sjöar indikerar att interaktion mellan sjöarna och grundvatten i underliggande kvartära avlagringar främst sker i strandnära områden.

Konceptuellt sker grundvattenströmning i de djupare delarna av berget i Laxemar främst i ett konnekterat system av deformationszoner, och tillhörande grundvattenuströmning sker där detta system konnekterar till zoner som har sitt utgående i dalgångarna. Enligt samutvärdering av grundvattennivåer i kvartära avlagringar och "point-water heads" i hammar- och kärnborrhål, råder det uppåtriktade hydrauliska gradienter från berg till jord främst där det finns deformationszoner i berget. Detta tyder på att topografin, i kombination med deformationszonernas geometri, hydrogeologiska egenskaper och deras kontakt med de kvartära avlagringarna, är viktiga faktorer för utströmning av grundvatten från berg till jord. Åtminstone i kvalitativt hänseende indikerar de interferenstester som summeras i denna studie att det existerar sådan hydraulisk konnektion mellan utgående deformationszoner och kvartära avlagringar.

Contents

1 Introduction

1.1 Background

During the period 2002–2007, the Swedish Nuclear Fuel and Waste Management Co (SKB) has undertaken multi-disciplinary site investigations at two different locations, Forsmark in mid-eastern Sweden and Laxemar-Simpevarp in the south-eastern part of the country. The overall objective of these investigations is the siting of a geological repository for spent nuclear fuel. The investigations were divided into an initial (ISI) and a complete site investigation (CSI) phase /SKB 2001/.

The results from the site investigations are used as a basic input to site descriptive modelling, in turn aiming to provide multi-disciplinary descriptions of current properties and processes at the investigated sites. Specifically, a site descriptive model (abbreviated SDM) is an integrated description of the site and its regional setting, covering the current state of the geosphere and the biosphere as well as ongoing natural processes of importance for long-term safety. The SDM shall summarise the current state of knowledge of the site, and provide parameters and models to be used in further analyses within Safety Assessment, Repository Design and Environmental Impact Assessment.

This report concerns data from the site investigations in the Laxemar-Simpevarp area. The site investigations at this site were conducted in campaigns, separated by so called data freezes (abbreviated DF). In Laxemar-Simpevarp, the data sets present at time of DF S1.1 (Simpevarp 1.1; July 1, 2003), DF S1.2 (Apr. 1, 2004), and DF L1.2 (Laxemar 1.2; Nov. 1, 2004) contain site data gathered during the initial (ISI) phase, whereas the complete (CSI) phase started in connection to DF L2.1 (Laxemar 2.1; Jun. 30, 2005), which was followed by the "interim" DF L2.2 (Dec. 31, 2006). The present report concerns site investigation data available in SKB's Sicada database at DF L2.3 (Laxemar 2.3; Aug. 31, 2007). This data set constitutes the basis for the final SDM for Laxemar-Simpevarp, referred to as SDM-Site Laxemar.

1.2 Scope and objective

This report is produced as one of the background reports for SDM-Site Laxemar /SKB 2009, Söderbäck and Lindborg 2009/. The site-descriptive modelling of hydrology and near-surface hydrogeology in Laxemar-Simpevarp is presented in /Werner et al. 2008/, whereas quantitative (MIKE SHE) water-flow modelling is reported by /Bosson et al. 2008/. The present report presents and analyses meteorological, hydrological and hydrogeological time-series data available in the Sicada database at time of DF L2.3. However, it should be noted that for some parameters, the considered time-series data set is not restricted in time to the actual data freeze. Specifically, for some parameters the report takes into account quality-controlled data available in Sicada up to Dec. 31, 2007. Besides time-series data, the report presents and analyses hydrogeological properties data available for the Quaternary deposits (in the remainder of this report referred to as QD) and the upper part of the underlying rock.

The overall objectives are to present the considered data sets, and to perform integrated data analyses with the overall purpose to further develop the conceptual model of meteorology, hydrology and near-surface hydrogeology in Laxemar. Further, as part of the SDM-Site work, input- and calibration data have also been assembled and delivered for the purposes of quantitative (numerical) water flow modelling, using the modelling tools MIKE SHE /Werner et al. 2006, Bosson 2006, Aneljung et al. 2007/ and CONNECTFLOW /Hartley et al. 2006, 2007/.

It should be noted that the SKB data considered in this report are restricted to those obtained from the site investigations 2002–2007. This implies that the report does not consider data from

previous investigations and/or from the Äspö Hard Rock Laboratory (located to the island of Äspö) and the Central interim storage facility for spent fuel (Clab, located to the Simpevarp peninsula). This is not considered to be an important limitation; the island of Äspö is not included in the geographical area considered in this report. Moreover, the present data evaluation inludes site-investigation data from the Simpevarp peninsula, e.g. monitoring time series from groundwater monitoring wells and boreholes in the rock.

1.3 The Laxemar-Simpevarp area

As mentioned previously, Laxemar-Simpevarp in south-eastern Sweden is one of two candidate sites for the siting of a geological repository for spent nuclear fuel in Sweden. Laxemar is located on the coast of the Baltic Sea, close to the Simpevarp nuclear power plant (Figure 1-1). During 2002–2007, site investigations were conducted within a square-shaped area referred to as the Laxemar-Simpevarp regional model area, covering c 273 km^2. The site investigations were initially focused on the so-called Simpevarp subarea (including the Simpevarp peninsula and the islands of Ävrö and Hålö), and later to the Laxemar subarea (i.e. the inland parts of the area).

Within the SDM-Site context, a smaller square-shaped area is defined within the regional area, referred to as the Laxemar local model area (see Figure 1-1). Note that the XY coordinate system throughout this report is RT 90 2.5 gon V 0:-15, whereas the height (Z) coordinate system is RHB 70. In principle, the Laxemar local model area encloses the Laxemar subarea. Obviously, site investigations and descriptive models within different disciplines focus on different areas, depending on the purpose and scope of the investigation or model. For simplicity, this report refers to the "Laxemar" area; when necessary, the actual area that the description refers to will be defined.

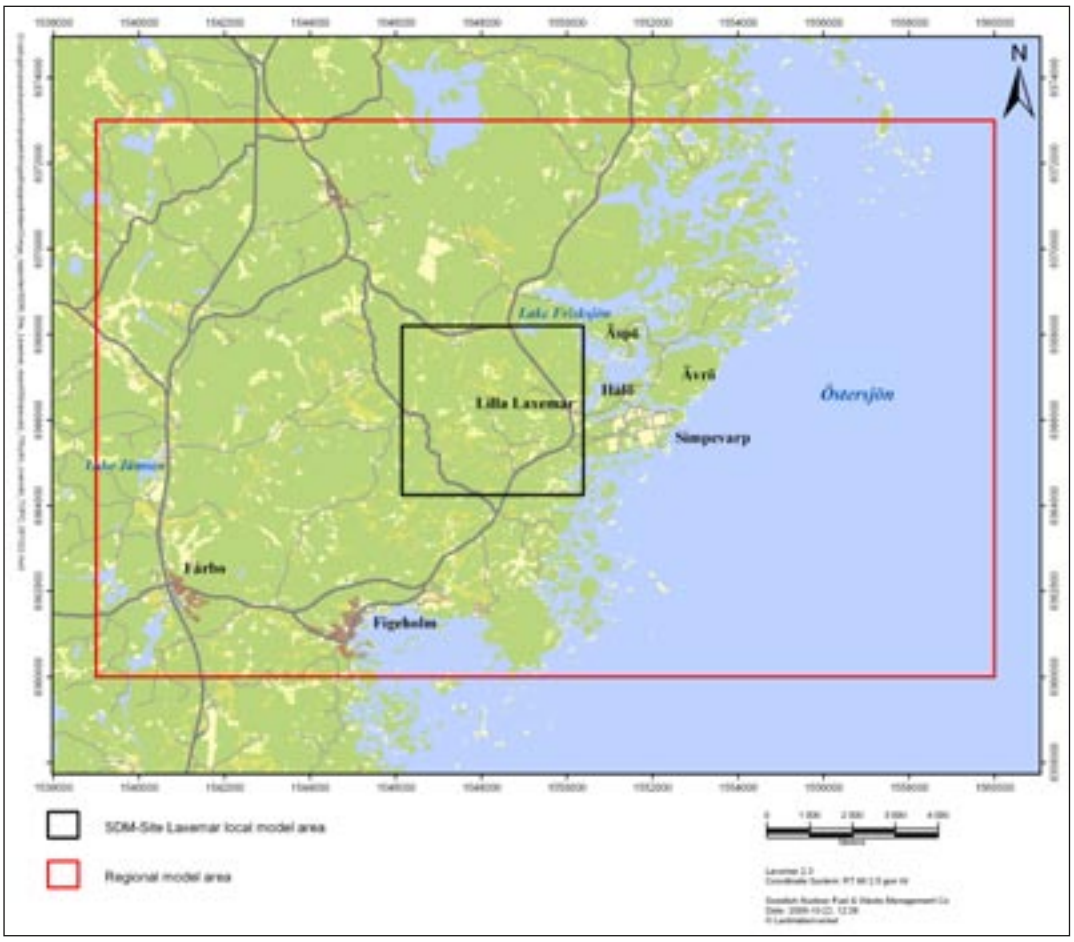

Figure 1-1. *Overview map of the Laxemar-Simpevarp regional model area and the SDM-Site Laxemar local model area.*

2 Presentation of time series data

2.1 Data overview

This report considers five types of time series data:

1. Meteorological data.
2. Surface-water levels measured in lakes and bays of the Baltic Sea.
3. Surface-water discharges measured in streams.
4. Groundwater levels measured in groundwater monitoring wells installed in Quaternary deposits.
5. Point-water heads measured in percussion and core boreholes in rock. As part of the present study, an attempt has also been made to transform point-water heads into environmental-water heads for a subset of the boreholes .

In order to provide an overview of the data availability, Figure 2-1 shows the number of meteorological and hydrological (discharge and water level) stations, groundwater monitoring wells, and monitored borehole sections during the period Jan. 1, 2003–Dec. 31, 2007. Note that Figure 2-1 only considers data from SKB's site investigations in Laxemar.

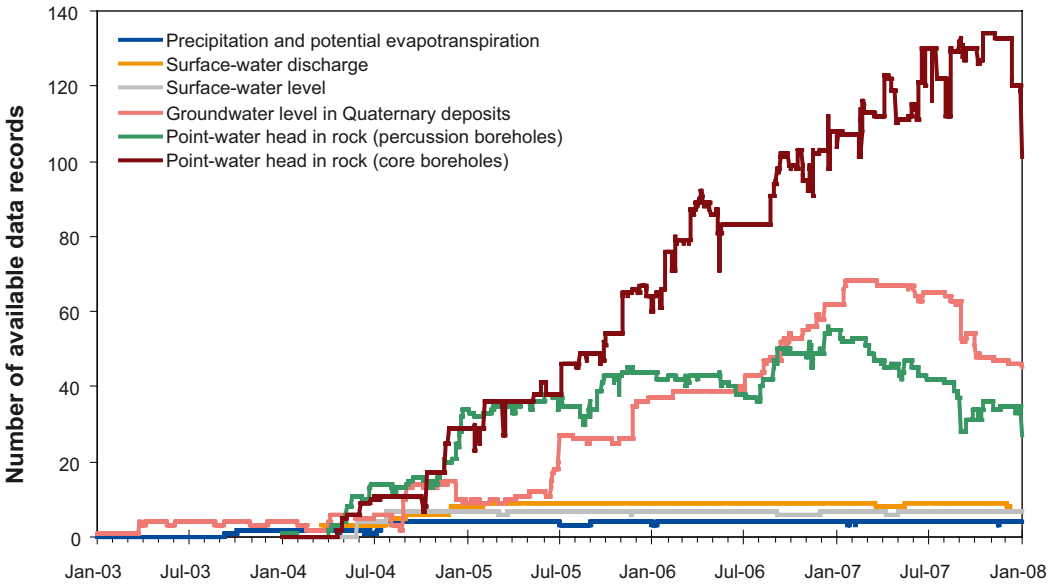

Figure 2-1. *Time-series plot illustrating the data availability during the period 2003–2007, in terms of the number of meteorological and hydrological (discharge and water level) stations, groundwater monitoring wells, and monitored borehole sections.*

At data freeze Laxemar 2.3 (Aug. 31, 2007), SKB's meteorological, hydrological and hydrogeological monitoring programme in Laxemar comprised the following:

- 2 meteorological stations.
- Observation points for winter parameters (snow depth at 1 location, ice freeze/breakup at 4 locations, and ground frost at 4 locations).
- 9 surface-water discharge gauging stations in 7 streams.
- 4 surface-water level gauging stations in lakes and 3 stations in bays of the Baltic Sea. The water-level gauging station in the downstream end of Lake Frisksjön is also a discharge-gauging station, measuring the stream discharge out from the lake.
- Groundwater-level monitoring in 62 groundwater monitoring wells, with their screens installed in the QD or across the QD-rock interface.
- 37 sections for monitoring of point-water heads in percussion boreholes.
- 132 sections for monitoring of point-water heads in core boreholes.

All time-series data presented and analysed in this report are obtained from Sicada deliveries #Sicada_07_370 (delivery date Oct. 16, 2007), #Sicada_07_386 (delivery date Oct. 19, 2007), and #Sicada_08_024 (partial deliveries on Feb. 22 and Mar. 3, 2008). These data deliveries contain all of the considered time series available from the site investigations in the Laxemar area up to Dec. 31, 2007. Table 2-1 summarises the corresponding meteorological, hydrological and groundwater monitoring reports, up to the 2.3 data freeze (Aug. 31, 2007).

2.2 Meteorological monitoring data

The most important meteorological time series data for a description of hydrology and hydrogeology include precipitation (P) and potential evapotranspiration (PET). The reason for this is that these parameters provide basic information on the site-specific driving forces of the hydrological cycle. In addition, time-series data on air temperature, snow accumulation and snowmelt are also important for a description of the water balance of the area and are therefore presented here, including comparisons with long-term data from the closest meteorological stations operated by the Swedish Meteorological and Hydrological Institute (SMHI). Figure 2-2 shows the locations of SKB's two meteorological stations in the Laxemar area, as well as the SMHI stations considered in this study. The enlarged map in Figure 2-3 shows the SKB meteorological and winter stations; the latter are used for observations of snow depth, ground frost and ice freeze/breakup.

Table 2-1. Meteorological, hydrological and groundwater monitoring reports from the site investigations in Laxemar.

Type of monitoring	Data period	P-report	Reference
Meteorological and hydrological monitoring	Jan. 2003–Oct. 2004	P-05-227	/Lärke et al. 2005a/
	Nov. 2004–Jun. 2005	P-06-19	/Lärke et al. 2005b/
	Jul. 2005–Dec. 2006	P-07-38	/Sjögren et al. 2007a/
	Jan.–Aug. 2007	P-07-172	/Sjögren et al. 2007b/
Groundwater monitoring	Dec. 2002–Oct. 2004	P-05-205	/Nyberg et al. 2005/
	Nov. 2004–Jun. 2005	P-05-282	/Nyberg and Wass 2005/
	Jul. 2005– Dec. 2006	P-07-219	/Nyberg and Wass 2007a/
	Jan.–Aug. 2007	P-08-28	/Nyberg and Wass 2007b/

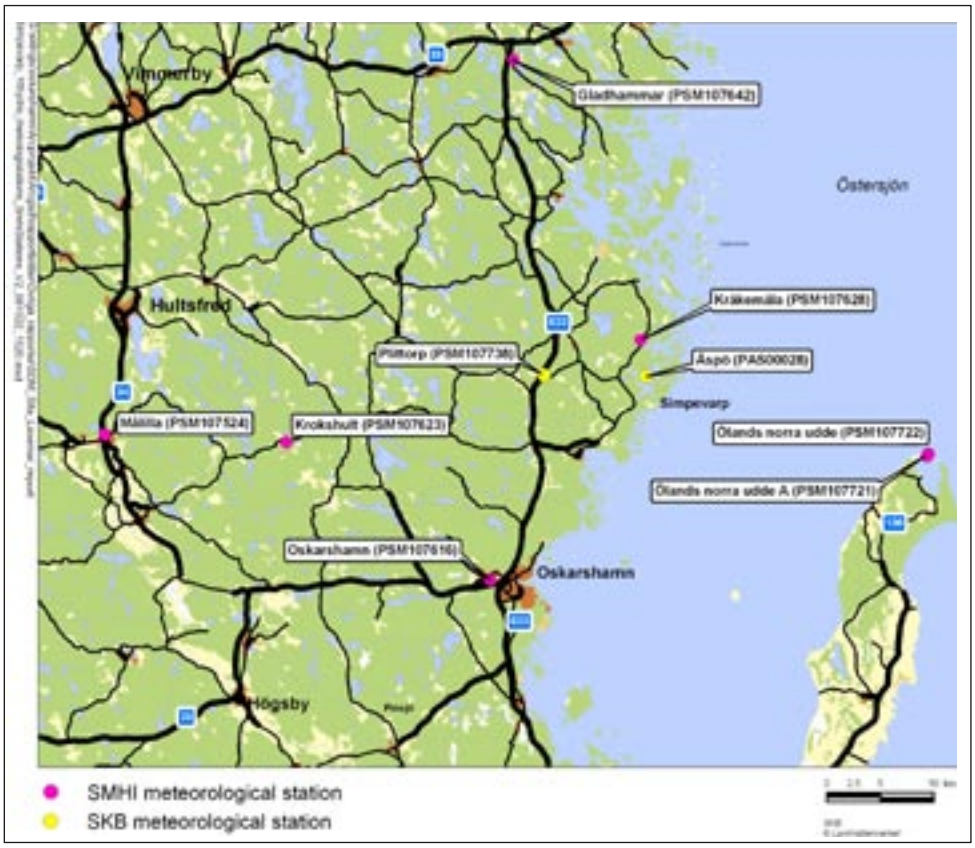

Figure 2-2. *Overview map of the local SKB meteorological stations and the closest SMHI stations.*

Figure 2-3. *Detailed map of the local SKB meteorological stations (yellow symbols; cf. Figure 2.2) and winter stations (snow depth, ground frost and ice freeze/breakup).*

Tables 2-2 to 2-7 summarise the meteorological data set available in the Sicada database at time of the Sicada delivery, in terms of parameter-specific data periods for the SKB (Tables 2-2 to 2-4) and SMHI (Tables 2-5 to 2-7) meteorological and winter stations. Note that the data periods refer to "complete data days", i.e. days for which daily sums or averages can be calculated. All SKB meteorological data are stored every half hour. Precipitation (P) is stored in form of the accumulated precipitation during 30 minutes, whereas air temperature, global radiation, air pressure, and relative humidity data are stored as 30-minutes (arithmetic) averages of 1-second readings. Specifically, wind speed and wind direction data are stored as the latest 10-minutes (arithmetic) average for the current half hour; e.g. for the 10.00 AM data, the stored data is the 10-minutes average for the period 09.51–10.00 AM. As can be seen from Tables 2-5 to 2-7, the temporal resolution for the SMHI data differs between parameters and data periods.

Table 2-2. Available data periods for precipitation (P), potential evapotranspiration (PET) and air temperature data from the SKB stations.

Station	P	PET	Air temperature
Äspö (PAS000028)	2003-09-10–2007-12-31 (no data 2003-10-04, 2004-04-21–26)	2003-10-05–2007-12-31 (no data 2004-04-21–26, 2004-06-11–18, 2004-06-22–07-06, 2007-01-22–25)	2003-09-09–2007-12-31
Plittorp (PSM107738)	2004-07-15–2007-12-31	2004-07-15–2007-12-31 (no data 2005-07-10–12, 2005-12-31–2006-01-10, 2006-05-06, 2006-06-30, 2006-07-08–09, 2006-07-11–16, 2007-02-05–07, 2007-11-14–16)	2004-07-14–2007-12-31

Table 2-3. Other meteorological parameters from the SKB stations.

Station	Global radiation	Wind direction/speed	Air pressure	Relative humidity
Äspö (PAS000028)	2003-09-09–2007-12-31	2003-09-10–2007-12-31	2003-09-09–2007-12-31	2003-10-04–2007-12-31
Plittorp (PSM107738)	-	2004-07-14–2007-12-31	2004-07-14–2007-12-31	2004-07-14–2007-12-31

Table 2-4. Parameters from the SKB winter stations.

Station	Snow depth (and snow weight)	Ground frost	Ice freeze/breakup
Grillplatsen, Äspö (ASM100224)	2002-12-18–2007-03-07	-	-
Grillplatsen, Äspö (PSM107724)	-	2003-01-14–2007-03-12	-
PSM006978	-	2005-01-17–2007-03-12	-
PSM006979	-	2005-01-17–2007-03-12	-
PSM006980	-	2005-01-27–2007-03-12	-
ASM100226	-	-	2002-11-07–2007-02-21
ASM100227	-	-	2002-11-07–2007-01-23
ASM100228	-	-	2002-11-07–2007-01-23
ASM100229	-	-	2002-11-07–2007-01-15

Table 2-5. Precipitation (P), potential evapotranspiration (PET) and air temperature data from the SMHI stations.

Station	P (daily values)	PET (daily values)	Air temperature (daily values)
Krokshult (PSM107623)	1994-01-01–2007-08-31	-	-
Ölands norra udde (PSM107722)	1994-01-01–2007-08-31 (no data 1995-08-01–09-30)	-	1994-01-01–2007-08-31 (no data 1995-08-01–09-30)
Ölands norra udde A (PSM107721)	1995-08-01–2007-08-31	1999-01-01–2006-08-31 (no data 1999-04-10, 1999-04-24–25, 2000-06-23–25, 2002-02-23–24, 2003-07-23–24, 2003-09-24–10-04, 2005-01-10–11, 2007-06-04–12)	1995-08-01–2007-08-31
Målilla (PSM107524), manual station	1994-01-01–2007-08-31 (no data 1999-06-01–07-31)	-	1994-01-01–2007-08-31 (no data 1999-06-19–07-18)
Oskarshamn (PSM107616), manual station	1994-01-01–2007-08-31 (no data 1994-07-01–1995-01-31) (monthly values 1961–2002; no data Jul. 1994–Jan. 1995)	-	1987-01-01–2007-08-31 (no data 1994-05-01–1995-06-30)
Gladhammar (PSM107642)	1995-08-01–2007-08-31	1999-01-01–2007-08-31 (no data 1999-02-17, 1999-04-10, 1999-04-24–25, 2007-01-15	1995-08-01–2007-08-31
Kråkemåla (PSM107628), manual station	1994-01-01–2007-08-31	-	-

Table 2-6. Other meteorological parameters from the SMHI stations.

Station	Global radiation	Wind direction/speed	Air pressure	Relative humidity
Ölands norra udde (PSM107722; 1880-)	1981 (hourly values)	1981 (each 3rd hour); wind rose 1968–1995	1981; 1991-01-01–1995-07-31 (each 3rd hour), 1961-01-01–1995-07-31 (monthly values)	1981 (each 3rd hour), 1963-01-01–1990-12-31 (monthly values)
Ölands norra udde A (PSM107721; 1996–)	-	2002 (daily values); wind rose 1968–1995	1995-08-01–2000-12-31, 2002-01-01–2002-12-31 (each 3rd hour)	2001 (each 3rd hour)

Table 2-7. Parameters from the SMHI winter stations.

Station	Snow depth (daily values, no data on snow weight)
Krokshult (PSM107623)	1994-01-01–2007-08-31
Målilla (PSM107524)	1994-01-01–2007-08-31
Oskarshamn (PSM107616)	1981, 1994-01-01–2007-08-31
Kråkemåla (PSM107628)	1994-01-01–2007-08-31

2.2.1 Precipitation

In this report, precipitation (P) refers to estimations of the actual precipitation. This implies that the measured precipitation has been corrected for various types of losses (see e.g. review papers by /Sieck et al. 2007ab/. The correction methodology, adopted for all precipitation data considered in this report, is described in /Alexandersson 2003, Wern and Jones 2006/. Since the estimation of P is a data uncertainty of relevance for the description of hydrology and near-surface hydrogeology, the estimation method is discussed in some detail below.

As shown by /Alexandersson 2003 and Sieck et al. 2007a/, precipitation corrections are subject to uncertainty, regardless of correction method. Precipitation measurements are generally considered to be subject to three main types of errors:

(1) Precipitation-catch errors caused by the wind, implying that some part of the precipitation that approaches a precipitation gauge from above does not reach the gauge. The so-called GEONOR type of automatic precipitation gauge is used at SKB's Äspö and Plittorp stations. Even though this gauge type is equipped with protective screens (of so-called Alter type), this gauge type is in fact subject to larger wind-loss errors compared to the traditional manual type of gauge, which has been and still is used by SMHI /Alexandersson 2003/.

(2) Measurement errors due to evaporation of water from the gauge. A thin oil film is used in the GEONOR type of gauge to prevent evaporation losses. Hence, it can be assumed that there is no need to correct GEONOR precipitation data for this type of loss /Alexandersson 2003/.

(3) Losses due to adhesion of precipitation within the gauge. For the GEONOR gauge, this type of error is corrected by a lumped "adhesion/evaporation" factor, taking into account errors due to evaporation of adhered precipitation /Alexandersson 2003/. Specifically, it is assumed that the adhesion/evaporation loss is 0.1 $mm \cdot d^{-1}$ for each day with precipitation.

Up to Jun. 2006, the precipitation measured at the Äspö and Plittorp stations were corrected according to a relatively simple correction method (see e.g. /Lärke et al. 2005b/). According to this method, the actual accumulated precipitation P during a specific 30-minutes period was estimated from the measured precipitation (P_m) as $P = P_m \cdot 1.10$ if the average air temperature during that time interval was less than +1°C, and as $P = P_m \cdot 1.06$ if the average air temperature was equal to or higher than +1°C. An updated correction method /Alexandersson 2003/ was introduced during 2006 /Wern and Jones 2006, Sjögren et al. 2007a/. All precipitation data used in this report, obtained from the Sicada database, are corrected according to the updated ("Alexandersson") method, which is described below.

The /Alexandersson 2003/ method is originally developed for correction of long-term precipitation time series. Specifically, it was first applied to the so-called "reference normal period"; the current such period encompasses the years 1961–1990. In a first step, wind losses are taken into account by selecting a reference station for air temperature (preferably the precipitation station itself). The reference station should have a long-term record of temperature measurements (i.e. preferably 1961–1990). Moving to the Äspö/Plittorp case, the Oskarshamn station (PSM107716) was chosen as reference station /Wern and Jones 2006/; it has an air temperature record for the period 1961–1990.

Next, assuming that the air temperature is normally distributed, the 1961–1990 temperature data are used to calculate monthly averages and standard deviations of the air temperature. For each month during the year, this operation then yields the monthly fraction (%) of each month of precipitation in the form of rain and snow, respectively. As in the previous correction method (cf. above), +1°C was adopted as the rainfall/snowfall air temperature threshold. Note that for the purposes of precipitation corrections, the /Alexandersson 2003/ method also implies that monthly average temperatures are adjusted by subtracting 1°C (during Jul.) and adding 2°C (during Jan.). This is done in order to mimic the fact that the air temperature usually drops in connection to rainfall in summer, and rises during snowfall in winter.

The (monthly) wind-correction factors depend on the "wind class", i.e. the degree of wind exposure for the gauging station in question. According to /Wern and Jones 2006/, the Äspö station is assigned wind class 4 ("rather open location in some directions, less open in others"). For this wind class, $P = P_m \cdot 1.115$ for rainfall and $P = P_m \cdot 1.19$ for snowfall. Further, The Plittorp station is assigned wind class 2 ("well protected for wind in all directions, and rather nearby forest"). For this wind class, $P = P_m \cdot 1.07$ for rainfall and $P = P_m \cdot 1.105$ for snowfall. For each month, this procedure gives (constant) rainfall/snowfall-weighted factors for wind-loss corrections. The monthly correction factors in /Wern and Jones 2006/ are hence constant, which implies that the correction methodology does not take into account the current wind speed or air temperature; note that the method used up to Jun. 2006 took into account the current air temperature.

In the second step, adhesion/evaporation are considered using the average (1961–1990) number of precipitation days per month in Sweden to estimate monthly correction factors. In the Äspö/Plittorp case, the estimated monthly adhesion/evaporation loss (mm per month) then corresponds to a certain fraction (%) of the monthly average (1961–1990) measured precipitation (mm) for the Oskarshamn station (PSM107716). The resulting monthly correction factors used for the SKB stations Äspö and Plittorp are presented in Table 2-8.

Table 2-8. Monthly precipitation correction factors (%) for the Äspö and Plittorp stations /Sjögren et al. 2007b/.

Station	Jan	Feb	Mar	Apr	May	Jun	Jul	Aug	Sep	Oct	Nov	Dec	Year
Äspö PAS000028	21	21	19	16	14	14	14	14	14	16	17	20	17
Plittorp PSM107738	12	13	12	10	10	9	9	10	10	10	10	12	11

Figure 2-4 shows bar plots of the monthly average precipitation at the Äspö (top plot) and Plittorp (bottom plot) stations for the indicated data periods. As can be seen in these plots, both stations demonstrate rather similar seasonal precipitation patterns, on average with least precipitation in Apr. and Sep. (on average c 20–30 mm per month). At Äspö, the precipitation is on average largest during the summer (May–Aug.) and the Oct.–Dec. periods (on average c 50–75 mm per month), whereas Jun. and Aug. are associated with most precipitation at Plittorp (on average c 75–85 mm per month).

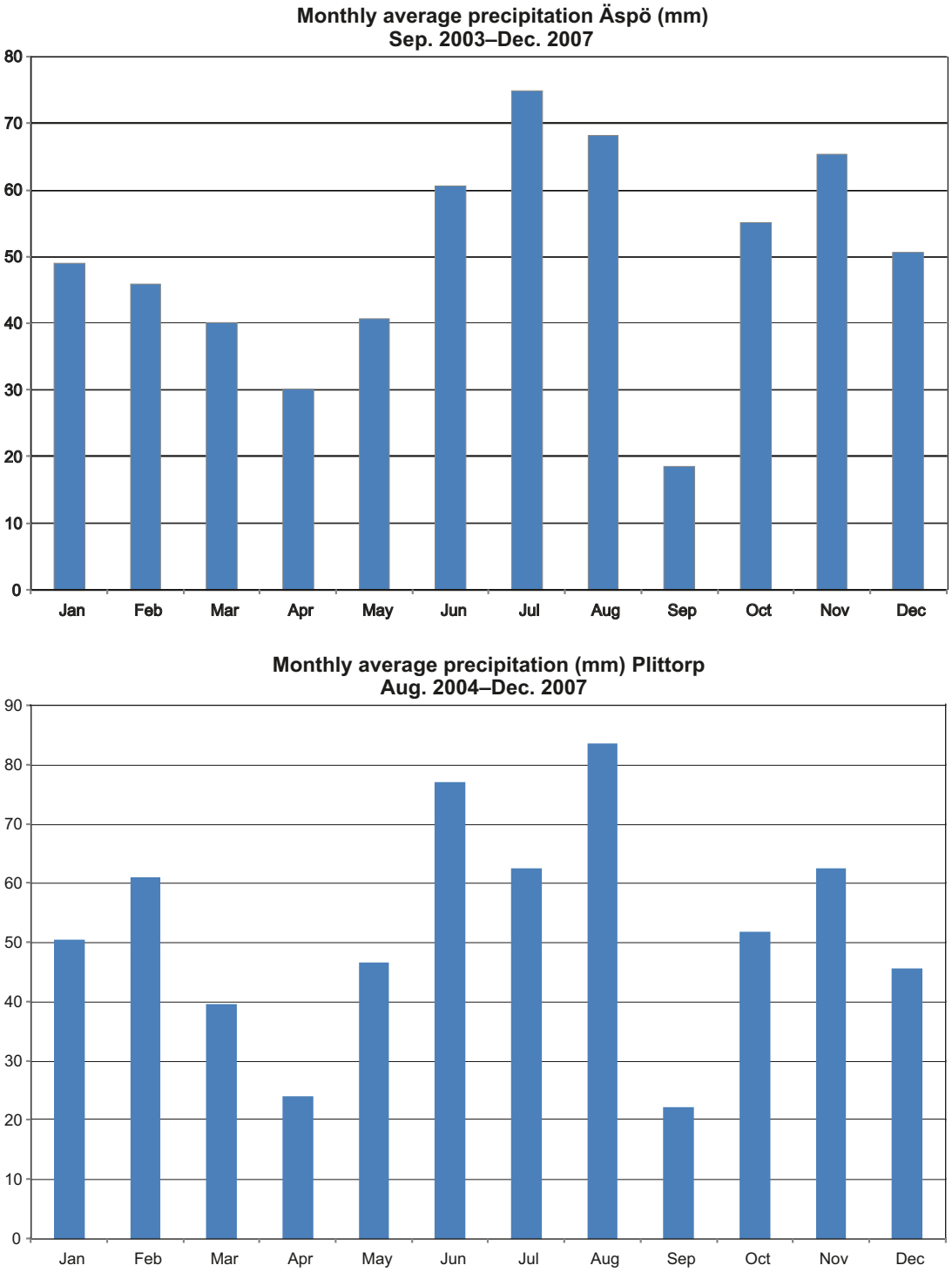

Figure 2-4. *Bar plots showing the monthly average precipitation at the Äspö (top plot) and Plittorp (bottom plot) stations for the indicated data periods.*

Figure 2-5 shows time series of the daily accumulated (corrected) precipitation at Äspö (from Sep. 10, 2003) and Plittorp (from Jul. 15, 2004). During the data period shown in the figure, the maximum recorded daily precipitation (rainfall) occurred on Jun. 26, 2007 (Äspö 51 mm and Plittorp 44 mm). At Äspö (2003-09-10–2007-12-31), there were precipitation c 60% of the days.

Figure 2-6 analyses the correlation between the daily precipitation at the Äspö and Plittorp stations, both for the whole common data period from Jul. 15, 2004 (top plot) and separately for the summer and non-summer periods (bottom plot). Note that there are some missing data days in the data set used to produce these plots (cf. Table 2-2); the correlation analysis only takes into account "complete data days" for which precipitation data are available for both stations. Also note that the top plot concerns data up to Dec. 31, 2007, whereas the bottom plot takes into account data up to Aug. 31, 2007.

According to Figure 2-6, the daily accumulated precipitation at Äspö and Plittorp has a correlation coefficient $R^2 = 0.79$ for the whole common period (Jul. 15, 2004–Dec. 31, 2007). According to this linear correlation model, the Plittorp/Äspö ratio of daily precipitation is 1.01. The corresponding ratios for the non-summer periods and the summer periods (Jul.–Aug.) are 1.01 ($R^2 = 0.84$) and 1.02 ($R^2 = 0.74$).

Precipitation ratios were used to complete the data set for both stations, i.e. the 7 days with no precipitation data for Äspö (see Table 2-2) and the period 2003-09-10–2004-07-14) for Plittorp. For Äspö, daily values from the SMHI station in Kråkemåla were used. Considering the accumulated precipitation during the period 2003-09-10–2008-08-31 (not including the 7 missing-data days), the Äspö/Kråkemåla ratio is c 0.94, which hence was used to complete the missing Äspö data. The correlation coefficient between these two stations is $R^2 = 0.77$ considering daily data and $R^2 = 0.96$ considering monthly data Oct. 2003–Aug. 2007 (not including incomplete data months); see Table 2-11. For Plittorp, daily values from the Äspö station were used. Considering the accumulated precipitation during the period 2004-07-15–2007-12-31 (no missing-data days), the Plittorp/Äspö ratio is c 1.07, which hence was used to complete the Plittorp data. The correlation coefficient between these two stations $R^2 = 0.89$ considering daily data and $R^2 = 0.95$ considering monthly data Aug. 2004–Dec. 2007; see Table 2-11.

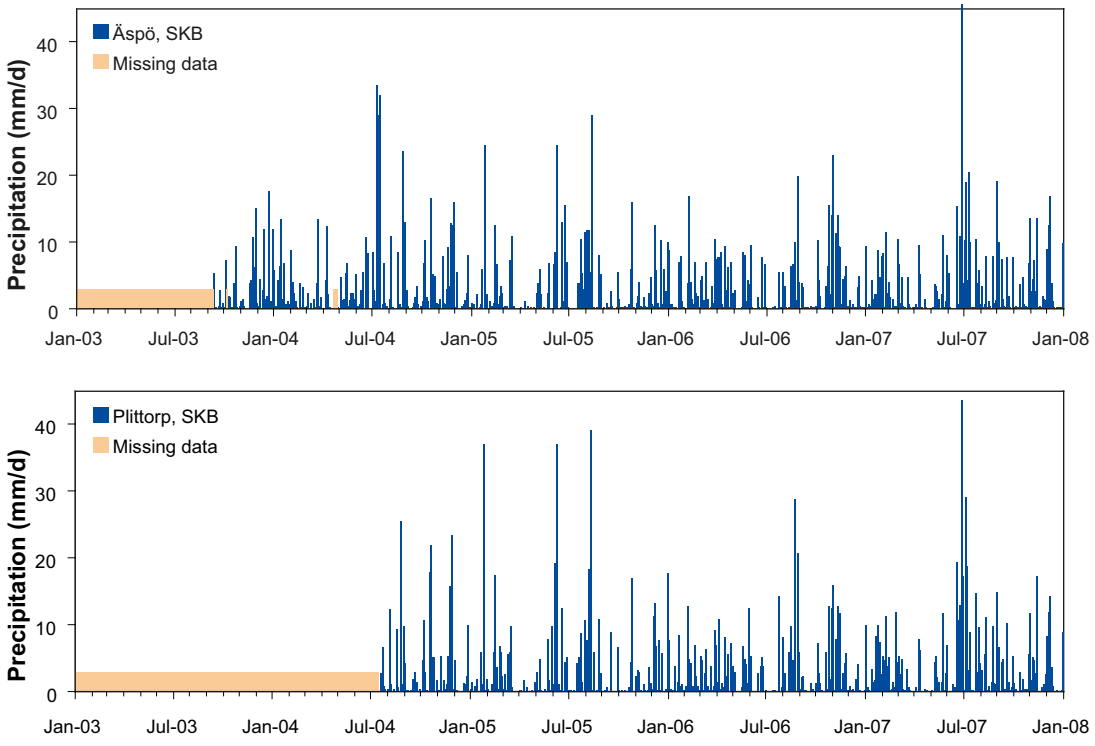

Figure 2-5. *Time series plots of daily accumulated precipitation at the Äspö (top) and Plittorp (bottom) stations.*

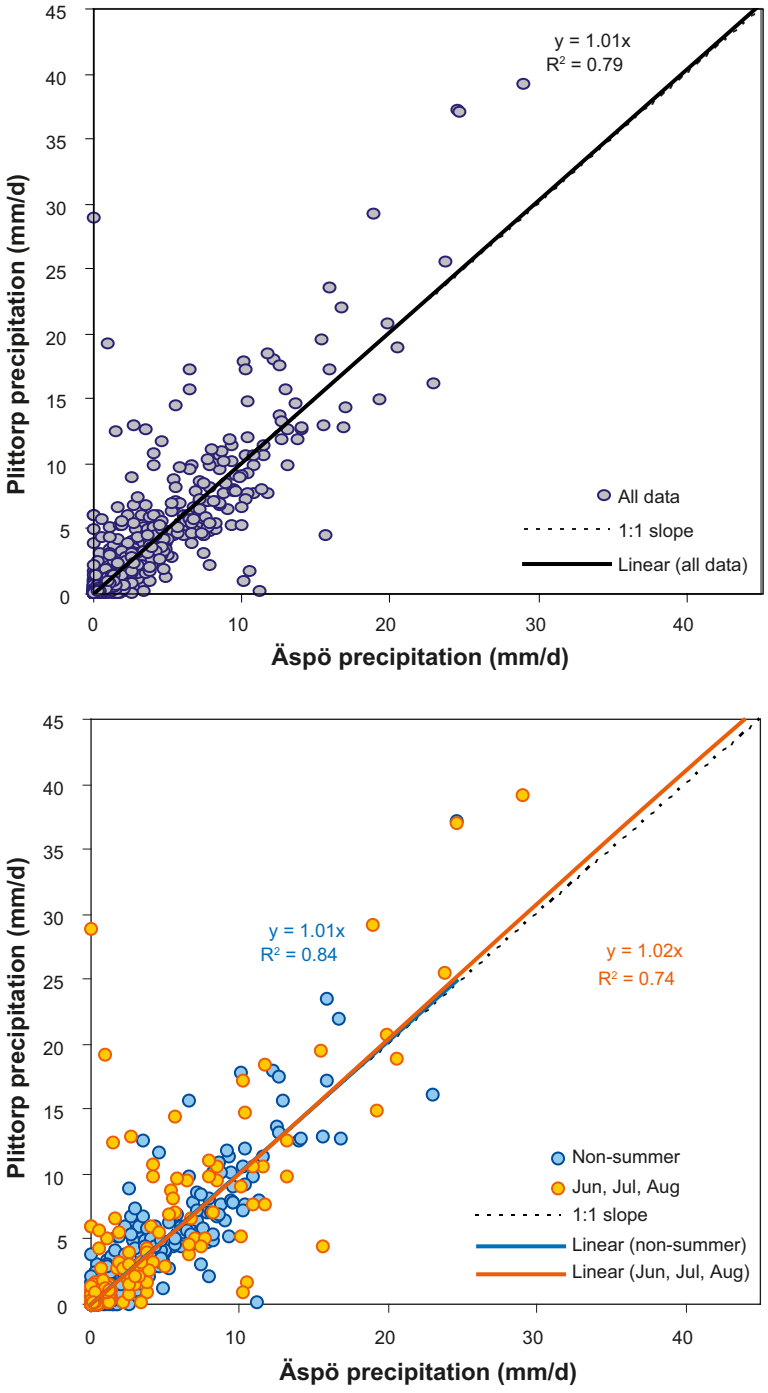

Figure 2-6. *Correlation plots between the daily accumulated precipitation at the Äspö and Plittorp stations. Whole data period in the top figure, and divided into non-summer and summer (Jun.–Aug.) below.*

Hence, a simple linear model (Figure 2-6) shows that for the non-summer periods (Sep. 1, 2004–May 31, 2007), the daily precipitation is 1% higher at Plittorp, whereas the daily precipitation is 2% higher during the summer periods. However, the overall correlation between the two stations is rather weak: $R^2 = 0.74$ for the summer periods (Jul–Aug.), $R^2 = 0.84$ for the non-summer periods, and $R^2 = 0.79$ for the whole data period. The long-term accumulated precipitation seems to be c 7% (6.6%) higher at Plittorp compared to Äspö, which indicates that there is some near-coastal west-to-east precipitation gradient, with more precipitation at the inland Plittorp station compared to the coastal Äspö station.

The observed precipitation gradient may cause differences in terms of the water balance and the specific discharge between different parts of the Laxemar area. For instance, in a numerical water flow model, one could in principle take this spatial variability into account explicitly by assigning different precipitation values in different subareas. There are rather sophisticated methods available for using precipitation gauge networks to perform spatial averaging and thereby assign a spatially variable precipitation (see e.g. /Chow et al. 1988/). In such methods, one may for example take into account geographical distances to gauging stations, differences in topographical elevations, distances to the coast, and so forth. Figure 2-7 illustrates the geographical relations between the Laxemar 2.2 MIKE SHE model area /Aneljung et al. 2007/, the SKB meteorological stations on Äspö and at Plittorp, and the relevant SMHI stations for which precipitation data are available in the Sicada database.

Given the relatively long distances from the SKB to the SMHI stations according to Figure 2-7, the issue of spatial precipitation variability is proposed to be taken into account by a relatively simple approach. The area between the Plittorp and Äspö stations can then be divided into 3 "zones", from west (Plittorp) to east (Äspö). Precipitation data from the Plittorp station is then proposed to be assigned to the westernmost zone (here denoted zone 1), data from the Äspö station to the easternmost zone (zone 3), and averages of Plittorp and Äspö to the middle zone (zone 2).

As can be seen in Figure 2-8, Plittorp acts as the western border of zone 1, Äspö the eastern border of zone 3, whereas the western and eastern borders of zone 2 are located 1/3 and 2/3, respectively, of the geographical distance from Plittorp to Äspö. The X-coordinates for the border lines then becomes (RT 90 2.5 gon V 0:-15):

- Zone 1: X = 1541657.50, X = 1544848.74.
- Zone 2: X = 1544848.74, X = 1548039.97.
- Zone 3: X = 1548039.97, X = 1551231.21.

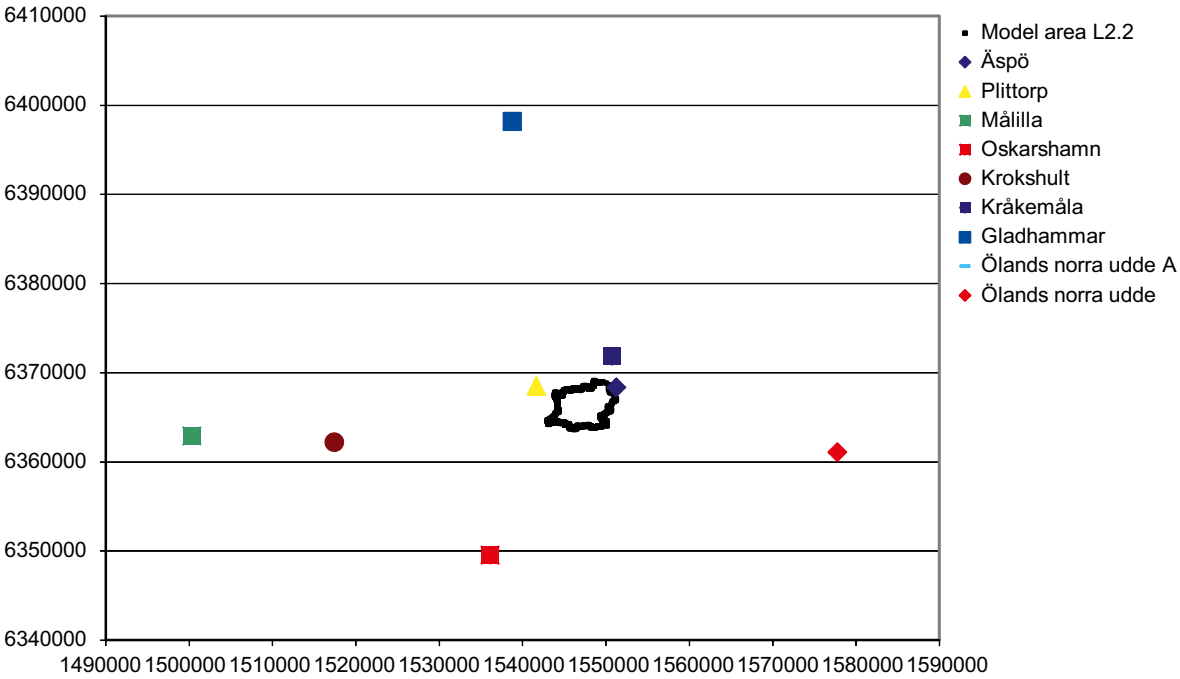

Figure 2-7. *Illustration of the geographical relations between the Laxemar 2.2 MIKE SHE model area /Aneljung et al. 2007/, SKB and SMHI meteorological stations.*

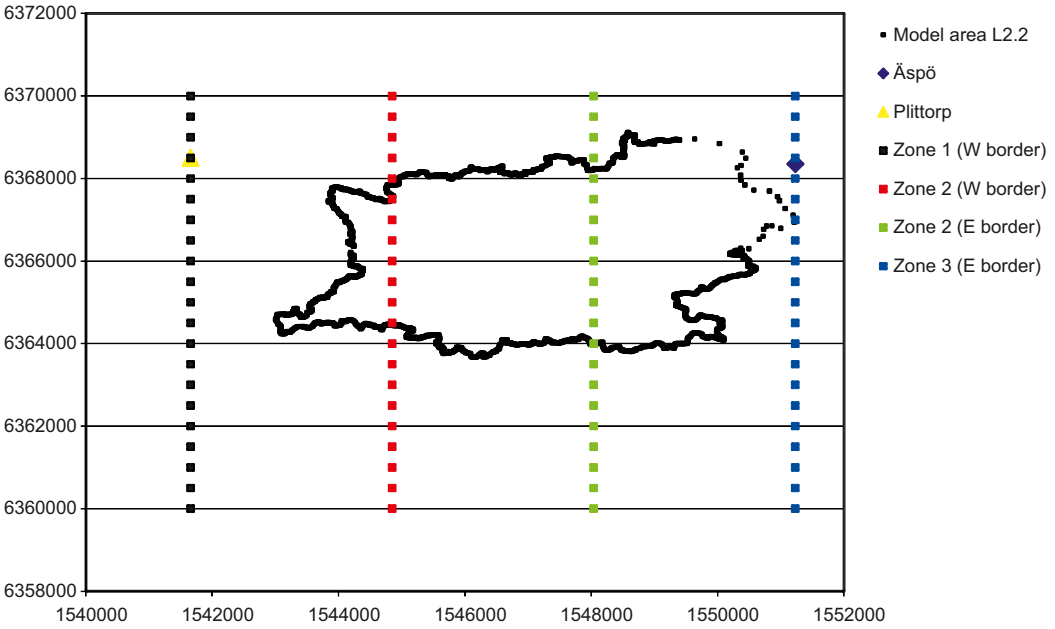

Figure 2-8. *Illustration of the proposed division of the area between the Plittorp and Äspö stations into 3 zones to take into account precipitation spatial variability.*

Figure 2-9 shows a time-series plot of the annual precipitation 1994–2007 at the SMHI stations, whereas some basic statistics of this data set are summarised in Table 2-9. "Typical" monthly values were used to complete the data set, estimated as the average of the available complete data months during the period Jan. 1994–Aug. 2007. The following comments can be made on the data shown in Figure 2-9:

- Oskarshamn: There are no data Jul. 1994–Jan. 1995.
- Målilla: There are no data Jun.–Jul. 1999.
- Gladhammar: There are no data Jan. 1994–Jul. 1995. Not that in Figure 2-9, Gladhammar data are plotted 1995 and onwards.
- For Ölands norra udde, Figure 2-9 shows the annual average of station PSM107721 (Ölands norra udde A) and station PSM107722 (Ölands norra udde). For the period Jan. 1994–Jul. 1995, PSM107722 data are used (at PSM107721, measurements started on Aug. 1, 1995). For PSM107722, there are no data for the period Aug. 1–Sep. 30, 1995; during this period, data are only available from station PSM107721.
- For all stations in Figure 2-9, "typical" monthly values are used for the period Sep.–Dec. 2007.

Figure 2-9 and Table 2-9 show that the average annual precipitation during the period 1994–2007 was lowest at Ölands norra udde (c. 490 mm/year), whereas Gladhammar (1995–) had the highest average annual precipitation (c. 750 mm/year).

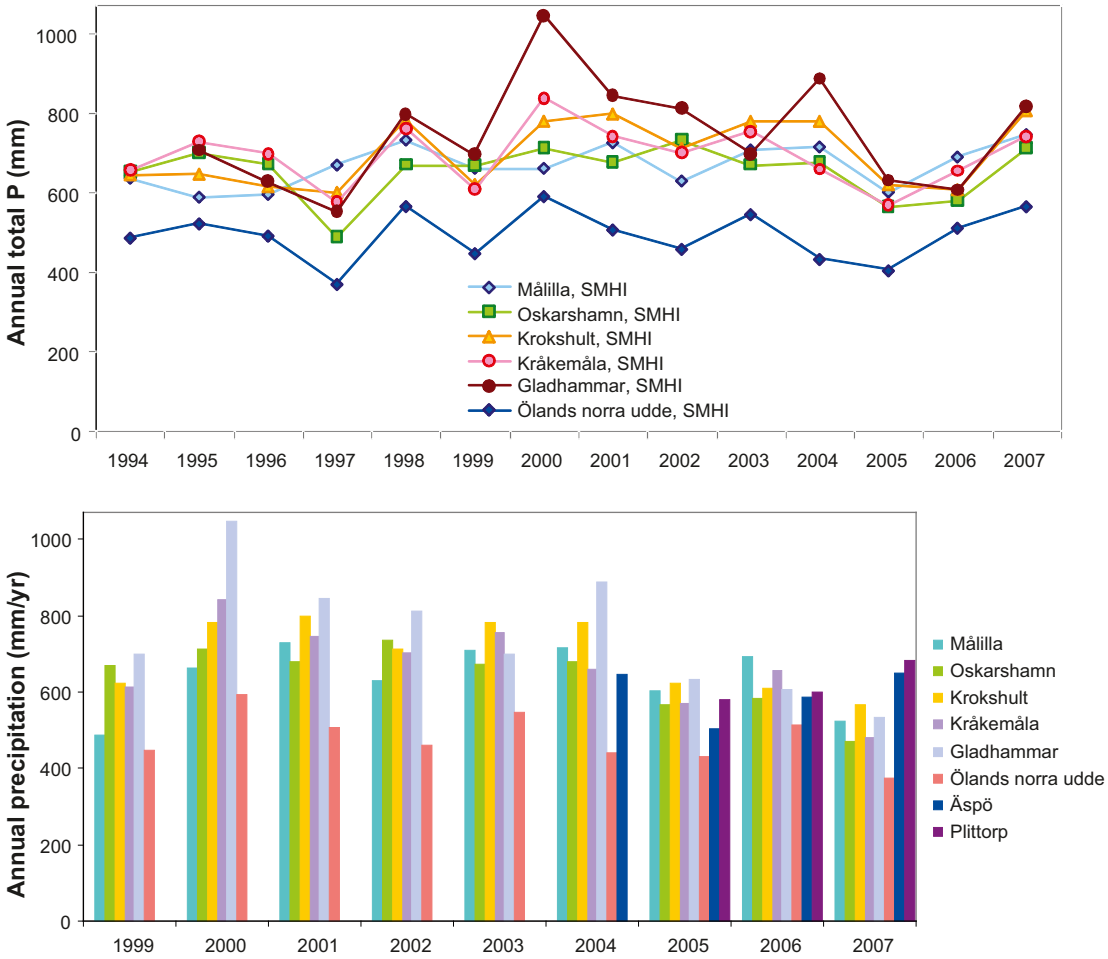

Figure 2-9. *Time-series plots of annual precipitation at the SMHI stations 1994–2007 (top plot; data period Jan. 1, 1994–Aug. 31, 2007) and the SKB and SMHI stations 1999–2007 (bottom plot; data period Jan. 1, 1999–Aug. 31, 2007). In the top plot, the annual precipitation 2007 is estimated by using the average monthly precipitation Sep.–Dec. during Sep.–Dec. 2007, whereas the period Sep.–Dec. 2007 are not included in the bottom plot.*

Table 2-9. Min, max and averages of the accumulated annual precipitation during different data periods 1961–2007. For the SMHI stations (Målilla to Ölands norra udde), monthly averages are used for the period Sep.–Dec. 2007.

Station	1961–2007			1994–2007			2003–2007	2005–2007
	Min	Max	Average	Min	Max	Average	Average	Average
Målilla				589.4	748.6	670.1	693.8	688.8
Oskarshamn	378.0	934.4	611.5	490.0	733.8	656.9	642.5	621.0
Krokshult				601.9	807.5	700.6	719.7	679.0
Kråkemåla				569.8	840.9	694.3	677.6	656.9
Gladhammar (1995-)				552.5	1,046.7	748.8	728.6	685.6
Ölands norra udde				371.8	591.5	493.9	492.9	494.7
Äspö (completed daily data set)								580.2
Plittorp (completed daily data set)								620.7

Figures 2-10 and 2-11 and Table 2-10 analyse the annual precipitation during the years 2003–2007. Figure 2-10 shows box plots, including ranges and averages, of the annual precipitation at each SMHI station for the displayed time periods. The annual precipitation at each station each of the years 2003–2007 is also shown. The monthly precipitation Sep.–Dec. 2007 is estimated as the average monthly precipitation Sep.–Dec. for the previous years. Note that in Table 2-10, "typical" monthly values are used for Äspö for the period Jan.–Oct. 2003, whereas the completed daily data set is used for 2004. Moreover, "typical" monthly values are used for Plittorp for the period Jan.–Jul. 2004. In the table, one can also note that the annual precipitation at Krokshult 2003 and 2004 were exactly equal; in fact, according to the data this happens to be the case and is not a calculation error.

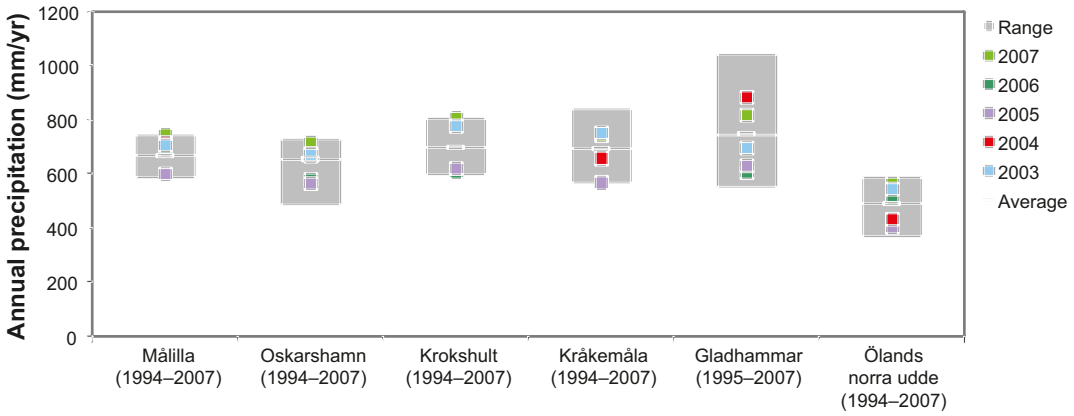

Figure 2-10. *Box plots showing ranges and averages of the annual precipitation for each SMHI station for the displayed time periods. The annual precipitation at each station each of the years 2003–2007 is also shown. The monthly precipitation Sep.–Dec. 2007 is estimated as the average monthly precipitation Sep.–Dec. for the previous years.*

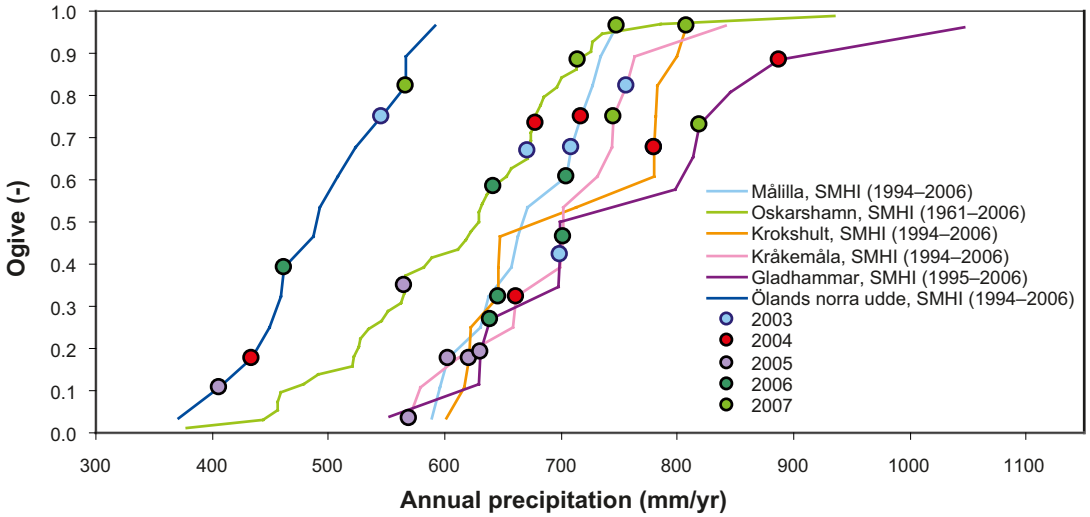

Figure 2-11. *Cumulative frequency plots of the annual precipitation at the SMHI stations for the displayed time periods. The annual precipitation at each station each of the years 2003–2007 is also shown. The monthly precipitation Sep.–Dec. 2007 is estimated by the average monthly precipitation Sep.–Dec. for the previous years.*

Table 2-10. Annual precipitation 2003–2007. For the SMHI stations, monthly averages from available data months are used for Sep.–Dec. 2007.

Station	2003	2004	2005	2006	2007	Average
Målilla	709.6	717.1	602.2	691.5	748.6	693.8
Oskarshamn	671.5	678.2	565.1	583.2	714.6	642.5
Krokshult	780.8	780.8	621.2	608.4	807.5	719.7
Kråkemåla	756.6	660.8	569.8	656.4	744.6	677.6
Gladhammar	698.7	887.4	631.1	607.1	818.7	728.6
Ölands norra udde	546.3	434.1	405.8	512.4	566.0	492.9
Äspö	593.3	658.1	503.0	587.7	649.9	598.4
Plittorp		643.8	581.3	598.9	681.8	626.5

According to Figures 2-10 and 2-11, the annual precipitation 2003 (except for Gladhammar) and 2007 was above average for all SMHI stations, and below average 2005. The annual precipitation 2004 and 2006 reveals two groups of stations: In 2004, the annual P was above average at Oskarshamn, Krokshult and Gladhammar and below average at Målilla, Kråkemåla, and Ölands Norra Udde. In 2006, the annual P was below average at Oskarshamn, Krokshult and Gladhammar, and close to average at Målilla, Kråkemåla, and Ölands Norra Udde. Considering all SMHI stations in Figure 2-11, the annual average percentiles are 2003: 0.67, 2004: 0.59, 2005: 0.17, 2006: 0.44, and 2007: 0.85. Specifically for the period 2003–2007 (Table 2-10), the average annual precipitation at both Äspö and Plittorp were below the corresponding averages for the SMHI stations (except for the station at Ölands norra udde).

Figure 2-12 shows a frequency plot of the annual precipitation at the Oskarshamn station for the period 1961–2002, and the annual precipitation for the period 2003–2007. For the 1961–2002 period, the average annual precipitation was 612 mm (median 623 mm), whereas the minimum and maximum values are 378 and 934 mm, respectively. Note that there are missing monthly data for the periods Jul. 1994–Jan. 1995 and Sep.–Dec. 2007. During these periods, "typical" monthly values (averages for available data months) are used. The precipitation sums 2005 (565 mm; 7.7% below) and 2006 (583 mm; 4.7% below) were below the annual average for the period 1961–2002. The precipitation sums 2003 (672 mm; 9.8% above), 2004 (678 mm; 10.8% above), and 2007 (715 mm, including an estimated precipitation during the period Sep.–Dec.; 16.8% above) were above the 1961–2002 average. Hence, for the years 2003–2007, the annual precipitation at the Oskarshamn station during 2006 was closest (4.7% below) to the 1961–2002 average.

Figure 2-13 shows the annual precipitation during the period Sep. 2003–Aug. 2007 at Äspö, Plittorp and the 6 SMHI stations, dividing the data into Sep. 1–Aug. 31 periods. In Figure 2-14, Äspö data are extrapolated for Oct. 2003 (1 missing data day) and Apr. 2004 (6 missing data days) using monthly averages from the period Sep. 2003–Aug. 2004. According to this figure, the annual precipitation at both the Äspö and Plittorp stations seems to be most similar to the Oskarshamn and Kråkemåla stations.

In order to illustrate typical intra-annual variations, Figure 2-14 shows bar plots of ranges and averages of the monthly precipitation at the Oskarshamn station 1961–2002, also displaying the monthly precipitation at Oskarshamn each of the years 2003–2007. Again, note that there are no data for Sep.–Dec. 2007. According to this figure, the average monthly precipitation is quite evenly distributed throughout the year. The highest average is in Jul. (c 67 mm), the lowest in Mar. (c 33 mm), whereas the average monthly precipitation for the Oskarshamn station (1961–2002) is c 51 mm. Figure 2-15 details the monthly accumulated precipitation during the period Oct. 2003–Aug. 2007. One can note that during the considered years, there was rather little precipitation during the spring periods, and relatively much precipitation during the summer and autumn period (except for the autumn of 2005).

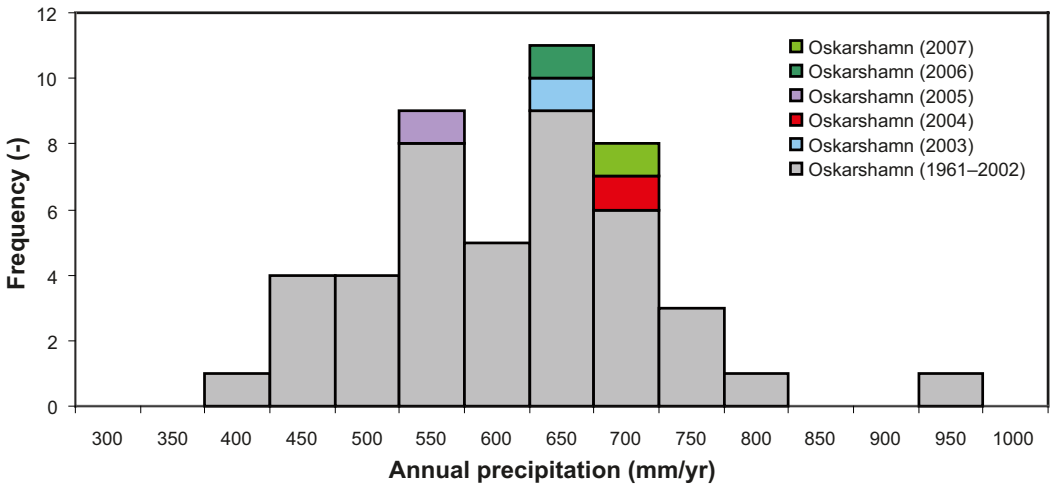

Figure 2-12. *Frequency plot of the annual precipitation at the Oskarshamn station 1961–2002, also displaying the annual precipitation each of the years 2003–2007. The annual precipitation 2007 is estimated using the average monthly precipitation Sep.–Dec. for the period Sep.–Dec. 2007.*

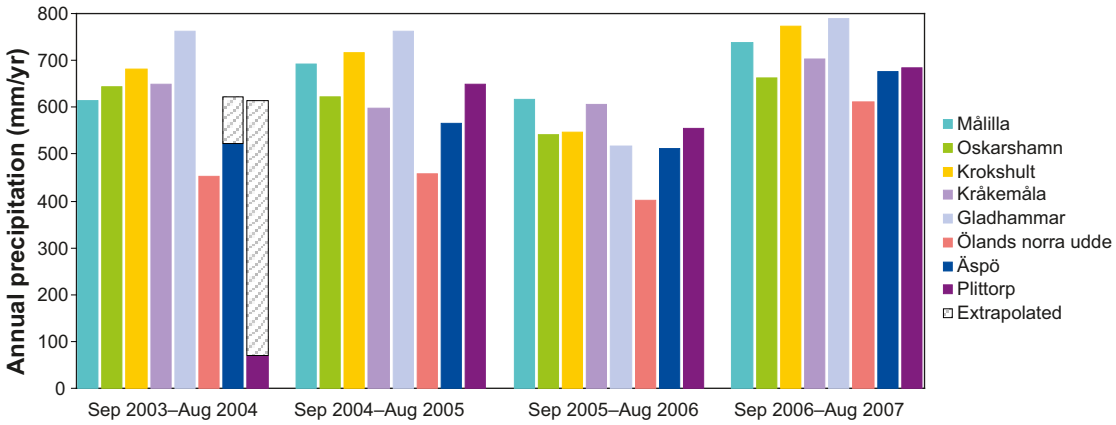

Figure 2-13. *Plot of the annual precipitation at the SKB and SMHI stations, divided into Sep. 1–Aug. 31 blocks.*

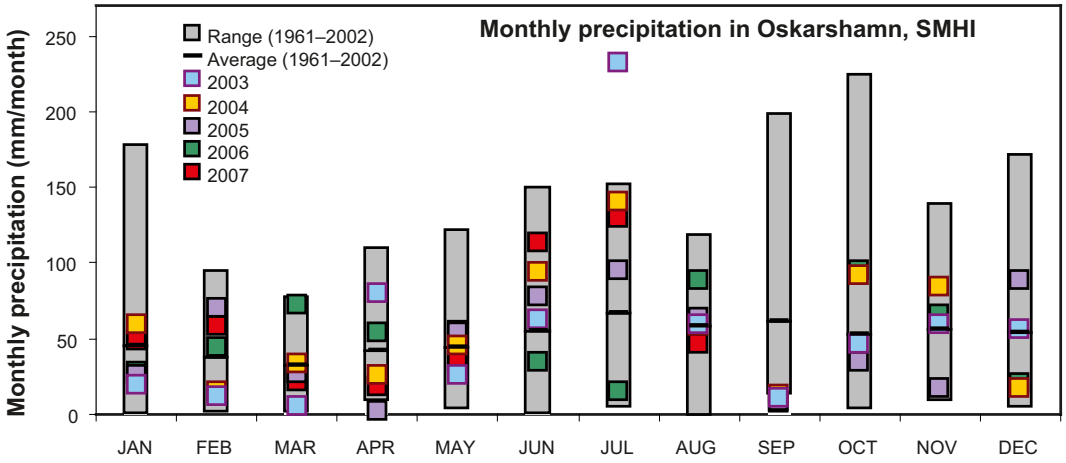

Figure 2-14. *Bar plots displaying ranges and averages of the monthly precipitation at the Oskarshamn station 1961–2002, also displaying the monthly precipitation at Oskarshamn each of the years 2003–2007. There are no data for Sep.–Dec. 2007.*

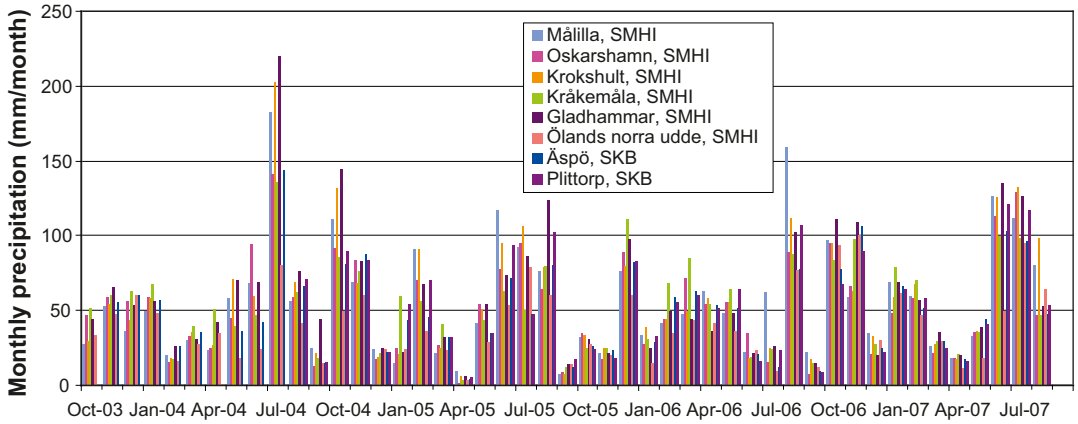

Figure 2-15. *Plot of the monthly precipitation at the SKB and SMHI stations Oct. 2003–Aug. 2007.*

Table 2-11 presents R^2-values for monthly precipitation sums at the SKB and SMHI stations for the period Oct. 2003–Aug. 2007, not including incomplete data months. According to the table, both the Äspö and Plittorp stations demonstrate the highest correlations to the SMHI Kråkemåla station (R^2 = 0.96 and 0.92, respectively), whereas the second highest correlation is to the SMHI Gladhammar station. On a monthly basis, the correlation coefficient between Äspö and Plittorp is 0.95.

To conclude this section on the evaluation of precipitation data, it should be mentioned that SMHI (included in /Johansson 2008/) performed a statistical analysis of long-term precipitation data to estimate the average and standard deviation of the long-term (1961–1990) precipitation at the Äspö and Plittorp stations. According to their analysis (see the results in Table 2-12), the precipitation at the Kråkemåla station demonstrates the best correlation to both Äspö and Plittorp, which is in accordance with the results of the analysis presented in this report (see above). The estimated 30-year average annual precipitation at Äspö and Plittorp is 553 mm and 630 mm, respectively. This yields a Plittorp/Äspö ratio of 1.13, which is higher than the ratio 1.07 according to the data period Jul. 2004–Dec. 2007. Based on these results, it can be concluded that the site-average long-term annual precipitation at the Laxemar site can be approximated as c 600 mm (the actual average of Äspö and Plittorp according to the SMHI analysis is 591.5 mm).

Table 2-11. Correlation coefficients (R^2) for monthly precipitation sums (Oct. 2003–Aug. 2007) at the SKB and SMHI stations, excluding incomplete data months.

	Äspö (Oct. 2003– Aug. 2007)	Plittorp (Aug. 2004–Aug. 2007)
Målilla	0.80	0.84
Oskarshamn	0.88	0.89
Krokshult	0.85	0.87
Kråkemåla	0.96	0.92
Gladhammar	0.91	0.90
Ölands norra udde	0.84	0.78
Äspö		0.95
Plittorp	0.95	

Table 2-12. Calculated long-term (1961–1990) averages and standard deviations (SD) of annual average precipitation at the Äspö and Plittorp stations /Johansson 2008/.

Station	Jan	Feb	Mar	Apr	May	Jun	Jul	Aug	Sep	Oct	Nov	Dec	Year
Äspö													
Average	49	35	32	38	39	44	64	53	55	45	49	50	553
SD	37	22	20	22	21	28	34	26	29	36	24	35	108
Plittorp													
Average	54	39	36	43	45	51	73	61	64	51	56	56	630
SD	41	25	23	25	24	32	39	30	34	41	27	39	122
Äspö/Plittorp (averages)	0.91	0.90	0.89	0.88	0.87	0.86	0.88	0.87	0.86	0.88	0.88	0.89	0.88

2.2.2 Potential evapotranspiration

The basis for calculation of the potential evapotranspiration (PET) is the Penman equation /Penman 1948, Eriksson 1981/ for a hypothetical grass reference crop (reference surface) with specific characteristics; the Penman equation is given as

$$PET = \frac{\Delta}{(\Delta + \gamma)} E_r + \frac{\gamma}{\Delta + \gamma} E_a$$

Two alternative methods have been used by SMHI to calculate PET for the meteorological stations on Äspö and in Plittorp. The first method (referred to as the "old" method) is formulated as /Nord et al. 2006, Sjögren et al. 2007a/

$$PET = \left[\frac{\Delta (R_n - G)}{L(\Delta + \gamma)} + \frac{\gamma f(u)(e_s - e)}{\Delta + \gamma} \right] tstep$$

where Δ is a proportionality constant (= $d(e_s)/d(T)$), R_n is the net radiation flux density, G is the heat flux density into ground ($W \cdot m^{-2}$), L is the latent heat of vaporisation, γ is the psychrometric constant, f(u) is a wind-speed function, e_s is the saturated water vapour pressure, e is the water vapour pressure, and tstep denotes the time step.

This method is based on daily values of air temperature (to obtain the net radiation R_n from the global radiation), steam pressure (e), wind speed (f(u)) and cloudiness (to obtain the global radiation, and hence the net radiation R_n). In /Eriksson 1981/, a simple equation is used to calculate the global radiation based on wind-speed data. The method neglects heat storage in the ground, which overestimates PET during spring and summer (when heat is stored in the ground), and underestimates PET during autumn (when heat is released from the ground). Global radiation is calculated based on observations of cloudiness from surrounding meteorological stations, and the albedo is set to 0.25, irrespective whether there is snow on the ground or not. The wind speed (which is measured at a height of 10 m above ground) at 2 m is calculated by multiplication by the factor 0.8.

The second method (referred to as the "new" method) is based on the same equation as above, but instead one uses half-hour values of air temperature (to obtain the net radiation from global radiation), relative humidity (e/e_s), wind speed (f(u)), and global radiation /Nord et al. 2006/. The main difference compared to the old method is that global radiation data are used directly, and not estimated by means of cloudiness observations. In addition, the new method takes into account heat storage in the ground. Moreover, the albedo is set to 0.12 if the ground is bare, and 0.5 when there is a snow cover.

Figure 2-16 presents time-series plots of daily PET sums and the rolling annual sums, calculated using the "new" method for the Äspö and Plittorp stations. According to this figure, PET demonstrates regular annual cycles, with high PET during late spring, summer and early autumn, and low or no PET during winter (note that the adopted method to calculate PET may produce negative PET during winter). Figures 2-17 and 2-18 compare annual PET sums at the stations Ölands norra udde A, Gladhammar, Äspö and Plittorp. The annual PET is highest at Ölands norra udde. The annual PET at the Äspö station 2004–2007 ranges from 450 (2004) to 591 mm·y^{-1} (2005), with an average of 541 mm·y^{-1}. The corresponding data for the Plittorp station 2005–2007 are 514 (2006) to 551 mm·y^{-1} (2005), with an average of 531 mm·y^{-1}.

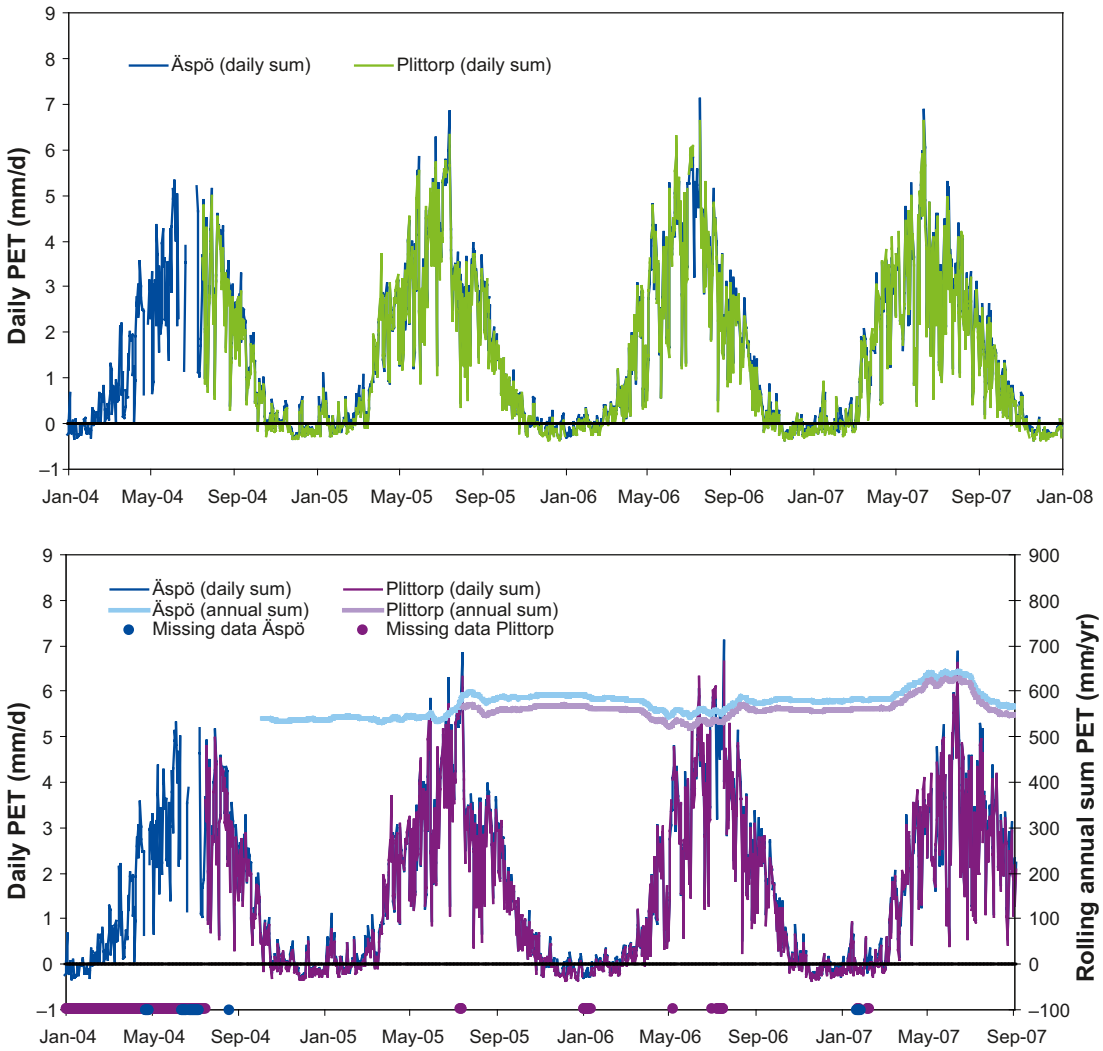

Figure 2-16. *Time-series plot of daily PET sums (mm·d^{-1}) at the Äspö and Plittorp stations for the period 2004–2007 (top plot) and in the bottom plot for the period Jan 1, 2004–Aug. 31, 2007, also showing rolling annual sums of daily PET for the period Oct. 4, 2004 (Äspö) and Jul. 14, 2005 (Plittorp) to Aug. 31, 2007.*

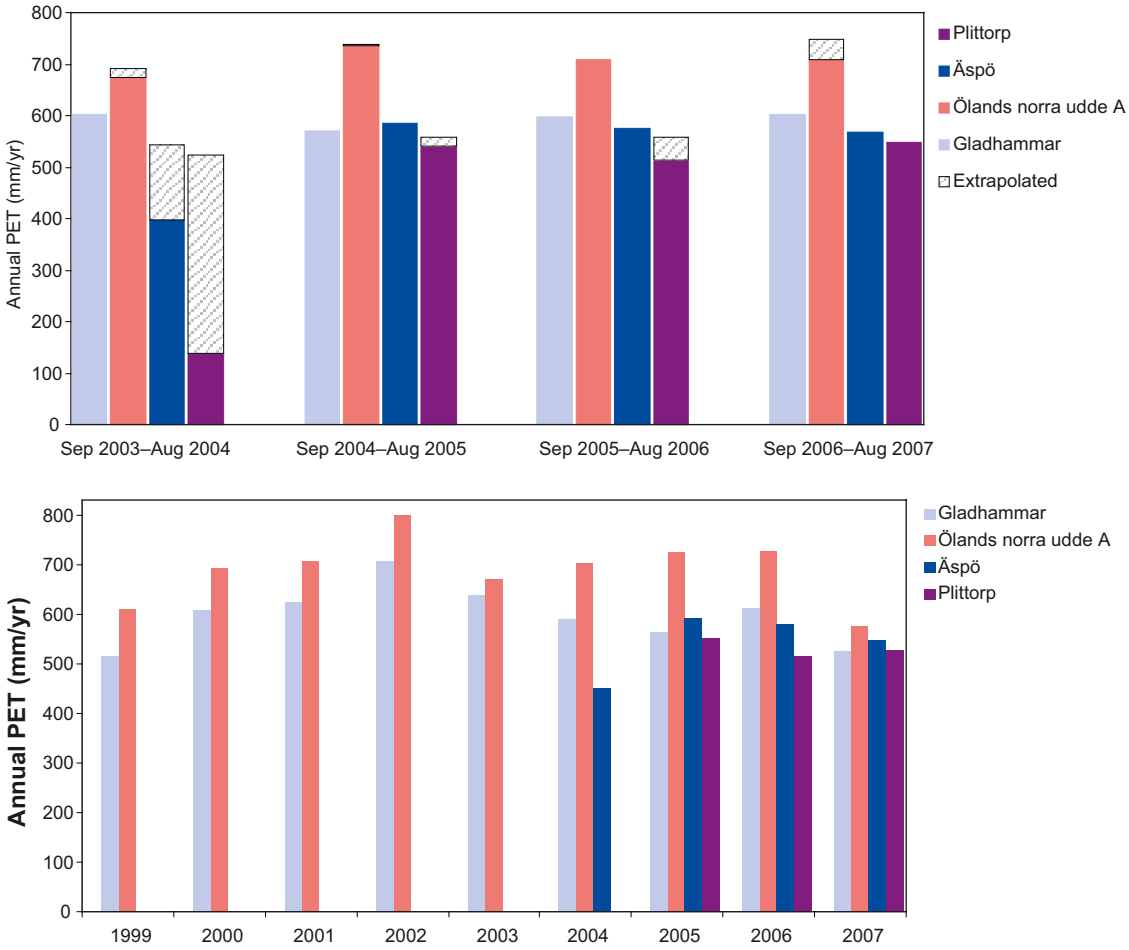

Figure 2-17. *Time-series bar plots of annual sums of PET at Äspö, Plittorp, Ölands norra udde A and Gladhammar, for calendar years (top plot) and divided into Sep. 1–Aug. 31 blocks (bottom plot).*

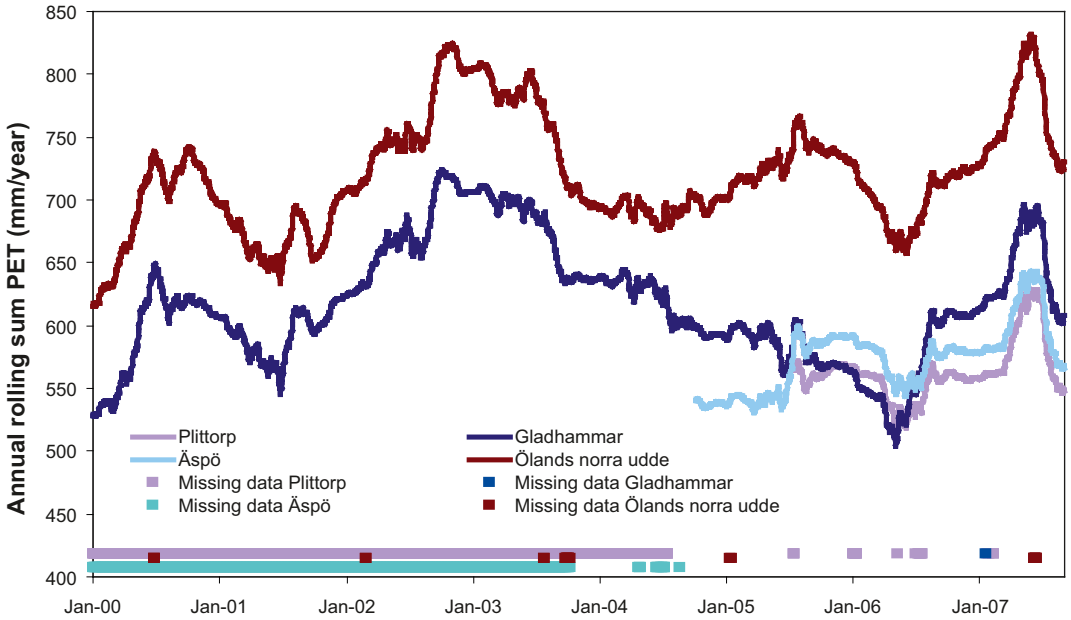

Figure 2-18. *Time-series plot of rolling annual PET sums at Äspö, Plittorp, Ölands norra udde and Gladhammar.*

2.2.3 Air temperature

Figure 2-19 shows a time-series plot of daily average air temperatures at the Äspö and Plittorp stations, whereas the two time-series plots of Figure 2-20 shows a typical annual air temperature cycle at the SMHI and SKB stations, based on data 1994–2007 and 2004–2007, respectively. As for the potential evapotranspiration, the air temperature demonstrates regular annual cycles, with high air temperatures during late spring, summer and early autumn, and low temperatures during late autumn and winter. During the available data periods for the Äspö and Plittorp stations, there were temperature conditions for snowfall (daily average air temperature < 1°C) during c 20% of the time at both stations, and hence conditions for rainfall during 80% of the time. Days with temperature conditions for snowfall commonly occur during the period from Oct.–Nov. to Mar.–Apr. the following year.

Figure 2-21 compares the seasonal temperature variations of inland and coastal areas, in terms of the difference in daily average air temperature between Äspö and Plittorp. It can be seen that Äspö generally is colder than Plittorp during the period Mar.– Jun. whereas Äspö is warmer during the period Jul.–Nov. This was also noted by /Larsson-McCann et al. 2002/, who state that there generally is an inland-coastline gradient of the air temperature; warmer winters and colder summers close to the coast, and corresponding similar day-night patterns (colder days and warmer nights).

According to /Larsson-McCann et al. 2002/, in the part of Sweden where Laxemar is located the annual average temperature can be estimated to be 6–7°C. The monthly average air temperature is lowest in Jan. (–2°C) and warmest in Jul. (16–17°C). At the Oskarshamn station, which was chosen as reference station for air temperature by /Larsson-McCann et al. 2002/, the long-term (1961–1990) monthly average air temperature ranges between –2.5°C (Feb.) and c 16°C (Jul.), with an annual average of 6.4°C (see Figure 2-22). The corresponding data for Ölands norra udde are –1.1°C (Feb.), 16.7°C (Jul.) and 7.3°C (long-term annual average), and for Målilla (c 45 km from the coast) –3.1 to –3.2°C (Jan.–Feb.), 15.9°C (Jul.) and 6.0°C (long-term annual average). Figure 2-22 shows that there generally are larger inter-year variations between winters compared to the summers.

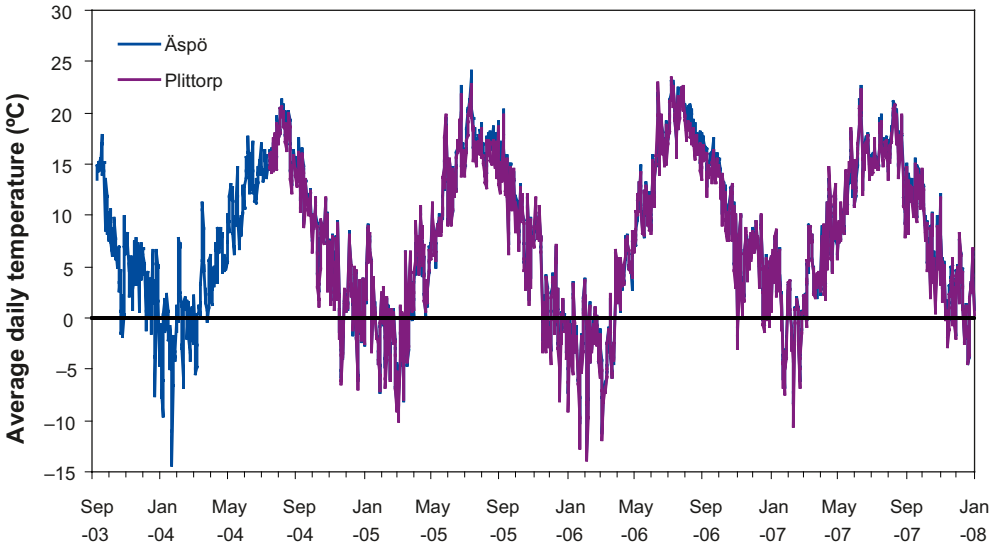

Figure 2-19. *Time-series plot of daily average air temperature at the Äspö and Plittorp stations.*

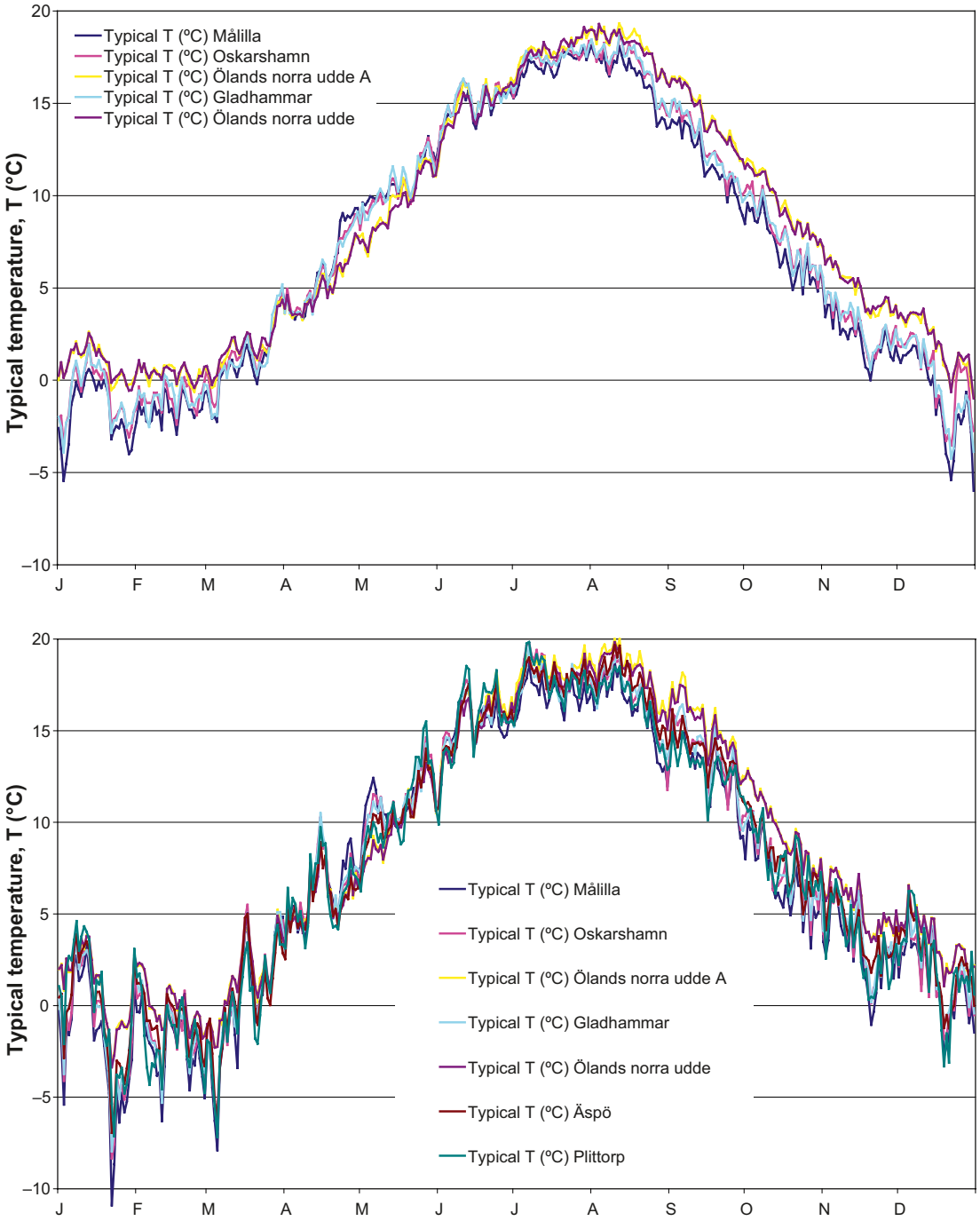

Figure 2-20. *Typical annual cycle of daily average air temperatures, based on data for the periods 1994–2007 (top plot) and 2004–2007 (bottom plot).*

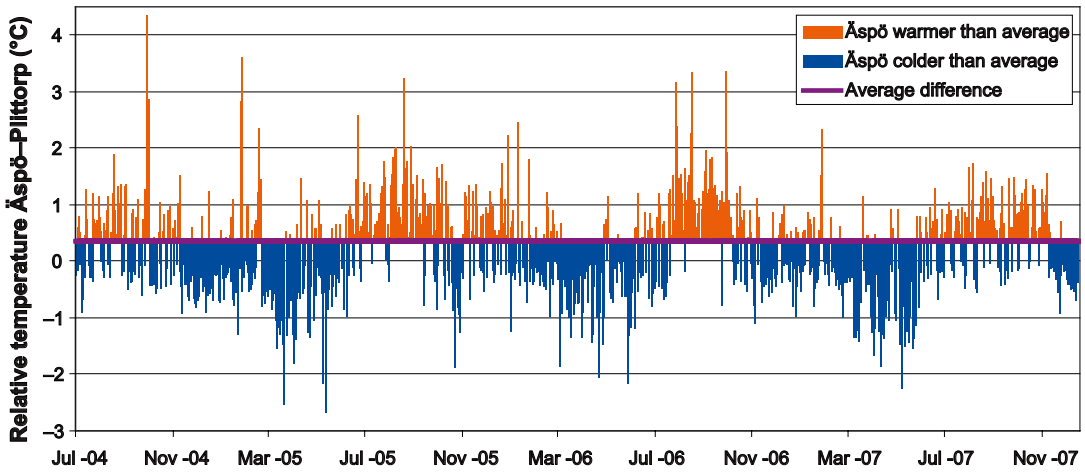

Figure 2-21. *Illustration of seasonal variations of the difference in air temperature between Äspö and Plittorp.*

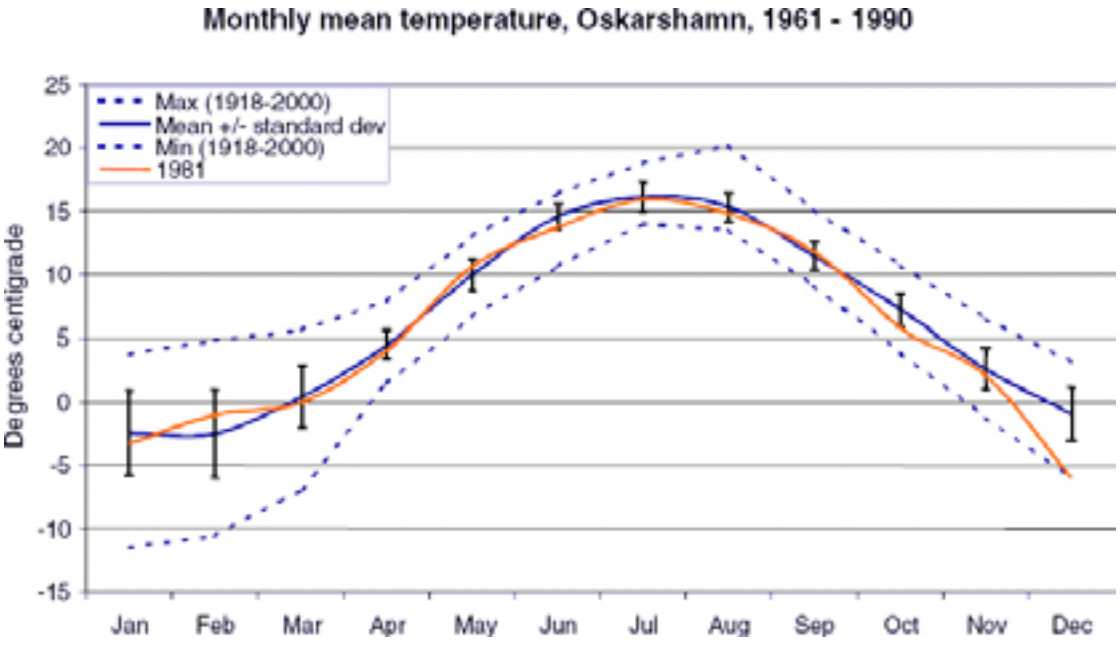

Figure 2-22. *Temperature statistics for the standard reference period 1961–1990, Oskarshamn, which was chosen as reference station (i.e. most representative for the Laxemar-Simpevarp area) by /Larsson-McCann et al. 2002/.*

Figure 2-23 shows the annual average air temperature of the available data at the SMHI and SKB stations during the period 1999–2007. For 2007, monthly averages were used for the period Sep.–Dec. 2007. The average of all stations (except Ölands norra udde, which on average is warmer than the other stations) for this data period is 7.7°C, varying between 6.5°C (Målilla 1999) and 9.4°C (Oskarshamn 2007). The annual average air temperature 1999–2007 is in fact relatively similar (again, except for Ölands norra udde), only varying between 7.3°C (Målilla) and 7.9°C (Äspö; the average for Plittorp was 7.8°C). The temperature correlation between the stations is quantified in Table 2-13, which presents R^2-values for average daily air temperatures at different stations. According to the table, the daily air temperature on the island of Äspö and at Plittorp are well correlated ($R^2 = 0.99$).

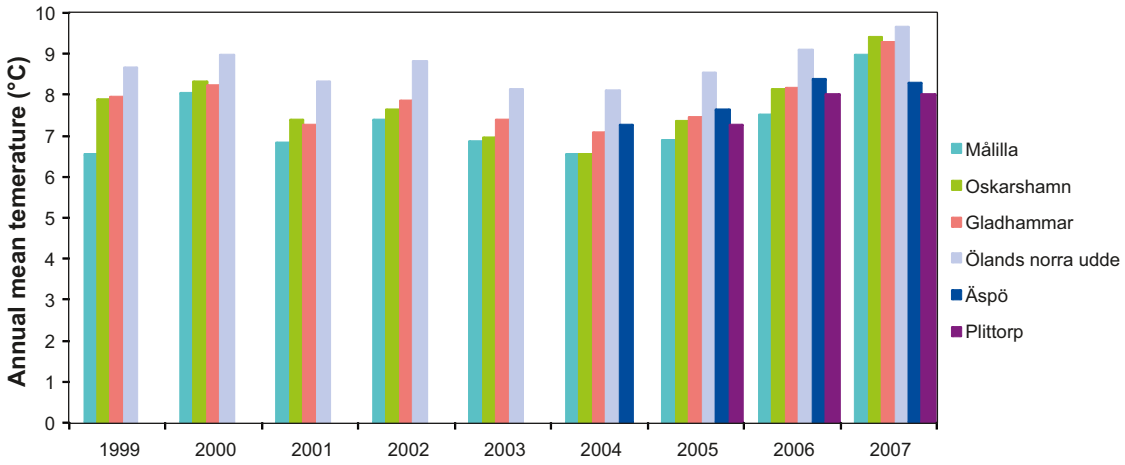

Figure 2-23. *Temperature statistics for the standard reference period 1961–1990.*

Table 2-13. Coefficients of determination (R^2-values) for the average daily air temperature at different stations.

Station	Målilla	Oskars-hamn	Glad-hammar	Ölands norra udde A	Ölands norra udde	Äspö	Plittorp
Målilla		0.98	0.98	0.91	0.91	0.97	0.98
Oskars-hamn			0.99	0.94	0.94	0.99	0.99
Glad-hammar				0.95	0.95	0.99	0.99
Ölands norra udde A					0.998	0.97	0.95
Ölands norra udde						0.97	0.96
Äspö							0.99

According to /Larsson-McCann et al. 2002/, the vegetation period in the Laxemar-Simpevarp area can be estimated to be c 200 days per year, i.e. there are on average 200 days per year with a daily average air temperature > 5°C. The length of the vegetation period is in Table 2-14 estimated for the periods 1994–2007 and 2004–2007, based on air temperature data from both the considered SMHI stations and the two SKB stations. According to this table, the vegetation period in Laxemar is on average in the interval 210–230 days per year, which is somewhat longer than stated in /Larsson-McCann et al. 2002/.

Table 2-14. Length of vegetation period (number of days with an average air temperature above 5°C).

Station	1994–2007			2004–2007		
	Min	Max	Average	Min	Max	Average
Målilla	184	241	209	214	228	220
Oskarshamn	194	244	213	219	219	219
Gladhammar	199	244	217	219	234	226
Ölands norra udde A	199	253	222	224	246	232
Ölands norra udde	200	253	223	225	244	232
Äspö				213	236	224
Plittorp				221	235	228

2.2.4 Snow depth and estimation of water content of snow

Site-specific data on snow depth and the water content of snow are important inputs to assessment of snow accumulation, snowmelt and the associated temporal distribution of surface runoff, infiltration and groundwater recharge. In /Larsson-McCann et al. 2002/, the Oskarshamn meteorological station was chosen to represent and characterise the snow-depth conditions in the part of Sweden where Laxemar is located. Their report briefly states that the ground is covered by snow c 70 days per year (i.e. per winter season), with a maximum depth typically on the order of 0.35–0.40 m, and that there are small differences in snow conditions between the coast and the inland.

In the Laxemar area, snow-depth observations were done on the island of Äspö (the Grillplatsen station; station ID ASM100224) at totally 60 occasions between Dec. 2002 and Mar. 2007. From these measurements, there are totally 49 snow-depth data (excluding occasions when measurements were not possible and occasions with zero snow depth). At 22 of these 49 occasions, the snow weight was also determined (i.e. there are 22 non-zero snow-weight data). However, there are no site-specific data on the water content of the snow. Figure 2-24 shows a time-series plot of snow depth (mm) at the Grillplatsen station and the SMHI stations at Krokshult, Oskarshamn, Kråkemåla and Målilla.

The Grillplatsen data show that during the considered data period (Dec. 2002–Mar. 2007) most years there was a snow cover from Dec./Jan. up to Mar./Apr. Short periods with a snow cover were recorded as early as Oct. and it was also recorded a snow cover in the late part of the winter season (in the end of Apr.). The average snow depth at Grillplatsen was c 120 mm, whereas the maximum observed snow depth was c 370 mm (Mar. 16, 2006). Overall, the recorded snow-cover data from Grillplatsen agree well with the snow-cover data from the four SMHI stations, as well as air temperature data (i.e. periods with an average air temperature < 1°C). Moreover, the similarities between stations are in accordance with the observed similarities between stations in terms of average air temperatures (cf. section 2.2.3).

Snow-depth measurements are done by a standardised procedure, using a sampling tube with certain dimensions. This implies that the cross-sectional area of each snow sample is known, which in turn means that even though no explicit determinations were done of the water content of the snow (i.e. the water content in melted form), the water content (mm) of the snow pack at a certain sampling occasion can be determined from the 22 available snow-weight data, based on the cross-sectional area of the sampling tube and by assuming the density of the melted water. The relationship between the weight of a snow sample and its water content (mm) is illustrated in Figure 2-25 using the Forsmark 2.2 data set, comprising data from the period Dec. 2002–Apr. 2006 /Johansson 2008/ and water-content data.

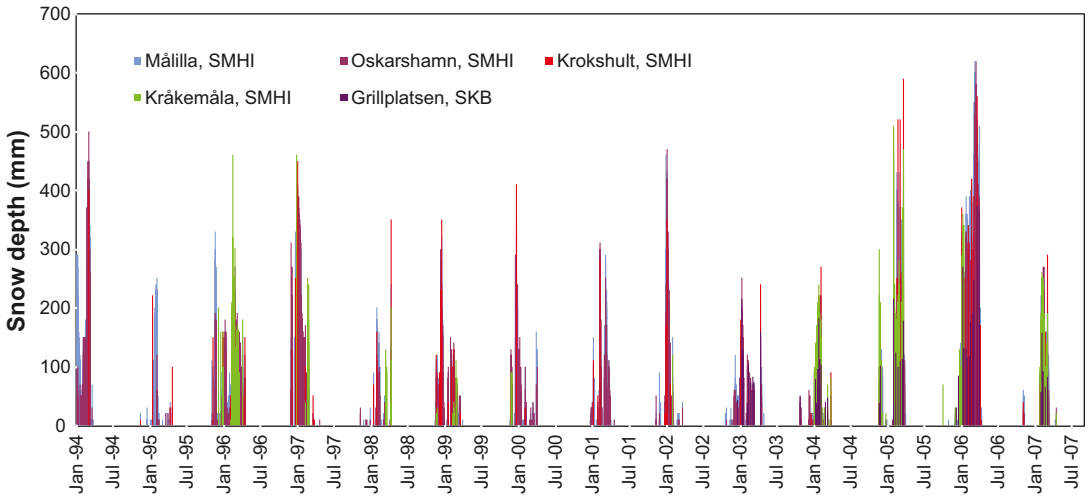

Figure 2-24. *Time series plot of snow cover (mm) at the Grillplatsen station on the island of Äspö, and the SMHI stations at Krokshult, Oskarshamn, Kråkemåla and Målilla.*

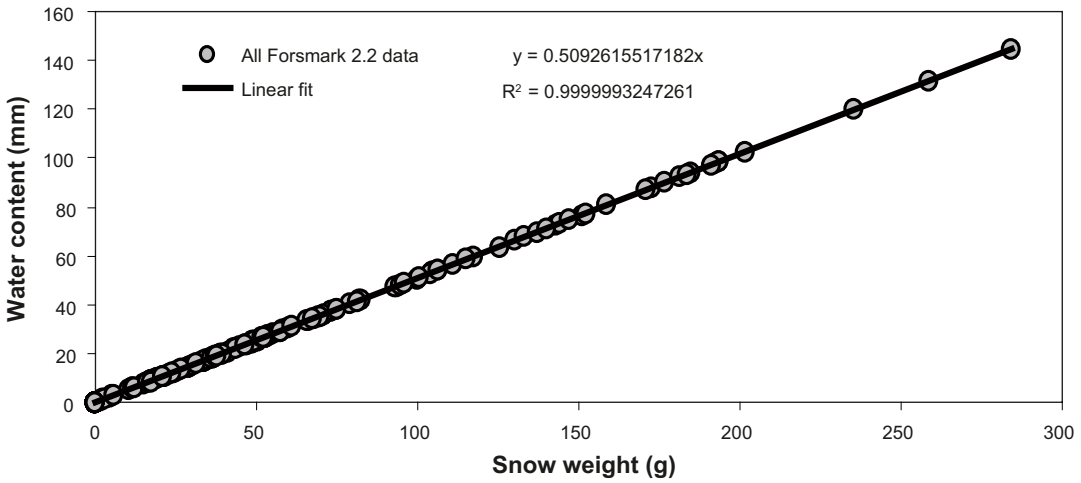

Figure 2-25. *Illustration of the relation between the water content (mm) and the weight (g) of snow, using data from the Forsmark data freeze 2.2 /Johansson 2008/.*

Figure 2-25 shows that snow-weight data can be recalculated into water contents, according to the linear expression water content (mm) = snow weight (g)·0.509. As mentioned previously, there are only 22 snow-weight data in the Laxemar 2.3 data set, whereas there are 49 snow-depth records from the ASM100224 station. Hence, a method is here sought to arrive at an approximation of water contents (in mm) based on snow-depth data only. One problem is that the Laxemar snow-depth data set is sparsely distributed in time, which again calls for supplementing the Laxemar data with data from Forsmark. Figure 2-26 shows the relation between snow weight (g) and snow depth (mm), including data from data freeze 2.2 from both the Laxemar ASM station and the three snow-depth (AFM) stations in Forsmark.

Using the linear relationship from Figure 2-25, snow water contents can be calculated using the available snow-weight data from both Laxemar and Forsmark (data freezes 2.2), see Figure 2-27. Note that the AFM001172 Forsmark data are excluded from Figure 2-27; these data deviate from the data from the other stations (cf. Figure 2-26). For the Laxemar data, the regression coefficient is 0.23 ($R^2 = 0.87$), and the obtained linear fit seems to agree quite well with the Forsmark data.

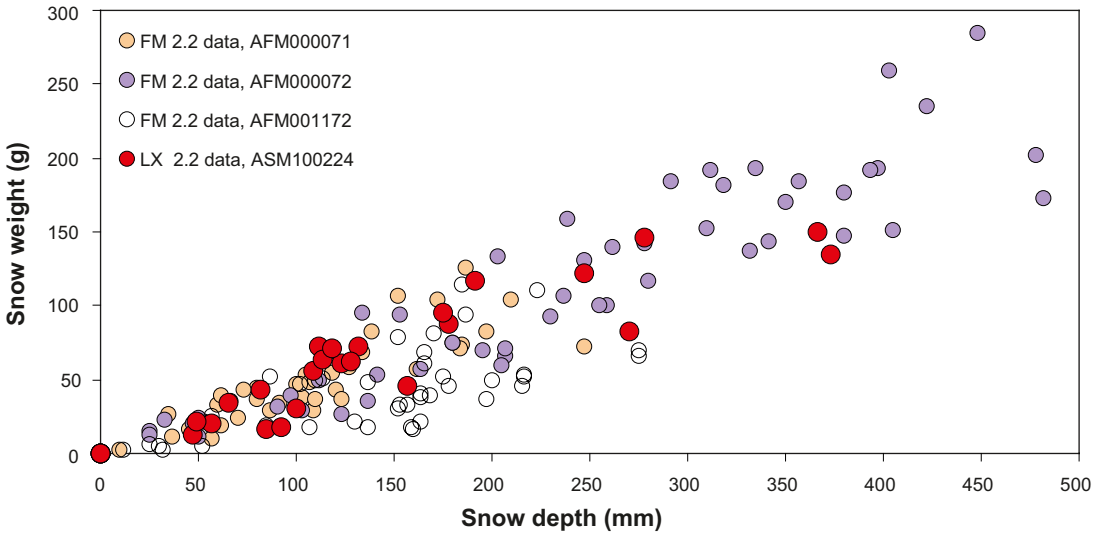

Figure 2-26. *Illustration of the relation between snow weight (g) and snow depth (mm), including data at the Laxemar (ASM) and Forsmark (AFM) 2.2 data freezes.*

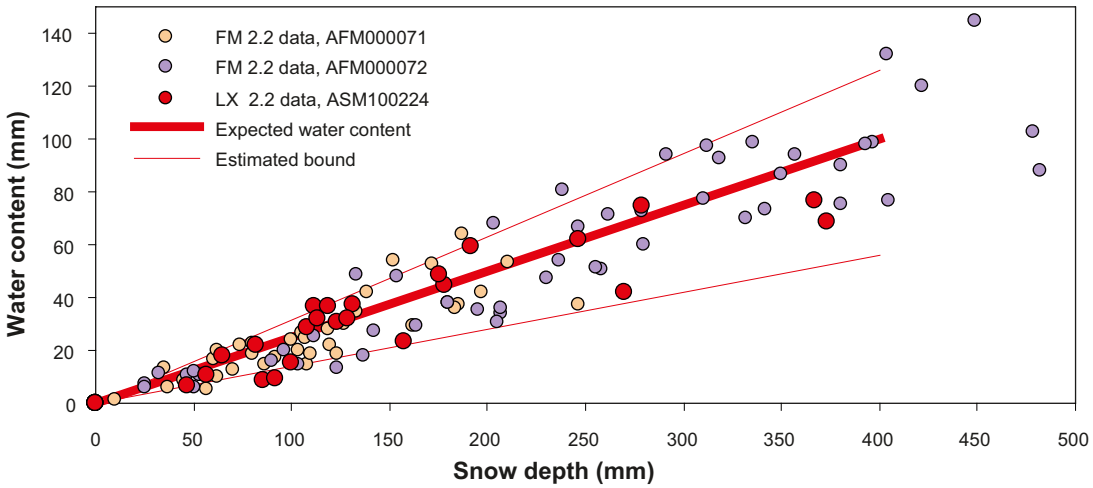

Figure 2-27. *Illustration of the relation between snow weight (g) and snow depth (mm), using data from the Laxemar (ASM) and Forsmark (AFM) 2.2 data freezes.*

It can be speculated that the data spread is due to seasonal variability, i.e. that the relation between snow depth and snow weight (and hence its water content) varies with season; at low temperatures, newly-fallen snow may have a lower water content compared to slushy snow during snowmelt periods. Using the data from Figure 2-27, this matter is explored in Figure 2-28, showing a time-series plot of the water content/snow depth ratio. As can be seen in this figure, there are no clear seasonal patterns, and the water content/snow depth ratio is therefore for simplicity assumed to be temporally constant.

Figure 2-29 plots the cumulative frequency of the water content/snow depth ratio (denoted "water content ratio") in the form of its ogive to determine the expected value of this ratio; ogives plot the cumulative frequencies at the class boundaries instead of the class marks. The median of the ratio (0.25) coincides with the type value, and was chosen as a "representative ratio". Based on this figure, it can be concluded that the water content (in mm) is c 0.25 times the snow depth (in mm). In order to verify this established relationship, its expected values and estimated bounds are in Figure 2-30 compared to the 22 data records of snow depth and snow weight, for which the water content hence can be calculated (Laxemar 2.3 data set). As anticipated, the expected water content agrees rather well with the water content data calculated directly from the snow-weight data.

The established relationships between snow weight/snow depth and its water content were used to recalculate all snow-depth and snow-weight data into water-content data, based on which a relatively simple snow accumulation/snowmelt model subsequently was calibrated. The overall objective is to obtain a fit between model-calculated and "measured" (in fact, calculated) snow water contents. In this exercise, snow-depth data (weekly averages) from three SMHI stations were also included: Krokshult, Oskarshamn and Kråkemåla. There are also snow-depth data from Målilla; this station is considered to be located too far away to be included in this context and was therefore not used.

The adopted model hence includes both snow accumulation ($mm \cdot d^{-1}$) and snowmelt ($mm \cdot d^{-1}$), where the daily sum of snowmelt is calculated according to a linear degree-day relationship: Snowmelt equals the daily average air temperature T (°C) times a degree-day factor (C_{melt}) with units $(mm \cdot d^{-1}) \cdot °C^{-1}$.

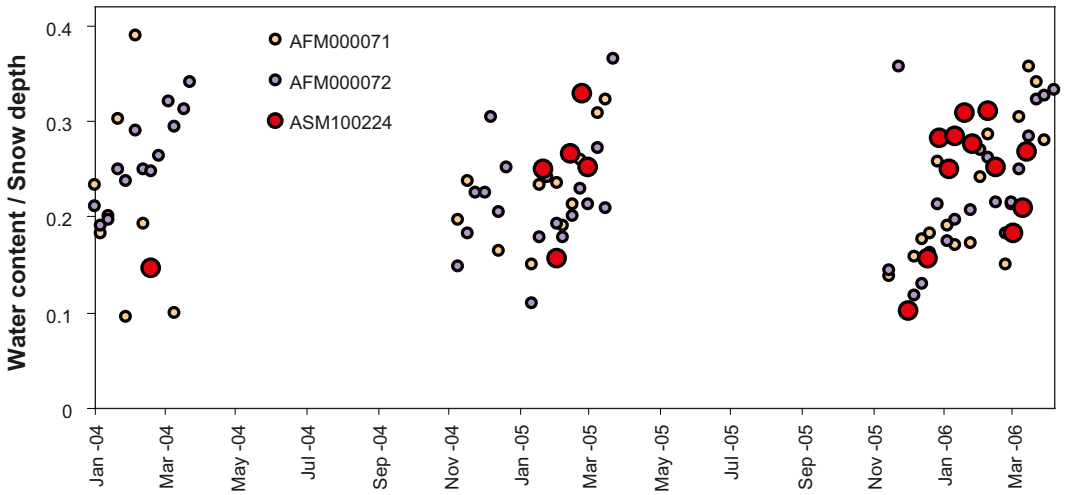

Figure 2-28. *Investigation of potential seasonal variability of the water content/snow depth ratio, using data from Figure 2-27.*

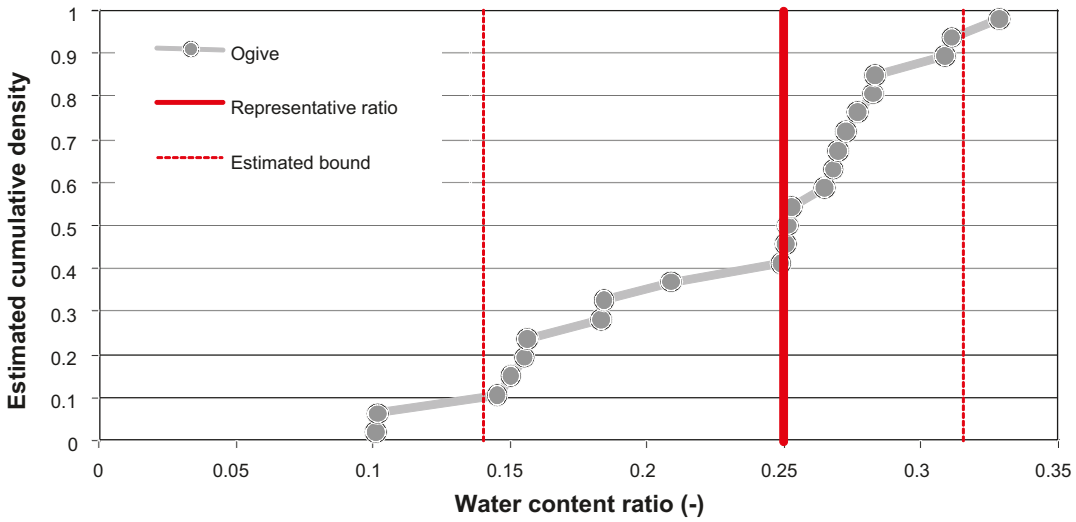

Figure 2-29. *Cumulative frequency of the water content/snow depth ratio ("water content ratio") in the form of its ogive. The "representative ratio" = median = type value = 0.25. The red dotted lines represent the estimated bounds for the ratio (min: 0.14, max: 0.31).*

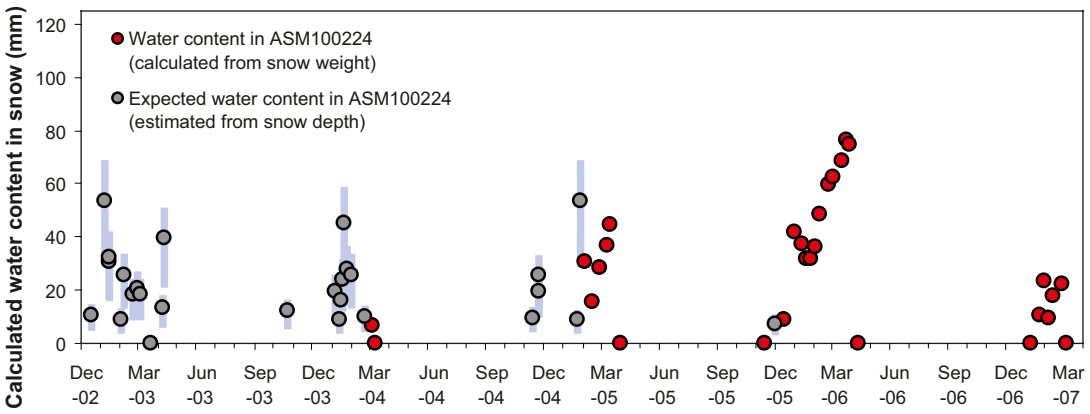

Figure 2-30. *Verification of the established water content/snow depth relation, showing expected water contents at ASM100224 calculated from snow depth (grey dots) and water contents calculated directly from snow weight (red dots; Laxemar 2.3 data set). The blue lines indicate the estimated bounds.*

Besides C_{melt}, model-fitting parameters include the air temperature threshold (T_{precip}) for rainfall/snowfall and the corresponding threshold for initiation of snowmelt (T_{melt}). The resulting calibrated time-series plot of daily values of the water content of snow is presented in Figure 2-31. Red dots represent data from the ASM100224 (Grillplatsen) station, whereas the grey dots represent "site-average" water-content data, calculated from the average of the snow depth at Grillplatsen and the three SMHI stations Krokshult, Oskarshamn and Kråkemåla (weekly averages). According to the figure, there are much smaller snow depths at ASM100224 compared to three SMHI stations. During some periods with snowfall (i.e. periods with increasing snow water content), the model tends to overestimate the snow water content. The underlying reason is likely that the water content/snow depth ratio is assumed to be temporally constant (the ratio is expected to be smaller during cold days with snowfall), due to that no clear seasonal patterns could be discriminated (cf. Figure 2-28).

The resulting model-fitting parameters are T_{precip} = 0.6°C, T_{melt} = 0.36°C and C_{melt} = 2.82 mm·d^{-1}·°C^{-1} (i.e. the rate of snowmelt during days with an average air temperature > T_{melt}). In this context, it can be noted that the method (cf. section 2.2.1) used up to Jun. 2006 to correct the measured precipitation at Äspö and Plittorp for wind losses used an air temperature rainfall/snowfall threshold of 1°C (corresponding to T_{precip} in this case). According to the calibrated air temperature threshold, approximately 17% of the accumulated precipitation in the Laxemar-Simpevarp area fell in the form of snow during the period Sep. 9, 2003–Dec. 31, 2007, which is in accordance with the estimated long-term, regional fraction of 20% /Larsson-McCann et al. 2002/, but obviously somewhat lower compared to the estimation in section 2.2.3 using a threshold of 1°C.

2.2.5 Global radiation

Global radiation is a key input parameter that is required when using the Penman formula to calculate the potential evapotranspiration. According to /Larsson-McCann et al. 2002/, the global radiation demonstrates large differences between inland and coastal areas during summers in Sweden, mainly due to differences in cloudiness. During winters, there are more pronounced differences between the northern and southern parts of the country. Global radiation is measured at the Äspö station, for which daily data are available for the period Sep. 9, 2003–Dec. 31, 2007. The plots in Figure 2-32 show average sums of monthly global radiation (top; kWh·m^{-2}) and monthly average global radiation (bottom; W·m^{-2}) at Äspö for the years 2004–2007.

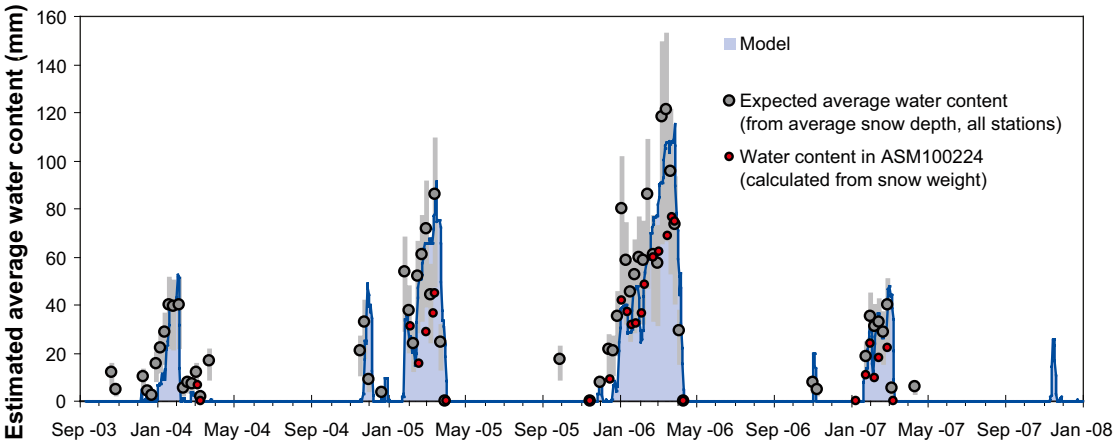

Figure 2-31. *Simulated time series plot of daily values of the water content of snow, calculated using calibrated models of snow accumulation (rainfall/snowmelt air temperature threshold) and a degree-day formulation for snowmelt. Red dots are data from the ASM100224 (Grillplatsen) station, and the grey dots represent a site-average water content data, calculated using snow-depth data (weekly averages) from Grillplatsen and the three SMHI stations Krokshult, Oskarshamn and Kråkemåla.*

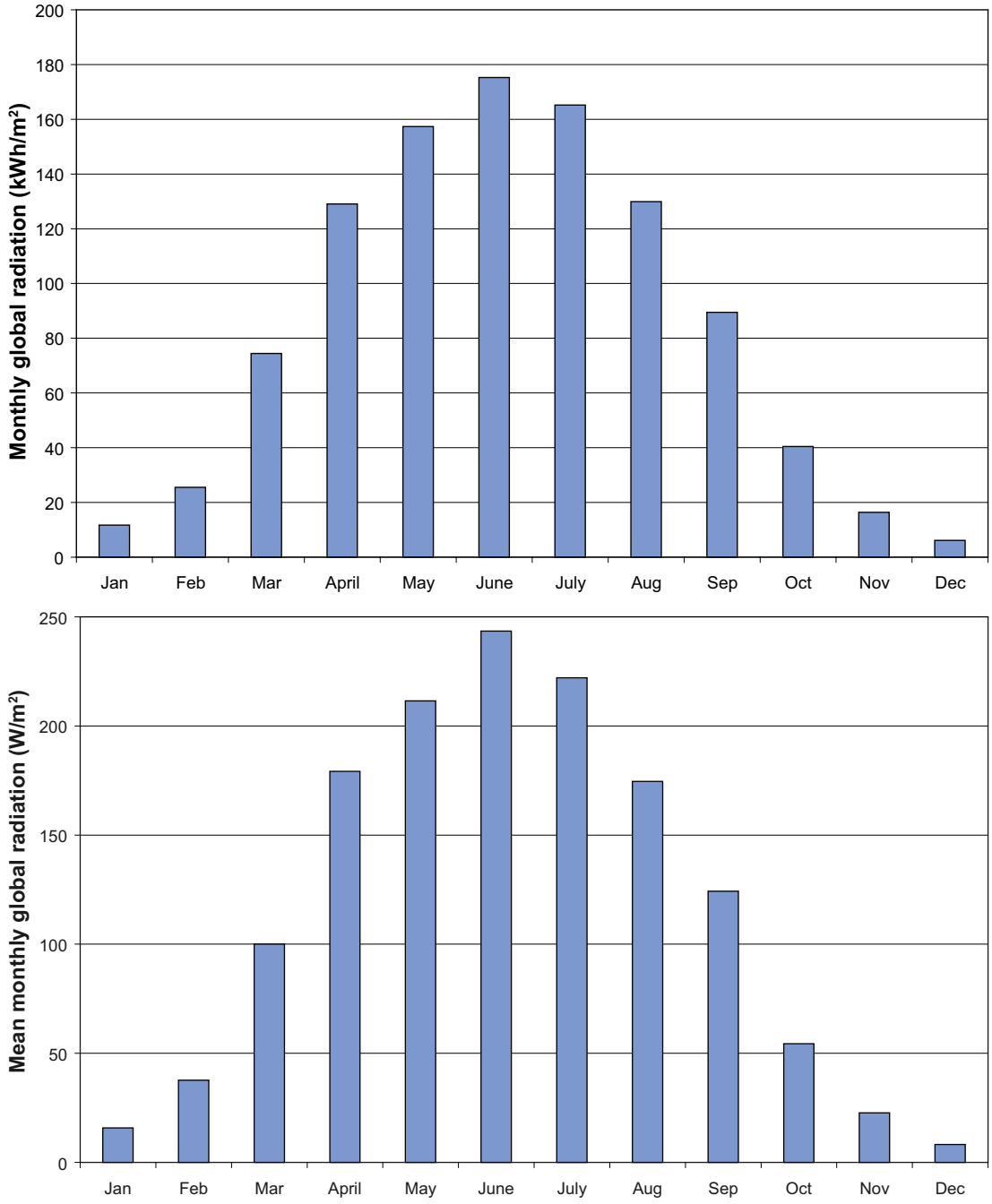

Figure 2-32. *Average monthly sums of global radiation (top) and average monthly global radiation (bottom) at Äspö, 2004–2007.*

As shown in the top plot, the average monthly sum of global radiation at Äspö varies between c 6 (Dec.) and 180 kWh·m^{-2} (Jun.), whereas the average annual sum is c 1,020 kWh·m^{-2} (min = 976, max = 1,079; standard deviation = 50 kWh·m^{-2}). The corresponding values for Dec., Jun. and the average annual sum at Ölands norra udde (1961–1990) are almost equal /Larsson-McCann et al. 2002/. It can be noted that the 1961–1990 range of the annual average global radiation at Ölands norra udde is just 934–1,116 kWh·m^{-2}, which shows that the global radiation demonstrates relatively small variations between years, and (based on the discussion above) likely also between different locations. As shown in the bottom plot, on average the global radiation at Äspö 2004–2007 is c 8 W·m^{-2} in Dec. and c 240 W·m^{-2} in Jun.

2.2.6 Ground frost and ice freeze/breakup

Ground frost

In Laxemar, ground-frost penetration depths have been measured at four locations: PSM107724 (Grillplatsen, Äspö; installed Jan. 2003), PSM006978 (Löv 1; installed Jan. 2005), PSM006979 (Grindstugan; installed Jan. 2005), and PSM006980 (Åker; installed Jan. 2005). These measurements show that the ground generally is frozen from approximately the middle of Nov. until the middle or end of Mar. the following year. When the ground is frozen, the measured frost depth is usually on the order of 0.05–0.15 m. Depending on the air temperature and the prevailing snow depth, the frost depth can be up to 0.5 m (Äspö, Grillplatsen, Feb. 2003), but there are also winter observations with zero frost depth (e.g. Grindstugan, Jan. 2006).

Ice freeze/breakup

Ice freeze/breakup has been inspected at three locations in the Baltic Sea: Äspö brygga (ASM100226), Kråkelund yttre (ASM100227), and Kråkelund inre (ASM100228). In addition, ice freeze/breakup inspections were also made at one location in Lake Jämsen (ASM100229). Table 2-15 summarises the results of these ice freeze/breakup inspections.

In general, the inspections indicate that the near-coastal sea bays (represented by ASM100226) are ice covered 1–4 months each winter (from Dec.–Jan. to Mar.–Apr. the following year). The ice conditions further offshore (ASM100227 and ASM100228) are variable, but the observations could be generalised to say that there is an ice cover between Jan. and Mar. The inspections in Lake Jämsen (ASM100229) show that the lake generally is ice covered from the end of Nov. and 2–4 months onwards (on average 96 days for the whole data period). However, during the 2003/2004 and 2006/2007 winter seasons, ice freeze did not occur until the end of Jan. /Larsson-McCann et al. 2002/ report that for the period 1957–2000, typically there is an ice coverage in Lake Gnötteln (located inland, c 30 km west of Lake Jämsen) from the beginning of Dec. to the beginning of Apr. (that is, during c 4 months), varying between a minimum period of 10 days and a maximum period of almost 6 months.

Table 2-15. Summary of observed ice freeze/breakup.

Gauging station	Winter period	Period with observed ice
ASM100226 (Baltic Sea; Äspö brygga)	2002–2003	2002-12-19–2003-03-27 (99 d)
	2003–2004	2004-01-07–2004-03-10 (62 d)
	2004–2005	2004-12-22–2005-01-23 (32 d)
		2005-01-28 – 2005-04-01 (63 d)
	2005–2006	2005-12-20 – 2006-04-18 (119 d)
	2006–2007	2007-01-29 – 2007-03-01 (31 d)
ASM100227 (Baltic Sea; Kråkelund yttre)	2002–2007	No ice
ASM100228 (Baltic Sea; Kråkelund inre)	2002–2003	2003-01-10 – 2003-03-21 (71 d)
	2003–2005	No ice
	2005–2006	2006-01-02–2006-01-12 (10 d)
		2006-01-26–2006-02-03 (8 d)
		2006-03-17 – 2006-03-29 (12 d)
	2006–2007	No ice
ASM100229 (Lake Jämsen)	2002–2003	2002-11-19–2002-11-22 (3 d)
		2002-12-19–2003-03-28 (100 d)
	2003–2004	2004-01-07–2004-03-10 (64 d)
	2004–2005	2004-11-22 – 2005-04-01 (129 d)
	2005–2006	2005-11-22 – 2006-04-18 (147 d)
	2006–2007	2007-01-23 – 2007-03-01 (37 d)

2.3 Hydrological monitoring data

2.3.1 Surface-water levels

In Laxemar, surface-water levels have been monitored in 4 lakes (Jämsen, Plittorpsgöl, Frisksjön and Sörå), and in 3 bays of the Baltic Sea. Water-level data are stored every full hour. Table 2-16 summarises the data periods for the level-gauging stations, and their locations are shown in Figure 2-33.

Table 2-16. Surface-water level gauging stations in lakes and the sea.

Gauging station	Data period
PSM000342 (Lake Jämsen)	2004-07-24–2007-12-31
PSM000344 (Lake Plittorpsgöl)	2004-07-24–2007-12-31
PSM000348 (Lake Frisksjön)	2004-07-24–2007-12-31
PSM000359 (Lake Sörå)	2004-05-27–2007-12-31 (no data 2006-09-04–2006-11-28)
PSM000369 (Baltic Sea; southern Äspö island)	2004-05-27–2007-12-31 (no data 2007-03-04–2007-03-20, 2007-04-07–2007-04-30)
PSM000370 (Baltic Sea; northern Äspö island)	2004-05-27–2007-12-31
PSM000371 (Baltic Sea; southern Simpevarp peninsula)	2004-05-27–2007-12-31

Figure 2-33. *Overview map showing the locations of surface-water level gauges in the Laxemar area.*

Figure 2-34 shows a time-series plot of daily average sea-water levels (metres above sea level) measured at the gauging stations PSM000369-371. The maximum and minimum daily average sea level during the considered period (May 2004–Dec. 2007) was –0.52 and 0.71 metres above sea level respectively, whereas the average sea-water level was 0.03 metres above sea level (RHB 70). The largest daily sea-level changes occurred on Nov. 1, 2006 (c +0.26 m) and Dec. 22, 2004 (c –0.23 m).

Figure 2-35 shows a time-series plots of daily average lake-water levels in Jämsen, Plittorpsgöl, Frisksjön and Sörå. During the considered period (May/Jul. 2004–Dec. 2007), the lake-water levels were always above sea-water level, including the near-coastal Lake Sörå; this lake was previously a sea bay, and is now used as a reserve-water supply for the Simpevarp power plant.

There is a strong co-variation among the lake-water levels, with maxima during spring and minima during late summer and early autumn. It can also be noted that the lake-water level amplitudes are relatively small: Jämsen 25.36–25.97 (average 25.56), Plittorpsgöl 24.75–25.37 (average 24.99), Frisksjön 1.29–2.19 (average 1.57), and Sörå 1.51–2.05 (average 1.77) metres above sea level. One can also note that the variability pattern of Lake Sörå deviates from the other three lakes, most likely because it is a man-made storage pond, with no surface in- or outlets. In particular, the variability pattern is "smoother" compared to the other lakes, indicating that the more pronounced water-level fluctuations of Jämsen, Plittorpsgöl and Frisksjön are caused by temporally variable stream in- and outflow.

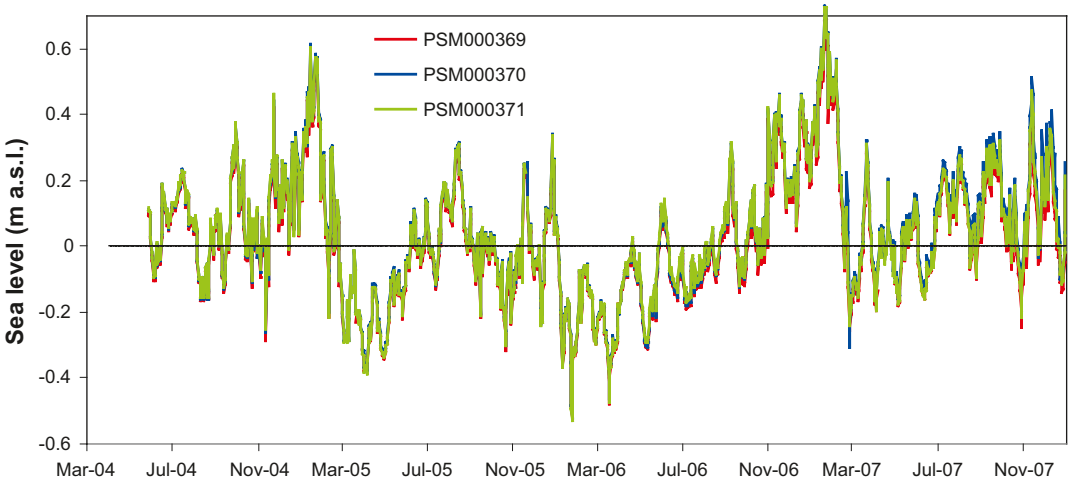

Figure 2-34. *Time-series plot of daily average sea-water levels between May 27, 2004 and Dec. 31, 2007.*

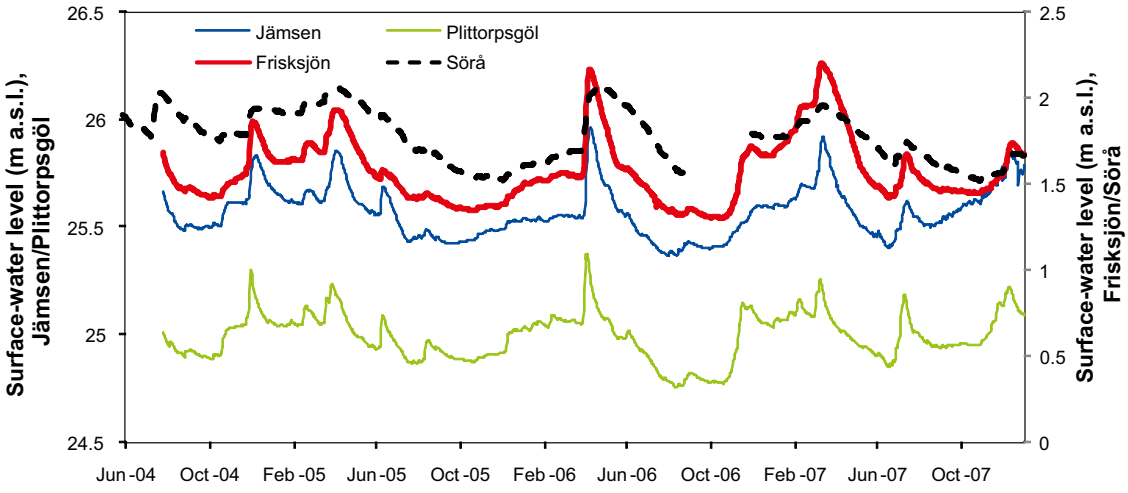

Figure 2-35. *Time-series plot of daily average lake-water levels in Jämsen and Plittorpsgöl (left vertical axis), Frisksjön and Sörå (right vertical axis).*

2.3.2 Surface-water discharge

Overview of discharge gauging stations and data handling

In Laxemar, stream discharge, surface-water temperature and electrical conductivity have been monitored at 9 gauging stations in 7 streams. For each of the 9 gauging stations, Table 2-17 summarises the locations, the size of the catchment areas, and the available data periods. Discharge data are stored every full hour. The locations of the gauging stations and their associated catchment areas are shown in Figure 2-36.

The discharge-data set is a key input to the description of hydrology and near-surface hydrogeology /Werner et al. 2008/. Moreover, discharge data provide an important basis for calibration of the MIKE SHE model /Bosson et al. 2008/. Preliminary data evaluations indicated that there are some uncertainties associated with the discharge data, in particular data from the PSM000348 station (located at the outlet from Lake Frisksjön). This motivated an overview of the discharge-gauging stations, with the purpose of identifying potential sources of uncertainty. In turn, this overview aimed to provide a basis for how the identified uncertainties should be characterised and taken into account in the conceptual and quantitative water-flow modelling.

Except from gauging station PSM000364, located in the stream Laxemarån, the gauging stations are of two types; constructed V-notch weirs and natural critical sections. The V-notch weirs (stations PSM000341, -343, -345, -347, -365) are constructed in concrete (thickness c 0.15 m), with a thinner V-shaped metal plate bolted to the downstream side of the concrete notch. The metal plate protrudes a small distance above the concrete V-notch (see example in Figure 2-37). On the upstream edge of the notch, an L-shaped metal plate is folded over the edge and bolted on the inside of the concrete V-notch. This plate is used for fastening a rubber tarpaulin. Upstream of the weir, there is a small excavated pool where measuring equipment is fastened in vertical pipes. A half-circle shaped net is also fastened to the upstream side of the V-notch, intended for intercepting debris. The underside of the net is open and the edge protrudes a small distance below the point of the V-notch.

Based on the measured water level upstream of the weir and the weir geometry, the discharge Q ($m^3 \cdot s^{-1}$) across the V-notch weirs is calculated according to the well-known discharge formula, $Q = (8/15)\mu(2g)^{½}h^{5/2}\tan(\alpha/2)$ where μ is a discharge coefficient (commonly $0.60 < \mu < 0.65$), g ($m \cdot s^{-2}$) is the coefficient of gravity, h (m) is the water level above the V-notch tip, and α is the angle of the V-notch opening /Lärke et al. 2005b/.

Table 2-17. Surface-water discharge gauging stations in streams.

Gauging station	Location	Catchment area size (km^2) /Sjögren et al. 2007ab/	Data period
PSM000341 (V-notch weir)	Vadvikebäcken, Ävrö	0.29	2004-03-18–2007-12-31
PSM000343 (V-notch weir)	Gloebäcken, Ävrö	0.11	2004-03-18–2007-12-31
PSM000345 (V-notch weir)	Skölkebäcken, Ävrö	0.16	2004-03-18–2007-12-31
PSM000347 (V-notch weir)	Kåreviksån, inlet to Lake Frisksjön	0.91	2004-11-30–2007-12-31
PSM000348 (natural section)	Kåreviksån, outlet from Lake Frisksjön (also measures the lake-water level)	1.88	2004-07-24–2007-12-31
PSM000353 (natural section)	Laxemarån (upstream part)	14.00	2004-09-02–2007-12-31 (no data 2007-12-02–2007-12-31)
PSM000364 (composite rectangular weirs, treated as a natural section)	Laxemarån (downstream part)	40.00	2004-11-24–2007-12-31
PSM000365 (V-notch weir)	Ekerumsån	2.38	2005-02-01–2007-12-31
PSM000368 (natural section)	Kärrviksån	27.00	2004-07-24–2007-12-31 (no data 2007-03-17 –2007-05-14 and 2007-12-09 –2007-12-31)

Figure 2-36. *Overview map of discharge-gauging stations and their associated catchment areas, as determined from the DEM.*

Figure 2-37. *Design of the V-notch gauging stations (station PSM000365 in Ekerumsån is shown in the picture).*

The natural critical sections are PSM000348, -353, and -368. PSM000364 is designed as a composite weir, consisting of two rectangular notches at different heights and with different widths. Based on this design, PSM000364 is considered as a natural critical section. This is because the discharge is calculated in the same manner as for natural sections, using empirical discharge (or rating) curves of the general form $Q = \alpha (w–b)^{\beta}$, where α and β are arbitrary (station-specific) constants, b is a reference level at which Q = 0, and w is the water level. In natural critical sections, seasonal variations in terms of e.g. vegetation growth, clogging by debris and by snow and ice during winter may lead to temporal variations of the section geometry and the flow resistance. This implies that a certain stream discharge may correspond to different water levels during the year, and that natural critical sections may be difficult to use in long-term monitoring programmes.

For the V-notch weirs, there is some deviations from the standard design proposed by /Lärke and Hillgren 2003/. The discharge formula given above is strictly applicable for weirs where (1) the V-shaped weir is thin and (razor) sharp, (2) the approach velocity is negligible (there is a more or less stagnant "pool" of water upstream from the station), (3) the downstream water surface is below the V-notch tip, and (4) the flow across the weir separates from the downstream side of the weir in the form of a nappe.

The gauging-station overview shows that for the present weirs, the blunt-edged V-shaped plate is fastened to the downstream side of a broad-crested concrete structure. Moreover, the second plate that is folded over the upstream edge of the notch, as well as the bolts used for fastening the plate, may protrude into the V-notch and thereby interfere with the flow across the weir. The principles of the different cross-weir flows for a standard design and the current weir design are illustrated in Figure 2-38. The designs of gauging stations PSM000341, -343, -345, and -347 are shown in the photographs in Figures 2-39 to 2-42.

Using analytical and numerical solutions for flow across different types of weirs, one can estimate the possible error introduced by calculating the discharge by the standard discharge formula. The analytical comparisons are made using discharge formulas valid for a rectangular thin plate weir and a rectangular broad-crested weir, simply because there are no analytical discharge formulas available for broad-crested V-shaped weirs. The analytical solutions show that the flow across a rectangular thin-plate weir is $3^{1/2}$ times the flow over a broad-crested weir, assuming that critical flow develops across the broad-crested weir. The (2D) numerical simulations consider a thin plate weir and a weir with a cross section similar to the one used at Laxemar. These results indicate that the deviation from the standard design is on the order of a few percent, and that the deviation is larger for small flows.

At gauging station PSM000348, the critical section is likely located below a large boulder, some metres downstream from the lake outlet (see Figure 2-43). The flow resistance beneath the boulder is likely to vary both on short time scales as well as seasonally. For instance, debris and ice may influence the flow resistance. Furthermore, it can be noted that the water level on the upstream side of the boulder depends on the water level on the downstream side. At gauging station PSM000353 (Figure 2-44), the natural critical section is likely a road culvert.

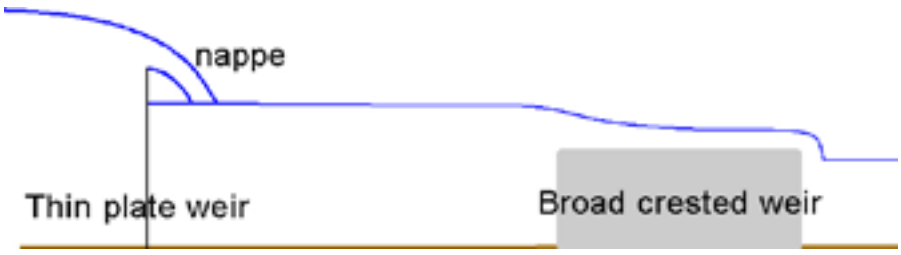

Figure 2-38. *Comparison of the flow across a sharp (left) and a broad-crested weir.*

Figure 2-39. *V-notch weir at gauging station PSM000341. The net has been removed to allow control measurements.*

Figure 2-40. *V-notch weir at gauging station PSM000343.*

Figure 2-41. *V-notch weir at gauging station PSM000345.*

Figure 2-42. *V-notch weir at gauging station PSM000347.*

Figure 2-43. *Probable critical section (below the boulder) downstream from gauging station PSM000348.*

Figure 2-44. *Water-level instrumentation at gauging station PSM000353. The natural critical section is likely a road culvert downstream from this site.*

Gauging station PSM000364 (Figures 2-45 and 2-46) was previously operated by the power company OKG, and is now used by SKB. The station consists of two rectangular notches, of which the lower (downstream) notch appears to be rather recent and not part of the original weir design. At the time of a field visit, the lower rectangular notch was submerged, which probably occurs at most flow situations. Consequently, the discharge across the weir is influenced by some critical section downstream from the gauging station, probably a shallow section a few metres downstream. Therefore, in order to calculate the flow, one would need information also on the water level at the downstream side of the weir. It can be noted that pipes containing measuring equipment may intercept debris and also may affect the cross-weir flow, since they are placed in front of the lower notch.

The V-notch weir at PSM000365 (Figure 2-47) has occasionally been submerged (e.g. during spring 2006), which lead to some uncertainties in the discharge data during such high-discharge events, possibly an order of magnitude higher than the uncertainties related to the weir design discussed above. One potentially useful method to further investigate the occurence of submergence may be to install a pressure sensor also on the downstream side of the V-notch. The discharge station PSM000368 (Figure 2-48) has a rather well-defined critical section. During small-discharge periods, the shallow area downstream of the measuring equipment may influence the cross-weir flow.

Based on the gauging-station overview, it can be concluded that the “error” in the discharge data for the V-notch weirs (PSM000341, -343, -345, -347 and -365) may be on the order of 5%, especially during small-discharge periods. During high-discharge periods, in particular in cases where the weirs are submerged, the discharge-data are associated with larger uncertainty. The discharge data from the natural critical section at PSM000348 are associated with relatively large uncertainty, due to seasonally variable flow resistance and possibly also different critical sections during different flow regimes.

Figure 2-45. *The two rectangular notches at PSM000364. The discharge is calculated in the same manner as for a natural critical section.*

Figure 2-46. *Close-up view of the submerged notch at PSM000364.*

Figure 2-47. *V-notch weir at gauging station PSM000365.*

Figure 2-48. *Water-level instrumentation at gauging station PSM000368.*

Presentation and interpretation of discharge data

Figure 2-49 presents time-series plots of daily average surface-water discharges, whereas the same data are shown in terms of monthly averages in Figure 2-50. In this context, it should be noted that water-level data from stations PSM000348 and PSM000353, and also at the V-notch weir station PSM000365 were adjusted down prior to the delivery to Sicada by c 0.02 m on Jul. 19, 2007. This was done due to an observed mis-match between the manually measured water level and the water level measured by the water-pressure meter. At the same date and for the same reason, the automatically measured water-level data were adjusted up c 0.01 m at the composite-weir station PSM000364. However, one does obviously not know the point in time when the automatic measurements started to deviate. The actual field check was done in May, 2007, whereas the data adjustments were initiated from Jul. 19, 2007.

The plots in Figures 2-49 and 2-50 show that stream discharges in Laxemar are characterised by large temporal variations; long periods with little or no discharge, interrupted by relatively short discharge periods. A more detailed analysis of the discharge data shows that stations PSM000343 and -345 demonstrate similar discharge patterns. Specifically, during the period 2004–2007, there was no discharge from mid-May to mid-Nov. 2004 (interrupted by a discharge period in Jul.), from mid-May to the end of Dec. 2005/beginning of Jan. 2006, from the beginning of Jun. to the beginning of Nov. 2006, and from the end of Apr. to the end of Nov. 2007 (except for a discharge period in Jul.).

At station PSM000347, there was no discharge from the end of Jun. to mid-Dec. 2005, from mid-Jun. to the beginning of Nov. 2006, and from mid-May to mid-Nov. (except for a discharge period in Jul.) 2007. Moreover, at station PSM000365 there was no discharge during parts of the periods Jul.–Oct. 2005, Aug.–Oct. 2006, and Jun. 2007. During the considered periods, there was discharge at all times at gauging stations PSM000341, -348, -353, -364 and -368.

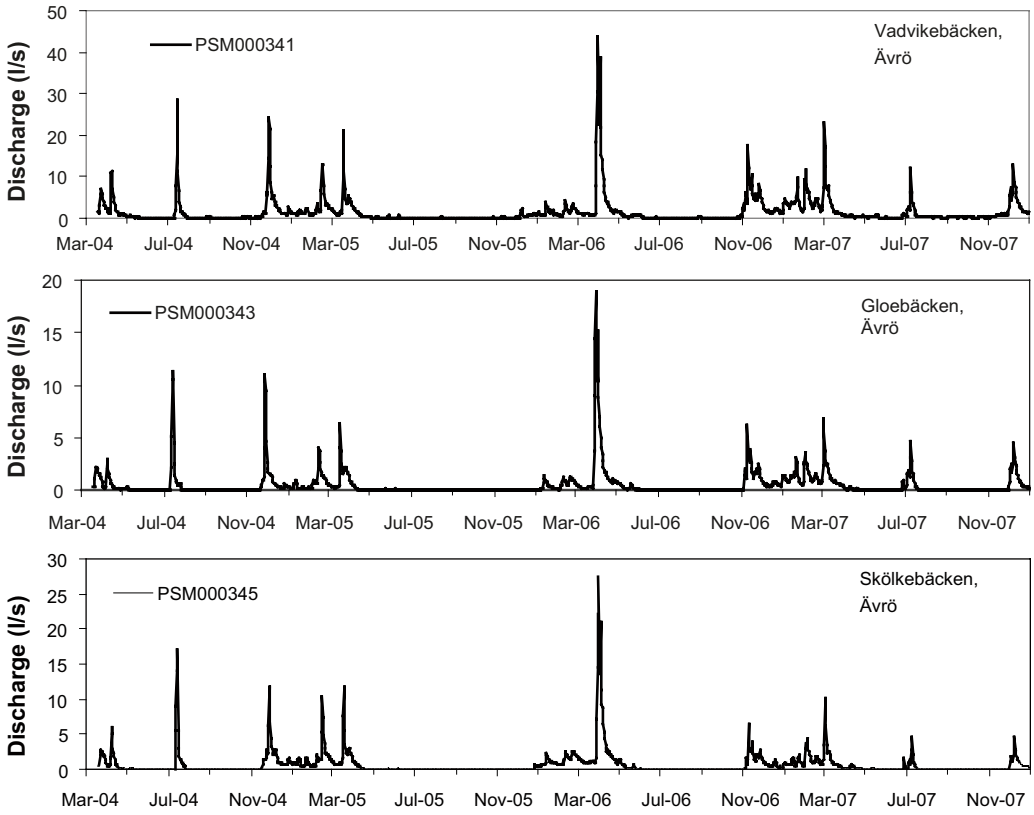

Figure 2-49a. *Time-series plots of daily average surface-water discharges at the discharge-gauging stations PSM000341, -343, and -345.*

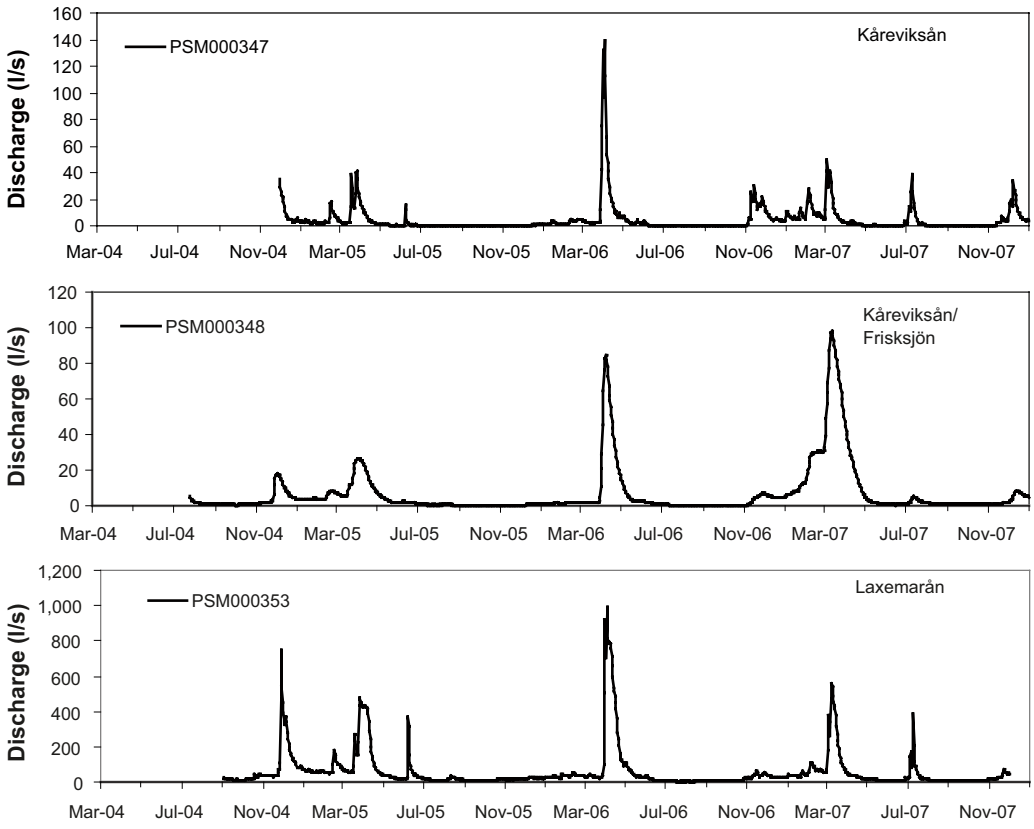

Figure 2-49b. *Time-series plots of daily average surface-water discharges at the discharge-gauging stations PSM000347, -348, and -353.*

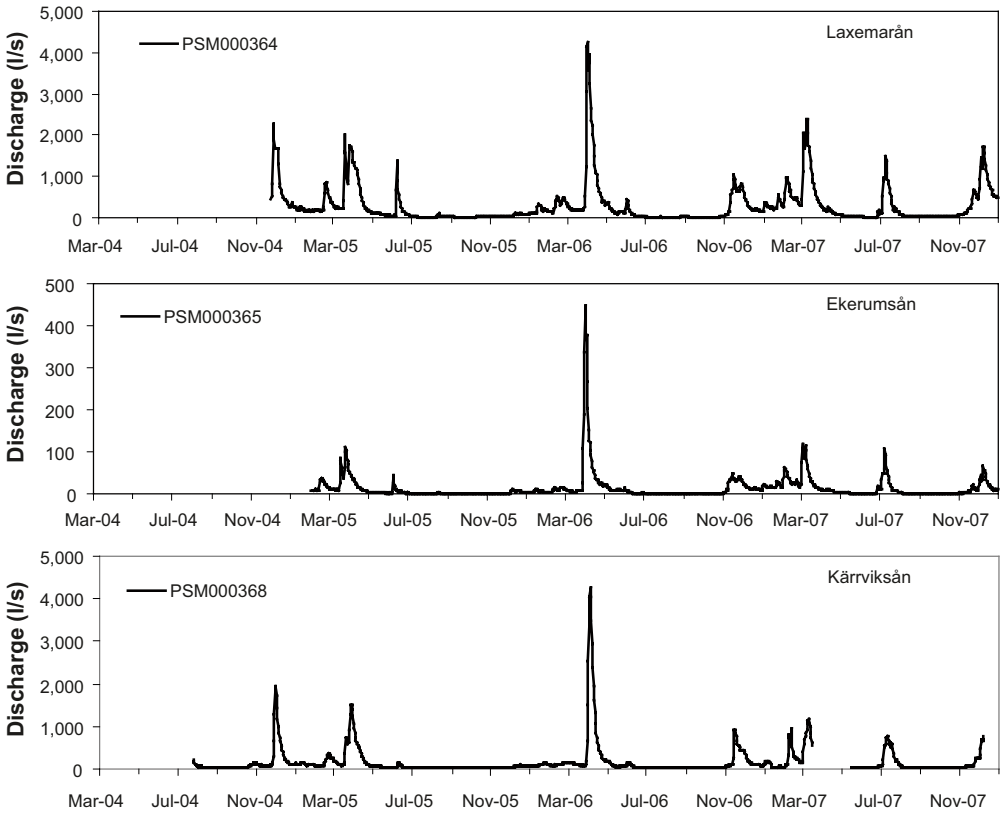

Figure 2-49c. *Time-series plots of daily average surface-water discharges at the discharge-gauging stations PSM000364, -365, and -368.*

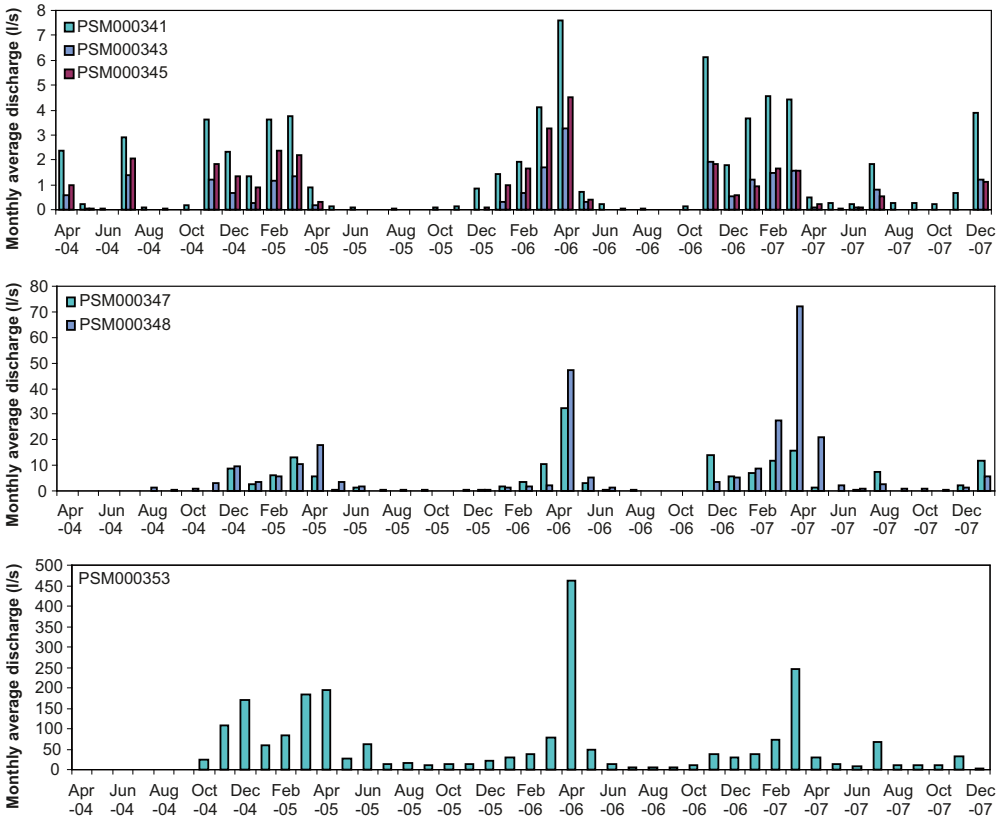

Figure 2-50a. *Time-series plots of monthly average surface-water discharges at discharge-gauging stations PSM000341, -343, -345, -347, -348, and -353.*

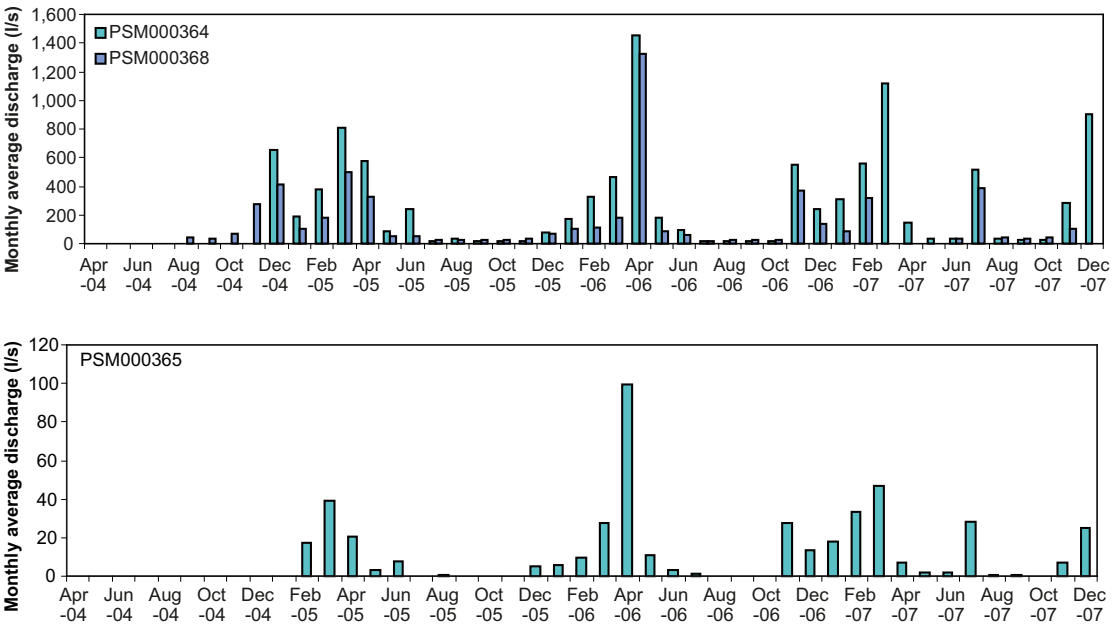

Figure 2-50b. *Time-series plots of monthly average surface-water discharges at discharge-gauging stations PSM000364, -368, and -365.*

To generalise, one may say that there is no discharge during approximately half of the year (from late spring/early summer (c. May–Jun.) up to late autumn/early winter (c. Nov.–Dec.) in most of the smaller streams in Laxemar, except from gauging station PSM000341 in the stream Vadvikebäcken. The underlying processes causing this large temporal variability and its implications for the conceptual water flow modelling are discussed further in chapters 3 and 5, based on joint interpretations of discharge data and other data sets.

Table 2-18 summarises the discharge data in terms of minimum, maximum and average discharges, for all 9 gauging stations and for the whole available data periods (see Table 2-17). In order to illustrate inter-annual variations, Table 2-19 shows the corresponding statistics for each of the years 2005–2007. As can be seen from Table 2-18 (cf. discussion above), the minimum discharge is zero at the stations installed in the smallest streams (PSM343 and -345) and at stations PSM000347 and -365. Moreover, the minimum discharge is very small at stations PSM000341 and -348. In comparison, the minimum discharge is larger in the larger streams (stations PSM000353, -364 and -368). Moreover, the maximum (and also average) discharges are largest at stations PSM000364 and -368, and also relatively large at stations PSM000353 and -365. From the data in Tables 2-18, one can conclude that the streams with small or zero minimum discharges are also associated with the smallest maximum discharges.

The inter-annual comparisons in Table 2-19 indicate that in a relative sense, variations are larger for the smaller streams compared to the larger streams, i.e. the streams with the largest maximum and average discharges. For instance, for station PSM000364, the largest and smallest annual average discharges are c 333 and 203 $L \cdot s^{-1}$, respectively, whereas the same data for station PSM000368 are c 173 and 117 $L \cdot s^{-1}$. These variability ranges correspond to c 34% and 44%, respectively, of the overall averages presented in Table 2-18. The variability ranges for stations PSM000341, -343, -345, -347 and -348 correspond to between c 73% (PSM000341) and 124% (PSM000348) of the overall averages.

Normalising the discharge ($L \cdot s^{-1}$) with the size of the catchment area (km^2) yields the so-called specific discharge, which commonly is used to facilitate comparisons of hydrological characteristics between catchment areas. Tables 2-20 to 2-22 present two alternative calculations of the specific discharge; for the whole available data periods (Table 2-20) and annual data for the years 2005-2007 (Tables 2-21 and 2-22). Further, Tables 2-20 and 2-21 are based on the average

Table 2-18. Minimum, maximum and average discharges ($L \cdot s^{-1}$) at the gauging stations for the whole available data periods. At station PSM000365, measurements started on Feb. 1, 2005. Numbers within brackets () denote the fraction of the average.

Gauging station	Min	Max	Average
PSM000341	0.0005 (0.03%)	43.9	1.5
PSM000343	0	18.9	0.5
PSM000345	0	27.4	0.7
PSM000347	0	139.6	4.6
PSM000348	0.08 (1.2%)	98.0	6.6
PSM000353	4.0 (6.7%)	988.1	59.4
PSM000364	9.6 (3.3%)	4,261.4	293.4
PSM000365	0	449.3	13.2
PSM000368	20.1 (12.2%)	4,260.4	164.0
All stations			60.4

Table 2-19. Annual minimum, maximum and average discharge ($L \cdot s^{-1}$) at the gauging stations for the individual years 2005–2007. At station PSM000365, measurements started on Feb. 1, 2005.

Gauging station	2005			2006			2007		
	Min	Max	Av.	Min	Max	Av.	Min	Max	Av.
PSM000341	$5 \cdot 10^{-4}$	21	0.9	$1 \cdot 10^{-3}$	44	2	$2 \cdot 10^{-2}$	23	2
PSM000343	0	6	0.2	0	19	0.7	0	7	0.5
PSM000345	0	12	0.5	0	27	1.1	0	10	0.5
PSM000347	0	41	2.5	0	140	5.9	0	49	4.8
PSM000348	0.2	27	3.8	$8 \cdot 10^{-2}$	84	5.7	0.4	98	12.0
PSM000353	9	475	57.8	4	988	63.2	5	563	49.2
PSM000364	13	2,024	202.8	10	4,261	293.3	11	2,404	332.9
PSM000365				0	449	16.5	0	119	14.1
PSM000368	21	1,522	117.3	20	4,260	204.1	22	1,166	172.9

Table 2-20. Average specific discharge for the whole available data periods, based on the average discharge ($L \cdot s^{-1}$), cf. Table 2-18. At station PSM000365, measurements started on Feb. 1, 2005. Values within brackets denote the average specific discharge excluding data from station PSM000348.

Gauging station	$L \cdot s^{-1} \cdot km^{-2}$	$mm \cdot y^{-1}$
PSM000341	5.2	164
PSM000343	4.5	142
PSM000345	4.4	139
PSM000347	5.0	158
PSM000348	3.5	111
PSM000353	4.2	134
PSM000364	7.3	231
PSM000365	5.5	175
PSM000368	6.1	192
All stations (excl. PSM000348)	5.1 (5.3)	161 (167)

Table 2-21. Specific discharge (mm·y^{-1}), based on the annual average discharge (L·s^{-1}), cf. Table 2-18. Values within brackets denote the average specific discharge excluding data from station PSM000348.

Gauging station	2005	2006	2007	2005–2007
PSM000341	97	216	187	167
PSM000343	70	207	153	143
PSM000345	95	215	101	137
PSM000347	85	204	168	153
PSM000348	63	95	201	120
PSM000353	130	142	111	128
PSM000364	160	231	262	218
PSM000365		218	187	203
PSM000368	137	238	202	192
All stations (excl. PSM000348)	105 (111)	196 (209)	175 (171)	162 (168)

Table 2-22. Specific discharge (mm·y^{-1}), based on annually accumulated values of daily specific discharge (mm·d^{-1}); cf. Table 2-21. Values within brackets denote the average specific discharge excluding data from station PSM000348.

Gauging station	2005	2006	2007	2005–2007
PSM000341	97	216	187	167
PSM000343	70	208	153	143
PSM000345	95	215	101	137
PSM000347	86	204	168	153
PSM000348	63	95	201	120
PSM000353	130	142	102	125
PSM000364	160	231	262	218
PSM000365		219	187	203
PSM000368	137	238	157	177
All stations (excl. PSM000348)	105 (111)	196 (209)	169 (165)	160 (165)

discharge (cf. Table 2-18), whereas Table 2-22 is based on annually accumulated values of daily specific discharges (given in terms of the units mm·d^{-1}). It can be seen that for most stations, there are small differences in the results using the annual average discharge (Table 2-21) or annually accumulated values of daily specific discharge (Table 2-22).

In this context, it should again be observed that some discharge-gauging stations (e.g. PSM000348 and -353) are natural sections (i.e. they are not constructed as V-notch weirs). For these stations, it may be difficult to establish correct rating curves (cf. above). Moreover, measurements at station PSM000365 started in Feb. 2005, which implies that the stream-flow data for this station do not include the autumn/winter 2004-2005. PSM000364 has the largest catchment area (40 km^2), and it can be speculated that this station may provide the most "site representative" specific-discharge data. As can be seen from the Tables 2-20 to 2-22, station PSM000348 yields exceptionally low specific discharges.

As indicated above, due to the possibly lower quality of the discharge data from station PSM000348, "site-average" specific discharges are in Tables 2-20 to 2-22 presented both with and without (within brackets) the PSM000348 data. The information on specific discharges in Laxemar is somewhat compressed in Figures 2-51 and 2-52. Figure 2-51 presents a "typical" seasonal cycle of the specific discharge at the 9 gauging stations. These data curves are calculated from daily average discharges, considering "same-day" daily average discharges.

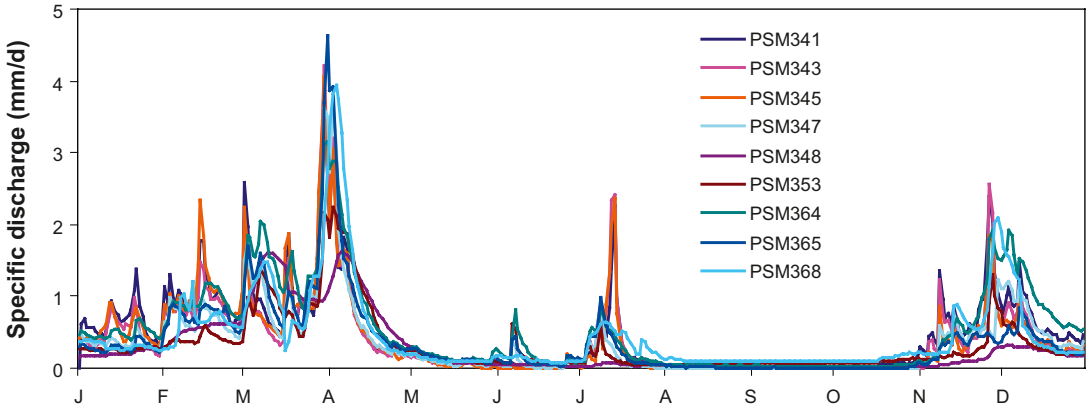

Figure 2-51. *Time-series plot of "daily average" specific discharges, calculated from "same-day" daily average discharges (cf. Figure 2-49) and the size of the catchment area for each discharge-gauging station (cf. Table 2-17).*

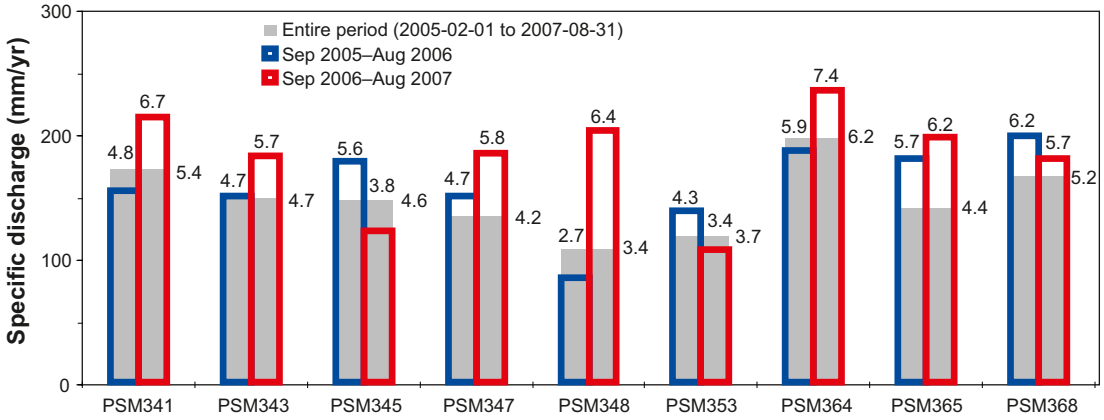

Figure 2-52. *Bar plot of the specific discharge during three different time periods. The specific discharge is expressed both in mm·y–1 (see the scale on the y-axis) and L·s–1·km–2 (the data above the bars).*

Moreover, the bar plots in Figure 2-52 complement the information in Tables 2-20 to 2-22; this figure visualises the average specific discharge during three different time periods, including two so-called "hydrological years" (here taken to be Sep. 1–Aug. 31).

Table 2-20 shows that for the whole available data period (excluding the PSM000348 data; see discussion above), the average specific discharge calculated for different gauging stations varies between c 134 (PSM000353) and 231 mm·y^{-1} (PSM000364). According to Tables 2-21 and 2-22, there are rather large inter-annual variations of the specific discharge (cf. Table 2-19), and as already mentioned also during individual years (Figure 2-51). During the period 2005–2007, the "site average" specific discharge (i.e. the average of all stations) varies between c 111 and 209 mm·y^{-1} (excluding PSM000348). Overall, Tables 2-20 to 2-22 and Figure 2-52 show that the site-average specific discharge for the considered period can be estimated to be on the order of 160–170 mm·y^{-1}, which is in accordance with the "regional" long-term (1961–1990) average of 150–180 mm·y^{-1} estimated by /Larsson-McCann et al. 2002/.

The specific discharges calculated for the gauging stations in Laxemar can be compared to the long-term discharge measurements (1955–) performed at the SMHI discharge-gauging station 1619 Forshultesjön, located some 35 km southwest of the Laxemar area. The station has a catchment area size of 103.2 km^2, with a lake area of 4.8%. /Larsson-McCann et al. 2002/ present pre-site investigation data from this gauging station (1955–2000), which here are extended with data from 2001 up to Aug. 31, 2007.

Table 2-23 presents some basic discharge statistics (see explanations below) for the 1955–2000 period /Larsson McCann et al. 2002/, whereas Table 2-24 takes into account the extended data set up, i.e. up to Aug. 31, 2007 (divided into the full-year period 1955–2006, and the part-year period 1955–Aug. 31, 2007). In these tables, MLQ denotes the average of the annual minimum discharge, MQ denotes the average discharge, and MHQ denotes the average of the annual maximum discharge. In Table 2-23, HHQ50 and HHQ100 denote the highest maximum discharge with a return period of 50 and 100 years, respectively. The statistics in Tables 2-25 and 2-26 are expressed in terms of specific discharge. Table 2-25 shows annual average specific discharges for the years 2005, 2006 and up to Aug. 31, 2007, calculated based on annual average discharges; see Table 2-26. Moreover, Figure 2-53 shows a bar plot of the annual average specific discharge at the Forshultesjön station for the period 1955–Aug. 31, 2007.

The long-term discharge data from the Forshultesjön station clearly demonstrate the large inter-year variability; according to Table 2-24, the coefficient of variation (CV = standard deviation/average) of the specific discharge is on the order of 0.4 (71/185). As shown in Figure 2-53, the annual average specific discharge during 1955–Aug. 31, 2007 varies between c 1.84 $L \cdot s^{-1} \cdot km^{-2}$ (or 58 $mm \cdot y^{-1}$) during 1989 and 12.60 $L \cdot s^{-1} \cdot km^{-2}$ (or 397 $mm \cdot y^{-1}$) during 1960. As can be seen in Tables 2-23 and 2-24, the long-term average specific discharge at Forshultesjön is slightly higher than that calculated for Laxemar for the years 2005–2007 (cf. Tables 2-20 and 2-21), in particular when the additional 2001–Aug. 31, 2007 data are taken into account (Tables 2-24 and 2-25). However, this result is in accordance with the observation of a west-east precipitation gradient, with more precipitation further inland (cf. section 2.2.1).

Table 2-23. Specific-discharge statistics for the SMHI gauging station 1619 Forshultesjön (1955–2000) /Larsson-McCann et al. 2002/.

Unit	Obs. minimum	MLQ	MQ	MHQ	HHQ50	HHQ100
$L \cdot s^{-1} \cdot km^{-2}$	0	0.58	5.72	26.4	59.2	66.1
$mm \cdot y^{-1}$	0	18.3	180.3	831.8	1,867.7	2,085.3

Table 2-24. Specific-discharge statistics for the SMHI gauging station 1619 Forshultesjön (1955–2006 and 1955–Aug. 31, 2007).

Unit	Period	MLQ	MQ (st. dev.)	MHQ
$L \cdot s^{-1} \cdot km^{-2}$	1955–2006	0.61	5.88 (2.27)	27.75
$mm \cdot y^{-1}$		19	185 (71)	875
$L \cdot s^{-1} \cdot km^{-2}$	1955–Aug. 31, 2007	0.61	5.90 (2.25)	27.7
$mm \cdot y^{-1}$		19	186 (71)	874

Table 2-25. Average specific discharge at the gauging station 1619 Forshultesjön, based on annual average discharge ($L \cdot s^{-1}$) data; cf. Table 2-24.

Unit	2005	2006	Jan. 1– Aug. 31, 2007	2005–Aug. 31, 2007
$L \cdot s^{-1} \cdot km^{-2}$	5.34	5.64	7.25	6.07
$mm \cdot y^{-1}$	168	178	229	192

Table 2-26. Annual minimum, maximum and average discharge ($L \cdot s^{-1}$) at the gauging station 1619 Forshultesjön.

2005			2006			Jan. 1–Aug. 31, 2007		
Min	Max	Av.	Min	Max	Av.	Min	Max	Av.
67	2,830	551	42	5,370	582	54	2,720	749

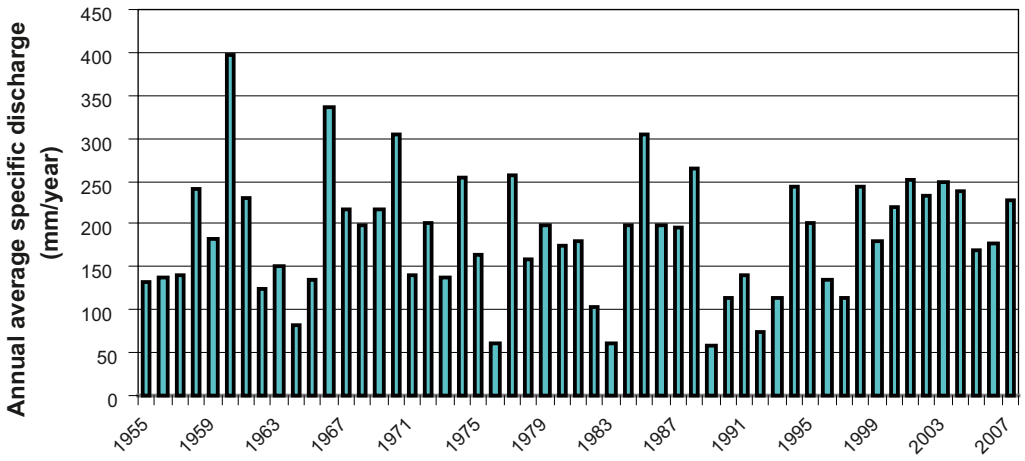

Figure 2-53. *Bar plot of the annual average specific discharge 1955–Aug. 31, 2007 for the SMHI gauging station 1619 Forshultesjön.*

2.4 Hydrogeological monitoring data

2.4.1 Data screening

The site investigation in Laxemar-Simpevarp has included a large number of activities that may disturb local hydrogeological conditions. In particular, drilling, pumping and other types of hydraulic tests in wells and boreholes may cause groundwater levels in QD and/or point-water heads in rock to deviate from natural (undisturbed) conditions, also in surrounding wells and boreholes. As "disturbed" data could affect the data interpretation, a pre-processing step was performed to identify potentially disturbing activities and to exclude the associated monitoring data periods. The objective of this exercise was hence to obtain a "screened" data set, providing an improved representation of undisturbed conditions compared to the unscreened data. The site investigation activities relevant to consider for this data screening according to /Ask et al. 2007b/ are summarised in the following sections. Note that the appendix numbers below refer to those of the Ask et al. report.

Core drilling

- Extraction and release of flush water during core drilling. Except for core borehole KSH02, the flush water was released to the Baltic Sea during core drilling on the Simpevarp peninsula and on the island of Ävrö (Ask et al. App. 3). In Laxemar, flush water was released on the ground, either close to or far from the core borehole. Relatively small flush-water volumes were used when drilling short core boreholes (so-called "MDZ boreholes"), which have no telescopic sections (Ask et al. App. 5.)
- Air-lift pumping of telescopic sections. The resulting flush water was usually released directly on the ground (Ask et al. App. 2).
- Nitrogen-gas flushing (so-called "air-lifting" with nitrogen gas) of core boreholes, performed after the borehole was completed. The resulting flush water was usually released directly on the ground (Ask et al. App. 7). Minor nitrogen-gas flushing was also made prior to overcoring-method rock stress measurements. The latter type of nitrogen-gas flushing is not considered as an important disturbance by /Ask et al. 2007b/.

Percussion drilling

Percussion drilling included activities such as air-lift pumping and water release, usually directly on the ground (Ask et al. App. 1).

Water-supply wells

A number of percussion boreholes were used to supply flush water during core drilling (Ask et al. App. 6). In addition, percussion borehole HLX22 is used as a (temporary) water-supply well for 14 households in the village Lilla Laxemar, with an extraction rate of approximately 3.3 $m^3 \cdot d^{-1}$ since Jan. 1, 2007. This well will be replaced by water supply from Lake Götemar if Laxemar is chosen as site for the geological repository.

Complete chemical characterisation

Water originating from rinse pumping between sampling events was released on the ground, whereas water pumped up during sampling was discharged into containers and thereafter released to the Baltic Sea (Ask et al. App. 9).

Groundwater monitoring wells

Groundwater monitoring wells were installed using air-blast drilling methods (NO-X 90 or similar), combined with auger drilling for soil sampling. Drilling with air-blast methods yields a local drawdown of the groundwater level. Air-blasting is not recorded as a separate activity in /Ask et al. 2007b/.

In so-called environmental monitoring wells, monitoring has included chemical sampling approximately every week or every two weeks. However, this sampling has not been recorded as a separate activity in /Ask et al. 2007b/.

Hydraulic borehole tests

- Wireline tests, performed during drilling. These tests are not recorded as separate activities in /Ask et al. 2007b).
- Injection tests, primarily made in core boreholes. These tests are not recorded as separate activities in /Ask et al. 2007b/.
- Pumping tests using a submersible pump, either performed as single-hole or interference (multiple-well) tests.
- PFL (single-hole) pumping tests, using a submersible pump.

The starting point for the actual data screening was data on daily average groundwater levels from groundwater monitoring wells and point-water heads from core and percussion boreholes on the islands of Ävrö and Hålö, the Simpevarp peninsula and in Laxemar. It should be noted that for the groundwater monitoring wells and the percussion boreholes, screening was only performed for data up to the L2.3 data freeze (Aug. 31, 2007). Data for the period Sep. 1–Dec. 31, 2007 were hence kept intact, but the risk of potential disturbances is assumed to be small subsequent to the data freeze. However, all core borehole data were screened for the period Sep. 1–Dec. 31, 2007.

The methodology for the data screening was to select all significant single-hole activities (in this context, the term (bore)hole refers both to groundwater monitoring wells installed in QD and boreholes in the rock), as well as activities that potentially could cause hydraulic disturbances in surrounding boreholes. Most of the activities considered relevant for the screening are available in the Sicada database in the form of coded activities with start- and stop dates. This information was obviously very useful for the data screening. All activities and associated data periods involving drilling, flush-water usage, water-release points, complete chemical characterisation and pumping tests were taken from the summary report by /Ask et al. 2007b/. A majority of the activities identified for the data screening were “embedded” in drilling periods and could therefore be disregarded immediately. It should be noted that the regular monitoring of groundwater levels and point-water heads (HMS, Hydro Monitoring System) usually started after completion of drilling, whereas monitoring data during drilling are stored separately in DMS (Drilling Monitoring System). A complete list of the totally 45 activity types used in the screening is shown in Table 2-27.

Table 2-27. Activity types considered in the data screening.

Activity type	Reference/Sicada activity code
Water release from percussion drilling	/Ask et al. 2007b/
Water release from percussion drilling of telescopic section	/Ask et al. 2007b/
Water release from deep core drilling	/Ask et al. 2007b/
Water release from short cored boreholes DFN and MDZ	/Ask et al. 2007b/
Water consumption from supply wells	/Ask et al. 2007b/
Water release point from drilling water	/Ask et al. 2007b/
Water release point from pumping tests	/Ask et al. 2007b/
Complete chemical characterisation	/Ask et al. 2007b/
Instrumentation, section installation	EG004
Pumping, stop	EG016
Pumping, start	EG017
Nitrogen lifting	EG036
Packer expansion	EG042
Packer release	EG043
Air lifting	EG044
Core drilling	EG050
Percussion drilling	EG051
Flush water in	EG081
Flush water source borehole	EG081
Flush water out	EG082
Flush water recipient borehole	EG084
Instrumentation, packer installation	EG505
BIPS-Logging in borehole	GE046
Recovery test	HY050
HMS Pumping flow rate from borehole	HY089
Test and rinse pumping	HY190
Radially converging test hole	HY230
Pumping test_wire line eq.	HY600
PLU Pumping test-Submers. pump	HY610
PLU Interference test-CRwr	HY641
Interference test-obs.holes	HY645
PFL Interference test anomaly obs	HY646
PFL Interference test section obs	HY647
Injection test	HY660
PLU Pulse test	HY665
PLU Slug test	HY670
Flowlogging-PFL-DIFF_sequential	HY680
PFL DIFF SPR and Caliper logging	HY681
PFL DIFF-EC Temp and Pressure measurements	HY683
PFL DIFF Fracture EC Measurements	HY684
Flowlogging-PFL-DIFF_overlapping	HY685
Water sampling, class 1	WC060
Water sampling, class 3	WC080
Water sampling, class 5	WC100
Hydrochemical water sampling series	WC120

Subsequent to identification of the recorded activities (either from Sicada or /Ask et al. 2007b/), there was a manual step involving analyses of time-series plots and even single (daily) data values. This manual screening took into account all single-hole activities, and also activities that potentially could yield interference effects, i.e. disturbances in surrounding boreholes. The latter analysis was done by analysing all boreholes located within a specified radius (initially set to 1 km) from half the borehole depth for each borehole. It was soon found that this radius was set too large, resulting in a vast amount of boreholes to include in each interference analysis. The analysis was therefore finalised manually, taking into account the locations of both major and minor fracture zones, as well as topography, geological aspects and the locations of streams, water divides and the sea.

In some cases, however, the initially set radius of 1 km was useful for identifying potential interference effects. For some interferences, the 1-km limit hid some disturbing activities, overlapping in time with the specific activity being analysed. Groundwater monitoring wells and boreholes in rock were also cross checked. Groundwater levels were compared with data from nearby boreholes, together with data on precipitation and in some cases also the sea-water level. In addition, the locations of flush-water release were considered in the screening. For post-pumping recovery, data were usually screened up to one week after pump stop.

The screening showed that the activities that resulted in the largest disturbances were core drilling, water sampling, pumping tests, and pumping from water-supply wells. In comparison, percussion drilling and flush-water release did not seem to cause any large disturbances for surrounding boreholes. Short-term activities only produced responses in the actual borehole; examples of such activities include rinse pumping, nitrogen- and air lifting, water sampling, pulse tests, BIPS logging, packer expansion and -release.

In multi-section boreholes, there were usually responses only in sections that were connected hydraulically. Between-borehole interferences were identified in two separate areas: In the central and south-western parts of Laxemar, there are some major and minor fracture zones, which in the data screening appear to be connected hydraulically. Such connections were even identified in boreholes close to boreholes subject to complete chemical characterisation. In cases where only short time series are available, it is obviously more difficult to analyse potential interference effects. In general, groundwater monitoring wells seem to be relatively unaffected by activities in surrounding boreholes. At the same time, interference effects are difficult to identify, since groundwater levels in the QD fluctuate in response to short-term meteorological processes such as precipitation events. In some cases, groundwater-level data were screened due to technical problems with the monitoring equipment.

It should be noted that there are some remaining unresolved issues, especially concerning some of the boreholes on the island of Ävrö and on the Simpevarp peninsula. Point-water head variations that could not be explained by any disturbing activity or other factors were (subjectively) screened. Potential explanations to the deviating point-water head variations could be equipment errors, hydrogeological influence due to the Äspö Hard Rock Laboratory or water handling within the industrial area around the Simpevarp nuclear power plant. However, analyses of potential disturbances due to activities outside of the site investigations were outside the scope of the present study.

In total, 4,947 separate activities were identified for the groundwater monitoring wells, whereas for percussion and core boreholes 4,396 single-hole disturbances and 14,539 interference disturbances were identified. The resulting screened data periods for groundwater monitoring wells and rock boreholes are shown in sections 2.4.2 and 2.4.3 below.

2.4.2 Groundwater levels in QD

During the period 2002–2007, totally 92 groundwater monitoring wells have been installed as part of the site investigations in Laxemar-Simpevarp (see Figure 2-54), of which data are available from totally 76 wells. In Sicada, simultaneous groundwater-level data are available from a maximum of 68 wells (Jan.–Mar. 2007). 62 wells were monitored at Aug. 31, 2007, and

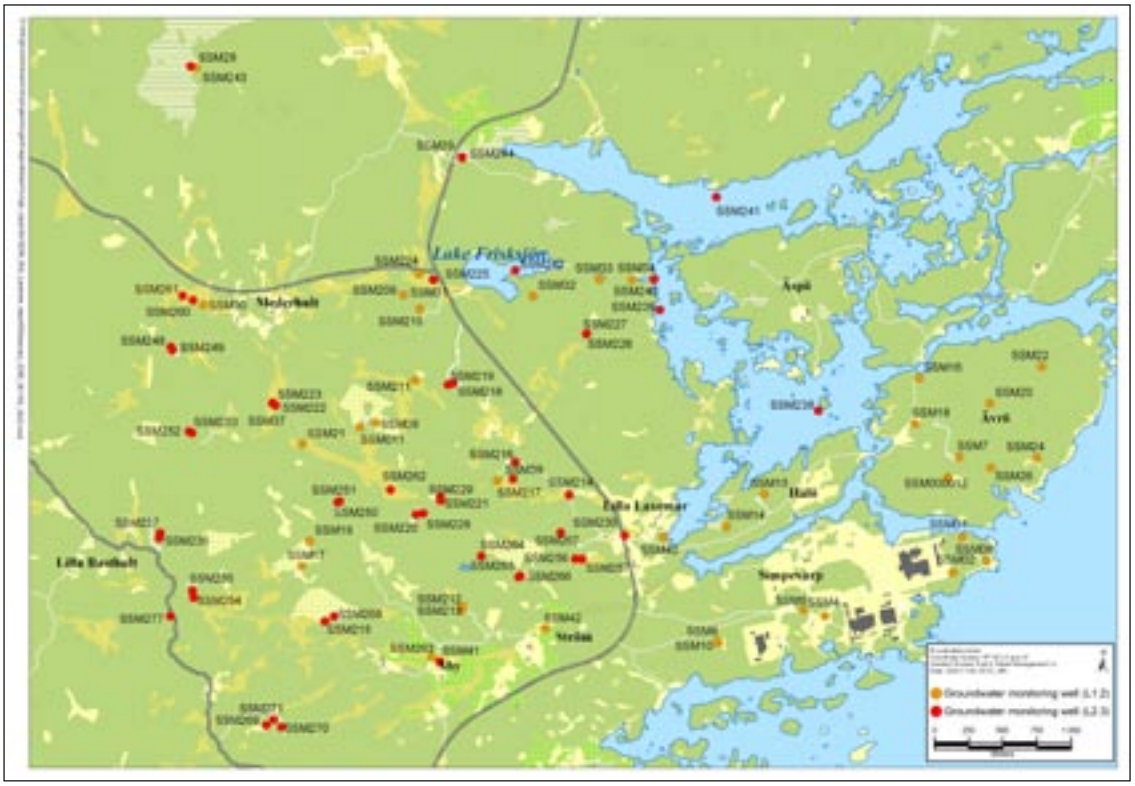

Figure 2-54a. *Overview map showing the locations of 91 of the totally 92 groundwater monitoring wells installed in Laxemar during the period 2002–2007 (see also Figure 2-54b). The colour of the well symbols indicates wells installed up to DF L1.2 (orange) and up to DF L2.3 (red).*

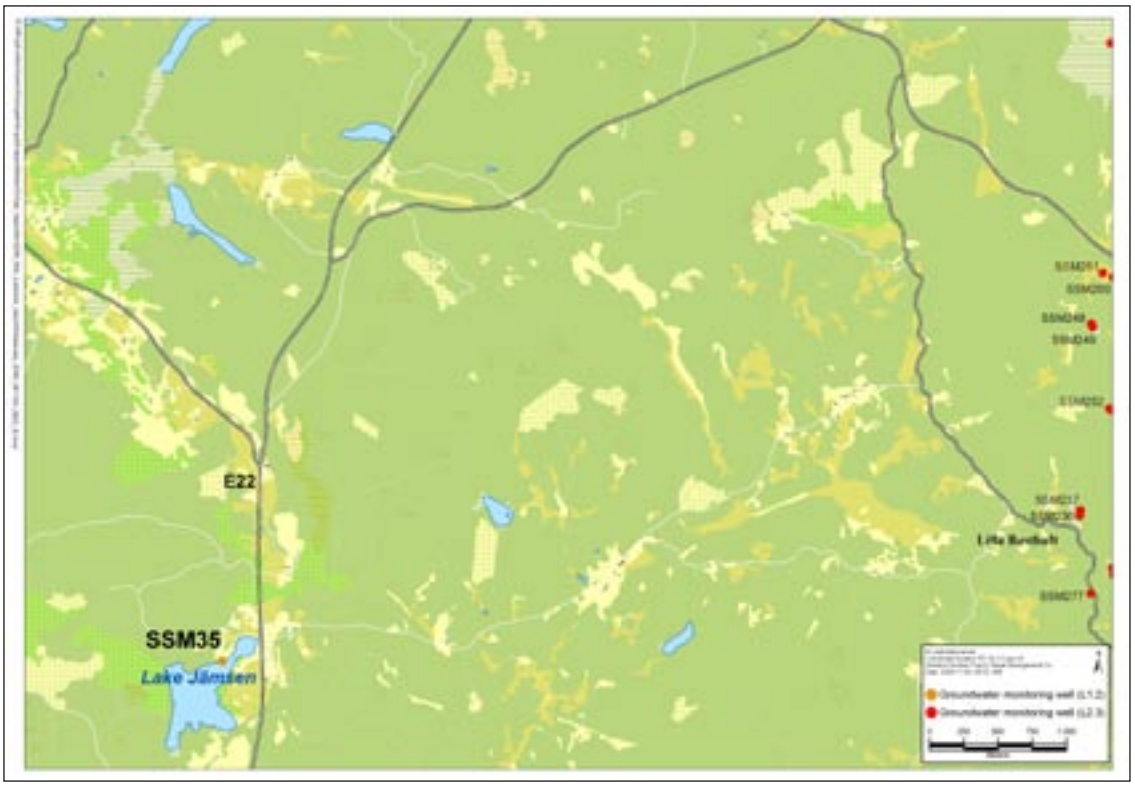

Figure 2-54b. *Overview map showing the location of groundwater monitoring well SSM000035. This well is installed at the shore of Lake Jämsen, west of the area shown in Figure 2-54a.*

45 wells at Dec. 31, 2007. The available data periods are illustrated in Figure 2-55, which also for each well shows data days that were removed as a result of the data screening (see section 2.4.1). On average 11 data days per well were removed in the data screening. No data days were removed for 29 wells, and the maximum number of removed data days was 127 (SSM000255). It should again be noted that no detailed screening was performed for the post data-freeze period (i.e. after Aug. 31, 2007). This implies that data for the period Sep. 1–Dec. 31, 2007 are kept intact, since the risk of potential disturbances is assumed to be small after the data freeze.

As can be seen in Figure 2-55, for many wells the data periods are interrupted by periods with missing data. In most cases, this is due to instrument problems as exemplified below (Lars Andersson, SKB, pers. comm. 2007):

- SSM000014: Data are missing Jun. 3–Sep. 12, 2007 due to data logger malfunction. The logger was replaced twice during this period.
- SSM000022: Data are missing from Jun. 4, 2007 due to that the data logger stores erroneous data. The logger has been replaced twice, and the latest replacement was done on Oct. 3, 2007, i.e. after data freeze Laxemar 2.3.
- SSM00041: Data are missing from Aug. 2, 2007 due to low battery level. The logger stopped Aug. 28, 2007.
- SSM000241: Data are missing from Nov. 27, 2006 due to erroneous groundwater-level measurements. The difference between the automatic and manual groundwater level data was on the order of 1 m. Well SSM000241 is installed at the bottom of a sea bay (Granholmsfjärden), and the manual groundwater-level readings are done in a PEM hose at the shore. The hose was replaced on Jun. 20, 2007, after which the difference between the manual and automatic readings is reduced but still not acceptable.
- SSM000269: Data are missing from May 7, 2007 due to data logger malfunction. The logger was replaced on Sep. 12, 2007, i.e. after data freeze Laxemar 2.3.

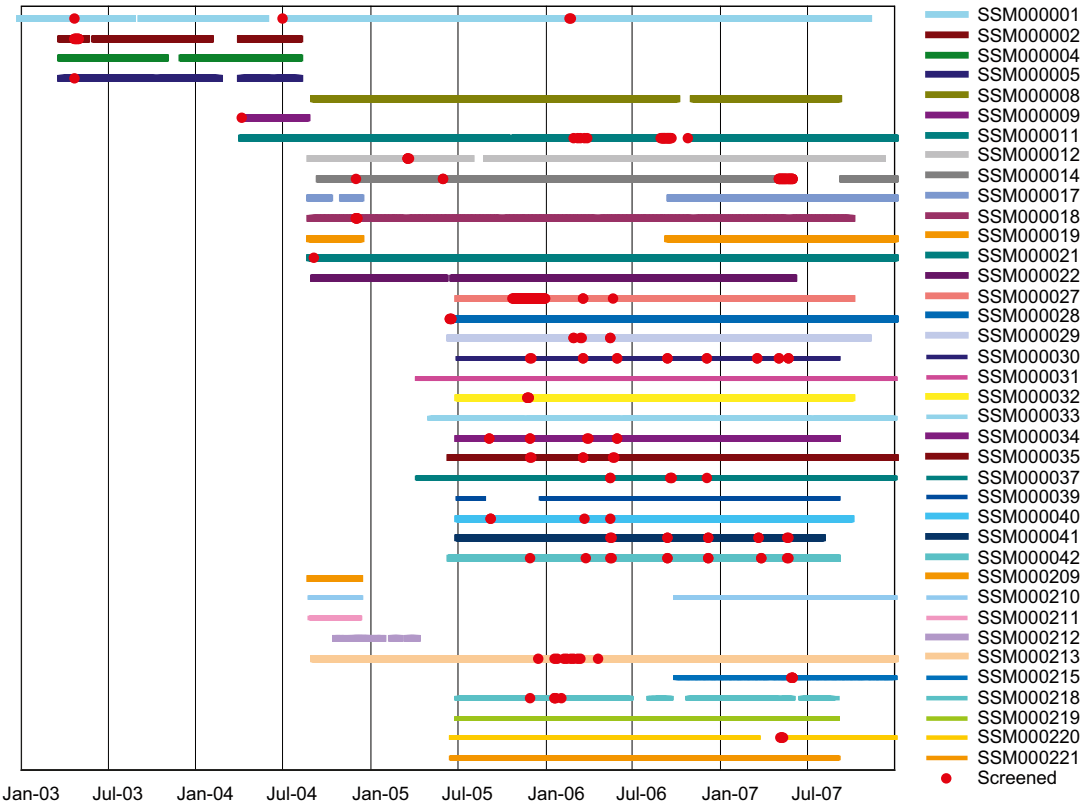

Figure 2-55a. *Overview of available groundwater-level time series from groundwater monitoring wells SSM000001-221. Red dots indicate screened (removed) data days.*

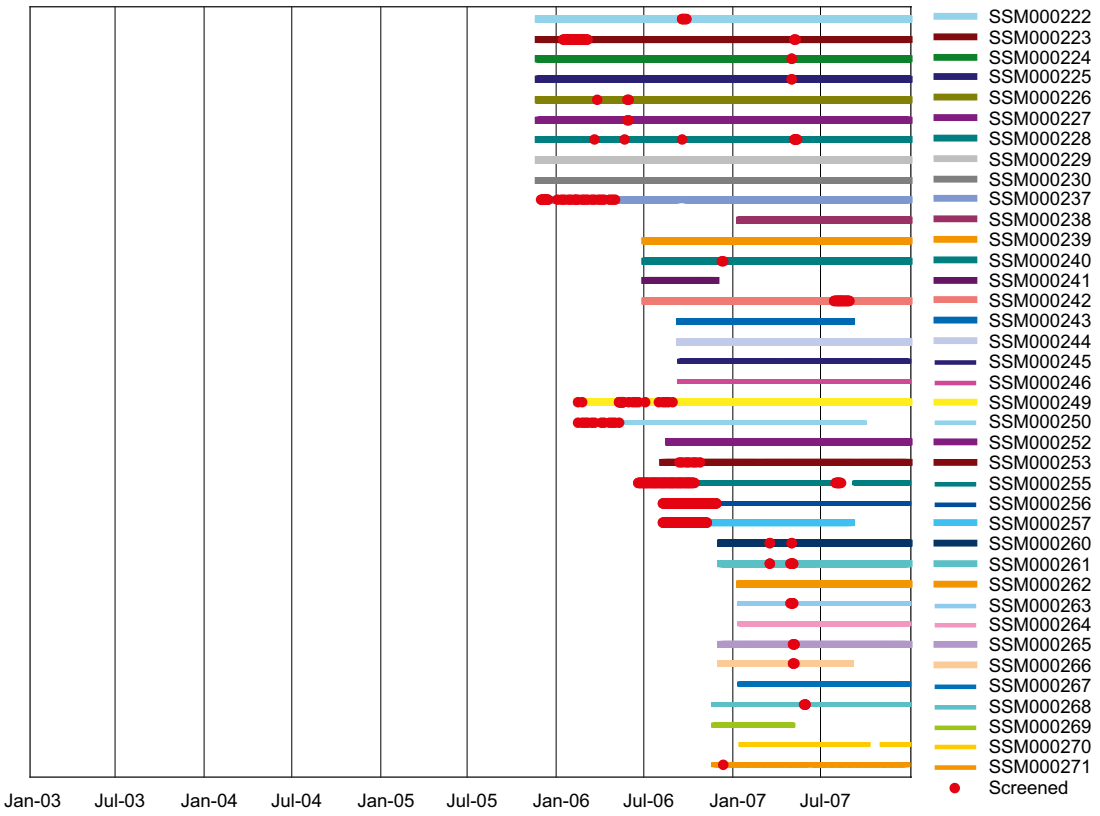

Figure 2-55b. *Overview of available groundwater-level time series from groundwater monitoring wells SSM000222-271. Red dots indicate screened (removed) data days.*

The well- and borehole casings were re-surveyed for a large number of groundwater monitoring wells and percussion- and core boreholes during Apr.–May 2008 (i.e. after data freeze Laxemar 2.3). Some errors were thereby identified, which led to corrections in the Sicada database of groundwater levels and point-water heads for a number of wells and boreholes. The identified errors that led to corrections larger than 0.1 m (i.e. <–0.1 m or > +0.1 m) are summarised below (Sicada Bug Report #3242):

- SSM000001:
  - –0.97 m (2003-01-01–2008-02-01)
  - –1.00 m (2008-02-01 –)
- SSM000008:
  - +0.60 m (2004-01-01–2008-01-01)
  - +0.55 m (2008-01-01 –)
- SSM000037:
  - +0.68 m (2005-04-01–2008-01-01)
  - +0.67 m (2008-01-01 –)
- SSM000040: +0.23 m (2005-07-01 –)
- SSM000041: +0.24 m (2005-07-01 –)
- HLX18.1: +0.21 m (2006-11-16 –)
- HLX18.2: +0.20 m (2006-11-16 –)

Moreover, corrections smaller than 0.1 m (i.e. >–0.1 and < +0.1 m) have also been made (for the data period 2008-01-01 –) for the following wells and boreholes considered in this report (Sicada Bug Report #3242): HAV06, HLX01, HLX07, HLX11, HLX21-26, HLX30, HLX36, HSH01, KAV03, SSM000012, SSM000014, SSM000018, SSM000022, SSM000027, SSM000031, SSM000039, SSM000213, and SSM000222-230.

It should be noted that the above data corrections were made after the Laxemar 2.3 data freeze. Even though the corrections could not be taken into account in figures and so forth in this report, they are considered and commented upon when applicable.

Figures 2-56 to 2-63 present plots of all screened daily average groundwater-level time series; data are shown both in terms of absolute levels (metres above sea level, RHB 70) and depth (metres below ground surface). Further, the data set is divided into wells installed in Laxemar (Figures 2-56 and 2-57), the Simpevarp peninsula (Figures 2-58 and 2-59), the island of Hålö (Figures 2-60 and 2-61), and the island of Ävrö (Figures 2-62 and 2-63).

Considering all available groundwater-level data, but only taking into account time series longer than 150 data days (which implies that 5 of the totally 76 data series are not included), the overall average groundwater level is c 8.0 metres above sea level and the overall average depth to the groundwater level is c 0.8 metres below ground surface. The lowest and highest average groundwater level, respectively, is –0.8 metres above sea level (SSM000018) and 26.4 metres above sea level (SSM000245 and -246). The average amplitude (maximum minus minimum groundwater level) is 1.29 m. The smallest amplitudes are observed for wells SSM000245 (0.17 m) and -246 (0.22 m), whereas the largest amplitude is observed for well SSM000039 (3.44 m). The groundwater level amplitudes are hence generally small, say on the order of 1 m. As can be seen in the figures below, groundwater levels are characterised by fluctuations on relatively small temporal scales. For many wells, these small-scale fluctuations are overlain by more or less typical seasonal variations; high groundwater levels during autumn, winter, and spring, and declining groundwater levels during the summer.

In Laxemar, the average depth to the groundwater level is in the approximate range 4.0 to –0.5 metres below ground surface (a negative number implies artesian conditions), c 0.5 to 2.0 metres below ground surface on the Simpevarp peninsula and c 0.5 to 1.5 metres below ground surface on the island of Ävrö (the average depth is 0.8 m for well SSM000014 on the island of Hålö). Considering each of these individual areas, the within-area difference of the average groundwater level is largest in Laxemar (c –1 to 26 metres above sea level) compared to the other areas; c 0.5 to 6.0 metres above sea level on the Simpevarp peninsula and –1.0 to 4.0 metres above sea level on the island of Ävrö (the average groundwater level is c 0 metres above sea level for well SSM000014 on the island of Hålö).

The larger variability in Laxemar is likely due to larger topographical variations in that area compared to the Simpevarp peninsula and the islands. It can be noted that in Laxemar, there is a much smaller range of depths to the groundwater level compared to groundwater levels; see discussion below on the topographical influence on groundwater levels. Note that post data-freeze data errors (cf. above) are taken into account in this data summary.

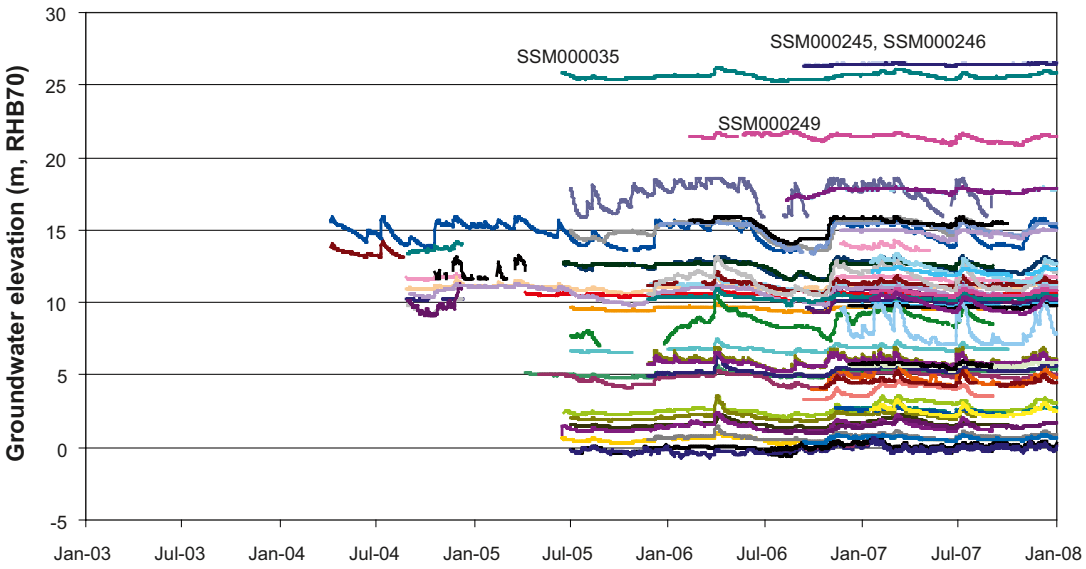

Figure 2-56. *Groundwater levels (metres above sea level) in monitoring wells in Laxemar.*

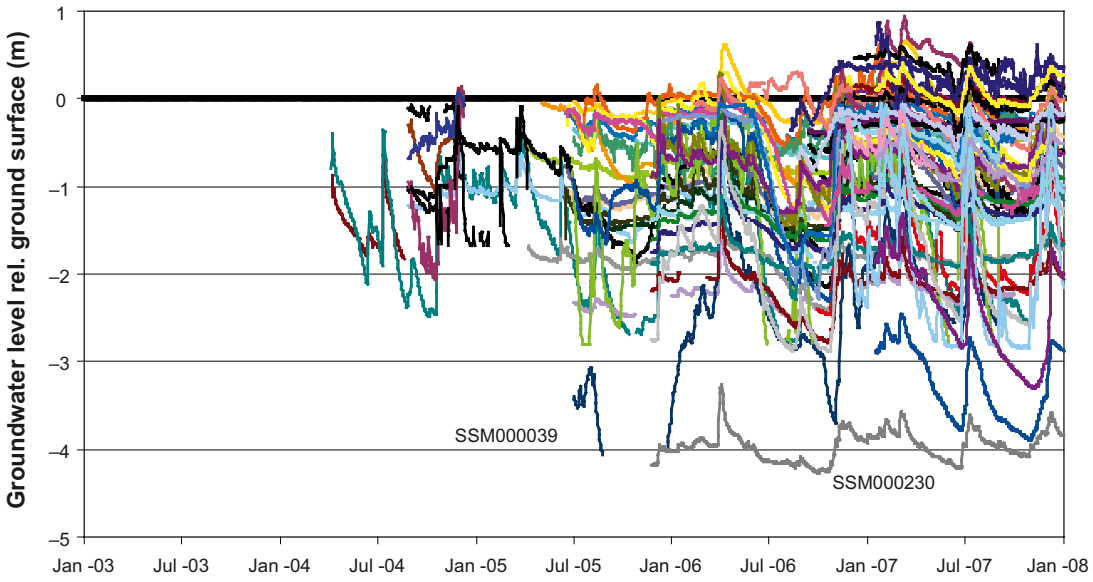

Figure 2-57. *Groundwater levels (metres below ground surface) in monitoring wells in Laxemar.*

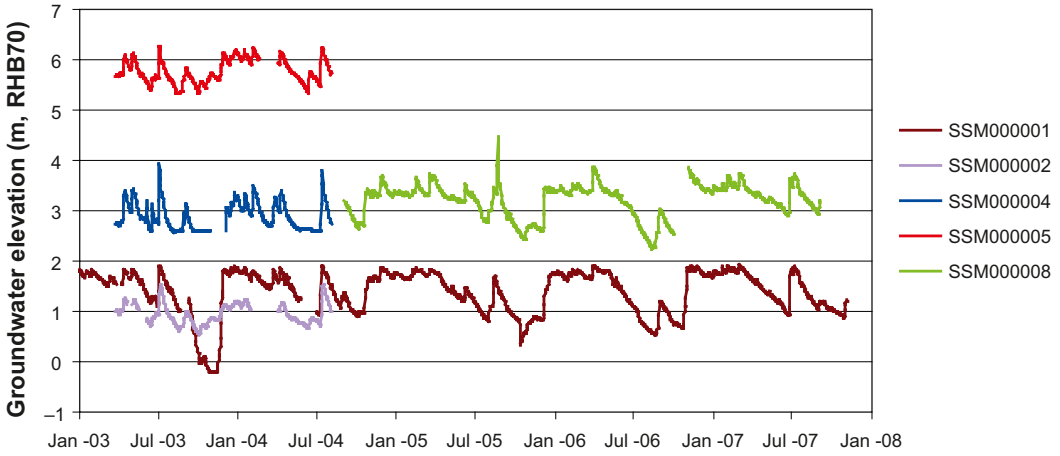

Figure 2-58. *Groundwater levels (metres above sea level) in monitoring wells on the Simpevarp peninsula.*

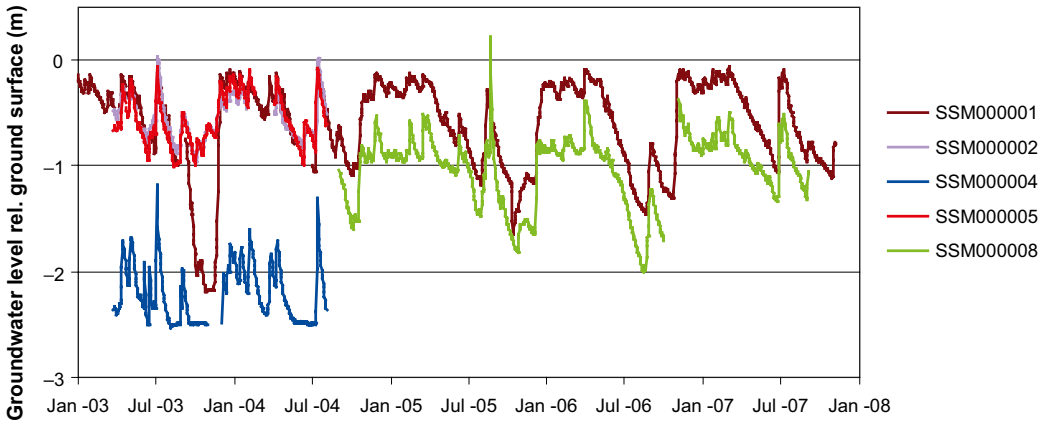

Figure 2-59. *Groundwater levels (metres below ground surface) in monitoring wells on the Simpevarp peninsula.*

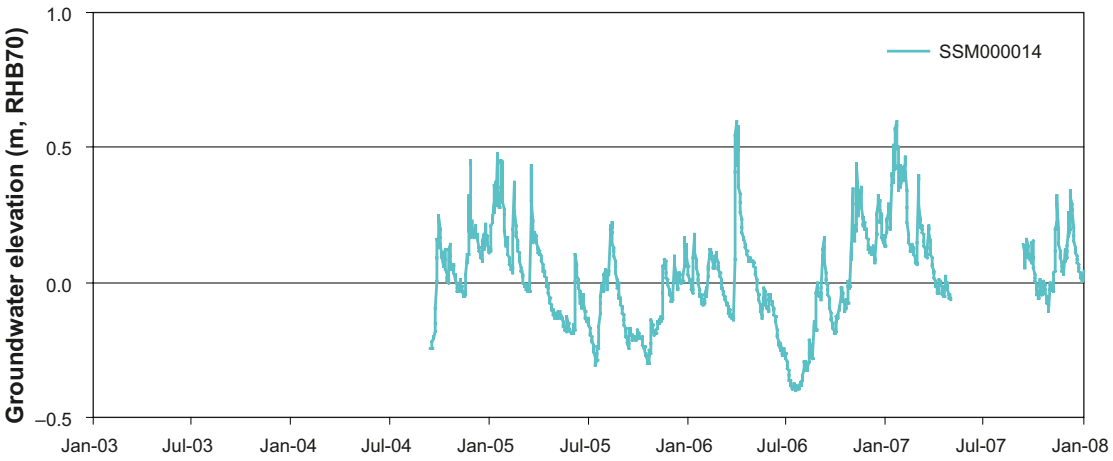

Figure 2-60. *Groundwater levels (metres above sea level) in monitoring well SSM000014 on the island of Hålö.*

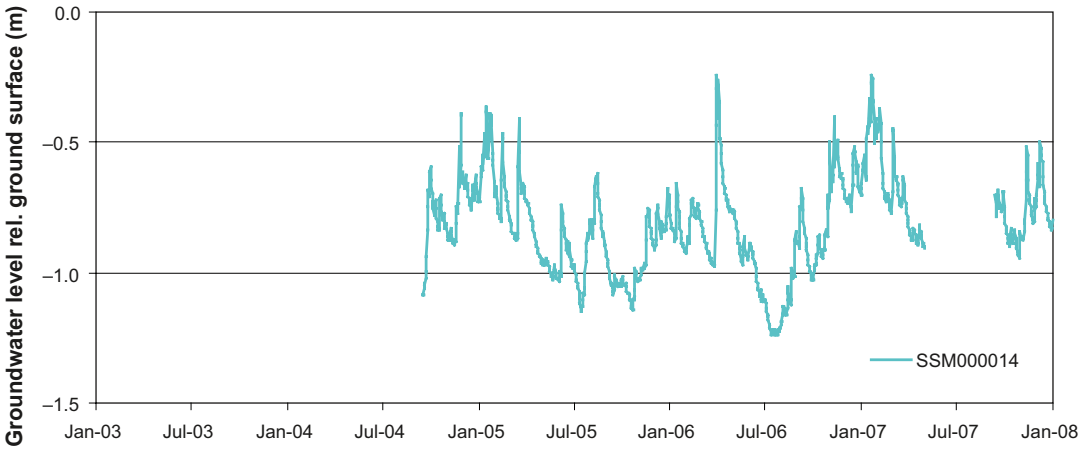

Figure 2-61. *Groundwater levels (metres below ground surface) in monitoring well SSM000014 on the island of Hålö.*

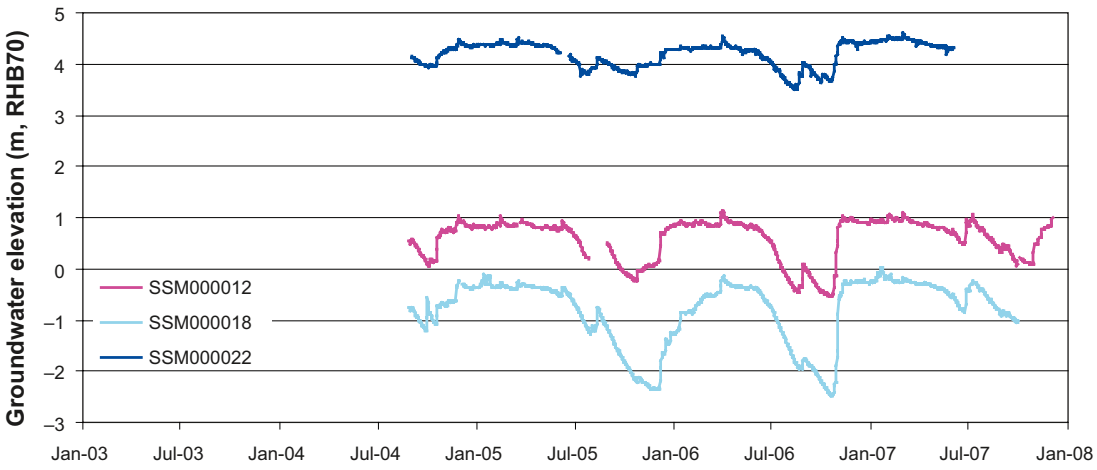

Figure 2-62. *Groundwater levels (metres above sea level) in monitoring wells on the island of Ävrö.*

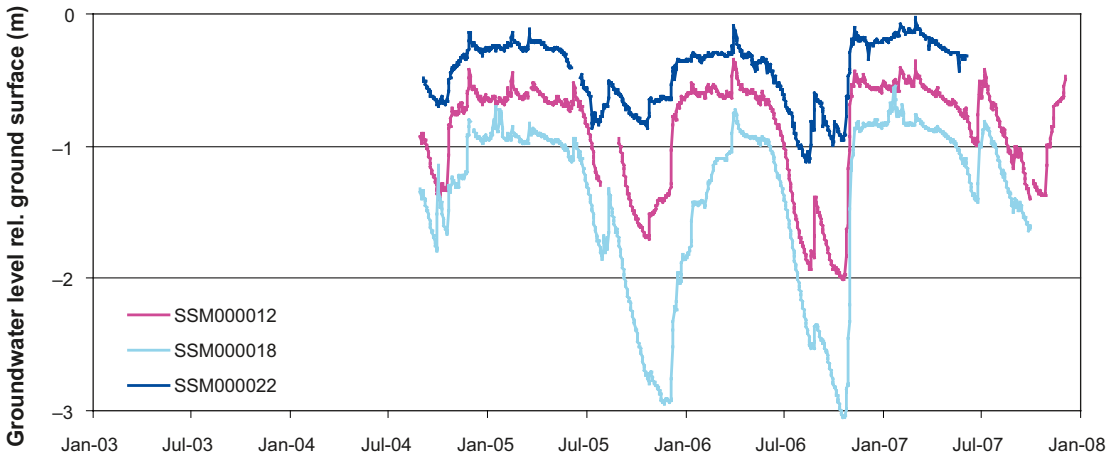

Figure 2-63. *Groundwater levels (metres below ground surface) in monitoring wells on the island of Ävrö.*

Figure 2-64 illustrates the temporal distribution of the depth to the groundwater level, in terms of the cumulative frequency distribution of daily values. The figure shows two data curves: The blue curve is calculated from all daily data, whereas the orange curve is calculated based on daily values of site-average depths to the groundwater level. The figure illustrates that the groundwater level is located at shallow depths; considering all daily data, the groundwater level is located within 2 m below ground during 90% of the time, whereas all daily site-average groundwater table depths are 2 m or less; the groundwater table depth is c 1 m or less about 50% of the time.

The near-surface groundwater level distributions indicated by Figure 2-64 imply that there is a strong correlation between the (elevation of) the groundwater level and the ground-surface elevation. This is further illustrated in the scattergram in Figure 2-65, plotting average groundwater levels versus ground-surface elevations. Note that the scattergram only includes wells with data periods longer than 150 days. There are 11 wells that on average are artesian: SSM000032, -238, -239, -240, -241, -243, -253, -260, -261, -262 and -266. On average for these wells, the groundwater level is located c 0.2 m above ground, whereas the strongest artesian conditions are found at SSM000239, -240 and -266 (average groundwater level c 0.4–0.5 m above ground). The largest average depth to the groundwater level (c 4 m) is found at well SSM000230 (the red dot in Figure 2-65).

The figures below further investigate the relationship between the groundwater level and the local topography of the ground surface, also taking into account the elevation of the rock surface. For each groundwater monitoring well, the plots in Figure 2-66 show the average depth to the groundwater level (including range bars) and the depth to the rock surface. In the upper plot, the data are ranked according to the depth to the groundwater level, whereas data are ranked according to the depth to the rock surface in the middle plot. The bottom plot, in which data are ranked according to the elevation of the rock surface, shows the data in terms of absolute levels (metres above sea level, RHB70), including the ground-surface elevation. One should note that these plots only take into account wells for which more than 150 data days are available. Further, in cases with no data on the depth to the rock surface or the rock-surface elevation, these data are estimated using the elevation of the top of the well casing minus the borehole length.

As illustrated in the upper and middle plots, there seems to be little correlation between the depth to the groundwater level and the depth to the rock surface, whereas the bottom plot emphasises the strong correlation between the groundwater level and the ground-surface elevation. Further, one can also observe that there appears to be some correlation to the elevation of the rock surface, indicating that the ground-surface topography is a suitable indicator not only of groundwater levels but also of the topography of the rock surface.

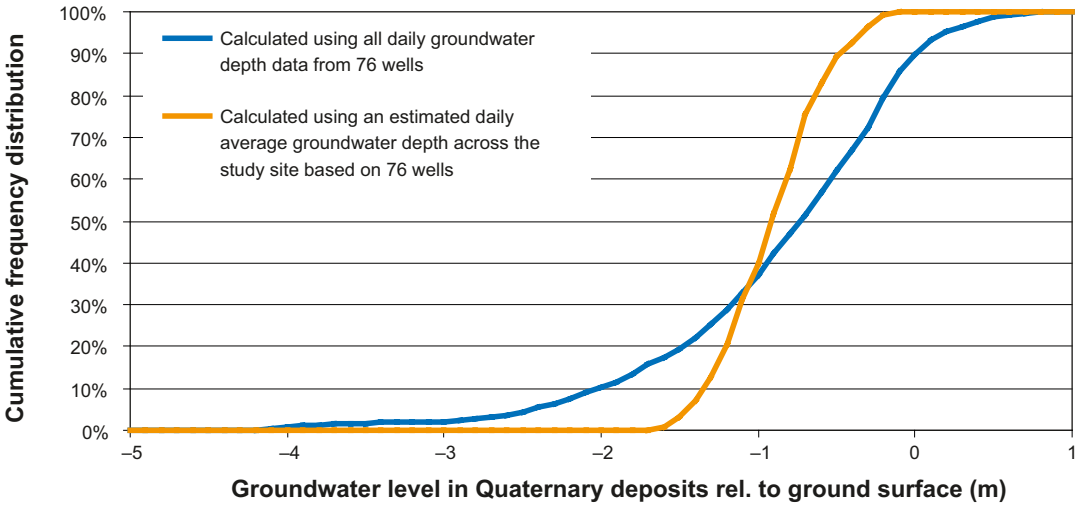

Figure 2-64. *Cumulative frequency distribution (CDF) plot, illustrating the temporal distribution of the groundwater table depth. The blue CDF is based on all daily groundwater level data, whereas the orange CDF uses the daily average of all groundwater wells.*

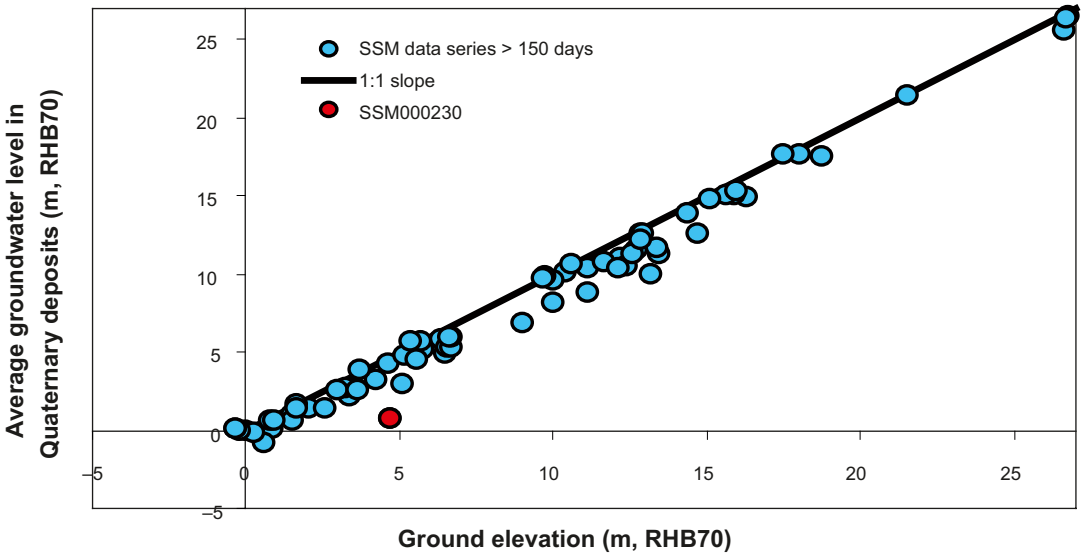

Figure 2-65. *Scattergram of average groundwater levels versus ground-surface elevations (metres above sea level).*

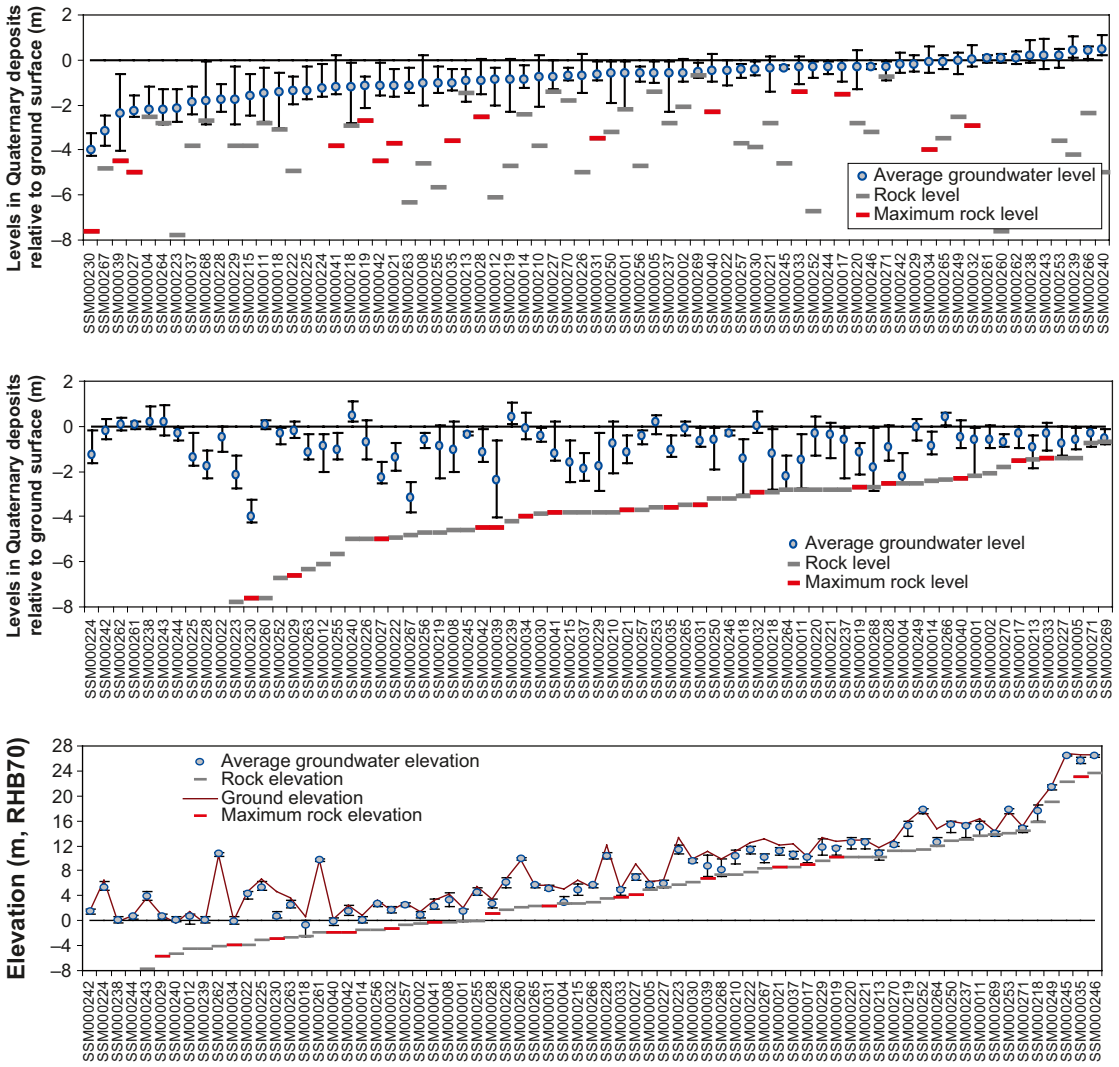

Figure 2-66. *Plots illustrating the relationship between the depth to the groundwater level and the depth to the rock surface (upper and middle plots), and between the groundwater level, the ground-surface elevation and the rock-surface elevation (bottom plot). "Maximum rock elevation" means that the depth to the rock surface and the rock-surface elevation are estimated using the elevation of the top of the well casing minus the borehole length.*

2.4.3 Point-water heads in rock

The Laxemar 2.3 data set includes point-water head data from 44 percussion boreholes and 37 core boreholes. As of Aug. 31, 2007, point-water heads in rock were monitored in 37 percussion borehole sections and 132 core borehole sections; as of Dec. 31, 2007, the corresponding numbers were 35 and 120. Figure 2-67 shows the locations of the monitored boreholes.

The figures below give an overview of the available point-water head time series, divided into percussion boreholes (Figure 2-68) and core boreholes (Figure 2-69). As indicated in these figures, most boreholes are divided into sections by means of packers. These sections are numbered from the borehole bottom and upwards. For instance, HAV06.1 and HAV06.2 denote the lower and upper section, respectively, in percussion borehole HAV06, which hence has two borehole sections. Note that open boreholes without packers (e.g. HLX02) contain a single section, denoted by index .1 (e.g. HLX02.1). For each borehole section in Figures 2-68 and 2-69, the red dots show data days that were removed during the data screening (see section 2.4.1). Note that for the core boreholes, Figure 2-69 only includes the upper sections, due to the large total number of borehole sections.

On average 170 data days per percussion borehole/borehole section were removed as a result of data screening, varying between 0 days in 8 borehole sections and a maximum of 1,043 data days for HSI04. For the core boreholes, the corresponding numbers are 158 data days (average), 0 data

days (minimum; 4 borehole sections), and 1,172 data days (maximum; the whole point-water head data set was removed for KSH01A.1). It should again be noted that for the percussion boreholes, no detailed screening was performed for the post data-freeze period (i.e. after Aug. 31, 2007). This implies that data for the period Sep. 1–Dec. 31, 2007 are kept intact, but, as mentioned previously the risk of potential disturbances is assumed to be small after the data freeze. For the core boreholes, all data were screened for the period Sep. 1–Dec. 31, 2007 (see Figure 2-69).

Figures 2-70 to 2-72 present plots of all (screened) daily average groundwater point-water head time series. The data are divided into boreholes in Laxemar (Figure 2-70), the Simpevarp peninsula (Figure 2-71), and the island of Ävrö (Figure 2-72). Note that there are no monitoring data from boreholes in rock on the island of Hålö.

Table 2-28 summarises the data set in terms of its extreme values (lowest of minimum, highest of maximum) and average-of-average point-water heads in boreholes in Laxemar, on the Simpevarp peninsula and on the island of Ävrö. According to this table, the overall average point-water heads are highest in Laxemar, and slightly above the sea-water level closer to the coast. Considering average point-water heads per area (Laxemar, Simpevarp, Ävrö), the lowest and highest average point-water heads are –0.6 to 20.1 metres above sea level respectively (percussion boreholes) and –2.1 to 15.5 metres above sea level (core boreholes) in Laxemar.

Moreover, the corresponding data are 0.19 to 0.50 metres above sea level (percussion boreholes) and –13.0 to 0.5 m (core boreholes; borehole section KSH02.1 is an outlier, having notably low point-water head) on the Simpevarp peninsula, and –5.6 to 10.9 metres above sea level (percussion boreholes) and –2.0 to 6.2 metres above sea level (core boreholes) on the island of Ävrö. Note that these analyses consider all borehole sections, i.e. also short time series with less than 150 data days, and that post data-freeze data corrections (cf. section 2.4.2) are taken into account in this data summary.

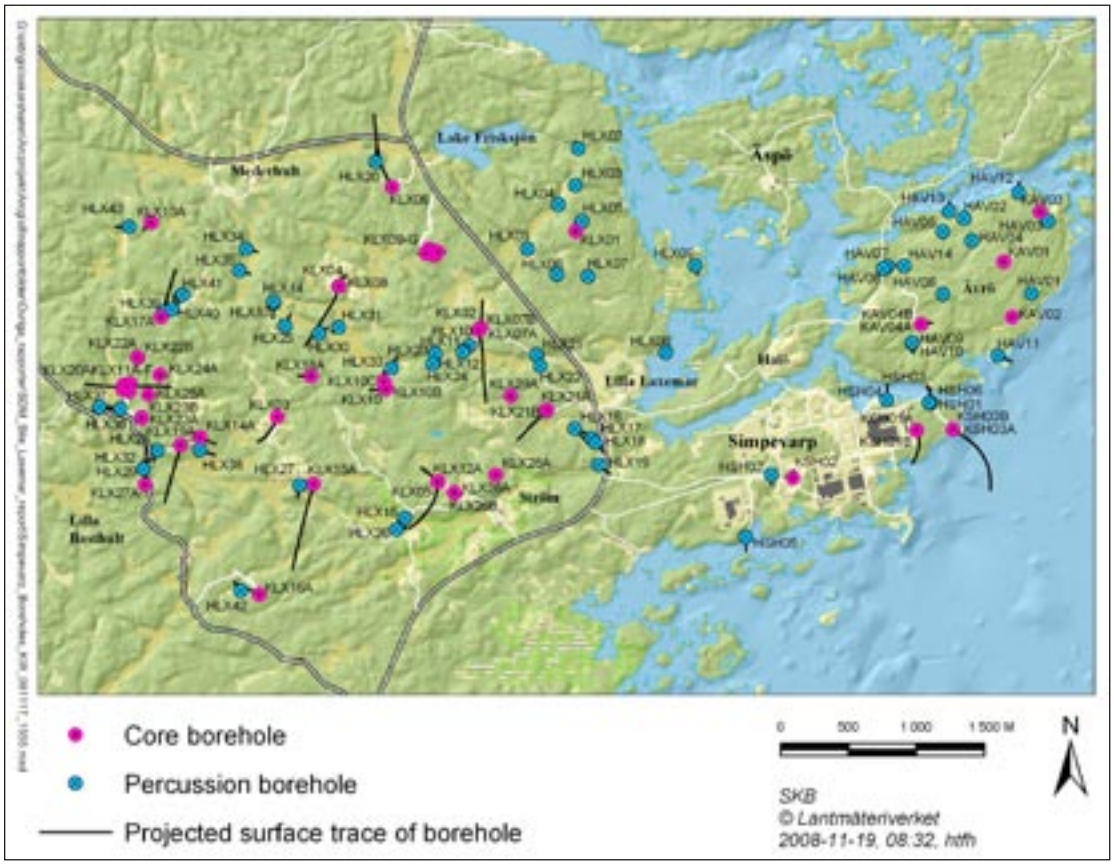

Figure 2-67. *Overview map showing the locations of percussion and core boreholes in Laxemar, among which point-water head data are available from 44 percussion boreholes and 37 core boreholes in the Laxemar 2.3 data set.*

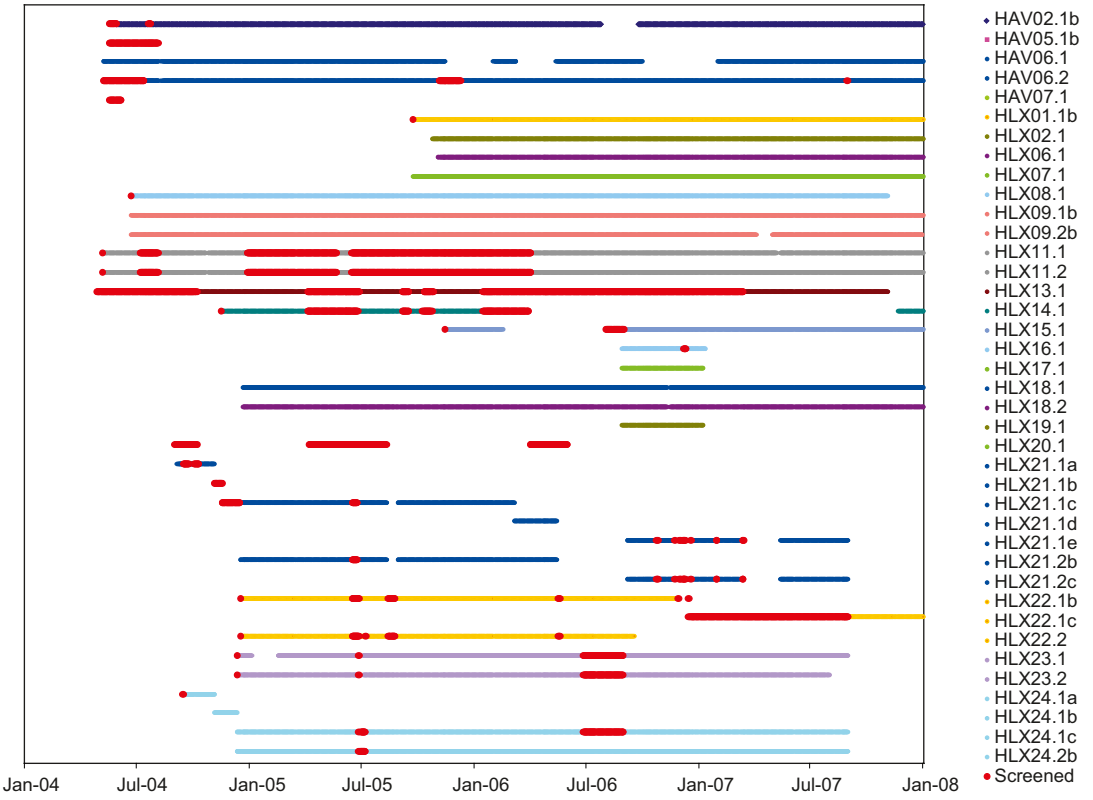

Figure 2-68a. *Overview of available point-water head time series from percussion boreholes HAV02-HLX24. Red dots indicate screened data days.*

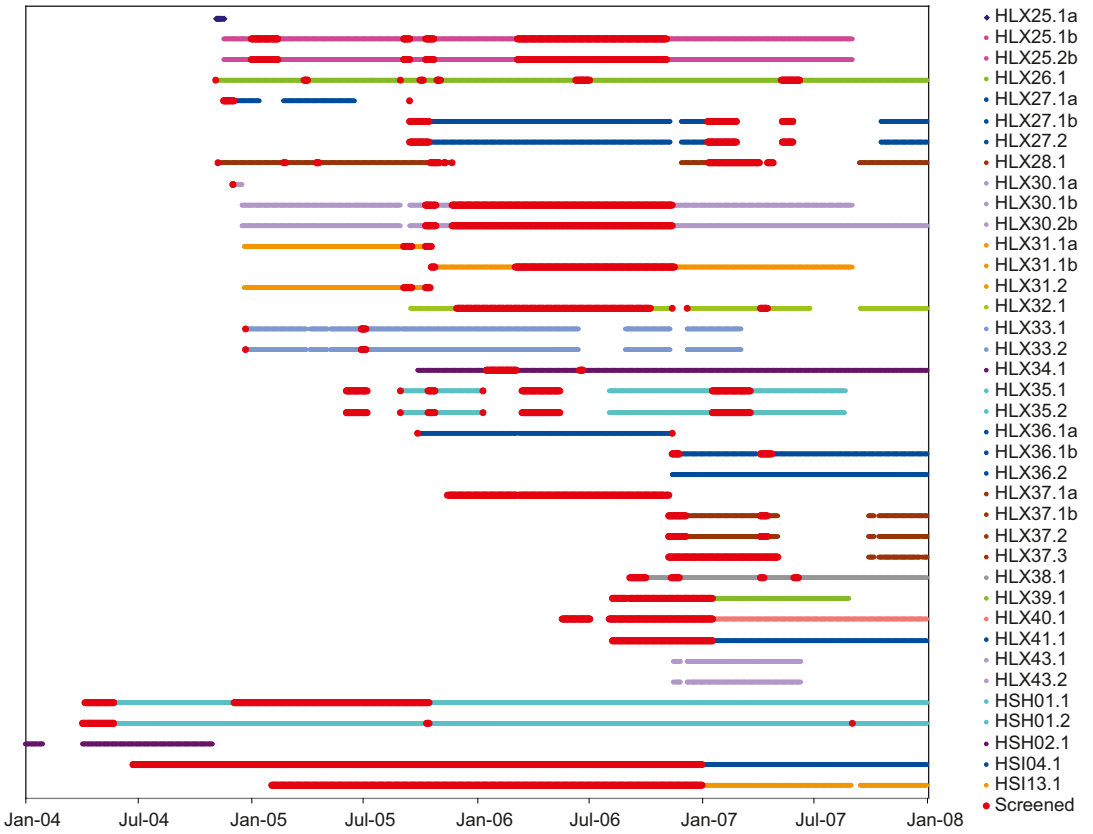

Figure 2-68b. *Overview of available point-water head time series from percussion boreholes HLX25-HSI13. Red dots indicate screened data days.*

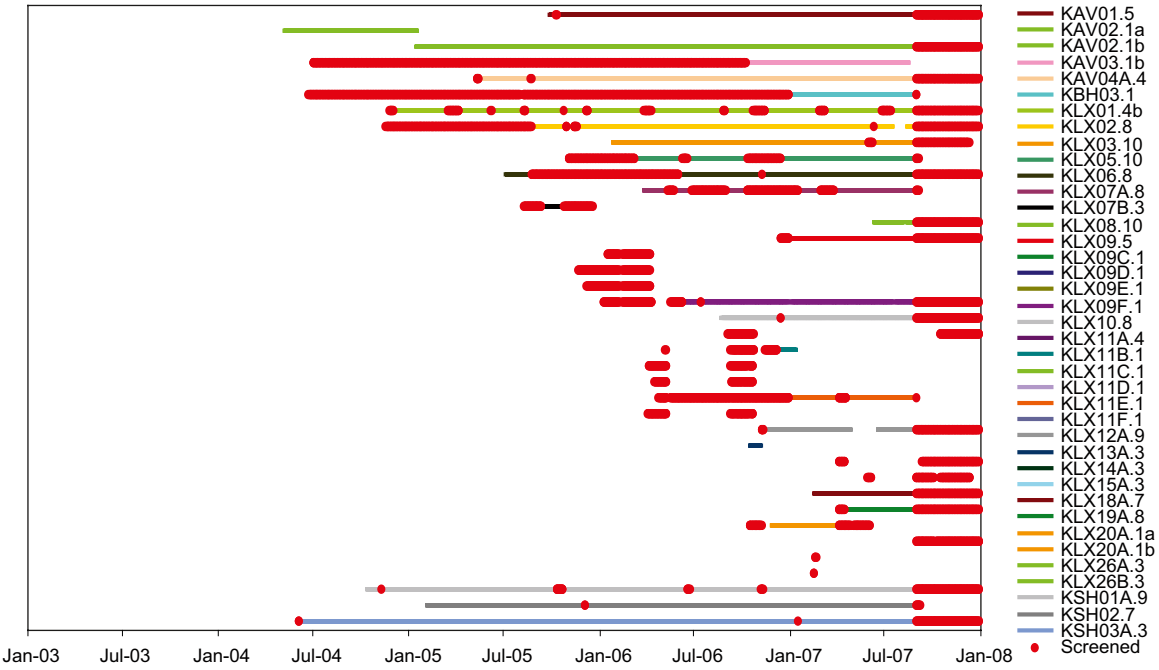

Figure 2-69. *Overview of available point-water head time series from core boreholes. Red dots indicate screened data days. Note that only the upper borehole sections are included in the figure, and that all post data-freeze data (i.e. Sep. 1, 2007 and onwards) are screened, since no actual detailed screening analysis was performed for the period Sep. 1–Dec. 31.*

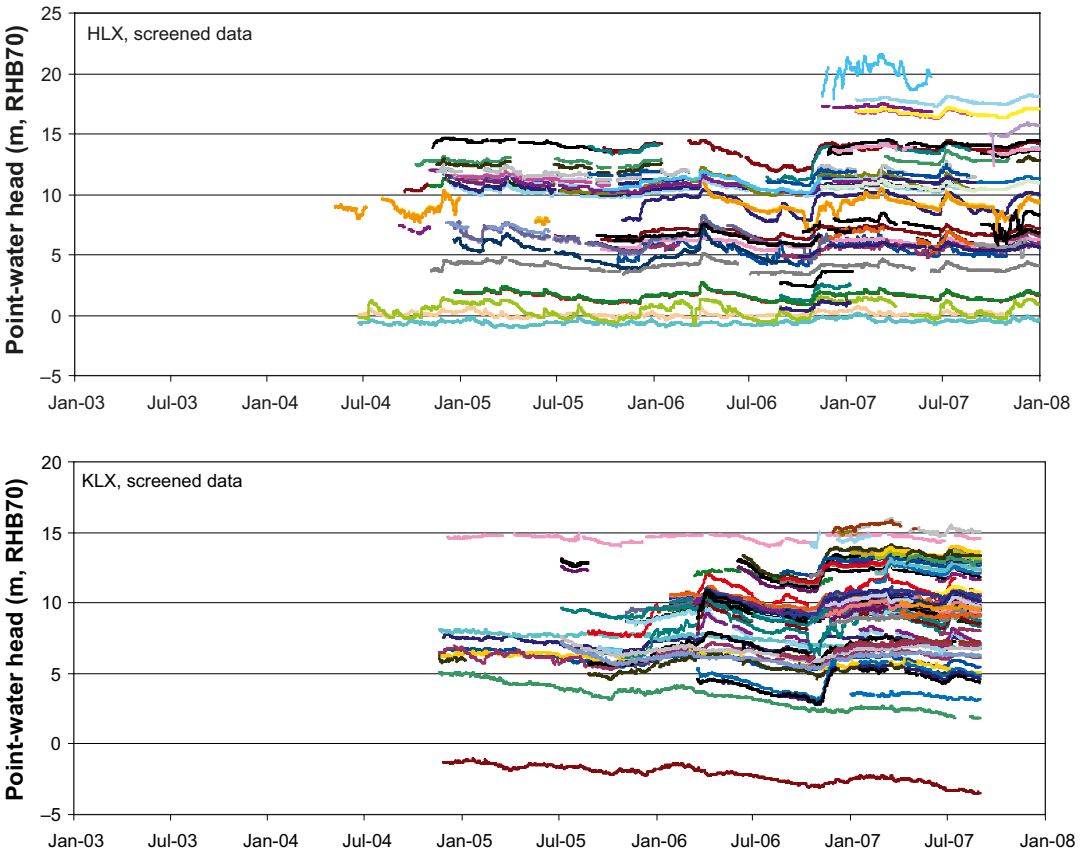

Figure 2-70. *Time-series plots of screened point-water heads in percussion boreholes (HLX) and core boreholes (KLX) in Laxemar.*

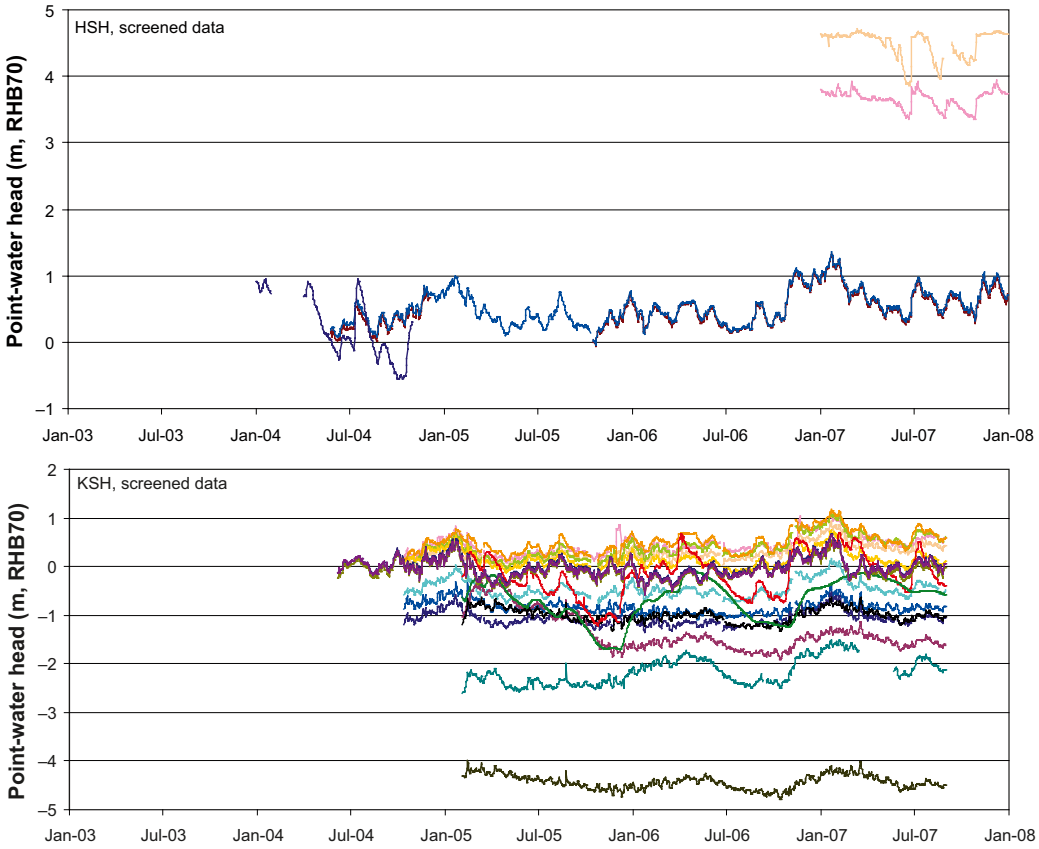

Figure 2-71. *Time-series plots of screened point-water heads in percussion boreholes (HSH) and core boreholes (KSH) on the Simpevarp peninsula.*

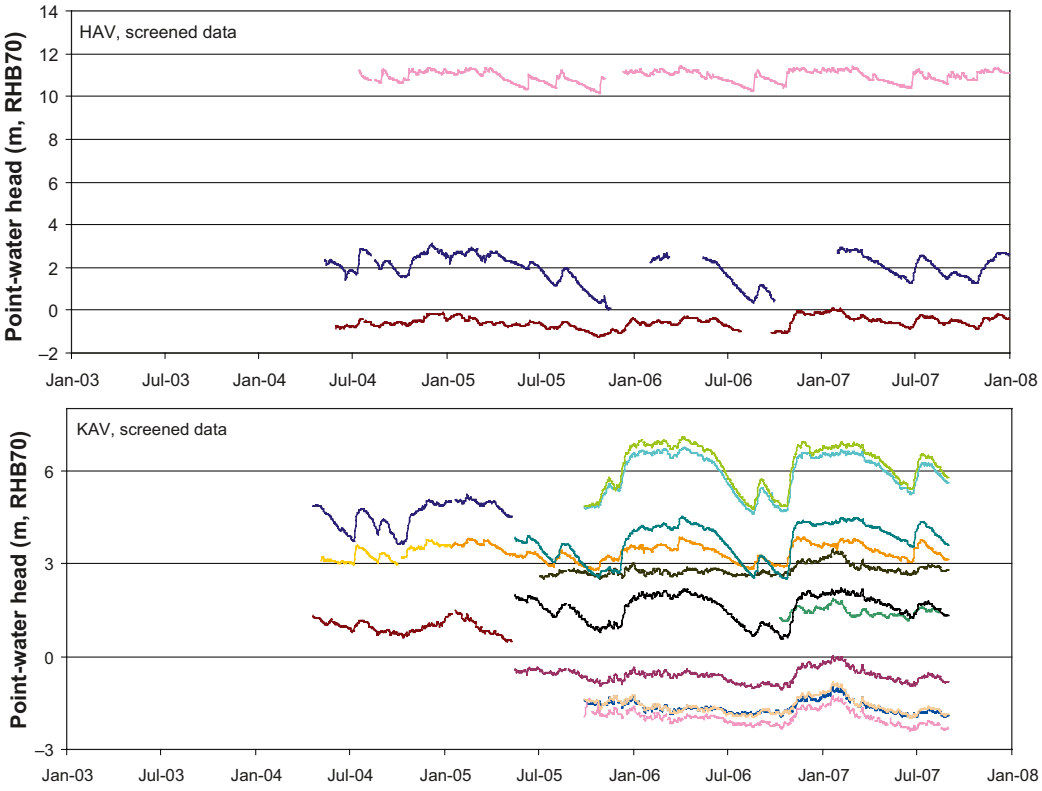

Figure 2-72. *Time-series plots of screened point-water heads in percussion boreholes (HAV) and core boreholes (KAV) on the island of Ävrö.*

Table 2-28. Summary statistics of point-water heads (m, RHB 70) in percussion (perc.) and core boreholes per area. The data represent all screened data up to Aug. 31, 2007.

Area/borehole type		Average	Min	Max
Laxemar	Perc. (HLX)	9.10	–1.01	21.54
	Core (KLX)	10.08	–3.48	16.04
Simpevarp peninsula	Perc. (HSH)	0.39	–0.55	1.35
	Core (KSH)	–1.30	–13.39	1.16
Island of Ävrö	Perc. (HAV)	4.11	–1.24	11.39
	Core (KAV)	2.00	–2.39	7.07

As indicated in Figure 2-70 to 2-72, there are relatively small temporal fluctuations of point-water heads in rock. Only taking into account borehole sections with 150 data days or more, the average point-water head amplitude (i.e. maximum minus minimum) is 1.9 m in the percussion boreholes and 1.5 m in the core boreholes. The smallest fluctuations are observed for HLX31 (borehole section HLX31.1b; 0.7 m) and KLX19A (borehole sections KLX19A.1-2; 0.5 m), whereas the largest fluctuations are observed for HLX11 (borehole section HLX11.2; 4.2 m) and KLX02 (borehole section KLX02.8; 4.4 m).

Figure 2-73 investigates possible correlations between point-water heads in percussion boreholes and the topography of the ground surface, plotting average groundwater levels versus ground-surface elevations. Note that this scattergram only includes borehole sections with more than 150 data days. For boreholes with packers, data are used for the upper borehole sections. Two artesian percussion boreholes can be observed, namely HLX15 and HLX28, with average point-water heads in the upper borehole sections approximately 0.9 m above the ground surface. Overall, there seem to be less correlation between point-water heads in the upper parts of the rock and ground-surface elevations, compared to groundwater levels in the QD (Figure 2-65), even though there is a general trend according to Figure 2-73.

The top plot of Figure 2-74 shows average point-water heads (including bar ranges) in percussion boreholes, and ground surface and rock elevations, ranked according to rock elevation. The bottom plot expresses the same data in terms of the depth below ground surface, ranked according to the rock-surface depth. Note that for boreholes with packers, data for the upper borehole sections are used. Also note that only sections with more than 150 days of data are shown, and that only data up to Aug. 31, 2007 are used. Percussion boreholes on the island of Ävrö (HAV boreholes) are not shown, because ground elevation and bedrock elevation data are missing for these boreholes. Moreover, there are ground elevation data (but no rock elevation data) for the boreholes HLX08, HLX09 and HLX11, located in Laxemar. For these boreholes, the maximum rock elevation is set equal to the ground elevation, motivated by a QD depth of 0 m at these boreholes according to Sicada.

According to Figure 2-74, there is a general trend with at least some correlation between point-water heads in the upper parts of the rock and ground-surface elevations (cf. Figure 2-73). However, there is no correlation between the "point-water depth" and the rock-surface depth. It is interesting to note that there seems to be a zone of unsaturated rock along some boreholes, i.e. locations where the point-water head is below the rock surface.

2.4.4 The influence of groundwater salinity on vertical head gradients in rock

Interpretation of the prevailing horisontal and vertical head gradients in a variable-density groundwater flow system requires transformation of measured point-water heads (h_{ip}) to fresh-water heads (h_{if}) and environmental-water heads (h_{in}), respectively /Lusczynski 1961, Acworth 2007, Post et al. 2007/. As illustrated in Figure 2-75, density measurements (made at the Äspö laboratory, at a temerature of 25°C) on groundwater samples from Laxemar show that the density of most groundwater samples is lower than 1 $g \cdot mL^{-3}$, even at relatively large depth in the rock. With a few exceptions, groundwater densities above 1 $g \cdot mL^{-3}$ occur below approximately –400 metres above sea level, and densities above 1.010 $g \cdot mL^{-3}$ below c –900 metres above sea level.

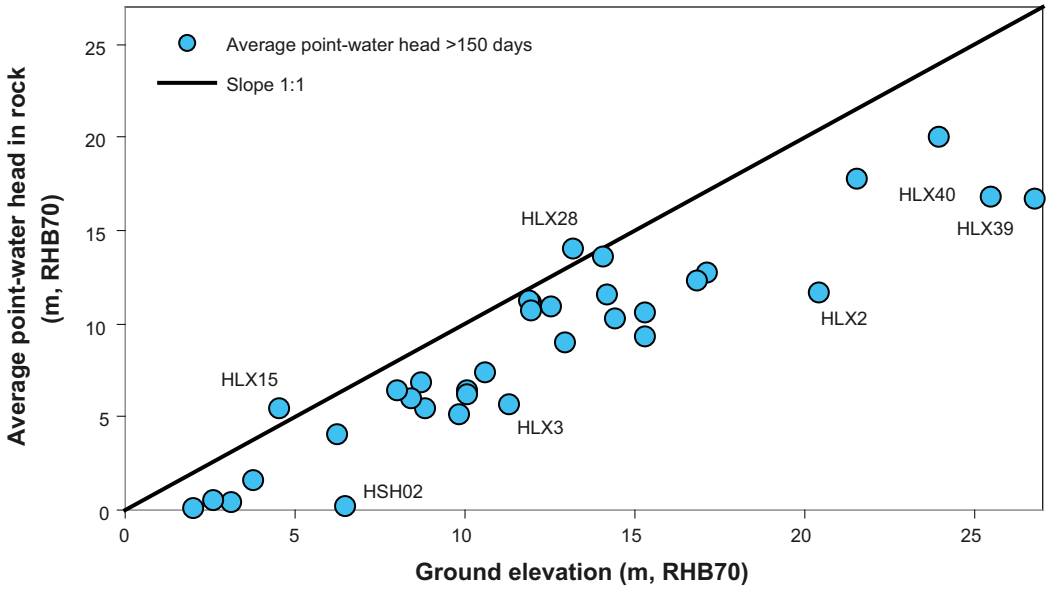

Figure 2-73. *Plot of ground elevation versus average point-water heads in percussion boreholes. Note that for boreholes with packers, data are used for the upper borehole section. Also note that only borehole sections with more than 150 data days are shown.*

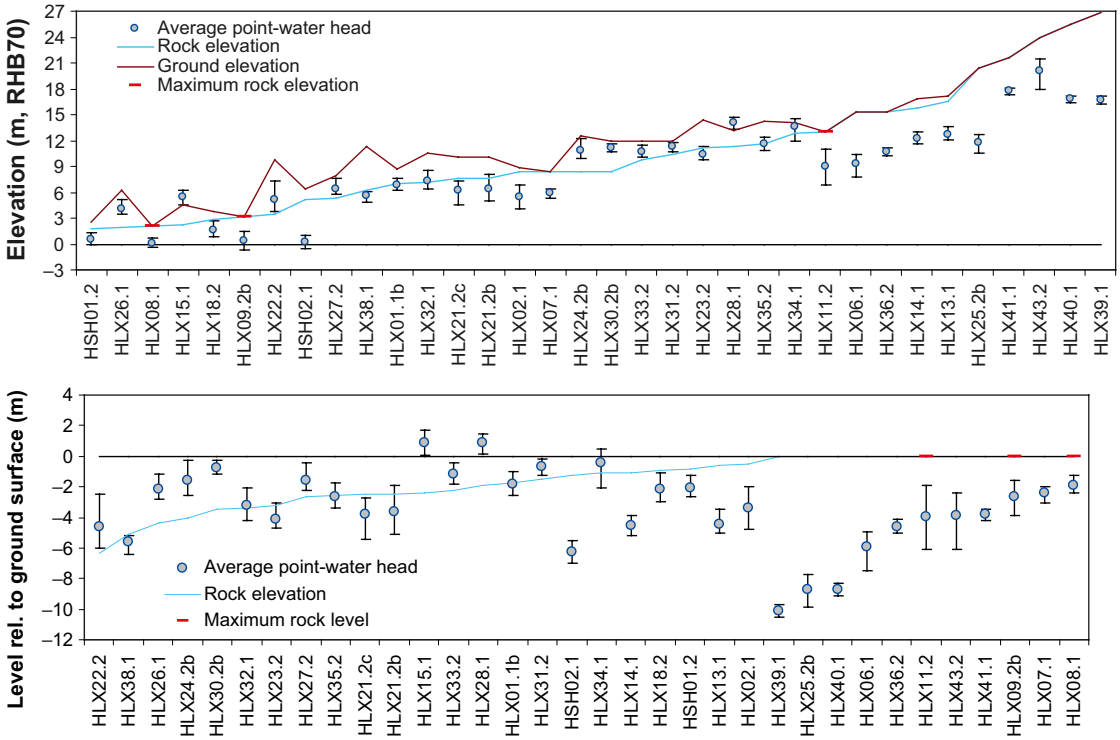

Figure 2-74. *Plots of averages, minimum and maximum point-water heads in percussion boreholes, ground-surface elevations, and rock-surface elevations. In the upper plot, data are ranked in terms of rock-surface elevation, and in terms of rock-surface depth in the lower plot. Note that for boreholes with packers, data for the upper borehole sections are used. Also note that only borehole sections with more than 150 data days are shown.*

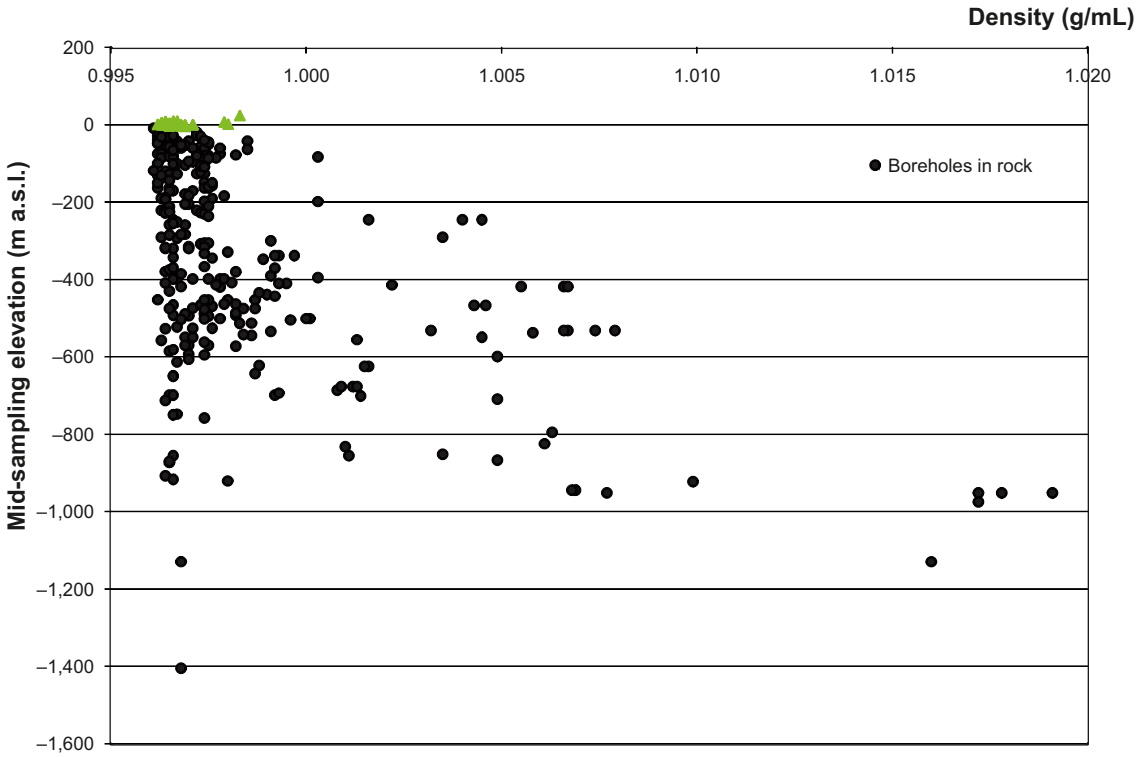

Figure 2-75. *Plot of laboratory-measured groundwater densities versus sampling depth for boreholes in rock and QD (green dots). The vertical axis shows mid-sampling elevations (metres above sea level) and the horisontal axis shows water densities in g·mL^{-3}.*

These data indicate that in general, density differences have only minor effects on groundwater head gradients in the Laxemar area. Note that of the totally 353 samples from boreholes and QD wells shown in Figure 2-75, 132 samples belong to hydrochemical sampling class 1 (which is associated with the highest chemical data quality), 126 samples belong to class 3, 5 to class 4 and 90 to class 5, which has lowest chemical data quality. In particular, 25 groundwater samples from core boreholes have a drilling-water residue > 20%, which obviously make these density data rather uncertain (this 25-sample data set has a max-, min- and average density of 1.0172, 0.9963 and 1.0011 g·mL^{-3}).

Table 2-29 summarises average water densities and electrical conductivities (EC) of water samples from the Baltic Sea, lakes, streams, groundwater monitoring wells, and boreholes in the rock. These results indicate that on average, there are rather small density differences between lakes, streams, groundwater in QD and groundwater in rock, whereas sea water obviously has the highest average density. Except from the sea, the highest average density is observed for the core boreholes, which in general are deeper than the percussion boreholes.

A general impression from the density data set is that many density values are lower than expected, even for fresh ("saline-free") water in lakes, streams and groundwater monitoring wells. Based on groundwater chemistry data from the Äspö Hard Rock Laboratory, /Rhén et al. 1997/ present an empirical relationship between the groundwater density ρ (kg·m^{-3}) and its electrical conductivity EC (mS·m^{-1}): $\rho = \rho_0 + 0.00467 \cdot EC$ where ρ_0 is the density of "pure" water, here taken as 997.3 kg·m^{-3}. This empirical result is used in the rightmost column of Table 2-29, which yields an average fresh-water density (based on the average of the EC data) for the groundwater monitoring wells of c 0.9975 g·mL^{-3}, and similar averages for lake- and stream water. In the corresponding exercise on the Forsmark data set /Juston et al. 2007, Johansson 2008/) a fresh-water density of 0.9976 g·mL^{-3} was used, which is also adopted here.

Table 2-29. Average water densities for different water systems in Laxemar.

Flow system	Average density (g·mL^{-3})	Average EC (mS·m^{-1})	Average calculated density (based on EC)
Baltic sea water	1.0009	1,019.46	1.0021
Lake water	0.9965	13.28	0.9974
Stream water	0.9965	13.82	0.9974
Groundwater monitoring wells	0.9966	41.82	0.9975
Percussion boreholes	0.9969	91.50	0.9977
Core boreholes	0.9987	486.44	0.9996

Using data on borehole geometries and groundwater densities, the time series of point-water heads measured in core- and percussion boreholes have been transformed to fresh-water heads and environmental-water heads (see Appendix 1). The primary objective is to investigate whether vertical groundwater density differences in the rock may be of importance for interpretation of vertical gradients within the rock, estimated by head gradients between borehole sections. The head-transformation methodology is based on the theory presented by /Lusczynski 1961/, according to which environmental-water heads h_{in} (used to interpret vertical head gradients) are calculated from measured point-water heads h_{ip} as

$$h_{in} = \frac{\rho_i h_{ip} - Z_i(\rho_i - \rho_a) - Z_r(\rho_a - \rho_f)}{\rho_f}$$

where ρ_i = density at point i, ρ_f = fresh-water density (0.9976 g·mL^{-3}), and Z_i = elevation of point i (positive upwards). ρ_a denotes the average density between Z_r and Z_i, where Z_r is the elevation of a reference point below which the average density is to be determined (and above which water is fresh):

$$\rho_a = \frac{1}{Z_r - Z_i} \int_{Z_i}^{Z_r} \rho(z)\, dz$$

Moreover, fresh-water heads h_{if} (used to interpret horisontal head gradients) are calculated from measured point-water heads h_{ip} according to the expression

$$h_{if} = \frac{\rho_i h_{ip} - Z_i(\rho_i - \rho_f)}{\rho_f}$$

As part of the corresponding Forsmark exercises /Johansson 2008/, three assumptions were tested concerning vertical density variations between borehole packers: (1) The density in each borehole section is constant. (2a) There is a linear variation of the density in each borehole section, estimated using density data from the current section as the “upper value” and data from the section below as the “lower value”. (2b) Likewise a linear variation, but instead estimated by density data from the section above as the “upper value” and data from the current section as the “lower value”. In general, these three different ways of calculating the average density ρ_a showed minor effects on the head transformations. Therefore, in the present report the density is for simplicity assumed to be constant within each borehole section. Groundwater levels in open boreholes by definition correspond to environmental-water heads, and head transformation exercises are therefore not necessary. On the other hand, groundwater-level measurements in a single open borehole cannot be used to assess vertical head gradients.

In cases where the measured groundwater density is below the adopted fresh-water density ($\rho < \rho_f = 0.9976$ g·mL^{-3}), the density obtained using the empirical expression was used instead. If also the empirically calculated density is lower than ρ_f, the density was set to $\rho = 0.9976$ g·mL^{-3}. In the calculation of the average density ρ_a, the upper section consists of groundwater in the QD. For each percussion borehole, the closest groundwater monitoring well was identified to provide transient data on the height of the overlying fresh-water column. A distance limit of 100 m was used, i.e. only groundwater monitoring wells located closer than 100 m from percussion boreholes were used.

There is only one percussion borehole with a nearby groundwater monitoring well, namely HLX21/SSM000214. However, there are no groundwater-level monitoring data from SSM000214. Hence, for all boreholes the point-water head data from the upper borehole section (i.e. the top section without an upper packer) were used to represent the groundwater density in the upper section. Appendix 1 presents the results of the calculations. There are sufficient data to allow head transformations for totally 19 boreholes (including percussion borehole HLX21): 16 boreholes in Laxemar, KSH01A and KSH02 on the Simpevarp peninsula, and KAV01 on the island of Ävrö.

As expected (cf. Figure 2-75), for most boreholes the calculations show relatively small differences between measured point-water heads (PWH) and calculated environmental-water heads (EWH). In terms of average differences for the whole data periods, the largest differences of EWH minus PWH are observed for KAV04 (5.16 m for section 1), KSH02 (5.09 m for section 1, 3.82 m for section 2 and 3.52 m for section 3), and KLX03 (4.41 m for section 2). Overall, density compensations are primarily made for the bottom borehole sections. Compensations of importance (larger than 0.1 m expressed in absolute values) are made for all considered boreholes except HLX21, KLX06, KLX07A, KLX07B, KLX18A, and KLX19A.

From the calculated environmental-water heads, there are no boreholes displaying a continuous upward or downward head gradient along the whole borehole. An upward gradient between the two topmost borehole sections (hence indicating groundwater discharge in the upper part of the rock) are only noted for percussion borehole HLX21 and core boreholes KLX03, KLX06, KLX15A (see below) and KSH02.

Using the relatively short time series from KLX15A, Figures 2-76 to 2-77 exemplify the effects of the head transformations (see further plots and evaluations in Appendix 1). Figure 2-76 shows measured point-water heads in the three borehole sections in KLX15A, whereas Figure 2-77 shows the corresponding calculated environmental-water heads. The density correction is large in the two bottom borehole sections (sections 1 and 2). In particular, the head correction for section 2 implies that the downward gradient, as indicated by measured point-water heads, in fact is an upward (environmental-water head) gradient in the upper rock.

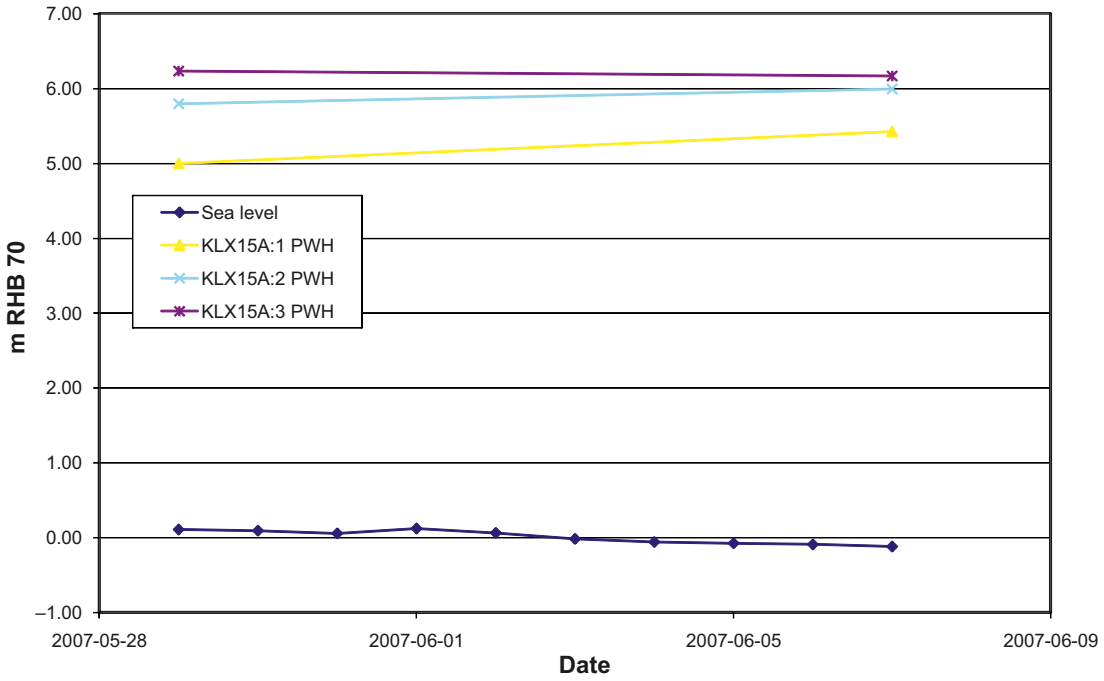

Figure 2-76. *Time-series plot of measured point-water heads in core borehole KLX15A.*

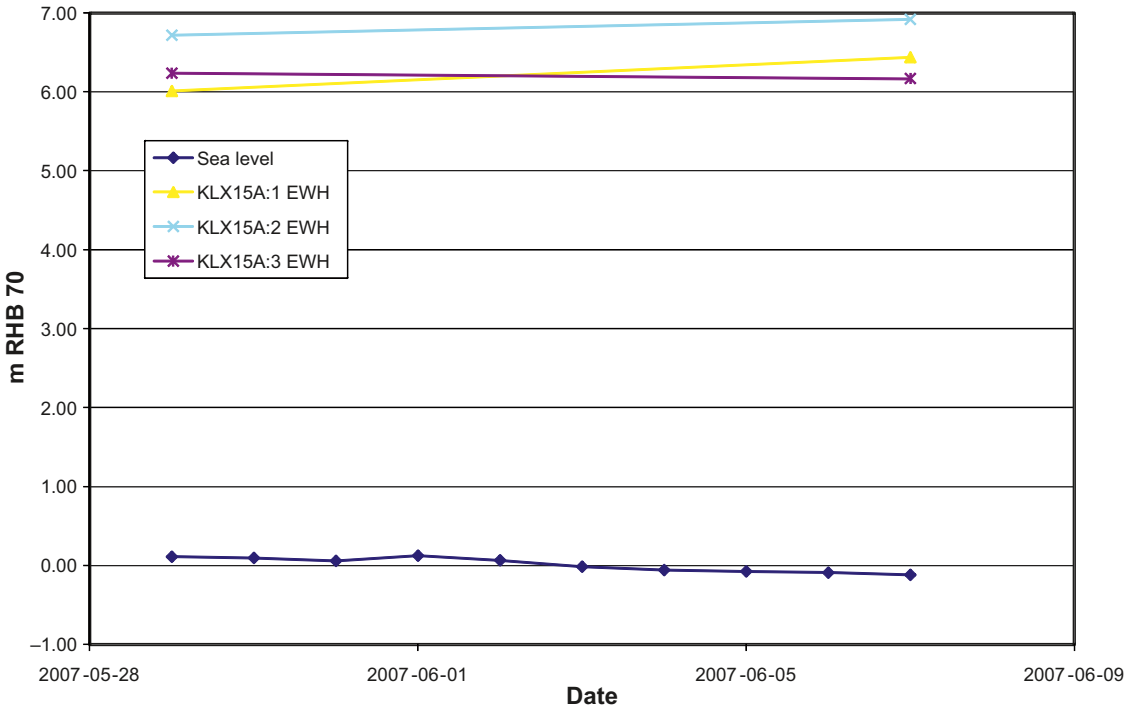

Figure 2-77. *Time-series plot of calculated environmental-water heads in core borehole KLX15A.*

3 Hydrological relationships between time-series data sets

3.1 Time series of rainfall, snowmelt and potential evapotranspiration

Rainfall and snowmelt (sources) and evapotranspiration (sinks) are the main driving forces of the hydrological cycle and they therefore have fundamental importance for the water balance of an area. This section investigates the relationships between these parameters, including their relationships to other monitored parameters. Specifically, different types of time-series data are compared, with the objective to explore the hydraulic responses in streams, QD and rock to the temporal variations of the above source/sink terms.

As described in section 2.2.4, a relatively simple model of snow accumulation and snowmelt was developed and used in conjunction with precipitation and air temperature data to derive a rainfall/snowmelt time series. The plot in Figure 3-1 shows calculated daily sums of rainfall/snowmelt (abbreviated R/S), produced using air temperature thresholds of 0.6°C for rainfall/snowfall and 0.36°C for snowmelt, and a degree-day factor of 2.82 $mm \cdot d^{-1} \cdot °C^{-1}$. The model distributes the precipitation, represented by the average of daily sums at Äspö and Plittorp, into snow accumulation and rainfall, which either add to the accumulated snow or falls directly on bare ground. Hence, the model takes into account snowmelt when there is accumulated snow. According to this model, even on an annual basis snowmelt (S) represents an important source term, contributing with totally c 26% of the sum of rainfall plus snowmelt (R + S) during the considered period (2003-09-10–2007-12-31). According to the model, the maximum snowmelt occurred on Dec. 5, 2004; 22 mm of water as snow melted in one day.

The lower plot in Figure 3-2 shows the corresponding monthly sums of R and S (upward bars), and monthly sums of potential evapotranspiration (downward bars) at the Äspö and Plittorp stations. The upward bars in the lower plot of Figure 3-2 hence represent the actual "source term" for surface runoff, infiltration and groundwater recharge; snowfall accumulates on the ground and does not act as a source term until the snow melts. On the other hand, the upward precipitation (P) bars in the upper plot of Figure 3-2 do not take into account whether precipitation falls in the form of rain or snow.

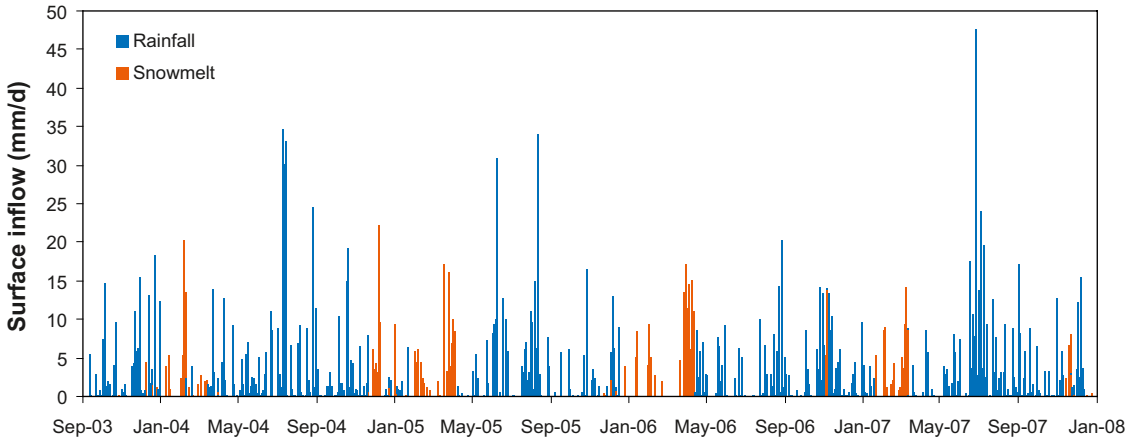

Figure 3-1. *Time-series plot of sums of calculated daily rainfall and snowmelt. Rainfall is calculated as the average of the Äspö and Plittorp stations. The snowmelt time series is simulated using a simple model of snow accumulation/snowmelt.*

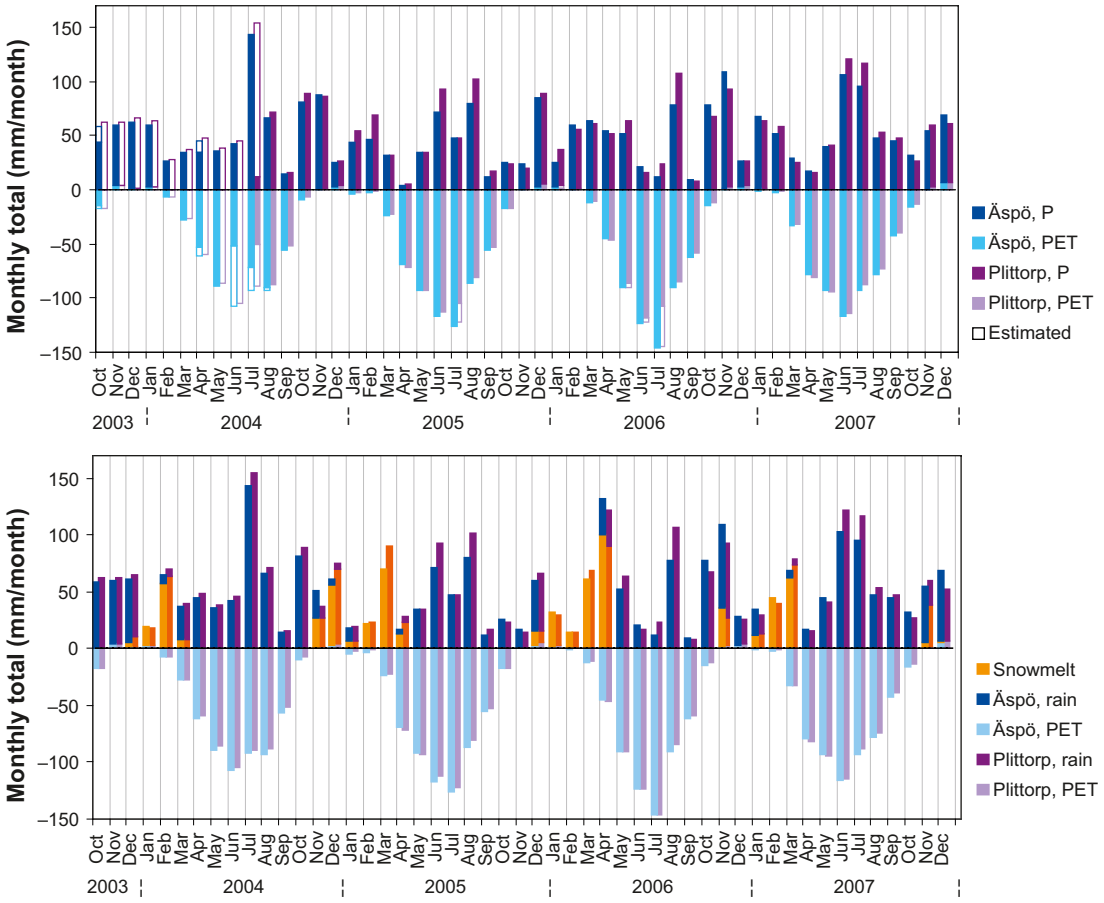

Figure 3-2. *Upper plot: Time-series plot of monthly sums of precipitation (P) and potential evapotranspiration (PET), respectively. Plittorp data are extrapolated based on Äspö data until Jul. 14, 2004, and Äspö data are extrapolated from Kråkemåla data during totally 7 days. Lower plot: Time series plot of monthly sums of snowmelt, rainfall and PET, respectively; data are extrapolated in the same manner as in the upper plot.*

A comparison between the upward bars in the upper and lower plots clearly shows that the temporal distribution of the source term appears quite different if snow accumulation/snowmelt is taken into account or not. Using the precipitation (P) as a measure of the source term does not properly represent the temporal distribution of the source term; snowmelt during parts of the winter but foremost during spring yields a large contribution to the surface runoff/infiltration/groundwater recharge source term, which is underestimated if represented by precipitation (P) only. Moreover, using P as the source term overestimates the actual source term during cold winter periods, when precipitation is accumulated in the form of snow. This is further illustrated in the plots of Figure 3-3, showing the time lag between the cumulative daily sums of precipitation (P) and rainfall plus snowmelt (R+S) at the Äspö and Plittorp stations. From these plots, it can be seen that there were cold periods during spring with much precipitation (i.e. snow accumulation), followed by warm periods with little precipitation (i.e. substantial snowmelt).

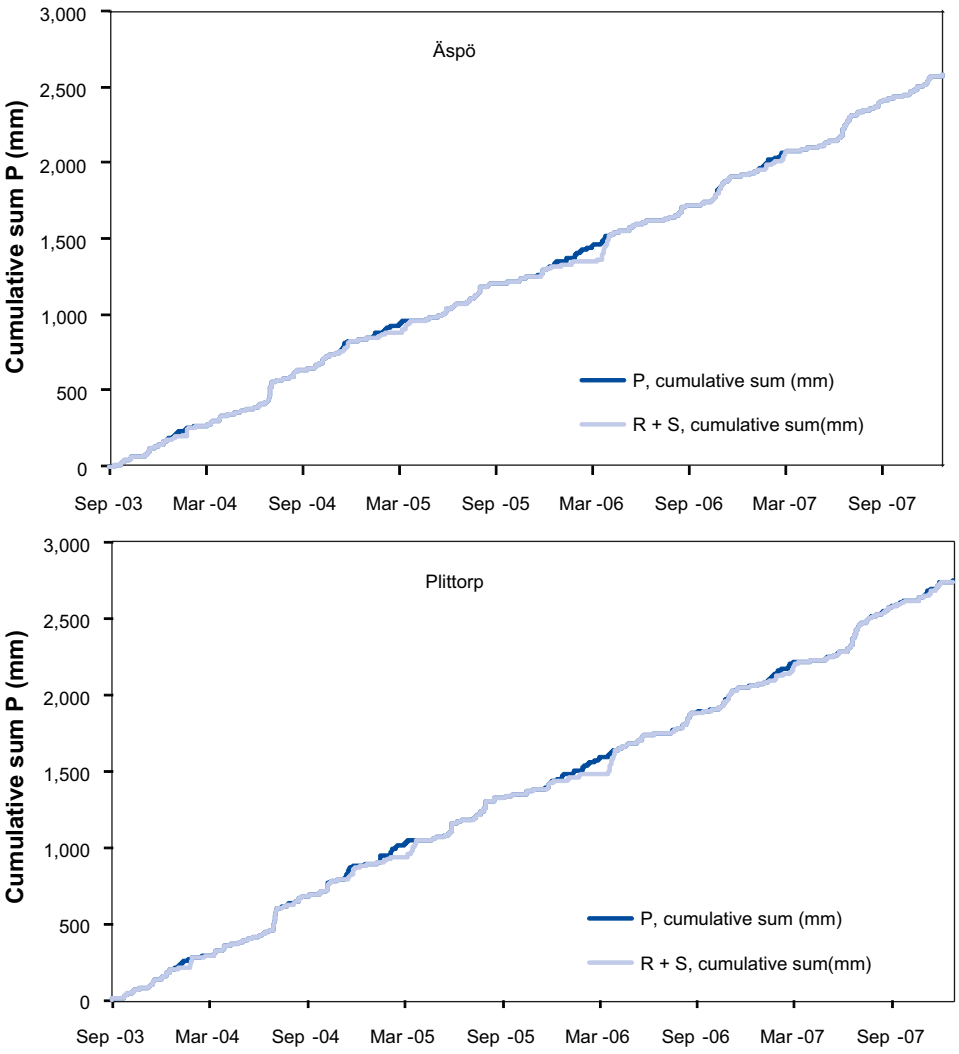

Figure 3-3. *Cumulative daily sums of precipitation (P) and rainfall plus snowmelt (R + S) at the Äspö and Plittorp stations during the period Sep. 10, 2003–Dec. 31, 2007.*

Figure 3-4 shows time-series plots of site-average daily sums of rainfall plus snowmelt (abbreviated R/S), PET, and a "net" source term defined as R/S minus PET. Data are shown in two ways: In the upper plot in terms of rolling annual sums (i.e. the rolling sum of the previous year), and in the lower plot in terms of annual accumulated sums during 1 Sep.–31 Aug. periods. The lower plot starts on Sep. 8, 2004, i.e. one year after local meteorological measurements started on the island of Äspö, whereas the lower plot starts on Sep. 9, 2003.

Also the plots in Figure 3-4 illustrate that the accumulated source term (R/S) is characterised by a large increase during spring (snowmelt), and for some years also in connection to periods with much rainfall during summer and autumn. Due to snow accumulation, the source term is generally small during winters. Moreover, the sink term (PET) demonstrates a large increase during spring and summer, which implies that the net source term (R/S-PET) increases during the whole summer until autumn, when the autumn rains combined with decreasing evapotranspiration results in an increase of the net source term. The source term demonstrates a particularly large increase during spring 2006, due to intense snowmelt and small evapotranspiration.

In order to explore the hydraulic responses in streams, QD and rock to the temporal variations of the source/sink terms discussed above, Figure 3-5 compares time-series plots of a) monthly values of the net source term R/S-PET and b) snowmelt, rainfall and PET, c) daily average stream discharges, d) daily average point-water heads in percussion boreholes, and e) daily average groundwater levels in QD.

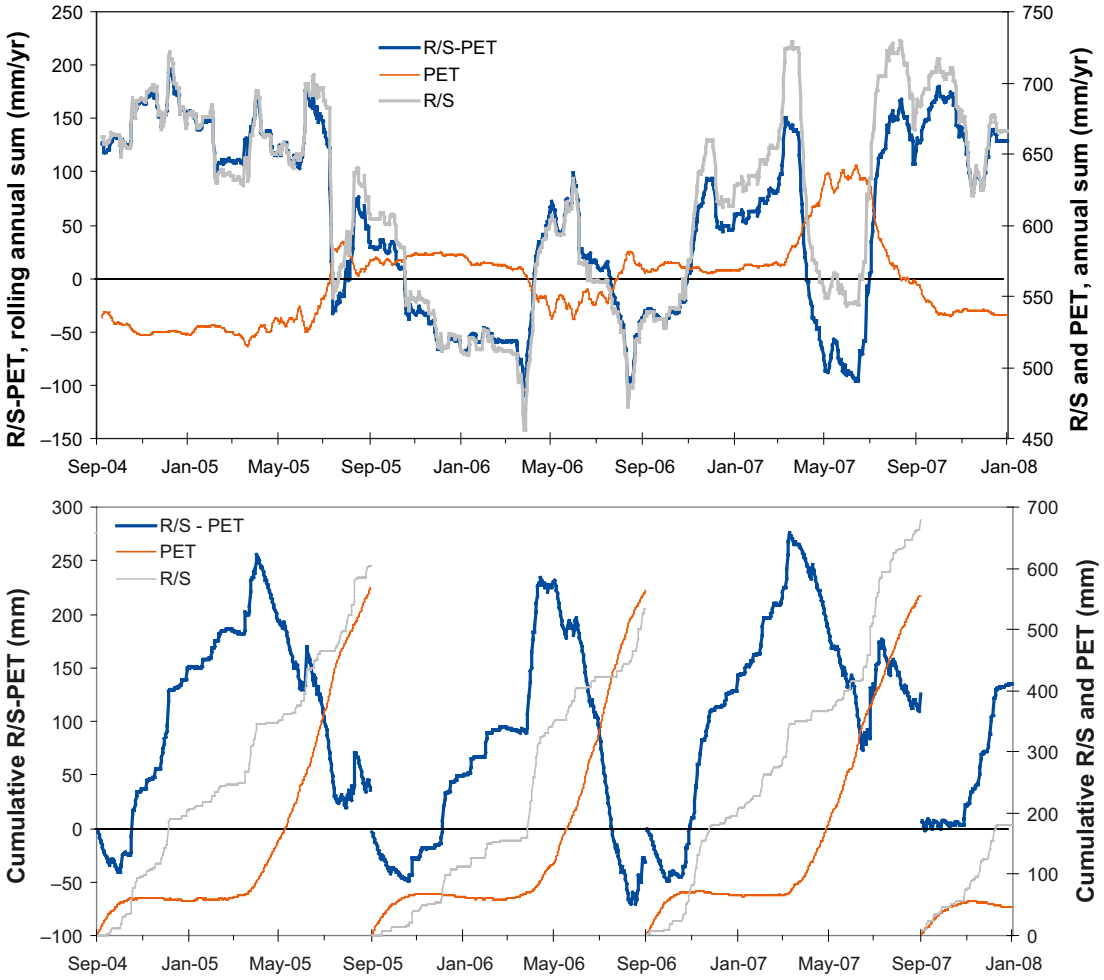

Figure 3-4. *Time-series plots based on daily sums of PET, R/S, and R/S minus PET. Upper plot: Time series of rolling annual sums (starting on Sep. 8, 2004). Lower plot: Time series of accumulated sums for 1 Sep.–31 Aug. periods (starting on Sep. 9, 2003). Rainfall and PET are represented as averages of the Äspö and Plittorp stations.*

The plots of Figure 3-5 illustrate the large influence of the net source term on the temporal variations of the stream discharge. For instance, there was some stream discharge during the rainy late parts of the summers 2004 and 2007, during which the net source term was positive. On the other hand, even though there was substantial rainfall also during the summers of 2005–2006, the net source term was then negative and the stream discharges very small. Moreover, the largest peaks in stream discharges appear to be associated with snowmelt in spring and to some extent also to warm and rainy winters. During these periods, PET is small and the net source term positive.

On the scale of the plots in Figure 3-5, one cannot explore the hydraulic responses in QD and rock to the temporal variations of the source/sink terms. Figures 3-6 and 3-7 therefore provide a more detailed correlation analysis on this matter. These figures are based on data up to Aug. 31, 2007 (i.e. the date of data freeze Laxemar 2.3), since no screening was performed for data after that date (cf. section 2.4.1). Further, only groundwater monitoring wells and percussion borehole sections with more than 150 data days are included in the analysis. The exception from this is borehole section HLX37.2 (137 days of monitoring data in the post-screening data set), which shows a strong correlation to the net source term R/S-PET also for the period Sep. 1–Dec. 31, 2007.

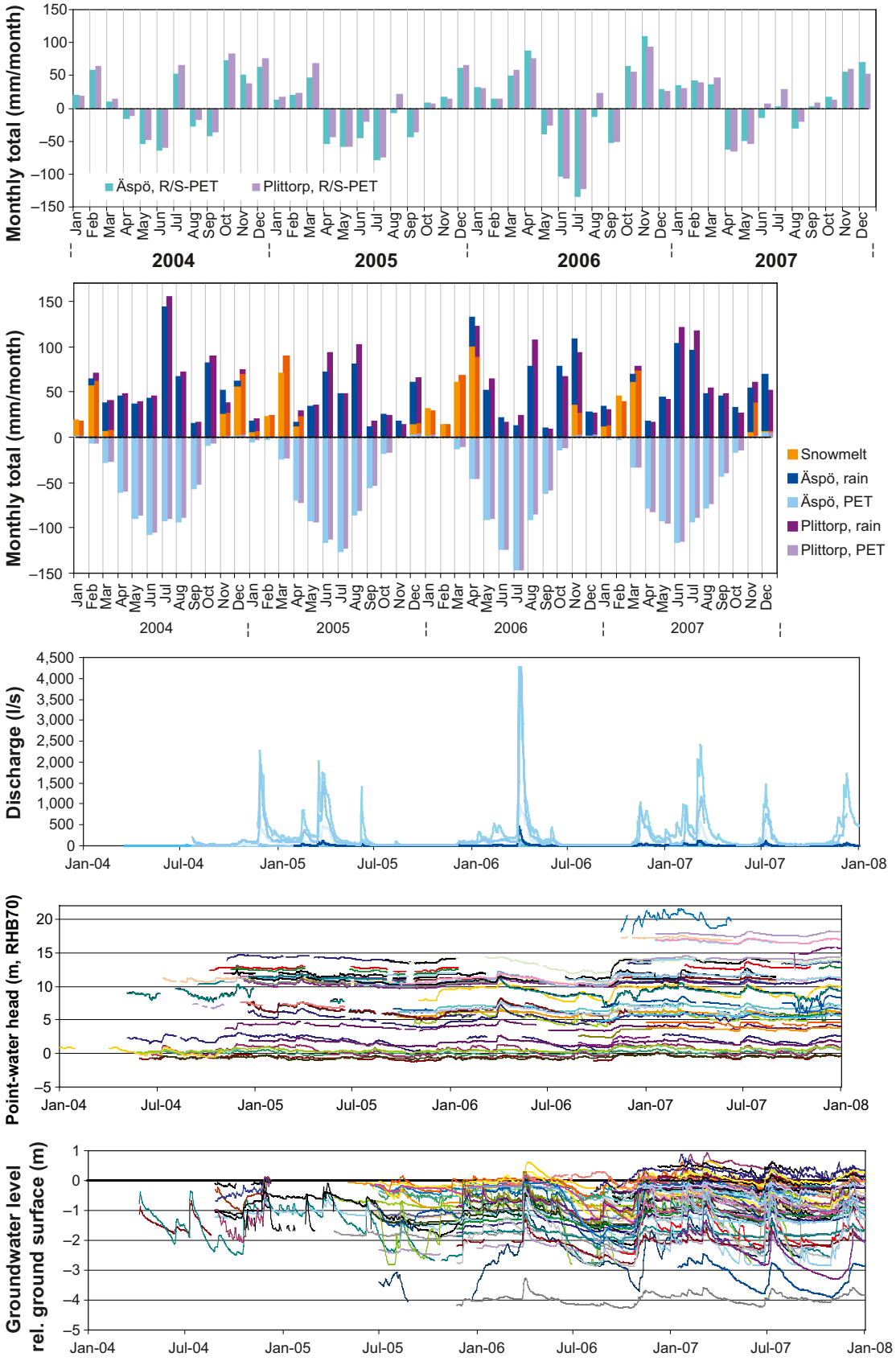

Figure 3-5. *Time-series plots of (from top to bottom) monthly values of R/S-PET, snowmelt, rainfall and PET, daily average stream discharges, daily average point-water heads in percussion boreholes, and daily average groundwater levels in the QD.*

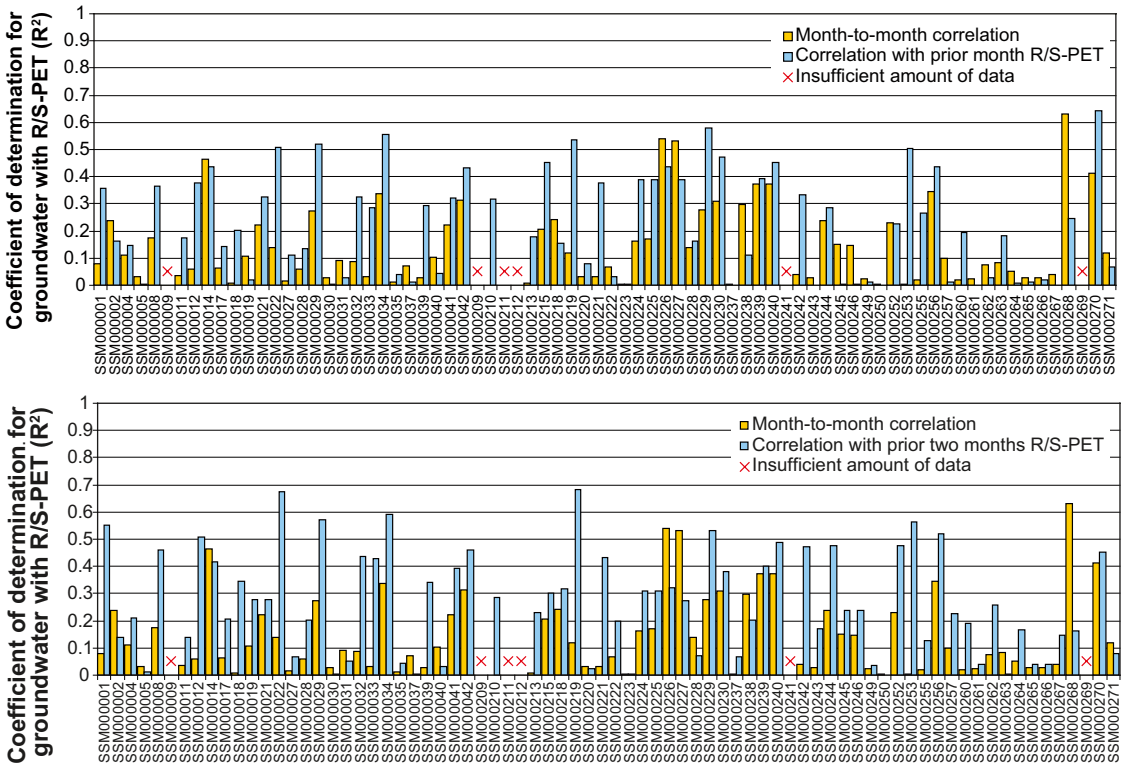

Figure 3-6. *Bar plots of R^2-values for monthly R/S-PET and monthly average groundwater levels in groundwater monitoring wells. Upper plot: R^2-values on a month-to-month basis, compared to R^2-values based on the prior month R/S-PET. Lower plot: R^2-values on a month-to-month basis, compared to R^2-values based on prior two months R/S-PET.*

In Figures 3-6 and 3-7, correlations between data are analysed on data with three different temporal separations; month-to-month, prior month, and prior two months. For instance, "month-to-month correlation" in Figure 3-6 implies that the results are based on monthly average groundwater levels and monthly values of R/S-PET for the same month. "Correlation with prior month R/S-PET" means that the results show correlations of average groundwater levels during one month ("month n") to monthly values of R/S-PET for the previous month ("month n –1"). The same principle applies to the "correlation with prior two months R/S-PET" case in Figure 3-6, as well as the analysis of data from percussion boreholes in Figure 3-7.

For the groundwater monitoring wells (Figure 3-6), the highest R^2-values (> 0.5) on a month-by-month basis are observed for wells SSM000226, -227 and -268. On a prior-month basis, the highest R^2-values are observed for groundwater monitoring wells SSM000022, -29, -34, -219, -253 and -270. Moreover, on a prior-two-months basis, the highest R^2-values are observed for wells SSM000001, -12, -22, -29, -34, -219, -229, -253 and -256. For the percussion boreholes (Figure 3-7), on a month-by-month basis, the highest R^2-values (> 0.5) are observed for borehole HLX37 (section HLX37.2), whereas on a previous-month basis, the highest R^2-values are noted for boreholes HLX01, -06, -07, -40 and -41. Finally, on a prior-two-months basis, the highest R^2-values are observed for HLX01, -06, and -07.

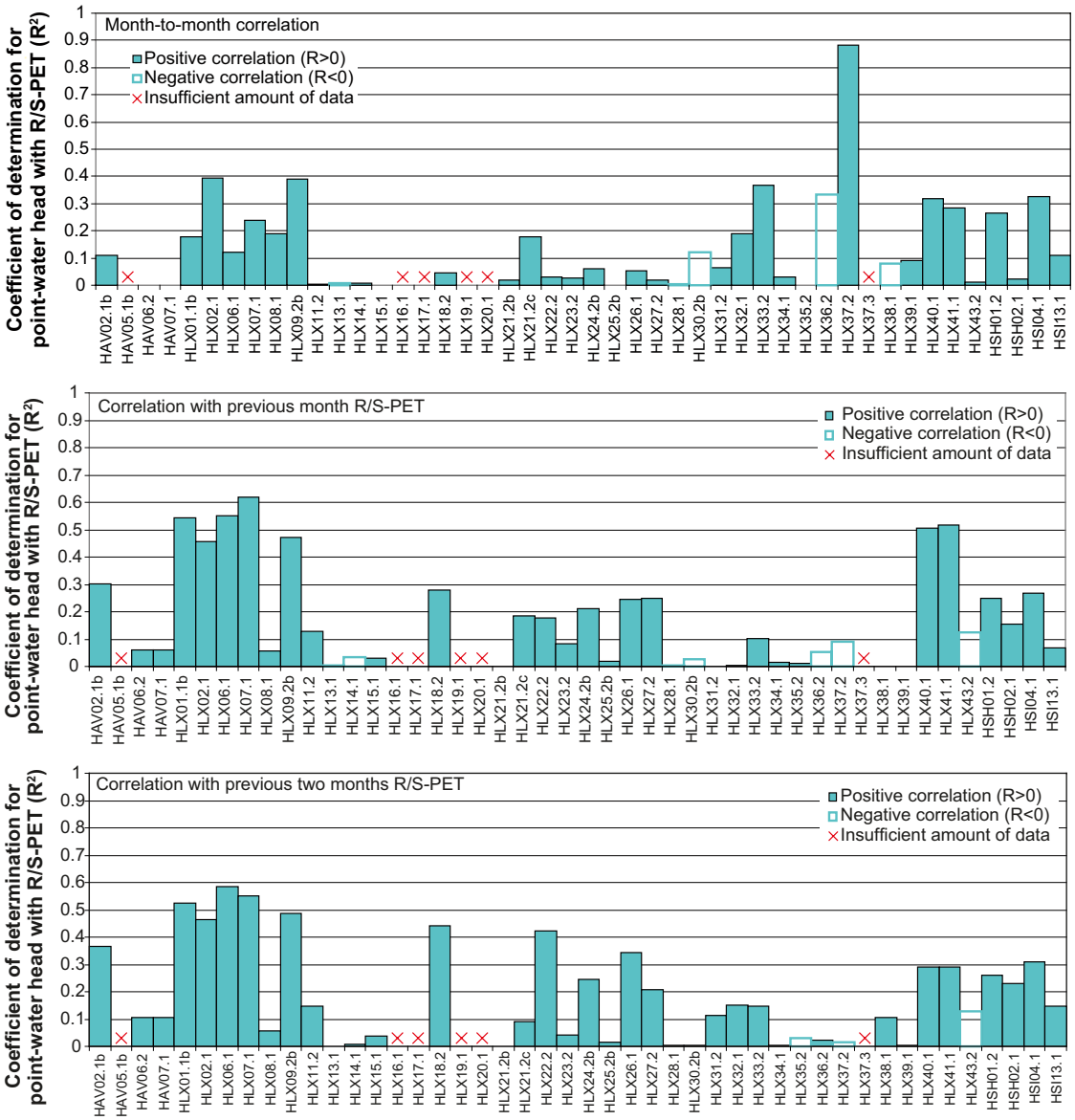

Figure 3-7. *Bar plots showing R^2-values for the monthly values of R/S-PET and monthly average point-water heads in percussion boreholes. Upper plot: R^2-values on a month-to-month basis. Middle plot: R^2-values based on prior month R/S-PET. Lower plot: R^2-values on prior two months R/S-PET.*

Interestingly, with exception of some groundwater monitoring wells, the correlation is stronger if one considers the net source term during the prior or prior two months; for some wells, the correlation is actually highest for the prior two months. Hence, relative to the temporal variations of the net source term, there appears to be a delay in the system monitored by the wells, whereas there seem to be faster responses in the system monitored by the discharge-gauging stations (cf. Figure 3-5) to temporal variations of the net source term. Delayed responses can also be observed for the percussion boreholes. For some boreholes, the correlations to the net source term are of the same order of magnitude as for the groundwater monitoring wells.

3.2 Relationships between groundwater levels in QD and stream discharges

Figures 3-8 to 3-13 investigate the relationship between groundwater levels in the QD and surface-water discharges in streams. Specifically, these figures show time-series co-plots of stream discharges and groundwater levels (in terms of depths below the ground surface) in monitoring wells installed within the catchment area of each gauging station. The considered streams and the associated gauging stations are Vadvikebäcken and Skölkebäcken on the island of Ävrö (gauging stations PSM000341 and -345), Laxemarån (PSM000364), Ekerumsån (PSM000365) and Kärrviksån (PSM000368).

Note that there is one groundwater monitoring well (SSM000007) installed in the stream Gloebäcken catchment area on the island of Ävrö (gauging station PSM000343) but there are no monitoring data from that well. Further, there are no groundwater monitoring wells installed upstream from gauging station PSM000353 in Laxemarån, which implies that stream discharge-groundwater level relationships cannot be investigated for those particular stations. There are also additional wells installed within the considered catchment areas, but they could not be included in the present investigation: Well SSM000020 is installed within the Vadvikebäcken catchment area, but there are no monitoring data from that well. Concerning the Laxemarån catchment area, there are no monitoring data from wells SSM000236 and -254. Moreover, wells SSM000009, -11, 214, -216 to -218, -248, and -251 are installed within the Ekerumsån catchment area, but there are either no monitoring data available or only very short monitoring data sets, in the latter case only for the period prior to the monitoring was initiated at station PSM000365.

For most streams, there appear to be "groundwater level thresholds" (in terms of the depth to the groundwater level), below which there is either no stream discharge or the discharge is very low. Considering groundwater monitoring wells that are located in the vicinity of streams in Figures 3-8 to 3-13, this threshold seems to be on the order of 0.5–2 m below the ground surface. This threshold range can be explained by the fact that the groundwater level at a stream may need to be above the stream bottom in order for stream discharge to occur. It can be speculated that confined conditions prevail in those areas where streams pass relatively conductive postglacial sediments (e.g. peat or postglacial sand) overlying less conductive sediments (e.g. glacial clay). The groundwater level then needs to be within the upper more conductive material, which interacts with the stream, for stream discharge to take place, and also above the stream bottom. In areas with relatively conductive types of QD throughout the QD profile (e.g. areas with till from the rock surface up to the ground surface), the condition for discharge to occur is simply that the groundwater level is above the stream bottom.

A general observation from the co-plots in Figures 3-8 to 3-13 is that periods with high stream discharges are associated with high groundwater levels in the vicinity of the streams; this simply shows that groundwater levels and stream discharges are governed by the same meteorological conditions. It can be seen that the peaks of the stream discharges occur more or less simultaneously as the corresponding peaks of the groundwater levels near the streams. However, groundwater levels do not reach the ground surface in most wells, even in those cases where they are located immediately at the streams. (Flowing) artesian conditions, i.e. the groundwater level is above the ground surface, are observed for wells SSM000041 and -253 within the Laxemarån catchment area, wells SSM000032, -33 and -226 within the Kåreviksån/Lake Frisksjön catchment area, wells SSM000220, -249 and -262 within the Ekerumsån catchment area, and well SSM000243 within the Kärrviksån catchment area.

In most cases, the actual stream furrow (and obviously the stream bottom) is substantially deeper than the surrounding terrain. The above analysis indicates that large part of the stream discharge (at least during peak-discharge periods) may consist of surface (overland) or near-surface groundwater flow, primarily in connection to periods with high groundwater levels and high water contents close to the ground surface. This hypothesis is investigated further in section 3.3.

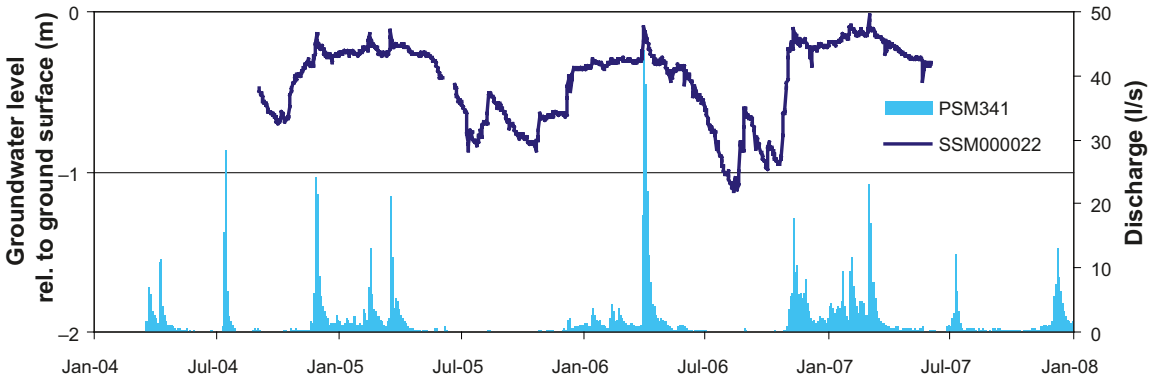

Figure 3-8. *Time-series plot of the groundwater level (metres below ground surface) in groundwater monitoring well SSM000022, installed within the catchment area of surface-water discharge gauging station PSM000341 (approximated by catchment area 23:1) in Vadvikebäcken, co-plotted with the discharge (L·s^{-1}) at PSM000341. Well SSM000022 is located c 10 m from Vadvikebäcken and approximately 350 m upstream (west of) PSM000341.*

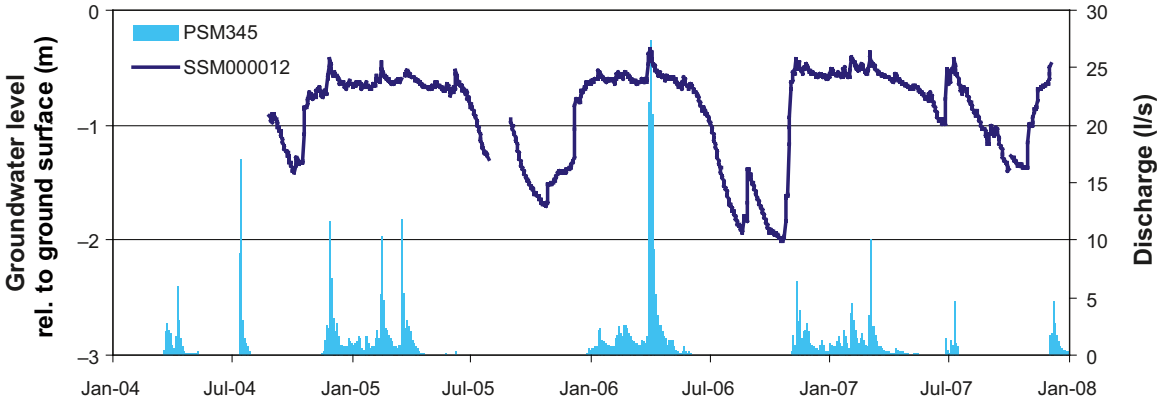

Figure 3-9. *Time-series plot of groundwater levels (metres below ground surface) in groundwater monitoring well SSM000012, installed within the catchment area of surface-water discharge gauging station PSM000345 (approximated by catchment area 26:1) in Skölkebäcken, co-plotted with the discharge (L·s^{-1}) at PSM00034. Well SSM000012 is located c 5 m from Skölkebäcken and approximately 260 m upstream (west of) PSM000345.*

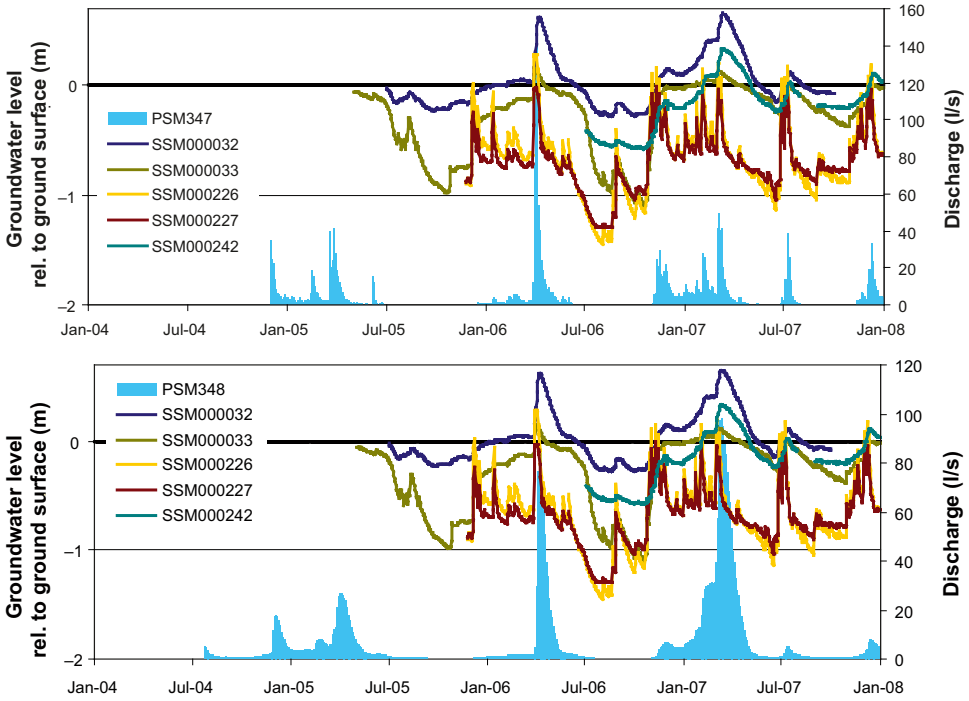

Figure 3-10. *Time-series plots of groundwater levels (metres below ground surface) in 5 groundwater monitoring wells, installed within the catchment area of Lake Frisksjön (catchment subareas 7:1–2), co-plotted with the discharge (L·s^{-1}) at PSM000347 (upper plot) and PSM000348 (lower plot) in Kåreviksån, the latter at the outlet from the lake. The wells are located on the order of 200–300 m from Kåreviksån and the lake, except from SSM000242 that is installed below the lake.*

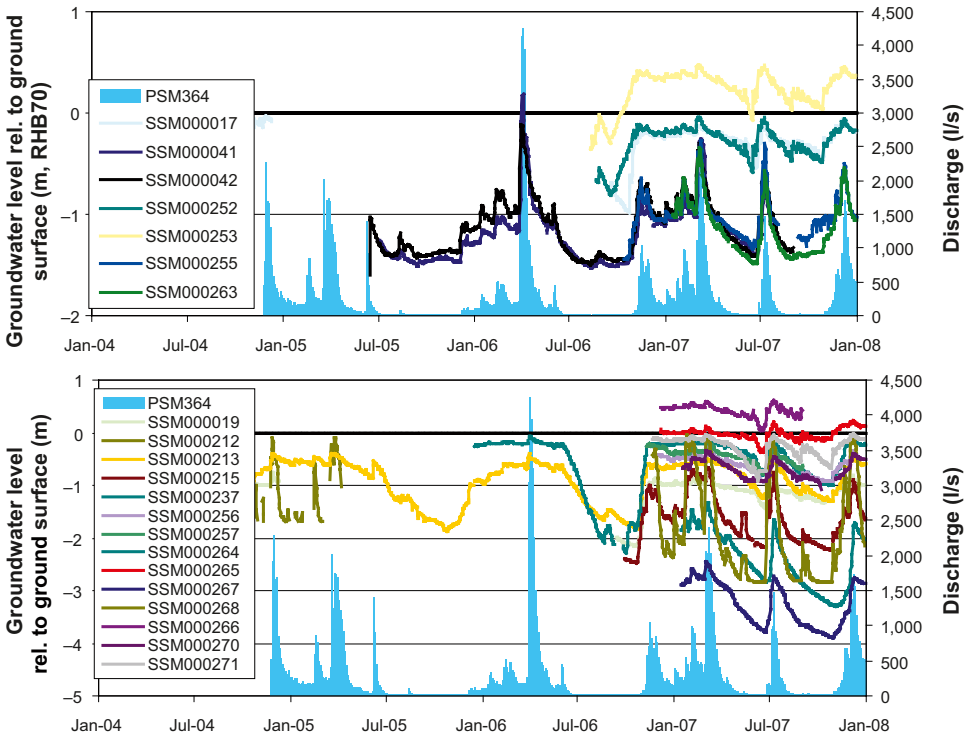

Figure 3-11. *Time-series plots of groundwater levels (metres below ground surface) in groundwater monitoring wells, installed within the catchment area of surface-water discharge gauging station PSM000364 (approximated by catchment subareas 10:1–32) in Laxemarån, co-plotted with the discharge (L·s^{-1}) at PSM000364. Upper plot: Wells located in the vicinity of Laxemarån or its tributaries: SSM000017 (c 50 m from a tributary), -41 and -263 (c 5 m from the stream), -42 (c 10 m from both the stream and PSM000364), -252 (c 5 m from the stream), -253 (at the stream), and -255 (c 80 m from the stream). Lower plot: Wells that are located relatively far away from the stream.*

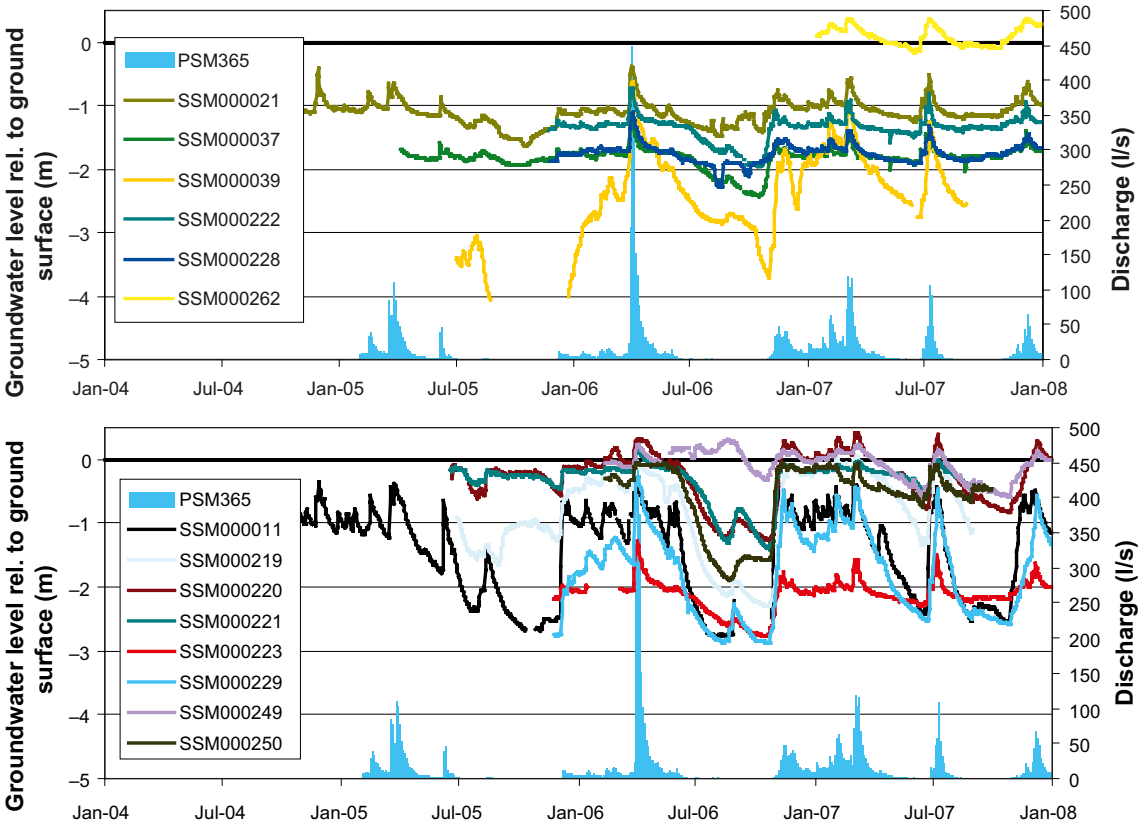

Figure 3-12. *Time-series plot of groundwater level (metres below ground surface) in groundwater monitoring wells installed within the catchment area of surface-water discharge gauging station PSM000365 (approximated by catchment subareas 9:1–3) in Ekerumsån, co-plotted with the discharge ($L \cdot s^{-1}$) at PSM000365. Upper plot: Wells located in the vicinity of Ekerumsån or its tributaries; SSM000021 (c 5 m from the stream), -37 and -222 (c 5 m from a tributary to the stream), -39 (c 50–60 m from the stream), SSM000262 (at the stream), and -228 (c 10 m from the stream). Lower plot: Wells that are located relatively far away from the stream.*

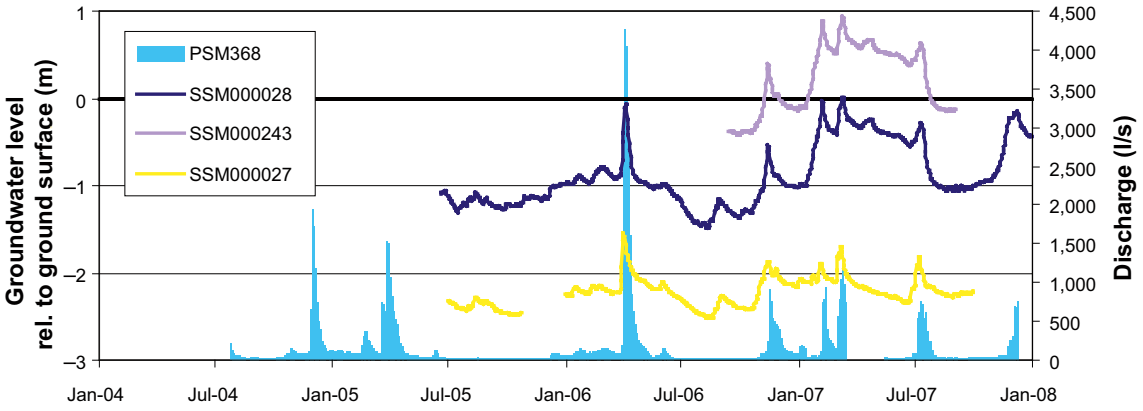

Figure 3-13. *Time-series plot of groundwater levels (metres below ground surface) in 3 groundwater monitoring wells, installed within the catchment area of surface-water discharge gauging station PSM000368 (approximated by catchment areas 5:1–20) in Kärrviksån, co-plotted with the discharge ($L \cdot s^{-1}$) at PSM000368. Well SSM000027 is located c 5 m from the stream, whereas SSM000028 and -243 are located c 170 m from a tributary to the stream.*

3.3 Relationship between stream discharge, electrical conductivity and temperature

This section aims to further investigate the origin (i.e. the dominant source) of stream discharges in Laxemar. Besides pressure transducers (providing water-level data and thereby discharge data), the discharge-gauging stations are equipped with instruments measuring the electrical conductivity (abbreviated EC) and the temperature of the stream water. As an overview of the data set, Figure 3-14 shows time-series summary plots of daily averages of EC (top) and water temperature (bottom) at the discharge-gauging stations.

At the scale of Figure 3-14, one cannot observe any clear seasonal patterns of the stream-water EC. The highest EC values (> 100 mS·m^{-1}) are noted for station PSM000365 in Ekerumsån. On the other hand, stream-water temperatures demonstrate small diurnal variations, overlain by seasonal temperature variations; the highest and lowest temperatures occur during summer and winter, respectively. Figures 3-15 and 3-16 present time-series co-plots of stream discharges, EC and temperature. Note that EC and temperature data at a specific station are not stored in the Sicada database when the calculated stream discharge is zero.

The plots of Figure 3-15 show that periods with large stream discharges generally are associated with a low EC of the stream water, and the opposite for periods with little discharge. It can be speculated that the underlying reason is that surface (overland) water, near-surface groundwater (from the very upper parts of the QD) and water originating from snowmelt act to dilute the stream water during periods with high discharges. On the other hand, during periods with small discharges the stream water may mainly consists of discharging groundwater ("baseflow"), associated with a higher EC. According to the time-series plots of Figure 3-16, the temperature of the stream water is characterised by small diurnal variations overlain by seasonal variations, which do not show any clear correlation to stream discharges.

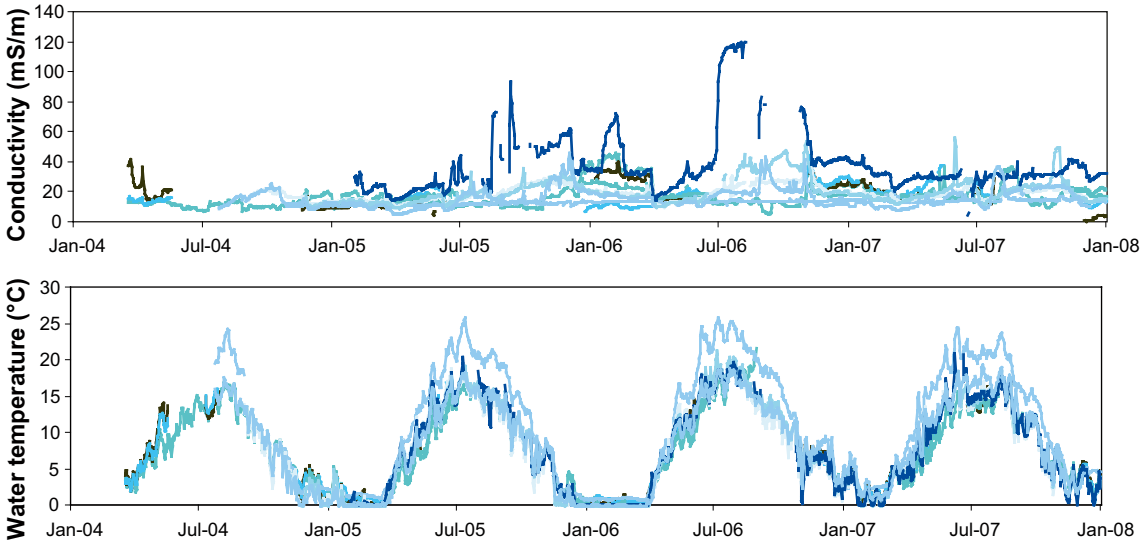

Figure 3-14. *Time-series summary plots of daily average electrical conductivity (top; mS·m^{-1}) and water temperature (bottom; °C) measured at the discharge-gauging stations.*

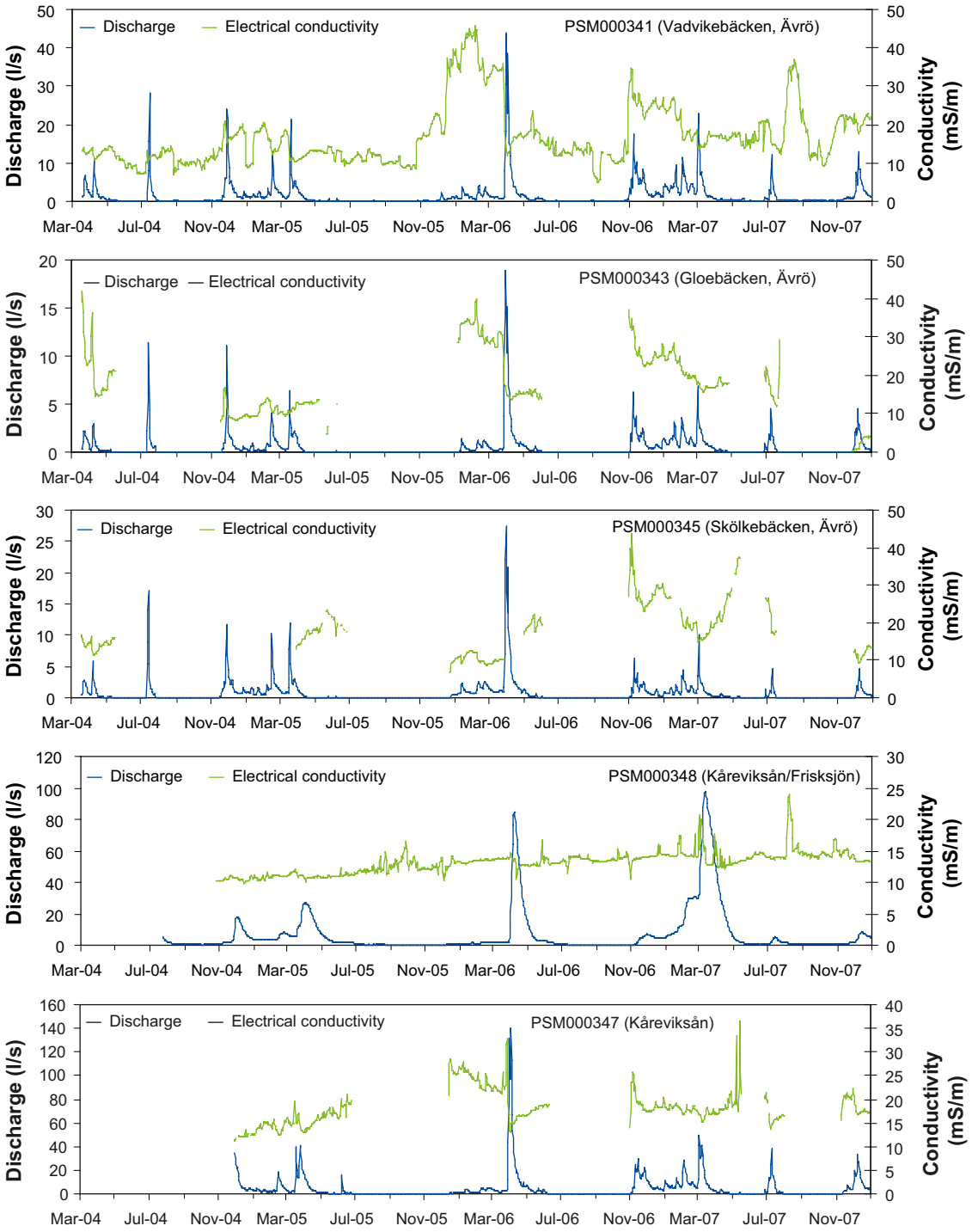

Figure 3-15a. *Time-series co-plots of daily average surface-water discharge and electrical conductivity at discharge-gauging stations PSM000341, -343, -345, -347, and -348.*

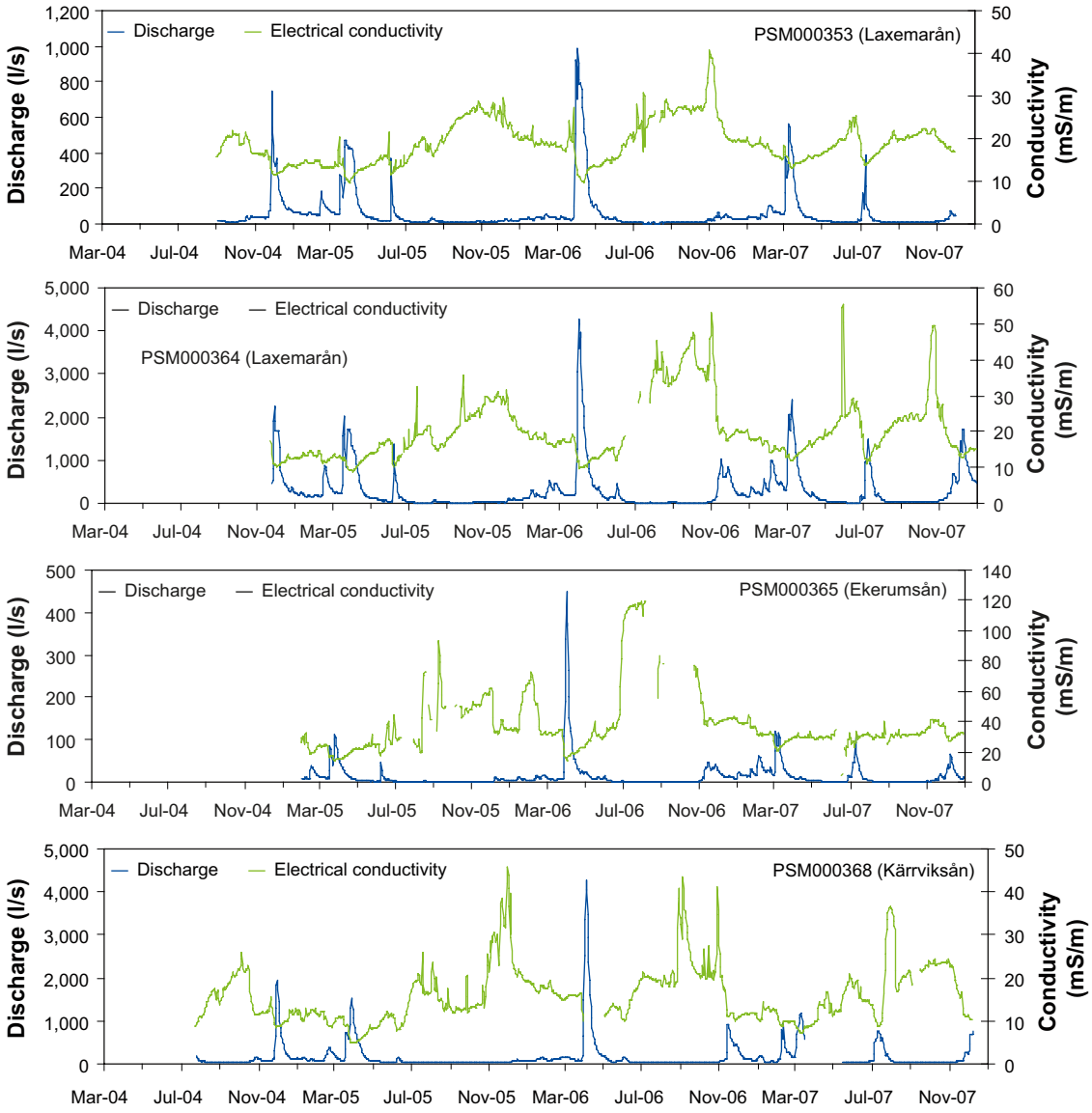

Figure 3-15b. *Time-series co-plots of daily average surface-water discharge and electrical conductivity at discharge-gauging stations PSM000353, -364, -365, and -368.*

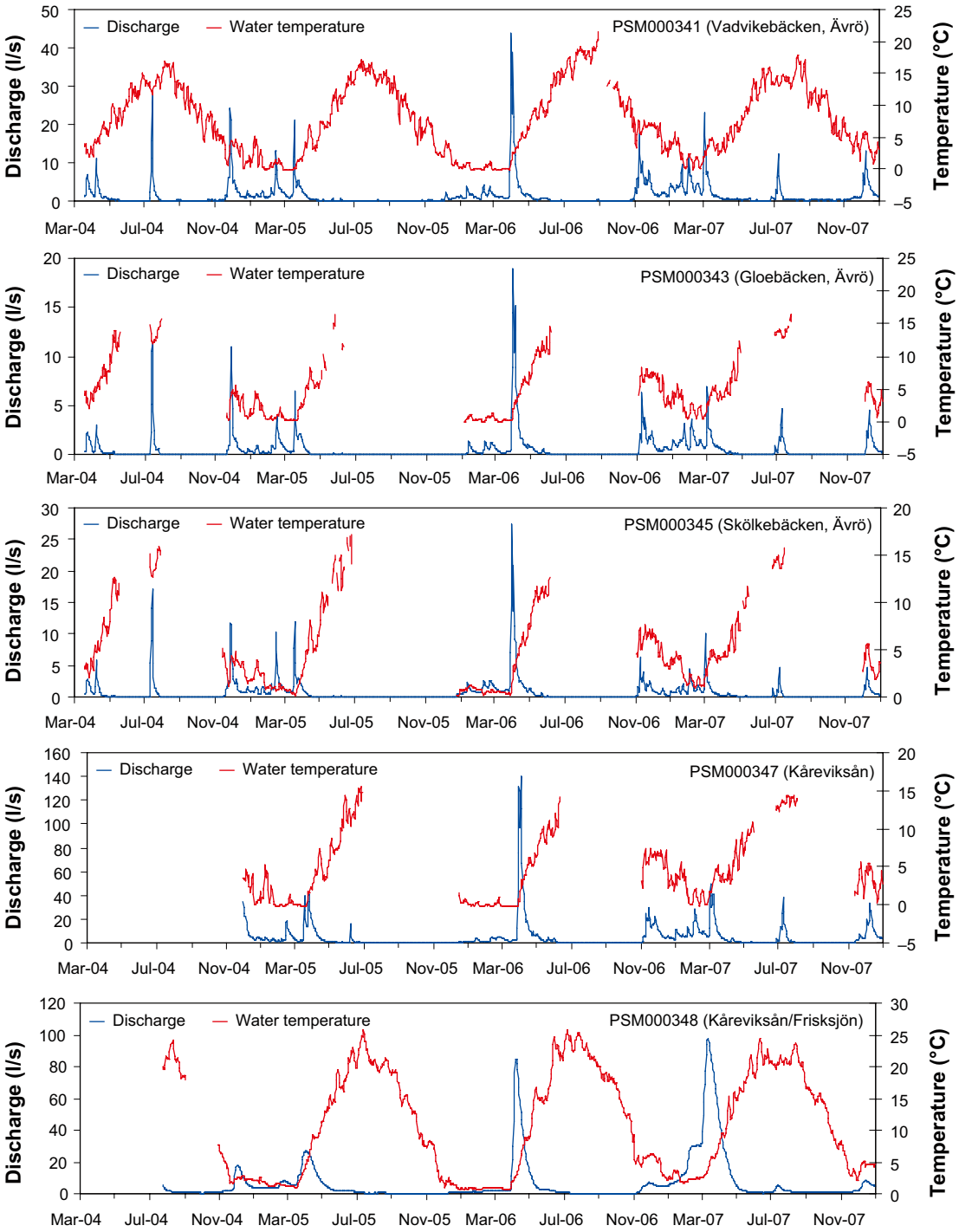

Figure 3-16a. *Time-series co-plots of daily average surface-water discharge and temperature at discharge-gauging stations PSM000341, -343, -345, -347, and -348.*

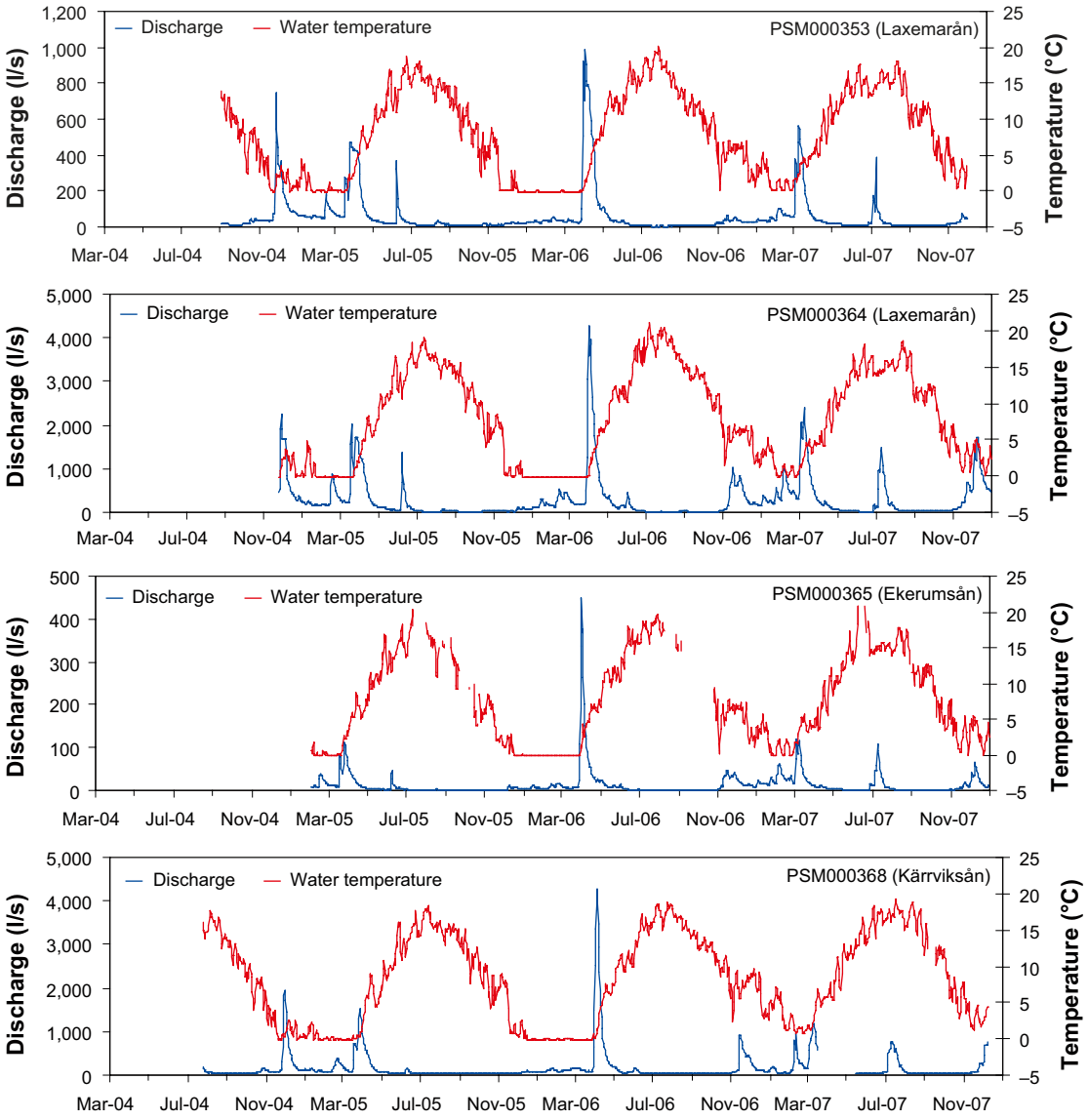

Figure 3-16b. *Time-series co-plots of daily average surface-water discharge and temperature at discharge-gauging stations PSM000353, -364, -365, and -368.*

3.4 Groundwater-wetland interactions

Figures 3-17 to 3-19 show time-series plots of daily average groundwater levels (metres below ground surface) in 6 groundwater monitoring wells installed below wetlands. The figures are presented in a west-to-east order: Wells SSM000245 and -246 are installed in the wetland (bog) Klarebäcksmossen, which is the westernmost and therefore oldest of the three investigated wetlands; it is located farthest from the sea. Moreover, wells SSM000028 and -243 are installed in the intermediate-age wetland Gäster, whereas wells SSM000029 and -244 are installed in a wetland at Kärrsvik, located close to the coast and therefore the youngest of these three wetlands.

In Klarebäcksmossen (Figure 3-17), the screen of well SSM000245 is installed in peat and underlying thin layers of gyttja-bearing peat, clayey gyttja, sandy till and also into the underlying rock. The well is installed at a somewhat lower elevation (22.76 metres above sea level) than the screen of SSM000246 (24.08 metres above sea level), installed in peat only. As indicated by Figure 3-16, the vertical hydraulic head gradient is very small; this can be expected for (raised) bogs /Kellner 2003, 2007/.

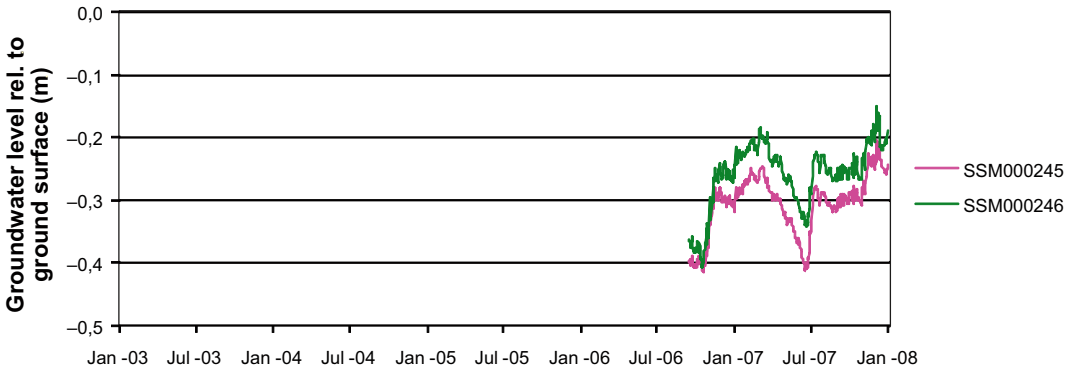

Figure 3-17. *Time-series plot of daily average groundwater levels (metres below ground surface) below the wetland Klarebäcksmossen.*

Figure 3-18. *Time-series plot of daily average groundwater levels (metres below ground surface) below the wetland Gäster.*

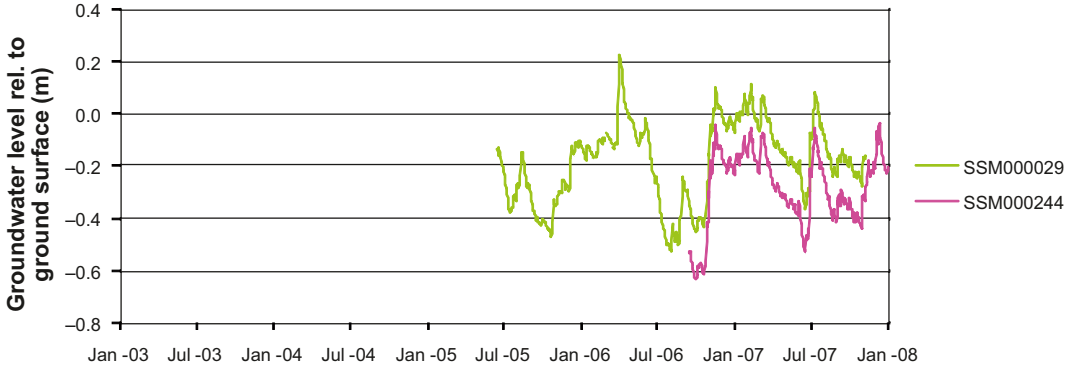

Figure 3-19. *Time-series plot of daily average groundwater levels (metres below ground surface) below the wetland at Kärrsvik.*

In Gäster (Figure 3-18), the screen of well SSM000243 is installed at a much lower elevation (–7.22 metres above sea level) in cobble-bearing clay and sandy till compared to the screen of SSM000028 (1.59 metres above sea level), installed in gyttja above the clay and till layers. The groundwater level is higher in well SSM000243, which hence indicates that there is groundwater discharge at Gäster.

In Kärrsvik (Figure 3-19), the screen of well SSM000244 is installed in sandy till at a lower elevation (–9.59 metres above sea level) than the screen of SSM000029 (–4.74 metres above sea level), installed in silty fine sand below peat and gyttja layers. As indicated by Figure 3-19, the vertical hydraulic head gradient is very small.

3.5 Relationships with the sea-water level

With the objective of investigating potential sea-groundwater interactions, Figures 3-20 to 3-23 show co-plots of the daily average sea-water level, groundwater levels and point-water heads in groundwater monitoring wells and percussion boreholes located below or close to the sea. The co-plots are divided into wells/boreholes in Laxemar (Figure 3-20), on the Simpevarp peninsula (Figure 3-21), and on the islands of Hålö (Figure 3-22) and Ävrö (Figure 3-23).

From Figures 3-20 to 3-23, one can note a co-variation between the sea-water level and the groundwater level in groundwater monitoring wells SSM000040 and SSM000238–240. This is not surprising, since the wells SSM000238–240 are installed below Borholmsfjärden (SSM000238 south of and SSM000239–240 west of the island of Äspö). Moreover, well SSM000040 is located at the coast, close to the outlet of stream Ekerumsån in Borholmsfjärden. Moreover, the point-water heads in percussion boreholes HLX08–09 (on the coast of Laxemar) and HSH01 (at the coast of the Simpevarp peninsula) show some co-variation with the sea-water level.

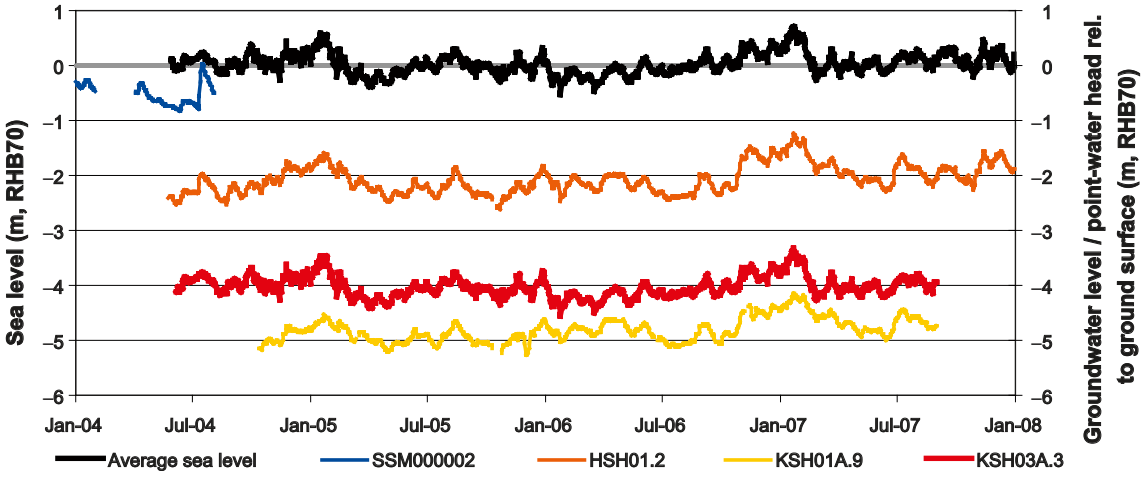

Figure 3-20. *Time series plot of the daily average sea level, groundwater levels in the QD, and point-water heads in percussion boreholes, located close to/below the sea in Laxemar. Groundwater data are shown in terms of the depth below the ground surface.*

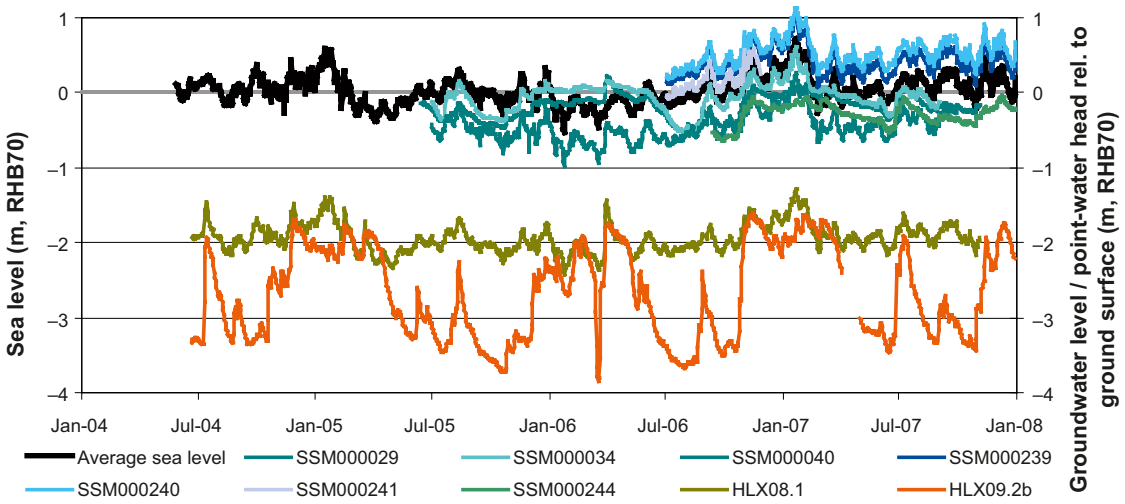

Figure 3-21. *Time series plot of the daily average sea level, groundwater levels in the QD, and point-water heads in percussion boreholes, located close to/below the sea on the Simpevarp peninsula. Groundwater data are shown in terms of the depth below the ground surface.*

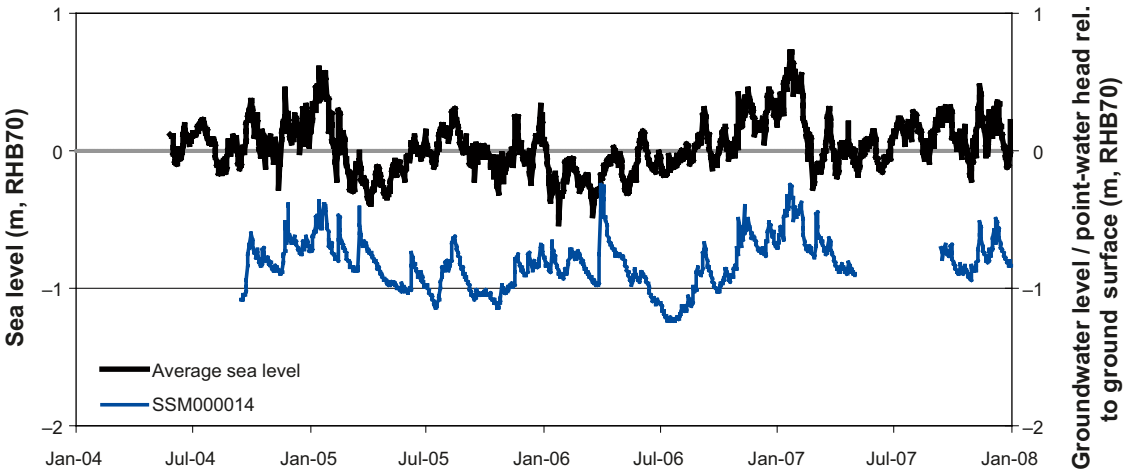

Figure 3-22. *Time series plot of the daily average sea level and the groundwater level in groundwater monitoring well SSM000014 on the island of Hålö. Groundwater data are shown in terms of the depth below the ground surface.*

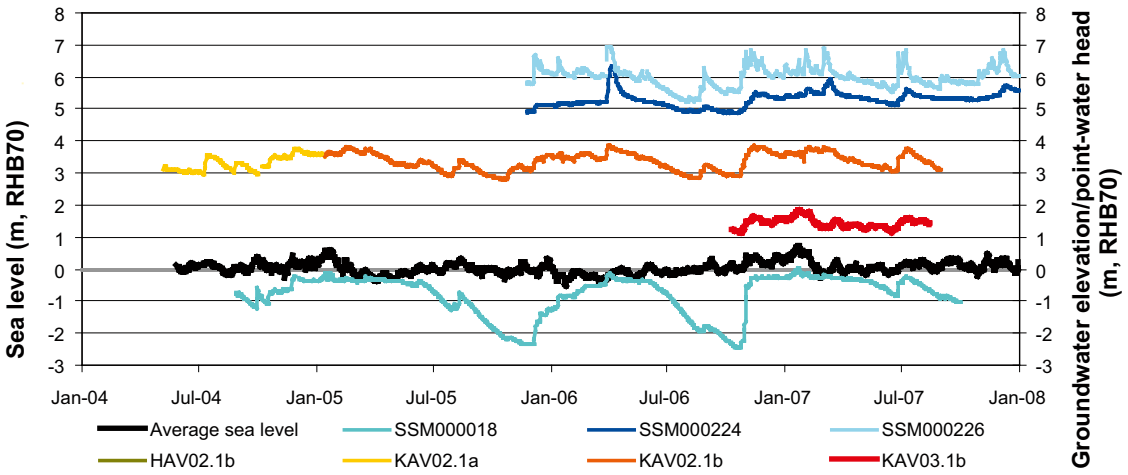

Figure 3-23. *Time series plot of the daily average sea level, groundwater levels in the QD, and point-water heads in percussion boreholes, located close to/below the sea on the island of Ävrö. Groundwater data are shown in terms of the depth below the ground surface.*

Figure 3-24 further explores sea-groundwater interactions, showing R^2-values (month-to-month basis) for groundwater monitoring wells (upper plot) and percussion boreholes (bottom plot), irrespective of location. Note that R^2-values are calculated only for data up to Aug. 31, 2007 (i.e. the date of data freeze Laxemar 2.3), since no screening has been performed for data after that date. Further, only groundwater monitoring wells and borehole sections with more than 6 data months (and only months with at least 15 data days) are considered in the analysis.

As expected (cf. above), the highest R^2-values (> 0.5) for the groundwater monitoring wells are observed for SSM000040 and SSM000238–240. One can also note that there are negative correlations for groundwater monitoring wells SSM000262–264 and -267. For the percussion boreholes, the highest R^2-values are observed for the previously mentioned boreholes HLX08–09 (R^2 = 0.8–0.9) and HSH01 (the R^2-value for section HSH.1 is just below 0.5). Borehole HAV02 (located c 70 m from the coast on the island of Ävrö) has an R^2-value of c 0.3.

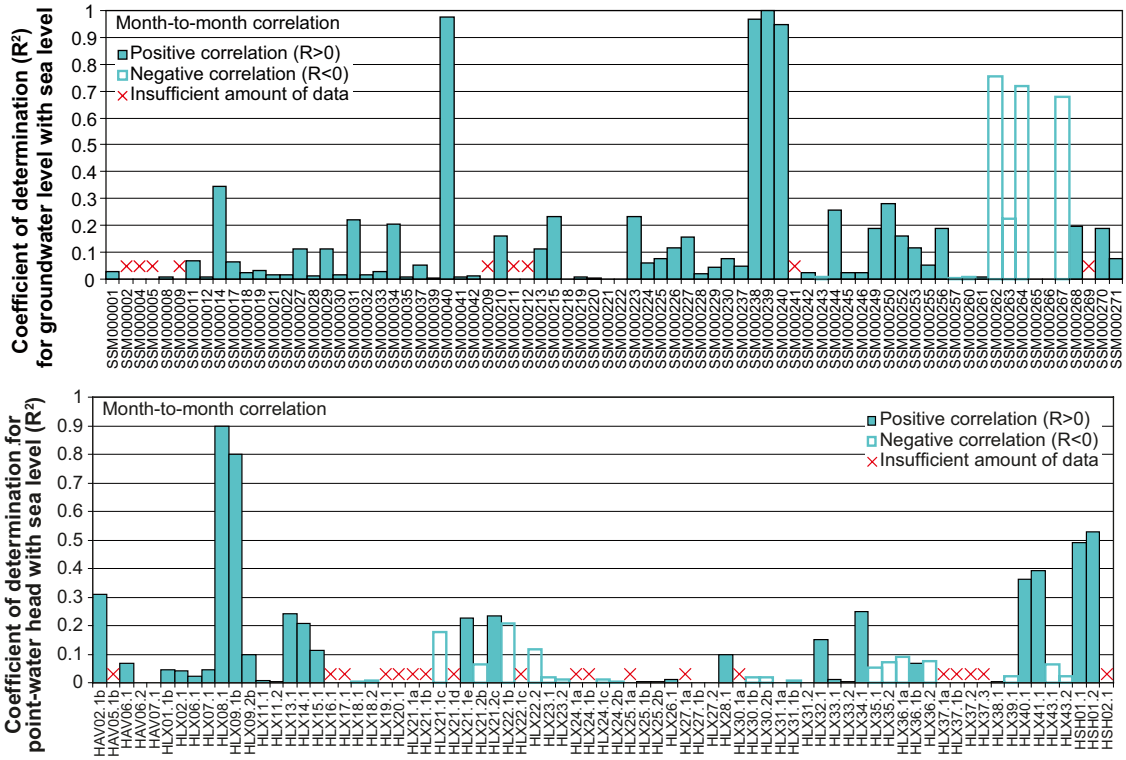

Figure 3-24. *Bar plots showing R^2-values for monthly average sea-water levels and monthly average groundwater levels in groundwater monitoring wells (upper plot) and point-water heads in percussion boreholes (lower plot) on a month-to-month basis.*

Interestingly, the point-water heads in boreholes HLX13, -14 and -21 have some correlation (R^2 = 0.20–0.25) with the sea-water level. These boreholes are located almost 3 km (HLX13 and -14) and c 850 m (HLX21) from the coast, in areas of the Ekerumsån stream valley that coincide with deformation zone ZSMEW007A. Moreover, boreholes HLX15 (R^2 = 0.10) and HLX32 are located c 1.5 km (HLX15) and 3.5 km (HLX32) from the coast, in areas of the Laxemarån stream valley that coincide with deformation zone ZSMNW042A. Borehole HLX34 (R^2 = 0.25) is located c 3 km from the coast in a small valley north of the Ekerumsån stream valley, in an area that coincides with deformation zone ZSMNS059A.

It may be speculated that these correlations across large distances are explained by an influence of the sea-water level on point-water heads within the deformation zones, which accordingly would influence the point-water heads measured in the mentioned boreholes. This explanation is however complicated by that it is difficult to explain the likewise relatively large correlations (R^2 = 0.3–0.4) for boreholes HLX40 and HLX41; these boreholes are located at large distances from the coast, in areas that do not coincide with any identified deformation zone.

3.6 Relationships between lake-water levels and groundwater levels in QD

Figure 3-25 shows time series co-plots of daily average lake-water levels and groundwater levels in groundwater monitoring wells installed below or in the vicinity of three lakes at the site: Lake Frisksjön, Lake Jämsen and Lake Sörå. The upper plot of Figure 3-25 also shows the discharge in the stream Kåreviksån, in which one surface-water discharge gauging station is located upstream of Lake Frisksjön (PSM000347) and another at the outlet from the lake (PSM000348). Figure 3-26 shows time series of the corresponding hydraulic head differentials (i.e. differences in hydraulic head between lakes and groundwater); negative values denote that the head gradient is directed downward, and the opposite for positive values.

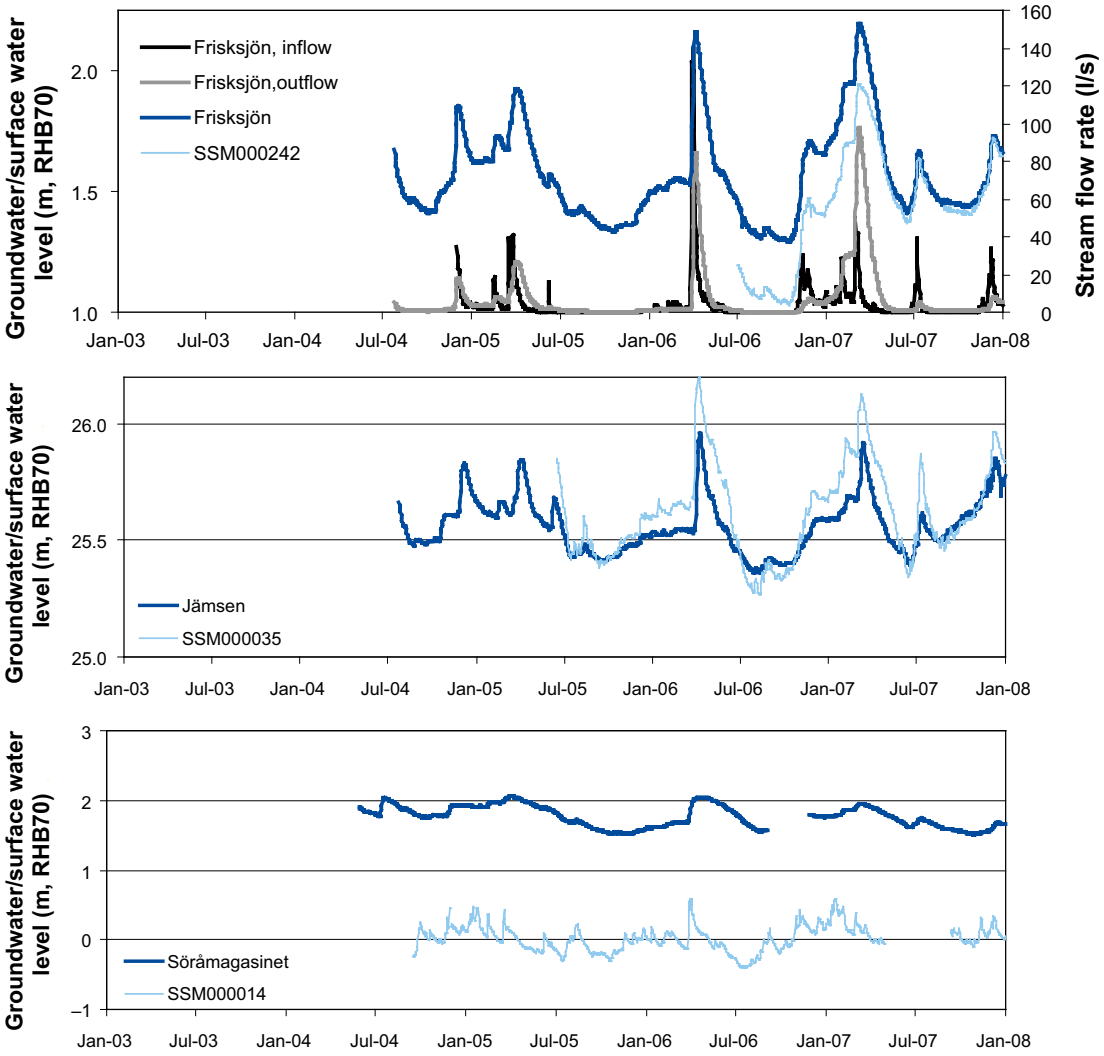

Figure 3-25. *Time series co-plots of daily average lake-water levels and groundwater levels in wells installed below Lake Frisksjön (SSM000242), at the shoreline of Lake Jämsen (SSM000035) and c 180 m from Lake Sörå (SSM000014). The upper plot also includes the daily average stream discharge into and out from Lake Frisksjön.*

The upper plots of Figures 3-25 and 3-26 indicate a small downward hydraulic head gradient from Lake Frisksjön to the till below the lake sediments, whereas the middle plots of the figures show a temporally variable gradient between Lake Jämsen and the till at the lake shoreline. The Lake Sörå data indicate a downward gradient, but the closest well (SSM000014) is located too far away from the lake to allow any conclusions to be drawn concerning groundwater-surface water interaction in that case.

According to the Lake Jämsen data, the shoreline areas of the lake act as groundwater discharge areas during most of the year, whereas these areas contribute to groundwater recharge during some relatively short periods during the summers of 2005–2007. The upper plot of Figure 3-25 shows that there is a large degree of co-variation between the lake-water level in Lake Frisksjön, the groundwater level below the lake and the stream discharge into and out from the lake. The upper plot of Figure 3-26 shows that there are conditions for groundwater recharge from Lake Frisksjön to the underlying QD, which may seem surprising considering the topographical location of the lake. In order to identify potential surveying errors, gauging station PSM000348 (which measures both the lake-water level and the (stream) discharge from the lake) was re-surveyed in Jun. 2007; no error was noted concerning the elevation data. It is not clear why there is a change of the head differential during spring 2007 and onwards, after which there is almost no head gradient between the lake and the underlying till.

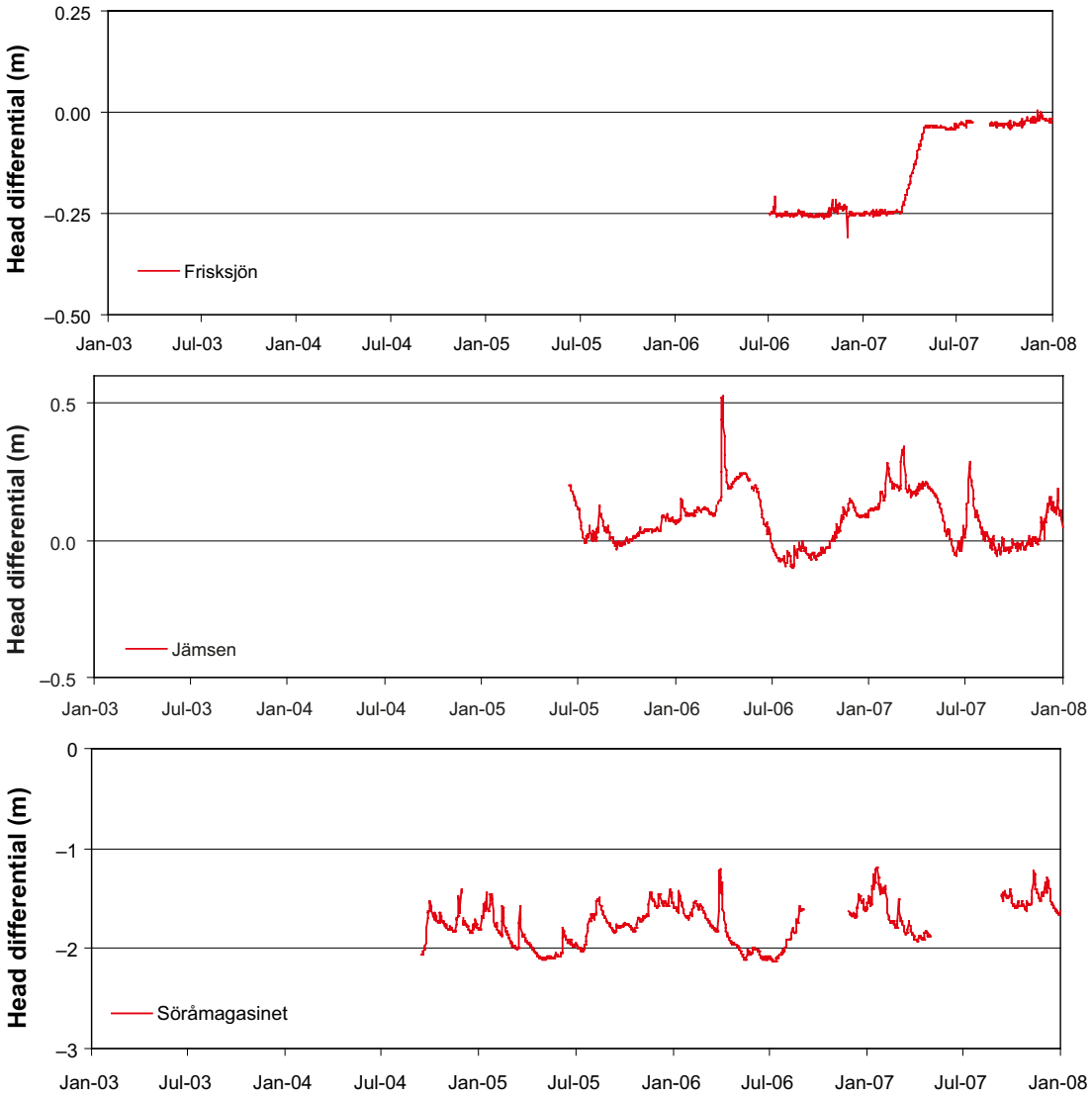

Figure 3-26. *Hydraulic head differentials between lakes and groundwater monitoring wells (cf. Figure. 3-25).*

3.7 Relationships between groundwater levels in QD and point-water heads in rock

This section examines relationships between groundwater levels in the QD and point-water heads in the rock. Specifically, monitoring time series from these two hydrogeological flow domains are compared in order to investigate hydraulic interactions, and to interpret to what extent such interactions are influenced by factors such as topography, type of QD, and the presence or absence of deformation zones in the rock. The overall objective is to generalise and try to draw useful conclusions from the field observations.

This type of analysis would preferably use monitoring data from wells in the QD and boreholes in the rock that are located in the immediate vicinity of each other (say, 10–20 m apart or so). However, there are few close wells and boreholes in Laxemar, which obviously limits the possibilities to make the intended comparisons. The comparisons are also complicated by the fact that many parts of the area are characterised by relatively large topographical variations over short distances. The criterion used in this report for selecting wells and boreholes for the comparison is (somewhat arbitrarily) set to 100 m, simply expressed as the horisontal (X,Y) distance between

the top of wells and borehole casings. Except for the mentioned complications due to topographical variations, a further difficulty is depth-dependent salinity of groundwater in rock, which results in a depth-dependent groundwater density. As far as possible, this latter issue is taken into account in the following, based on the findings in section 2.4.4 and Appendix 1.

The following sections present time-series plots of groundwater levels and point-water heads, and the same data sets in terms of depths below the ground surface. Both these ways of representing the data are used to assess groundwater interactions between QD and rock. Each comparative analysis below includes a brief summary of local conditions in terms of topography, type of QD and whether any deformation zones in rock have been identified in the vicinity of the wells and boreholes being analysed. In order to facilitate for the reader to understand how data are evaluated, these types of information (which are available in the SKB GIS database) are exemplified in Figures 3-27 to 3-30, which show the locations of groundwater monitoring wells overlain on the detailed QD map (Figures 3-27 and 3-28) and a map of the QD depth according to the regolith depth and stratigraphy model (Figures 3-29 and 3-30).

In addition, Figure 3-31 shows the locations of a subset of the groundwater monitoring wells, in which each well has been classified in terms of its topographical position and the type of QD at the ground surface. The data comparisons in the following sections are divided into three parts: Potential groundwater recharge areas (section 3.7.1), potential groundwater discharge areas (section 3.7.2) and areas with small gradients between QD and rock (section 3.7.3). It should be observed that this simply is a manner of organising the data presentation; the division is based on observed hydraulic gradients, and not any sort of á priori assumption concerning groundwater flow directions.

It should be noted that there are additional well-borehole pairs that potentially could be used for the present type of data comparison. However, the following wells and boreholes could not be analysed here since no monitoring data were available in the Laxemar 2.3 data freeze:

- SSM000226/-227 vs. HLX04.
- SSM000214 vs. HLX21 and -22.
- SSM000209 vs. HLX20.
- SSM000216 vs. KLX02, -07A and -07B.
- SSM000254 vs. HLX28.
- SSM000269/-270 vs. HLX42.
- SSM000271 vs. KLX16A.
- SSM236/-237 vs. KLX11E.
- SSM000012 vs. HAV09 and -10.
- SSM000006 vs. KSH03A and -03B.
- SSM000007 vs. KAV04A and -04B.
- SSM000024 vs. KAV02.

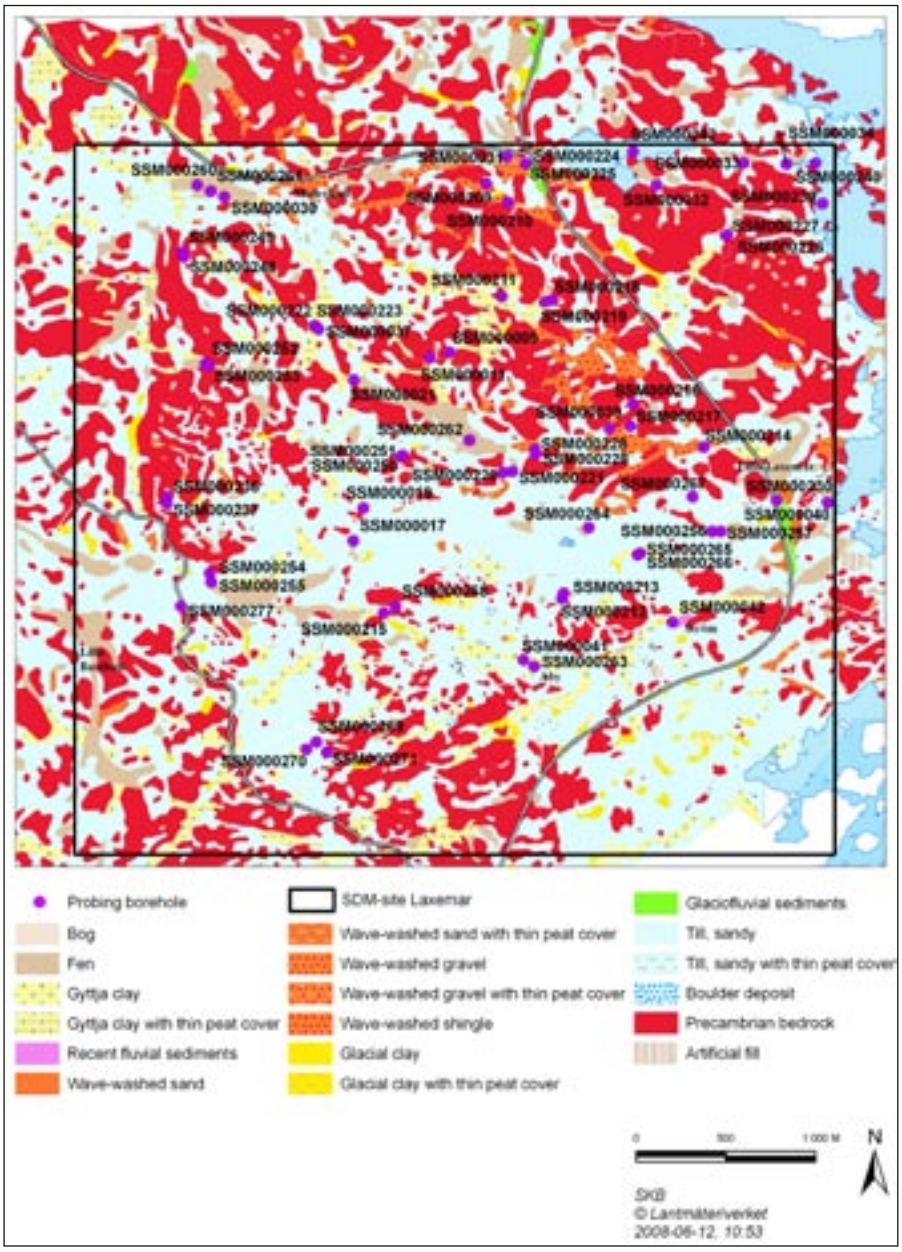

Figure 3-27. *Map of groundwater monitoring wells (denoted "Probing boreholes" in the map) inside the Laxemar local model area, overlain on the detailed QD map.*

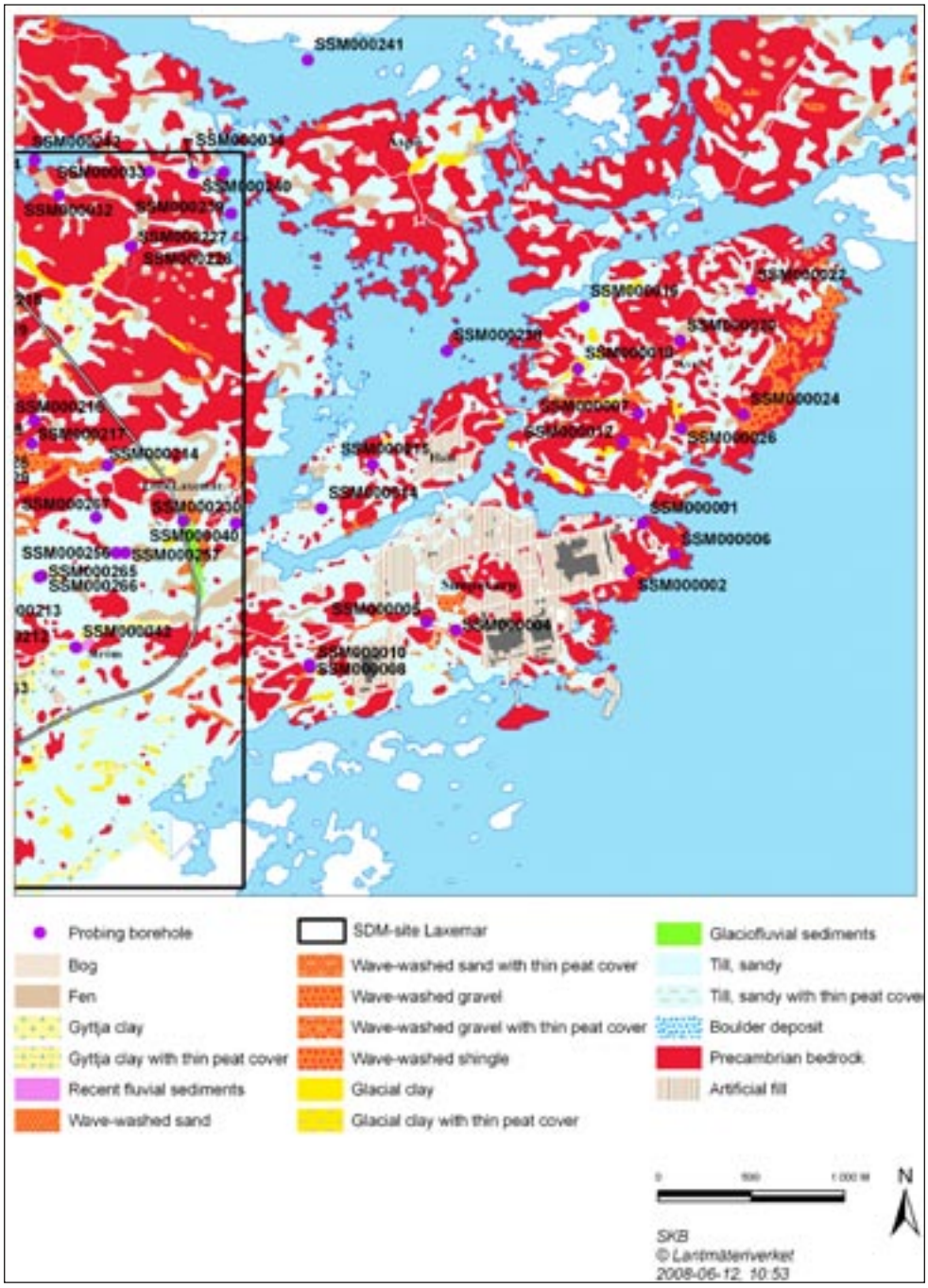

Figure 3-28. *Map of groundwater monitoring wells (denoted "Probing boreholes" in the map) outside the Laxemar local model area, overlain on the detailed QD map.*

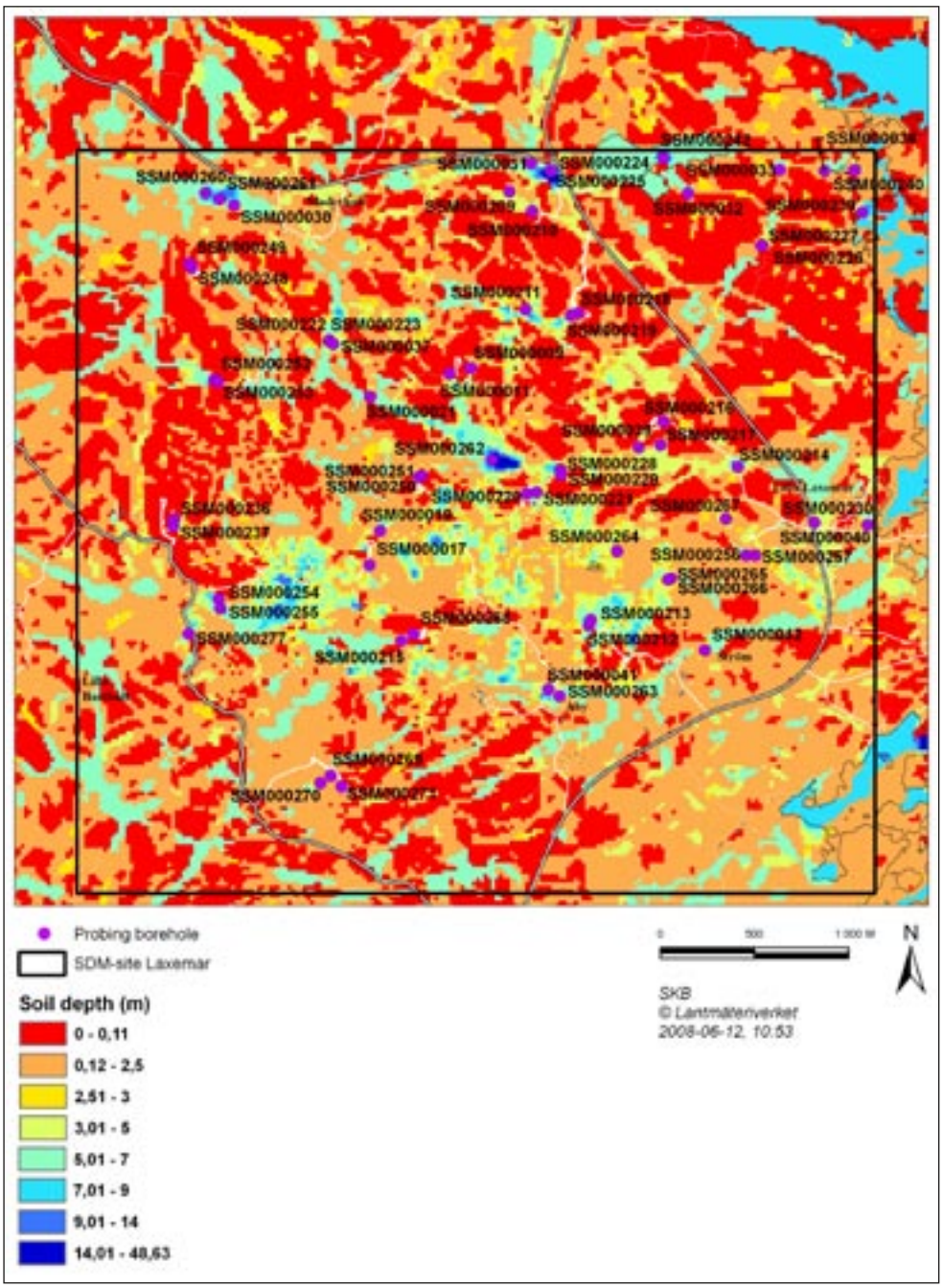

Figure 3-29. *Map of groundwater monitoring wells (denoted "Probing borehole" in the map) inside the Laxemar local model area, overlain on a map of the QD depth (denoted "Soil depth" in the map).*

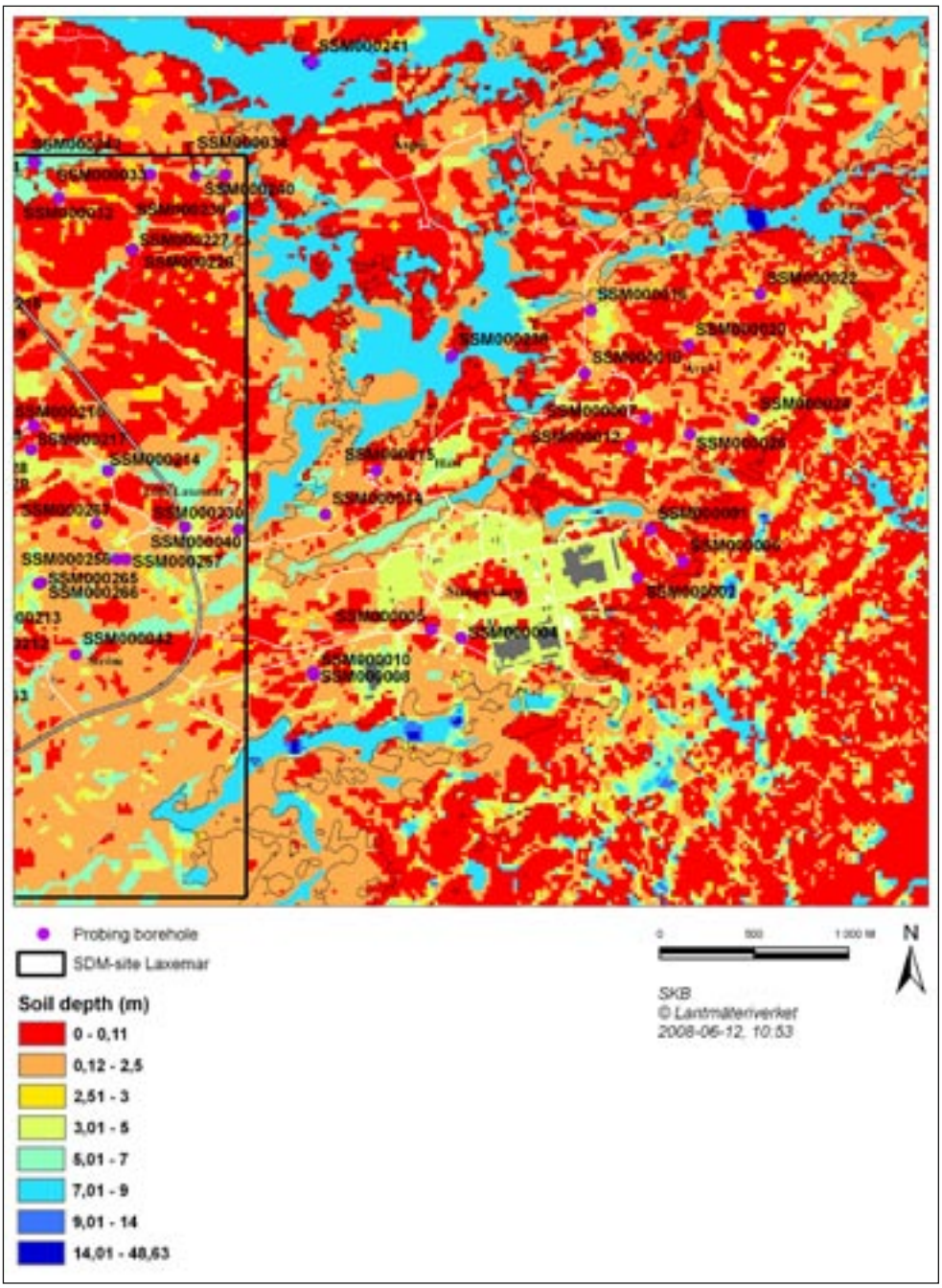

Figure 3-30. *Map of groundwater monitoring wells (denoted "Probing borehole" in the map) outside the Laxemar local model area, overlain on a map of the QD depth (denoted "Soil depth" in the map).*

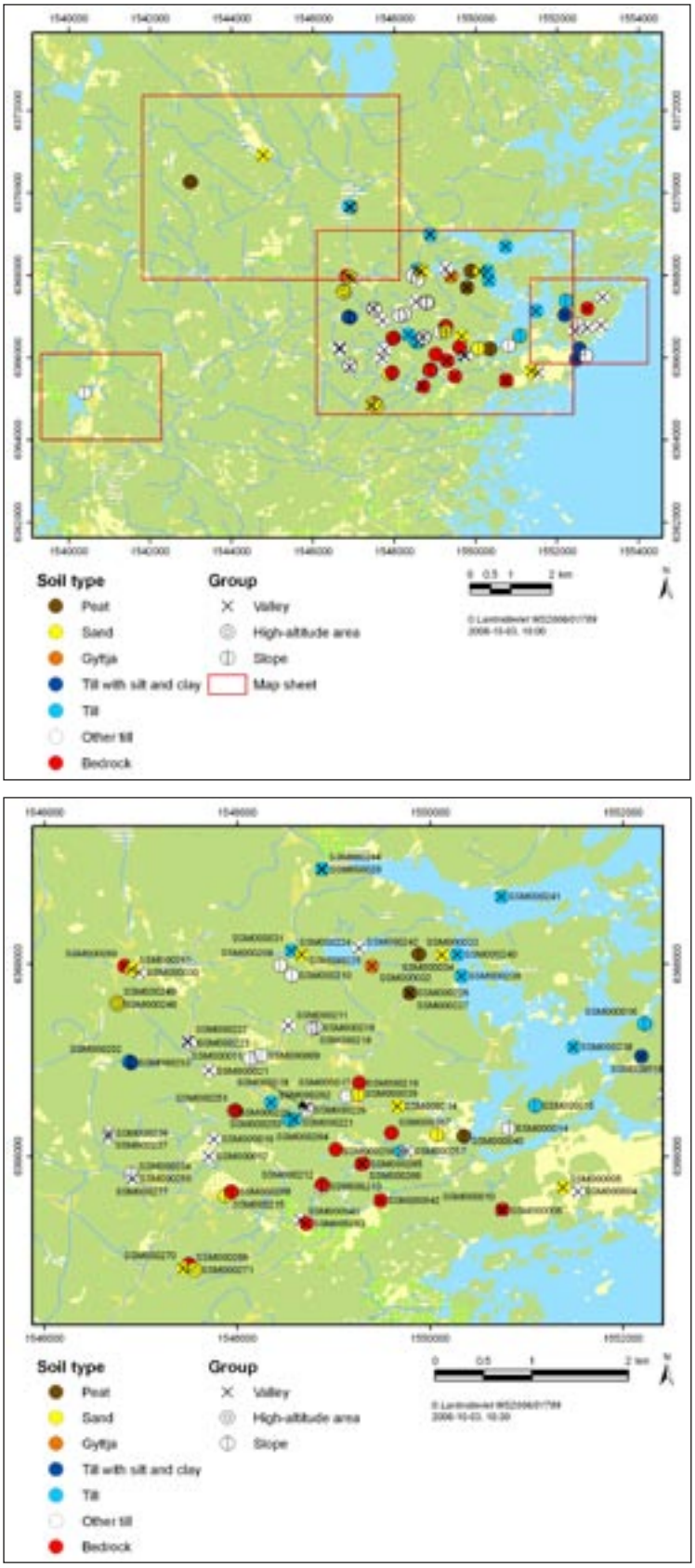

Figure 3-31a. *Overview map (top) and a map of groundwater monitoring wells, classified according to topography and type of QD at well-screen depth.*

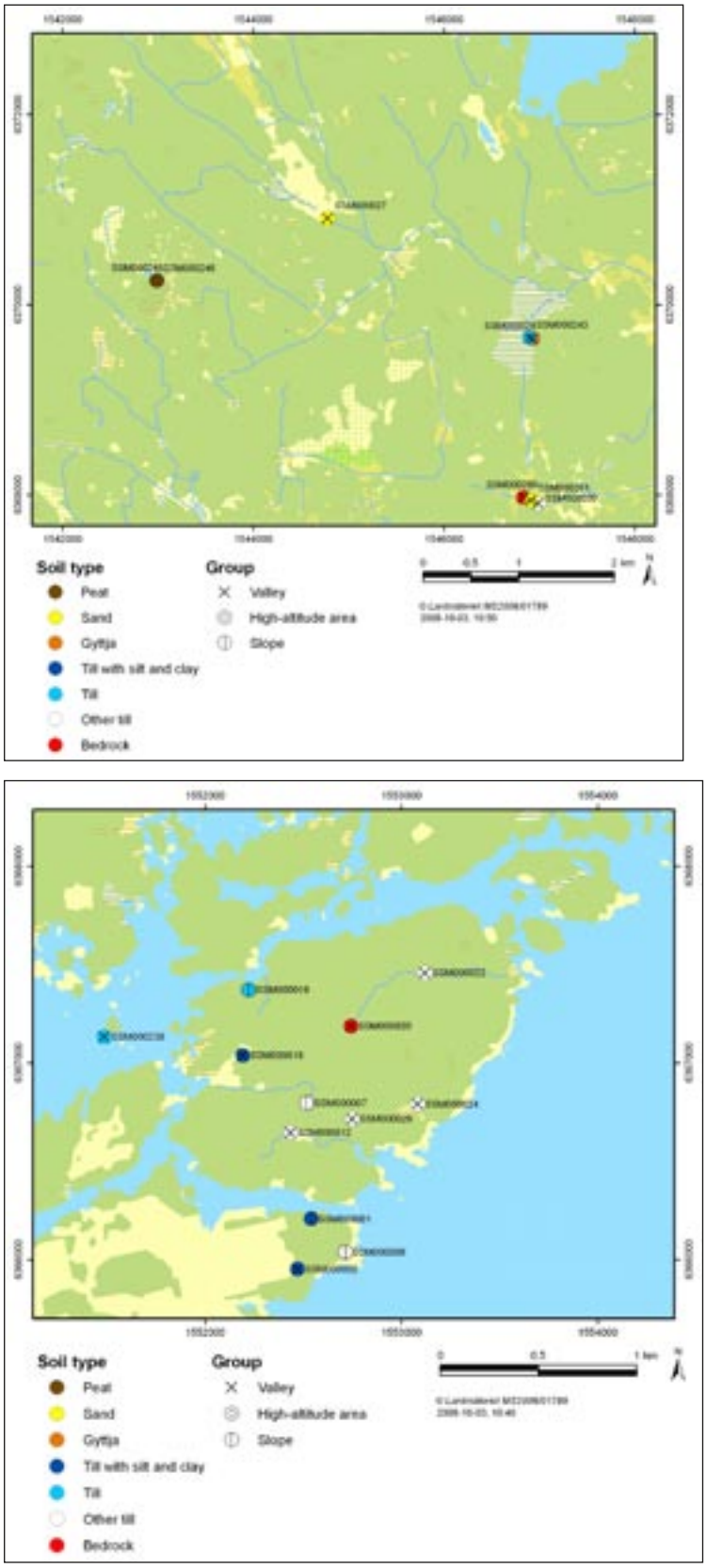

Figure 3-31b. *Maps of groundwater monitoring wells (continued), classified according to topography and type of QD at well-screen depth.*

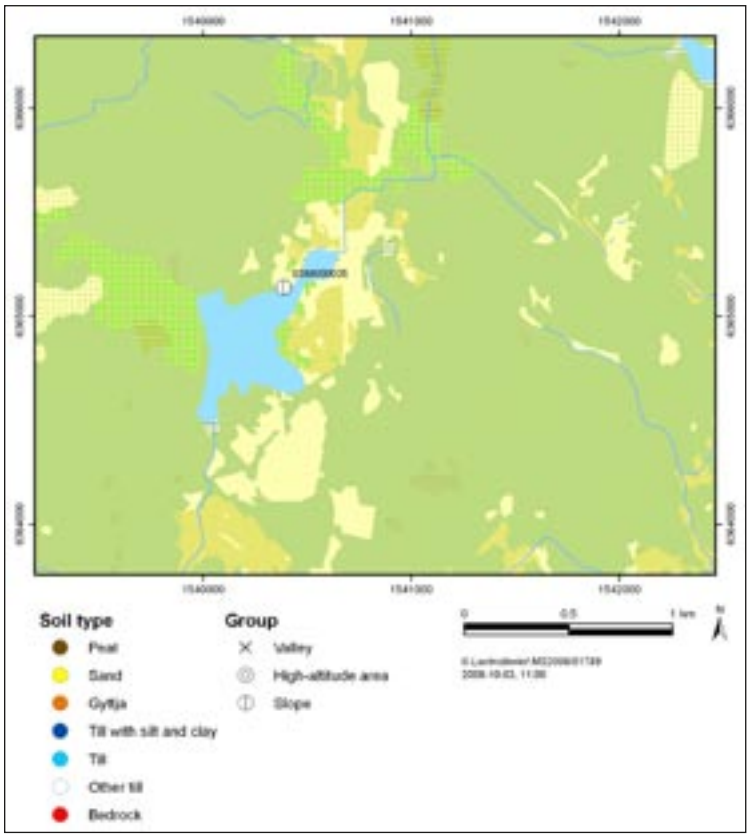

Figure 3-31c. *Map of groundwater monitoring wells (continued), classified according to topography and type of QD at well-screen depth.*

3.7.1 Potential recharge areas: Higher groundwater levels in QD than point-water heads in rock

Table 3-1 summarises some basic geometrical data for the well-borehole pairs that are analysed in this section, whereas the overview map in Figure 3-32 for orientation shows their locations in terms of sites (Site 1-8). Note that horisontal (XY) distances in Table 3-1 are approximate.

Table 3-1. Geometrical data for wells and boreholes. G.s.e. = Ground-surface elevation. R.s.e. = Rock-surface elevation. Hor. dist. = Horisontal well-borehole distance.

Gw. monitoring well ID	G.s.e. (m.a.s.l.)	R.s.e. (m.a.s.l.)	Perc./core borehole ID	G.s.e. (m.a.s.l.)	B.s.e. (m.a.s.l.)	Hor. dist. (m)
SSM000218	18.73	15.83	KLX09	23.33	22.69	50
SSM000219	15.87	11.17	KLX09			90
SSM000218			KLX09F	19.31	19.31	15
SSM000219			KLX09F			40
SSM000009	14.92	10.82	KLX08	24.05	21.62	75
SSM000011	16.30	11.50	KLX08			80
SSM000212	13.28	9.49	KLX05	17.54	17.54	55
SSM000212			KLX12A	17.59	16.09	55
SSM000220	12.83	10.04	KLX10	18.16	17.86	60
SSM000019	12.71	10.01	KLX03	18.39	17.42	80
SSM000250	15.94	12.74	KLX18A	20.71	20.22	50
SSM000252	17.99	11.29	HLX39	26.79	26.79	95
SSM000252			HLX40	25.48	25.48	95
SSM000253	17.46	13.86	HLX39			85
SSM000253			HLX40			75
SSM000002	1.50	–0.60	KSH01A	5.32	No data	70

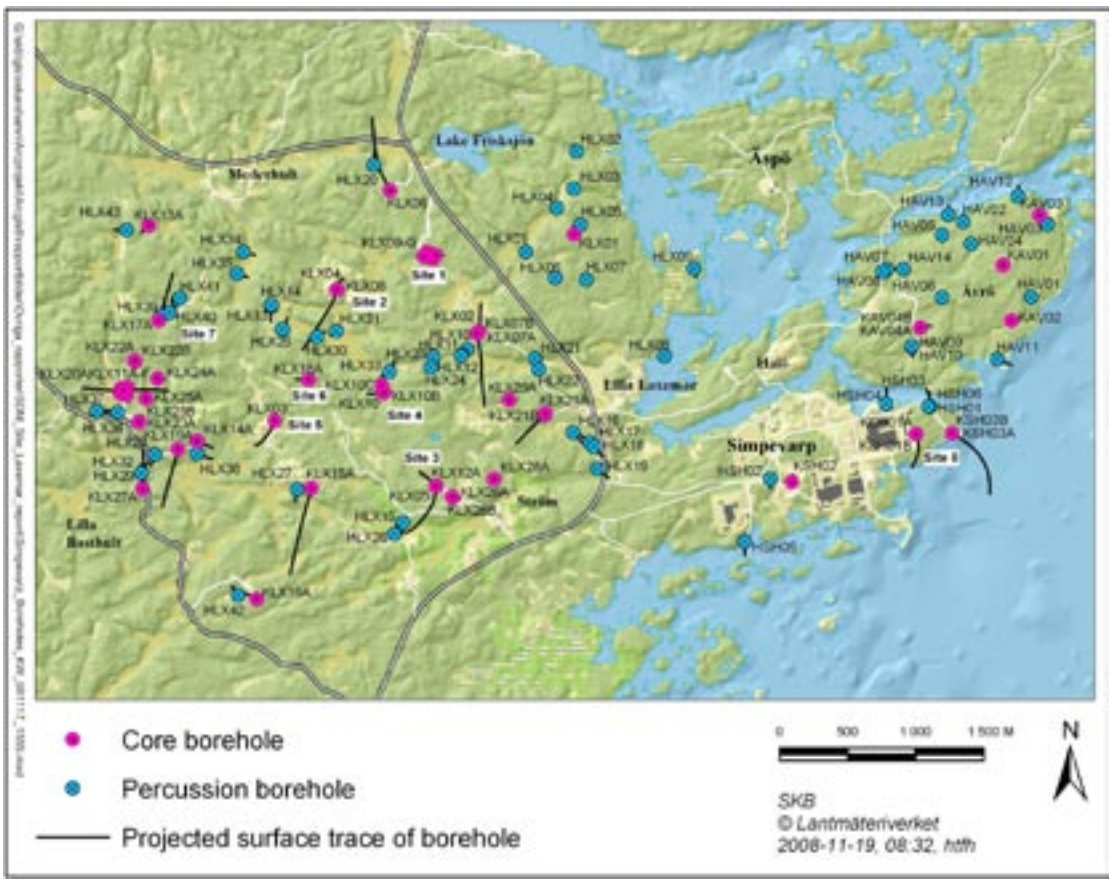

Figure 3-32. *Overview map of percussion and core boreholes in Laxemar, showing the locations of the sites (Site 1-8) discussed in this section.*

Site 1: SSM000218, -219, KLX09 and -09F

Groundwater monitoring wells SSM000218 and SSM000219 are located along a slope in a small valley, north of the Ekerumsån stream valley. The width of the small valley is on the order of 50 m, whereas the QD depth is modest (c 2–5 m). The QD in the valley are dominated by clay gyttja with a thin peat cover, till and postglacial gravel at the surface, whereas no deformation zone in rock has been identified along the small valley. The core boreholes KLX09 and KLX09F are drilled east of the valley, from an higher-altitude area with exposed or shallow rock.

The comparison in Figure 3-33 indicates that there is a downward hydraulic gradient from QD to rock in this area. According to Appendix 1, vertical groundwater-density differences are small along the upper borehole sections of KLX09. Therefore, the use of point-water heads should give realistic indications of prevailing vertical gradients. However, it was not possible to calculate environmental-water heads for KLX09F. According to the field classification in Appendix 2, SSM000218 was classified as a "recharge well" and SSM000219 as a "discharge well". It can also be noted that the average point-water heads (metres above sea level) in the borehole sections of KLX09 are KLX09.1 = 3.42, KLX09.2 = 13.36, KLX09.3 = 13.48, KLX09.4 = 13.6, and KLX09.5 = 13.64. Hence, the point-water head data from KLX09 indicate a downward hydraulic gradient along this borehole.

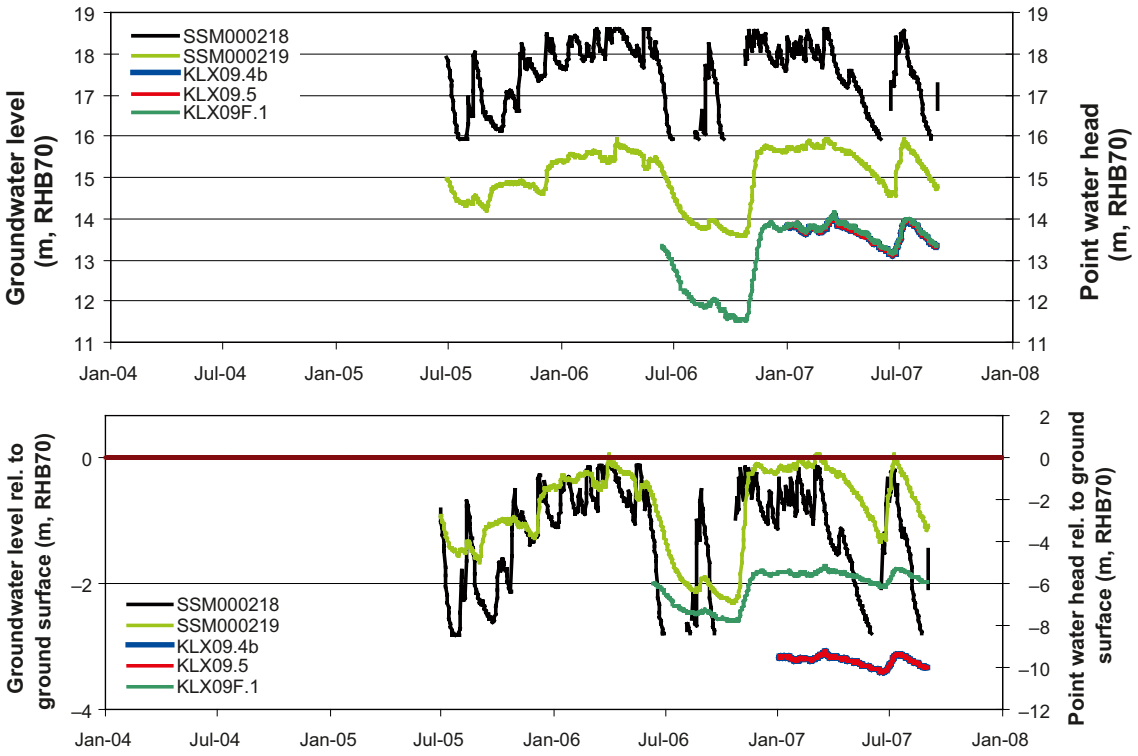

Figure 3-33. *Comparison of groundwater levels in SSM000218 and -219, and point-water heads in KLX09 and -09F.*

Site 2: SSM00009, -11 and KLX08

Groundwater monitoring wells SSM000009 and -11 are located in a slope of a small valley north of the Ekerumsån stream valley. The small valley has a width on the order of 50–100 m and a modest QD depth (c 2–5 m). The QD of the valley are dominated by clay gyttja with a thin peat cover, till, postglacial gravel and some glacial clay at the surface, whereas no deformation zone in rock has been identified along the valley. The core borehole KLX08 is drilled west of the valley, from an higher-altitude area with exposed or shallow rock.

The comparison in Figure 3-34 indicates that there is a downward hydraulic gradient from QD to rock in this area. According to Appendix 1, vertical groundwater-density differences are small along the upper borehole sections of KLX08. Therefore, the use of point-water heads should give realistic indications of prevailing vertical gradients.

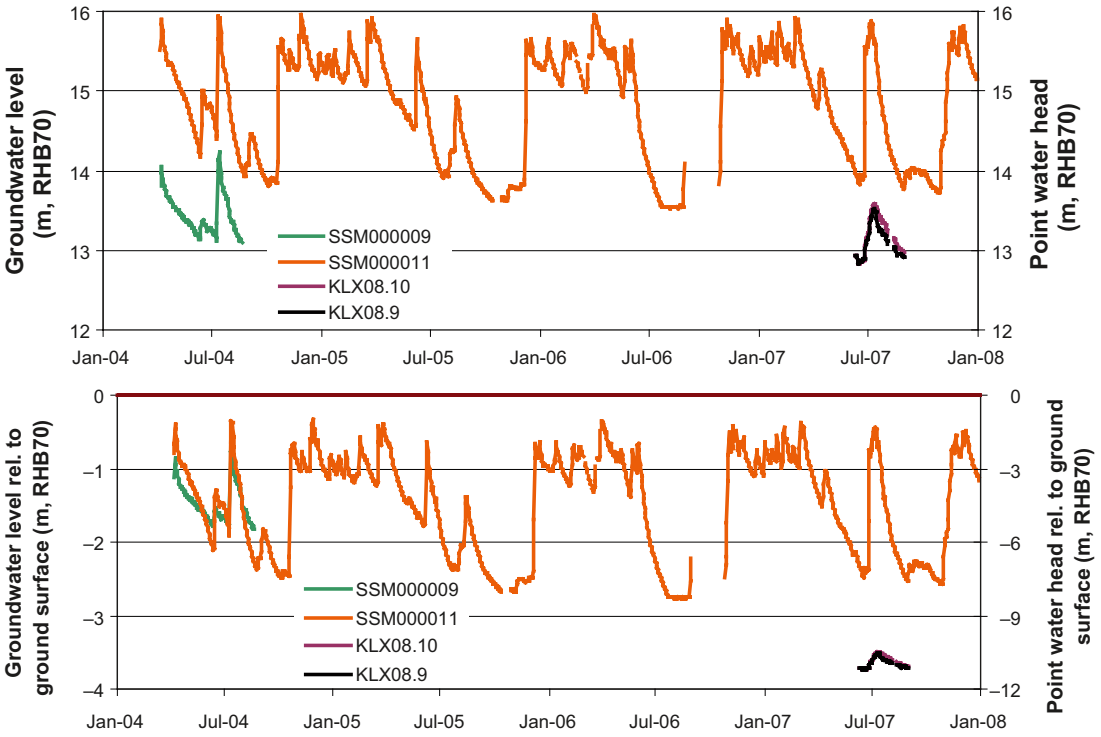

Figure 3-34. *Comparison of groundwater levels in SSM000009 and -11, and point-water heads in KLX08.*

Site 3: SSM000212, KLX05 and -12A

Groundwater monitoring well SSM000212 is installed in a slope in a hummocky moraine area, dominated by till and with a QD depth on the order of 6–8 m. The core boreholes KLX05 and -12A are drilled from a small higher-altitude area, south of well SSM000212. No deformation zone in rock has been identified along the valley.

The comparison in Figure 3-35 indicates that there is a downward hydraulic gradient from QD to rock in this area. According to Appendix 1, vertical groundwater-density differences are small along the upper borehole sections of KLX05 and -12A. Therefore, the use of point-water heads should give realistic indications of prevailing vertical gradients. According to the field classification in Appendix 2, SSM000212 was classified as a "probable recharge well".

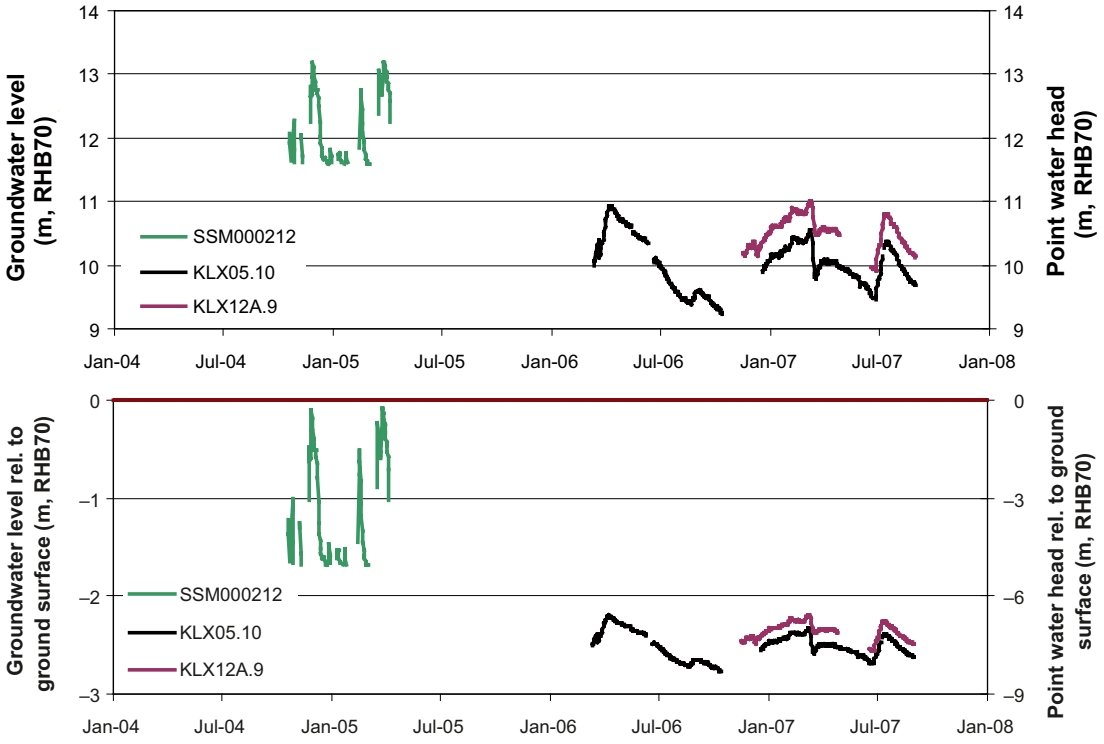

Figure 3-35. *Comparison of groundwater levels in SSM000212, and point-water heads in KLX05 and -12A.*

Site 4: SSM0000220 and KLX10

Groundwater monitoring well SSM000220 is installed in a slope of small valley, south of the Laxemarån stream valley. The small valley has a width of c 100 m and a QD depth on the order of 2–6 m. The QD are dominated by till, fen bog and postglacial sand with a thin layer of peat at the surface. Deformation zone ZSMNE942A coincides with the small valley in this area. However, borehole KLX10 is not drilled across the deformation zone.

The comparison in Figure 3-36 indicates that there is a downward hydraulic gradient from QD to rock in this area. According to Appendix 1, vertical groundwater-density differences are small along the upper borehole sections of KLX10. Therefore, the use of point-water heads should give realistic indications of prevailing vertical gradients. According to the field classification in Appendix 2, SSM000220 was classified as a "discharge well".

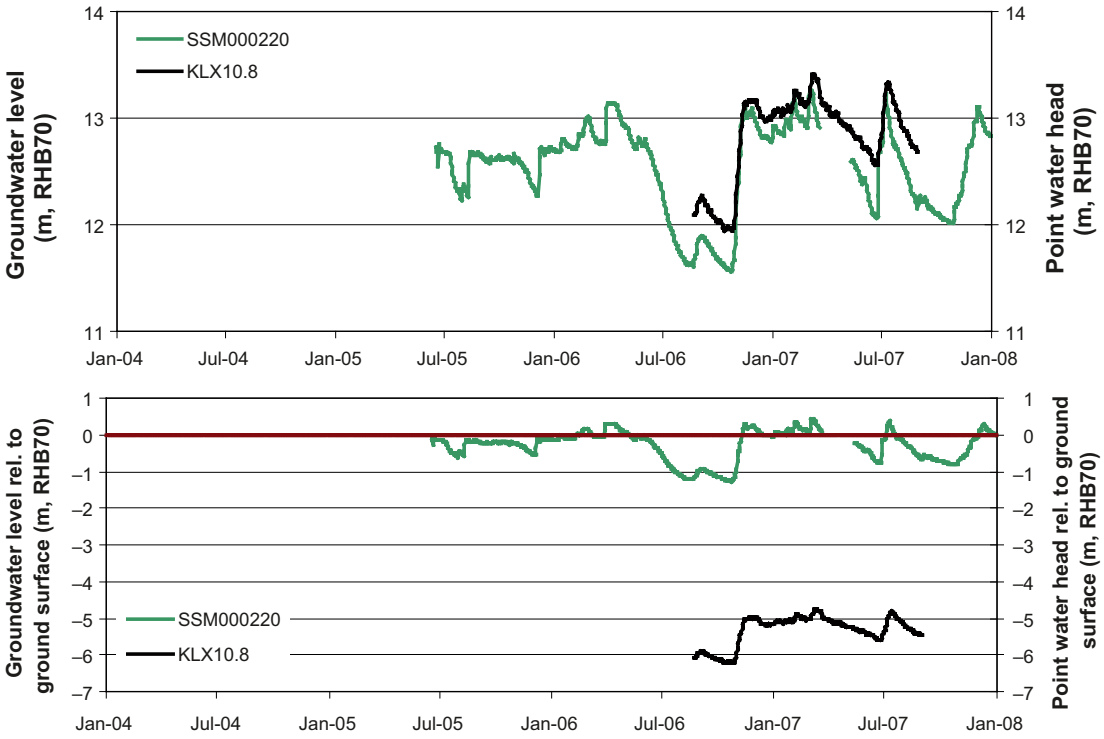

Figure 3-36. *Comparison of groundwater levels in SSM000220 and point-water heads in KLX10.*

Site 5: SSM000019 and KLX03

Groundwater monitoring well SSM000019 is installed in a hummocky moraine area dominated by till at the surface, with a QD depth on the order of 2–3 m. The core borehole KLX03 is drilled from a higher-altitude area with exposed or shallow rock, south of well SSM000019. The area is transect by (medium confidence) deformation zone ZSMNS945A.

The comparison in Figure 3-37 indicates that there is a downward hydraulic gradient from QD to rock in this area. According to Appendix 1, vertical groundwater-density differences are small along the upper borehole sections of KLX03. Therefore, the use of point-water heads should give realistic indications of prevailing vertical gradients.

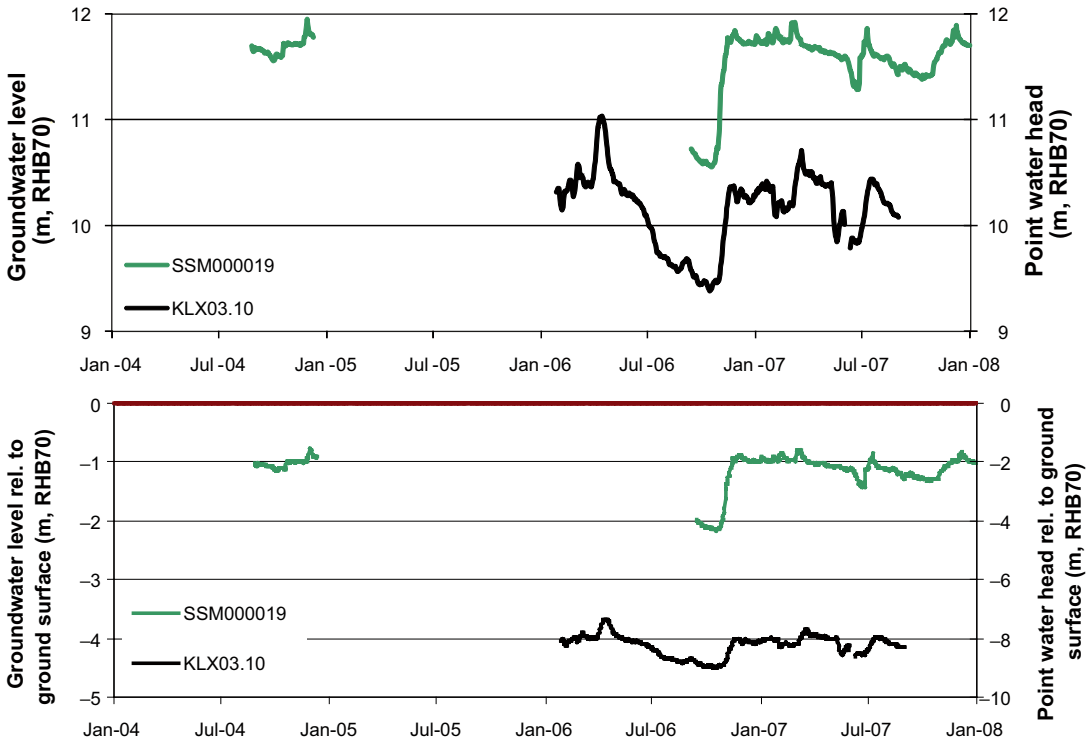

Figure 3-37. *Comparison of groundwater levels in SSM000019 and point-water heads in KLX03.*

Site 6: SSM000250 and KLX18A

Groundwater monitoring well SSM000250 is installed on the edge of an area with exposed or shallow rock, in a hummocky moraine area dominated by till and with a QD depth of c 2–4 m. Core borehole KLX18A is drilled from the higher-altitude area south of well SSM000250. No deformation zone has been identified in this area.

The comparison in Figure 3-38 indicates that there is a downward hydraulic gradient from QD to rock. According to Appendix 1, vertical groundwater-density differences are small along the upper borehole sections of KLX18A. Therefore, the use of point-water heads should give realistic indications of prevailing vertical gradients. According to the field classification in Appendix 2, SSM000250 was classified as a "probable recharge well".

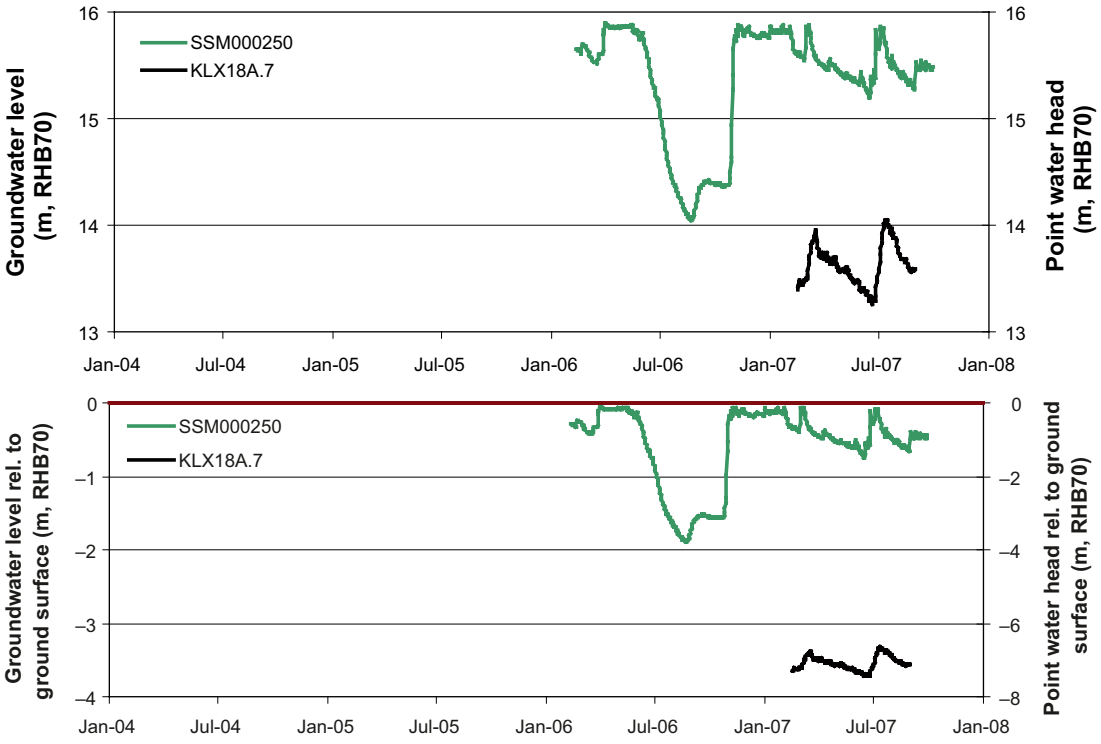

Figure 3-38. *Comparison of groundwater levels in SSM000250 and point-water heads in KLX18A.*

Site 7: SSM0000252, -253, HLX39 and -40

Groundwater monitoring wells SSM000252 and -253 are installed in a narrow valley with a width of c 30–40 m. The QD in the small valley is dominated by fen peat at the surface, with a modest QD depth (c 3–7 m). No deformation zone in the rock has been identified in this area.

The comparison in Figure 3-39 indicates that there is a downward hydraulic gradient from QD to rock. It was not possible to calculate environmental-water heads for HLX39 and -40. According to the field classification in Appendix 2, both SSM000252 and -253 were classified as “discharge wells”.

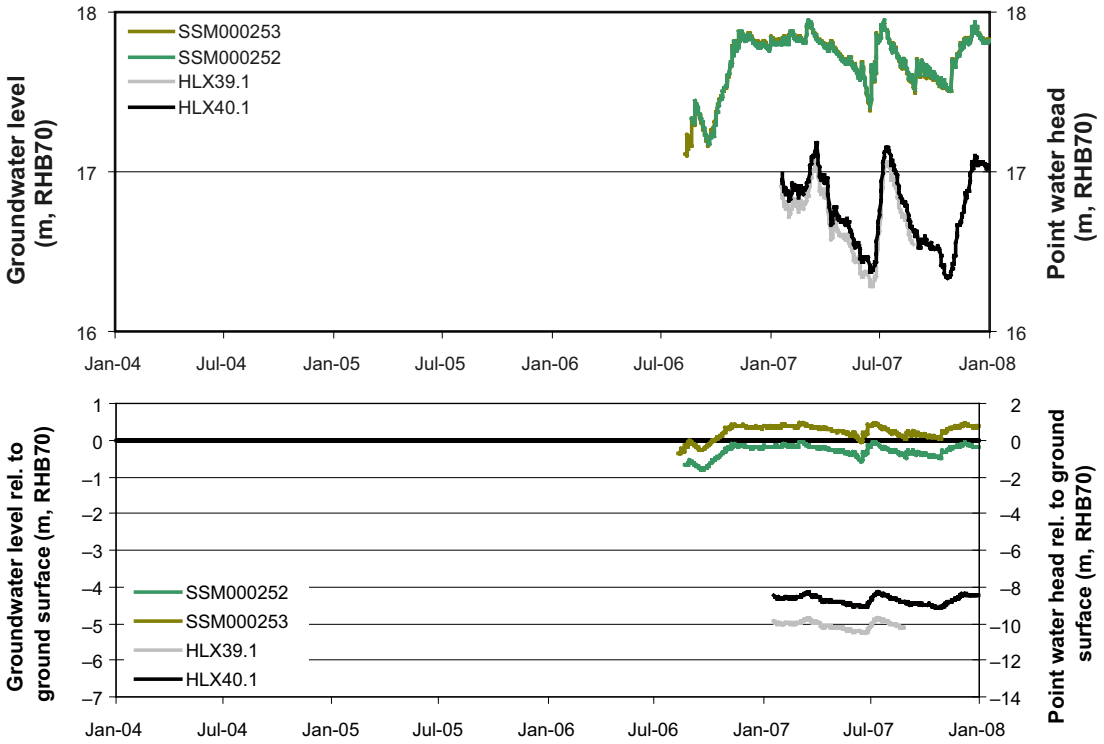

Figure 3-39. *Comparison of groundwater levels in SSM000252 and -253, and point-water heads in HLX39 and -40.*

Site 8: SSM000002 and KSH01A

Groundwater monitoring well SSM000002 and core borehole KSH01A are installed/drilled in the eastern part of the Simpevarp peninsula. The QD are in this area dominated by artificial fill and postglacial gravel at the surface, with a modest QD depth (c. 0.5–2 m) at SSM000002, but with a larger thickness to the west in the artificial-fill area. Deformation zone ZSMNE930A transects the Simpevarp peninsula, north of SSM000002 and KSH01A.

The comparison in Figure 3-40 indicates that there is a downward hydraulic gradient from QD to rock in this area. According to Appendix 1, vertical groundwater-density differences are small along the upper borehole sections of KSH01A. Therefore, the use of point-water heads should give realistic indications of prevailing vertical gradients.

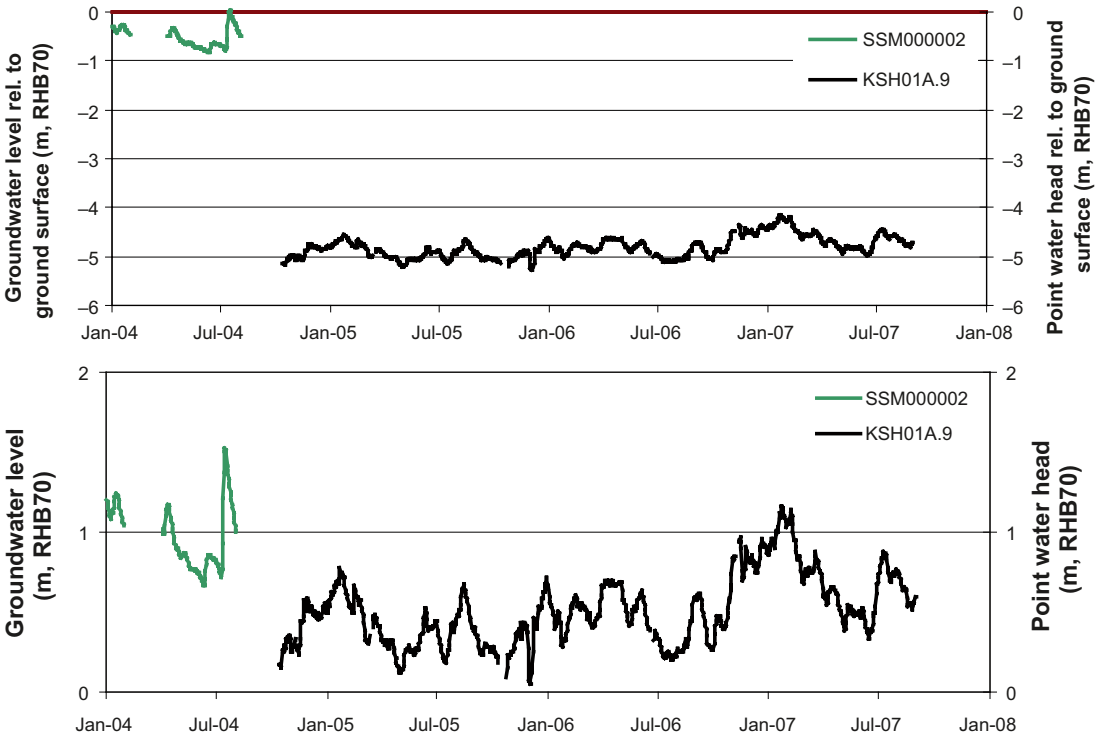

Figure 3-40. *Comparison of groundwater levels in SSM000002 and point-water heads in KSH01A.*

3.7.2 Potential groundwater discharge areas: Lower groundwater levels in QD than point-water heads in rock

Table 3-2 summarises some basic geometrical data for the well-borehole pairs that are analysed in this section, whereas the overview map in Figure 3-41 for orientation shows their locations in terms of sites (Site 1-8). Note that horisontal (XY) distances in Table 3-2 are approximate.

Table 3-2. Geometrical data for wells and boreholes. G.s.e. = Ground-surface elevation. R.s.e. = Rock-surface elevation. Hor. dist. = Horisontal well-borehole distance.

Gw. monitoring well ID	G.s.e. (m.a.s.l.)	R.s.e. (m.a.s.l.)	Perc./core borehole ID	G.s.e. (m.a.s.l.)	B.s.e. (m.a.s.l.)	Hor. dist. (m)
SSM000041	3.36	–0.45	HLX15	4.55	2.17	30
SSM000263	3.61	–2.69	HLX26	6.22	1.87	80
SSM000033	5.12	3.72	HLX02	8.84	No data	35
SSM000210	11.11	7.32	KLX06	17.59	16.68	70
SSM000037	12.35		HLX35	14.18	11.58	35
SSM000222	12.59	7.69	HLX35			35
SSM000223	13.39	5.60	HLX35			80
SSM000039	11.10	6.60	HLX11	12.95	No data	55
SSM000221	12.87	10.08	HLX33	11.94	9.72	95
SSM000221			KLX10	18.16	17.86	100
SSM000021	12.18	8.48	HLX13	17.14	16.54	65
SSM000021			HLX14	16.83	15.72	75
SSM000215	6.44	2.64	HLX27	7.99	5.32	15
SSM000268	9.95	7.26	HLX27			60
SSM000268			KLX15A	14.35	12.26	45

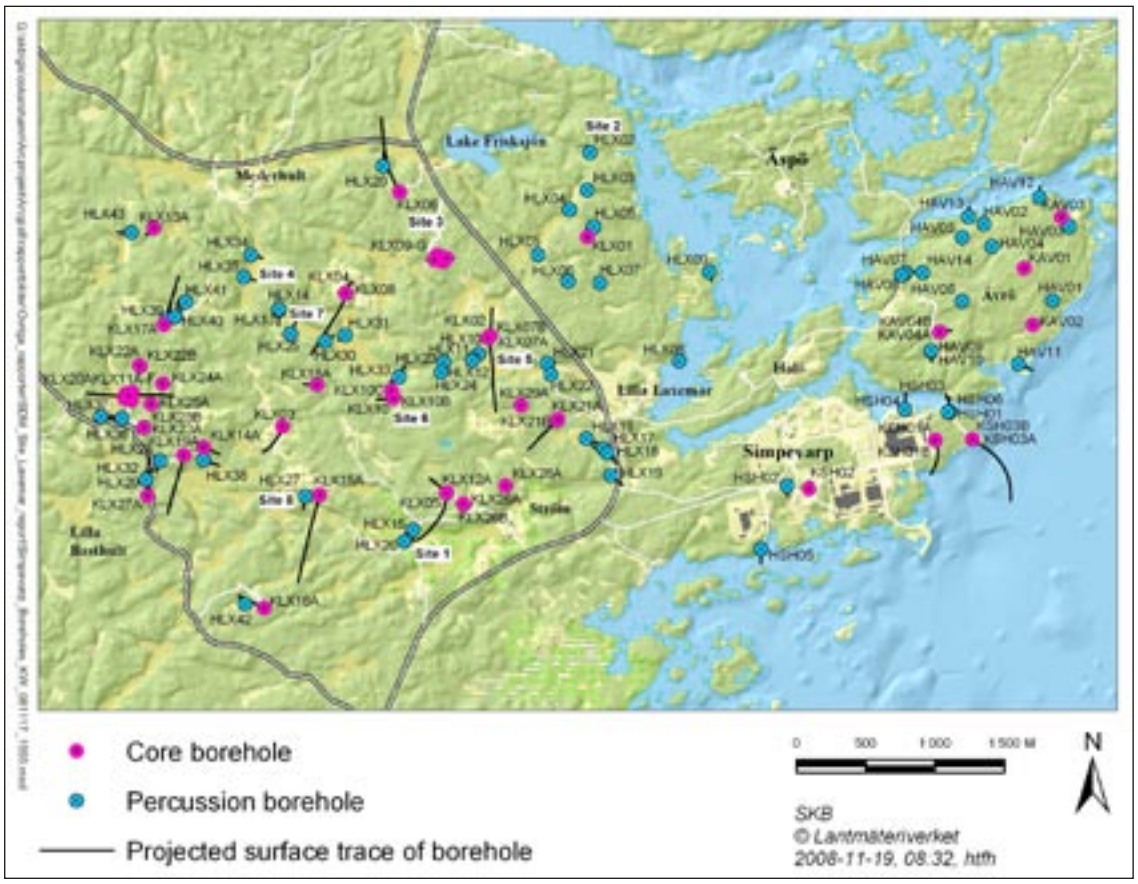

Figure 3-41. *Overview map of percussion and core boreholes in Laxemar, showing the locations of the sites (Site 1-8) discussed in this section.*

Site 1: SSM000041, -263, HLX15 and -26

Groundwater monitoring wells SSM000041 and -263 are installed in the vicinity of the stream Laxemarån, in an area dominated by clay gyttja at the surface. The QD depth is c 3–6 m. Percussion boreholes HLX15 and -26 are drilled further north and south of the stream, respectively. Deformation zone ZSMNW042A coincides with the Laxemarån stream valley in this area.

The comparison between SSM000041, -263, HLX15 and -26 in Figure 3-42 indicates that there is an upward hydraulic gradient from rock to QD. The post data-freeze data corrections (cf. section 2.4.2) for well SSM000041 imply an increase of the groundwater level in the well of 0.24 m compared to the data shown in Figure 3-42, which however does not affect the conclusions on vertical gradients. Taking into account the post data-freeze data corrections, the average groundwater levels in SSM000041 is c 2.4 m (the average is c 2.5 metres above sea level in SSM000263), whereas the average point-water heads in HLX15 and -26 are in the range 4–5.5 metres above sea level.

It was not possible to calculate environmental-water heads for HLX15 and -26. According to the field classification in Appendix 2, both SSM00004 and -263 were classified as "discharge wells". It is interesting to note that percussion borehole HLX15 is artesian, whereas HLX26 is not. This indicates an influence of the deformation zone, which likely yields the artesian conditions in HLX15.

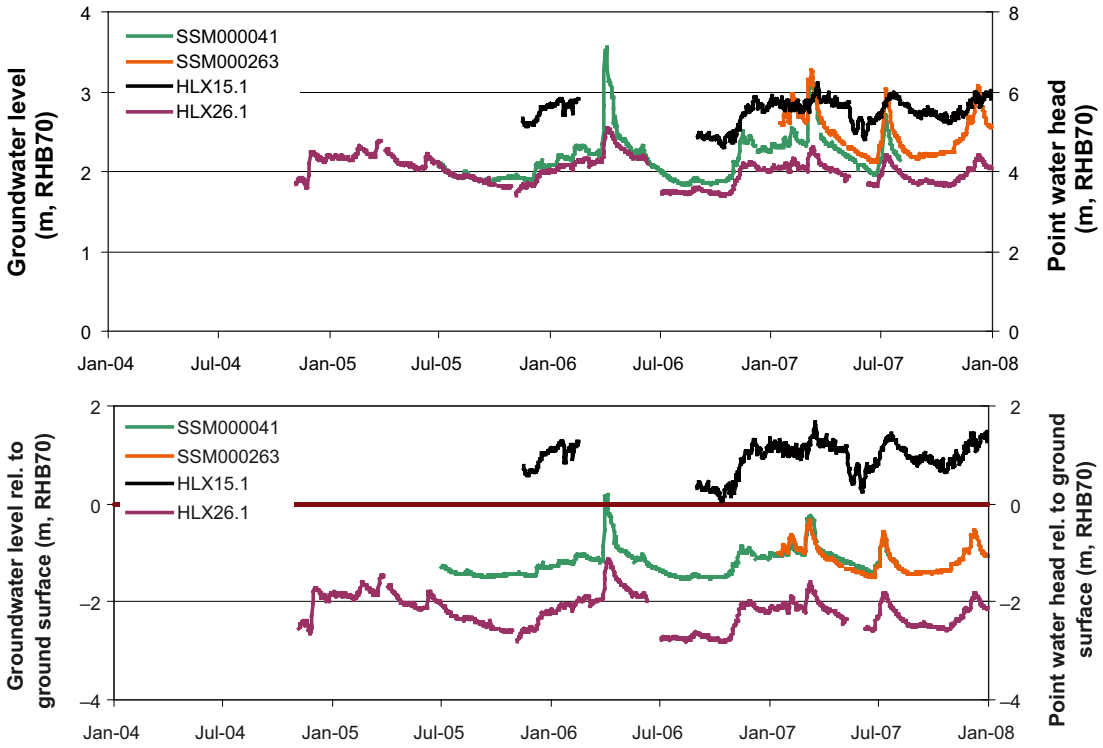

Figure 3-42. *Comparison of groundwater levels in SSM000041 and -263, and point-water heads in HLX15 and -26.*

Site 2: SSM000033 and HLX02

Groundwater monitoring well SSM000033 is installed in a slope of a small valley, close to the coast. The width of the valley is c 20–40 m, whereas the QD are dominated by till and fen peat at the surface. The QD depth is on the order of c 2–7 m. Deformation zone ZSMEW002A transects this area, and deformation zone ZSMNE040A terminates at ZSMEW002A in the vicinity of well SSM000033.

The comparison in Figure 3-43 indicates that there is an upward hydraulic gradient from rock to QD. It was not possible to calculate environmental-water heads for HLX02. According to the field classification in Appendix 2, SSM000033 was classified as a "discharge well". It is interesting to note the relative large fluctuations of the point-water head in HLX02.

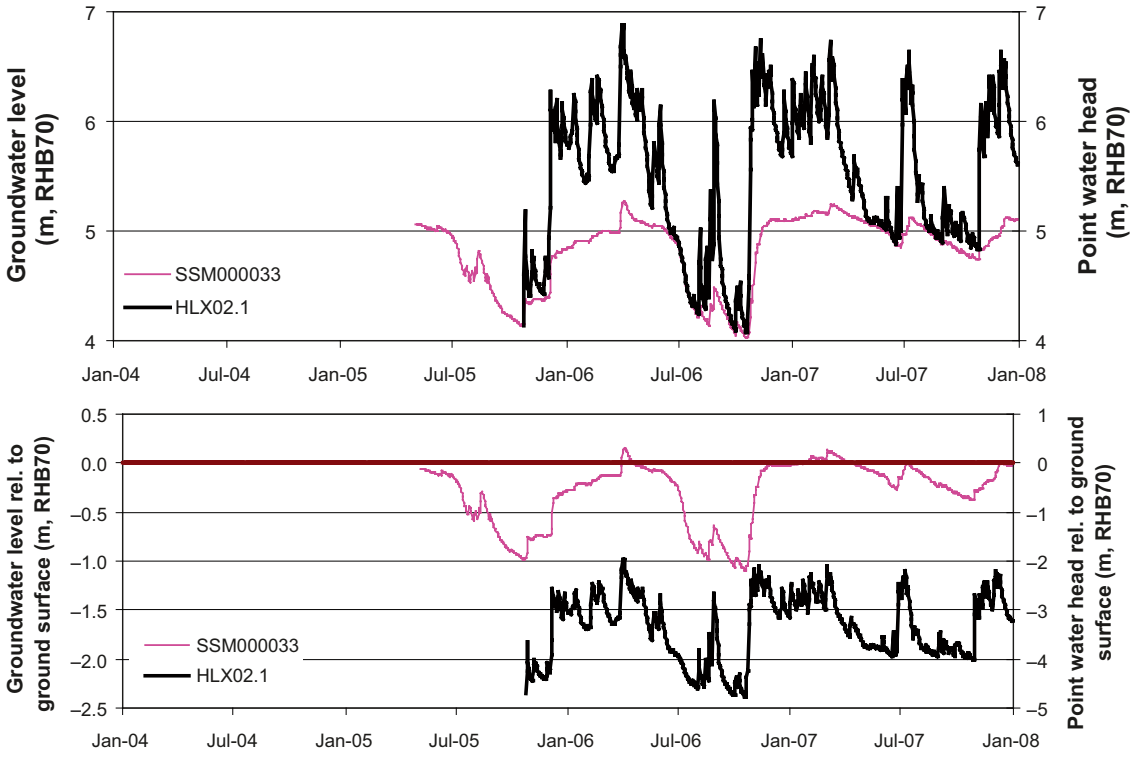

Figure 3-43. *Comparison of groundwater levels in SSM000033 and point-water heads in HLX02.*

Site 3: SSM000210 and KLX06

Groundwater monitoring well SSM000210 is installed in the southern part of the Mederhultsån stream valley. The QD in this area are dominated by till and postglacial gravel at the surface, with a QD depth of c 2–4 m. Core borehole KLX06 is drilled from an higher-altitude area south of the valley. Deformation zone ZSMEW002A coincides with the stream valley in this area.

The comparison in Figure 3-44 indicates that there is an upward hydraulic gradient from rock to QD. According to Appendix 1, vertical groundwater-density differences are small along the upper borehole sections of KLX06. Therefore, the use of point-water heads should give realistic indications of prevailing vertical gradients.

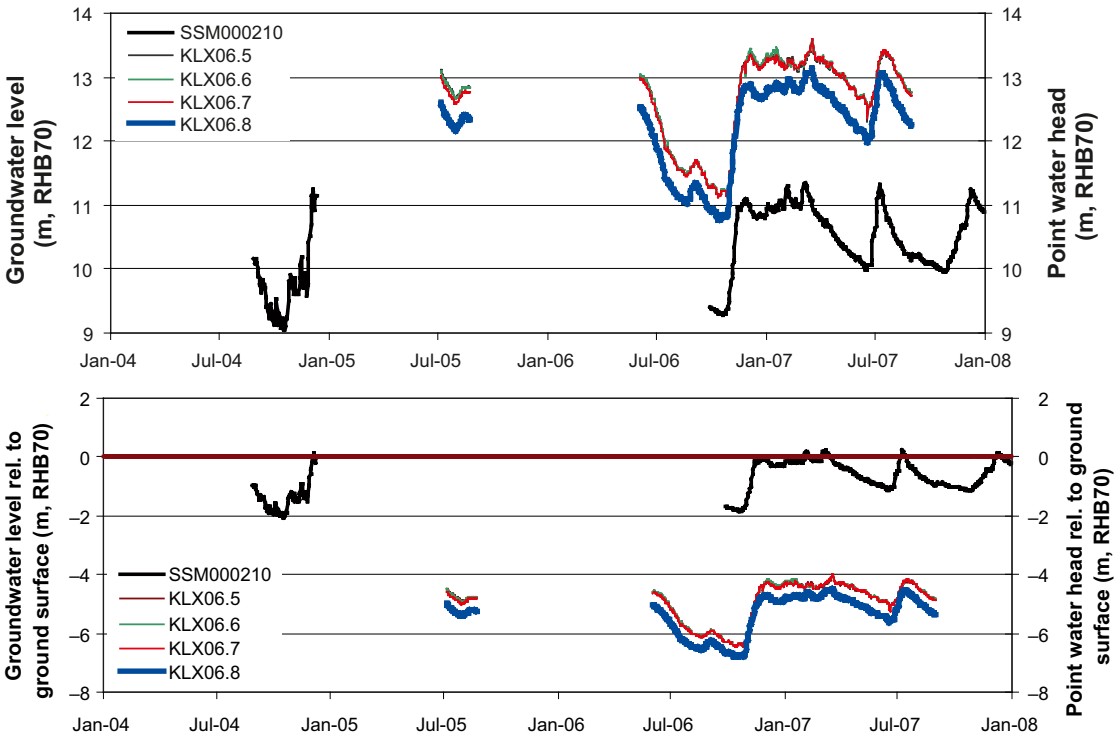

Figure 3-44. *Comparison of groundwater levels in SSM000210, and point-water heads in KLX06.*

Site 4: SSM000037, -222, -223 and HLX35

Groundwater monitoring wells SSM000037, -222 and -223 are installed in a valley north of the Ekerumsån stream valley. The width of the valley is on the order of 100–150 m. The QD are dominated by clay gyttja, at some locations also with a thin peat cover, and the QD depth is c 3–6 m. Deformation zone ZSMNS059A coincides with the valley in this area.

The comparison in Figure 3-45 indicates that there is an upward hydraulic gradient from rock to QD. The post data-freeze data corrections (cf. section 2.4.2) for well SSM000037 imply an increase of the groundwater level in the well of c 0.7 m compared to the data shown in Figure 3-45, which however does not affect the conclusions on vertical gradients. Taking into account the post data-freeze data corrections, the average groundwater levels in SSM000037 is c 11.2 m (the average groundwater levels are c 11.2 metres above sea level also in SSM000222 and -223), whereas the average point-water head in the borehole sections of HLX35 is HLX35.1 = 13.2 metres above sea level and HLX35.2 = 11.6 metres above sea level. It was not possible to calculate environmental-water heads for HLX35. According to the field classification in Appendix 2, SSM000222 was classified as a "discharge well" and SSM000223 as a "probable discharge well".

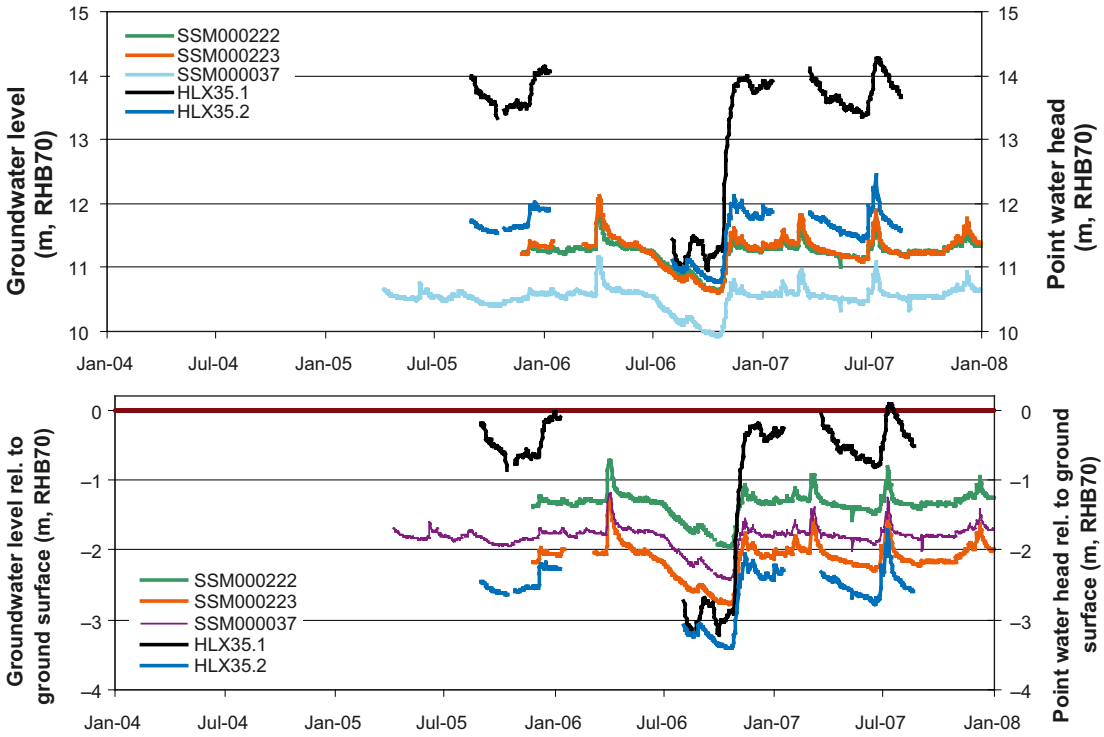

Figure 3-45. *Comparison of groundwater levels in SSM000222, -223 and -37, and point-water heads in HLX35.*

Site 5: SSM000039 and HLX11

Groundwater monitoring well SSM000039 is installed in a slope of the Ekerumsån stream valley, in an area dominated by postglacial gravel at the surface and with a QD depth of c 2–4 m. The percussion borehole HLX11 is drilled from an area dominated by till, southwest of well SSM000039. Deformation zone ZSMEW007A here coincides with the stream valley, and there are also three other deformation zones identified in this area: ZSMNS046A, ZSMNE107A and ZSMNE942A.

The comparison in Figure 3-46 indicates that there is a small upward gradient from rock to QD. It was not possible to calculate environmental-water heads for HLX11. According to the field classification in Appendix 2, SSM000039 was classified as a "recharge well".

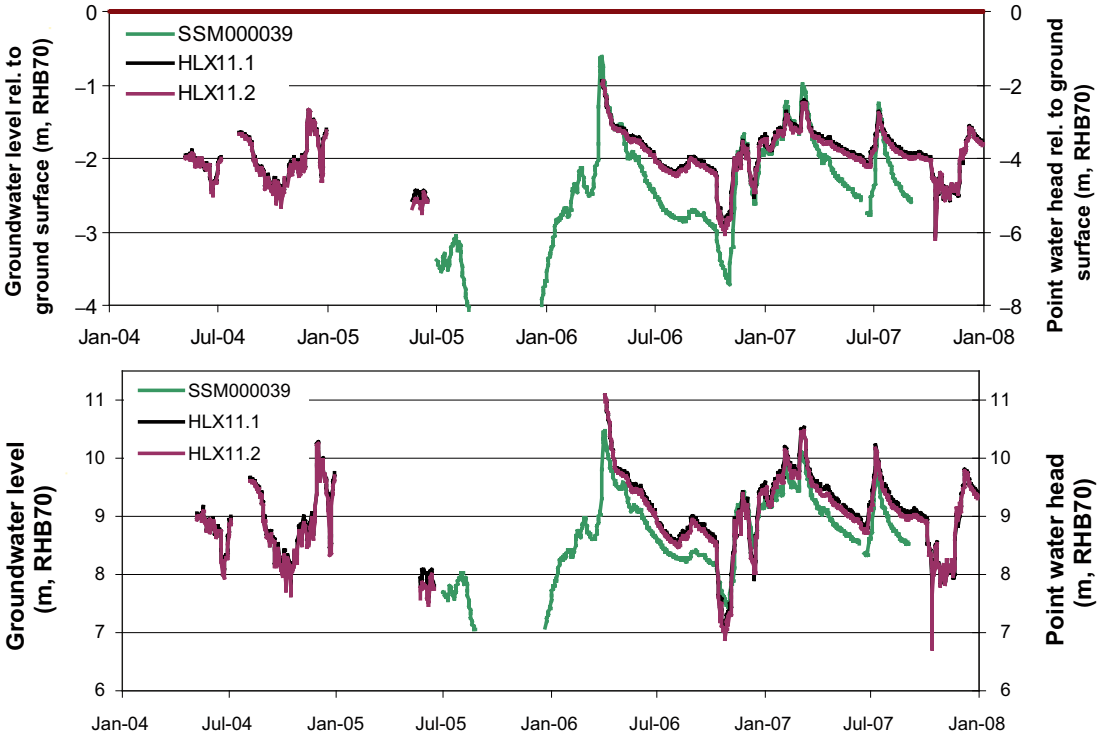

Figure 3-46. *Comparison of groundwater levels in SSM000039 and point-water heads in HLX11.*

Site 6: SSM000221, HLX33 and KLX10

Groundwater monitoring well SSM000221 and percussion borehole HLX33 are installed/drilled in the Ekerumsån stream valley. The QD in this area are dominated by till, locally also post-glacial sand with a thin peat cover at the surface. The QD depth is very variable (c 2–8 m). The core borehole KLX10 is drilled from a higher-altitude area south of SSM000221 and HLX33. Deformation zones ZSMEW007A and ZSMNE942A transect the area in the direct vicinity of HLX33 and KLX10, respectively.

The comparison between SSM000221 and KLX10 in Figure 3-47 indicates that there is an upward hydraulic gradient from rock to QD. On the other hand, comparison between SSM000221 and HLX33 indicates a downward gradient. According to Appendix 1, vertical groundwater-density differences are small along the upper borehole sections of KLX10. Therefore, the use of point-water heads should give realistic indications of prevailing vertical gradients. It was not possible to calculate environmental-water heads for HLX33. According to the field classification in Appendix 2, SSM000221 was classified as a "discharge well".

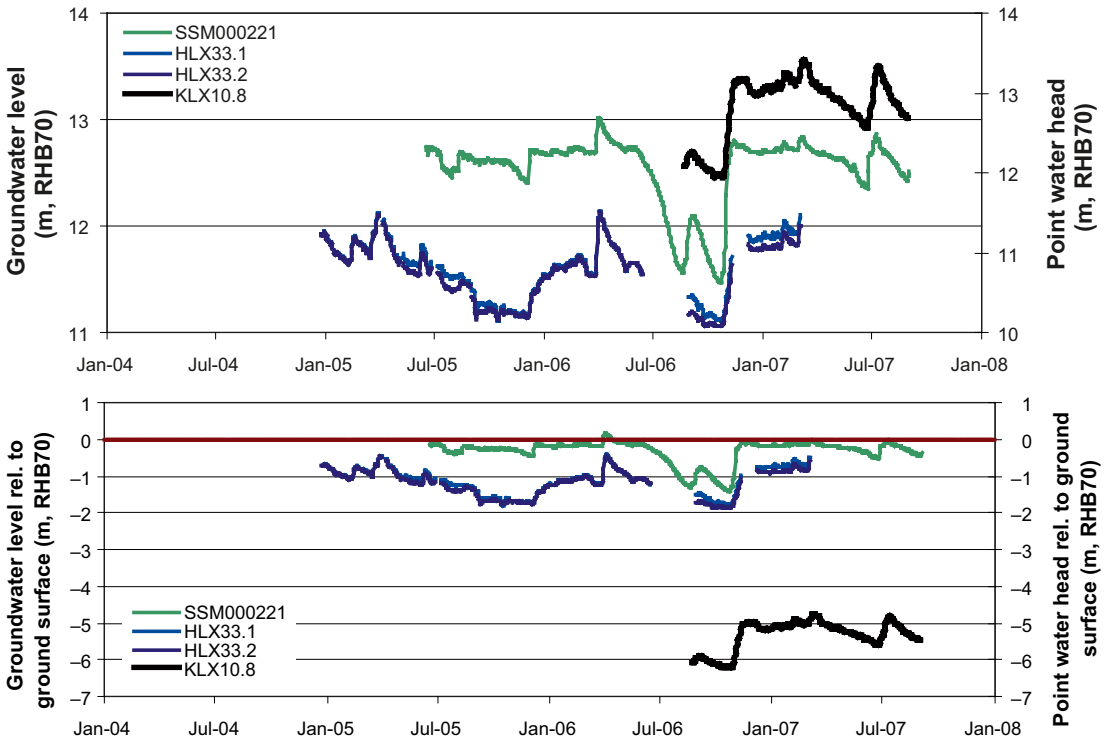

Figure 3-47. *Comparison of groundwater levels in SSM000221, and point-water heads in HLX33 and KLX10.*

Site 7: SM000021, HLX13 and -14

Groundwater monitoring well SSM000021 is installed in the Ekerumsån stream valley. The QD are dominated by fen peat and clay gyttja at the surface, and the QD depth in this area is c 2–6 m. Percussion boreholes HLX13 and -14 are drilled from an higher-altitude area north of the stream, dominated by exposed/shallow rock and till. Deformation zone ZSMEW007A coincides with the valley in this area.

The comparison in Figure 3-48 indicates that there is an upward hydraulic gradient from rock to QD. It was not possible to calculate environmental-water heads for percussion boreholes HLX13 and -14. According to the field classification in Appendix 2, SSM000021 was classified as a "discharge well".

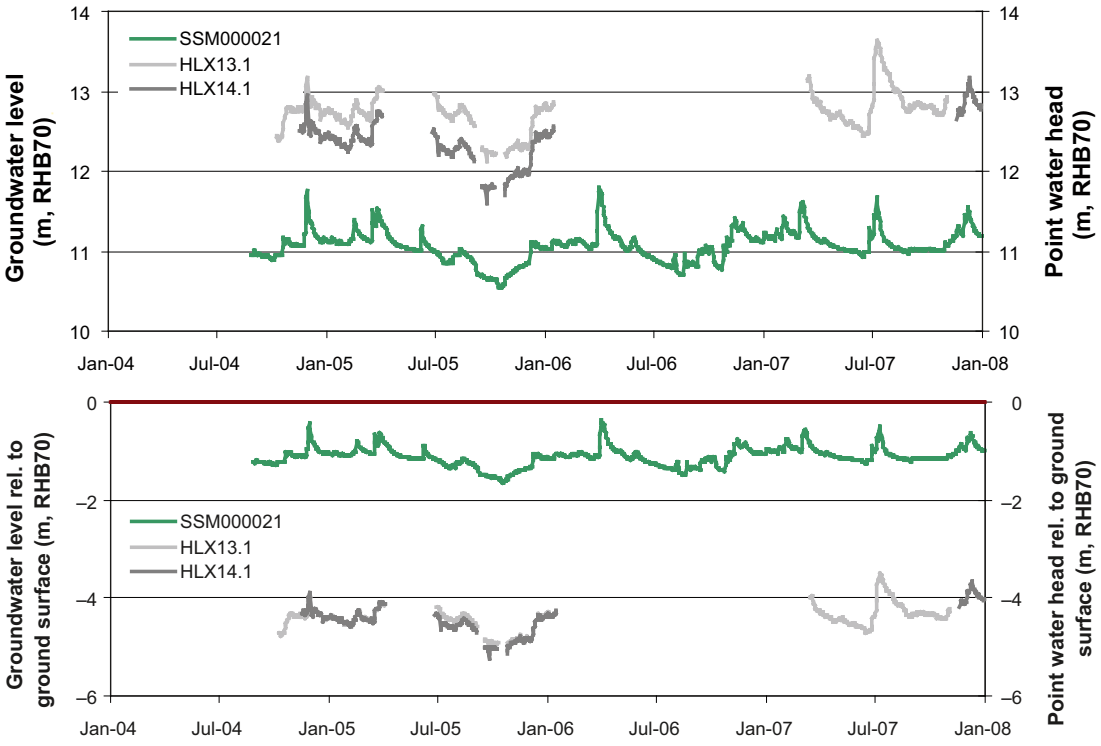

Figure 3-48. *Comparison of groundwater levels in SSM000021, and point-water heads in HLX13 and -14.*

Site 8: SM000215, -268 and HLX27

Groundwater monitoring wells SSM215 and -268 and percussion borehole HLX27 are installed/ drilled in a slope in the northern part of the Laxemarån stream valley. The QD in this area are dominated by till, with a QD depth of c 1–3 m. Deformation zone ZSMNW042A coincides with the valley in this area. Core borehole KLX15A is drilled from an higher-altitude area with exposed/shallow rock, east of the groundwater monitoring wells and HLX27.

The comparison between SSM000215 and HLX27 in Figure 3-49 indicates that there is an upward hydraulic gradient from rock to QD, whereas the reverse flow conditions are indicated by the comparison between SSM000268 and HLX27. There are only two days of point-water head data from KLX15A. The average point-water heads in the three borehole sections of KLX15A (see Appendix 1) are KLX15A.1 = 5.2, KLX15A.2 = 5.9 and KLX15A.3 = 6.2 metres above sea level. In terms of environmental-water heads, the corresponding averages are 6.2, 6.8 and 6.2 metres above sea level. Environmental-water heads in KLX15A are hence above the groundwater level in the QD at well SSM000215, but below the groundwater level at SSM000268. It was not possible to calculate environmental-water heads for HLX27. According to the field classification in Appendix 2, both SSM000215 and -268 were classified as “discharge wells”.

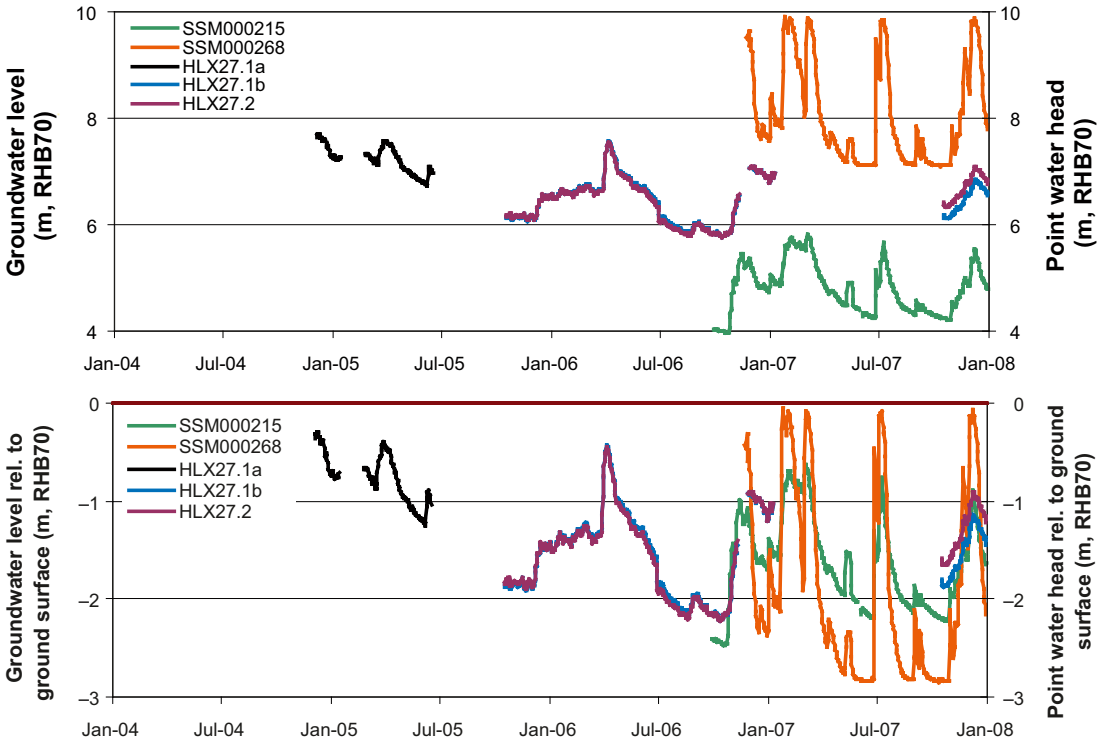

Figure 3-49. *Comparison of groundwater levels in SSM000215 and -268, and point-water heads in HLX27.*

3.7.3 Areas with small hydraulic gradients between QD and rock

SSM000005 and HSH02

Groundwater monitoring well SSM000005 (ground-surface elevation = 6.33 metres above sea level, rock-surface elevation = 4.95 metres above sea level) is installed c 10 m from percussion borehole HSH02 (ground-surface elevation = 6.45 metres above sea level, no data on rock-surface elevation). Also this well-borehole pair is located on the Simpevarp peninsula, between Clab and the Simpevarp power plant. The QD in this area are dominated by till and exposed/shallow rock, hence with a shallow QD (depth c 0.5–1 m). Deformation zone ZSMNE930A transects the area north of SSM000005 and HSH02, in which area deformation zone ZSMNE019A also terminates at ZSMNE930A.

The comparison in Figure 3-50 indicates that there is only a small hydraulic gradient between rock and QD in this area. It was not possible to calculate environmental-water heads for HSH02.

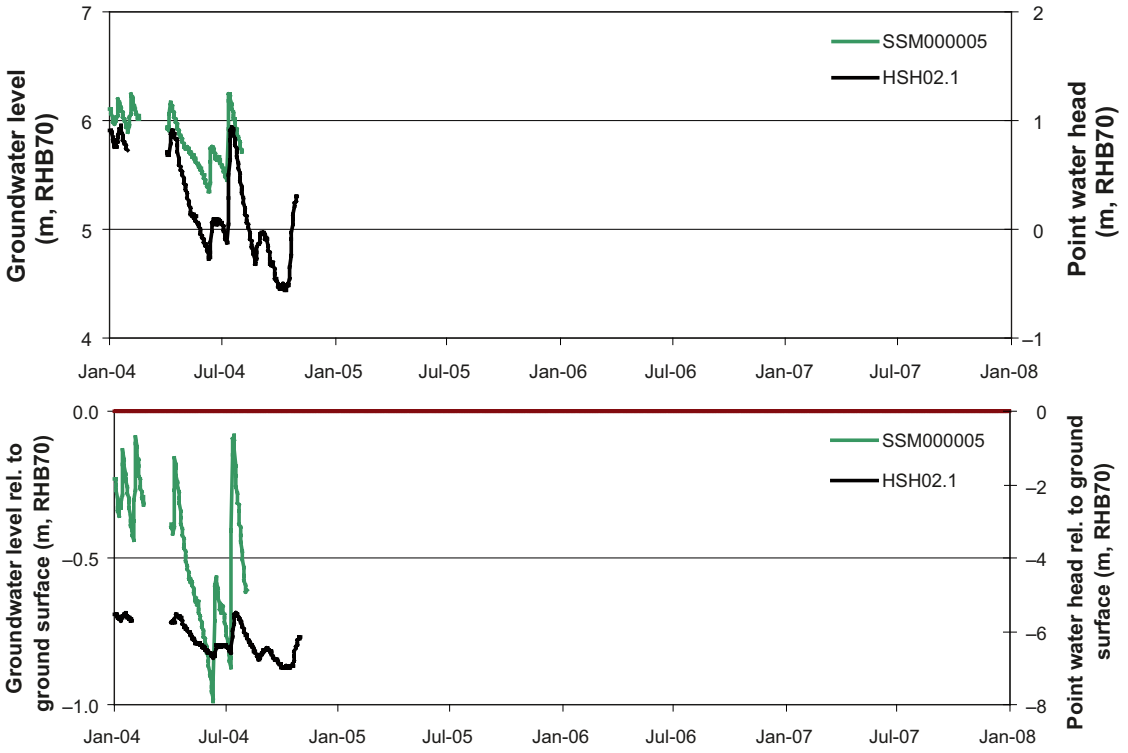

Figure 3-50. *Comparison of groundwater levels in SSM000005 and point-water heads in HSH02.*

SSM000001 and HSH01

Groundwater monitoring well SSM000001 and percussion borehole HSH01 are installed/drilled on the eastern edge of the Simpevarp peninsula. The QD in this area are thin (c 2–3 m) and dominated by till at the surface. Deformation zone ZSMNE930A transects the Simpevarp peninsula in the vicinity of SSM00001 and HSH01.

The comparison in Figure 3-51 indicates that there is a downward hydraulic gradient from QD to rock. However, the post data-freeze data corrections (cf. section 2.4.2) for well SSM000001 imply a lowering of c 1 m of the groundwater level compared to the data shown in Figure 3-51. The average groundwater level in SSM00001 as shown in Figure 3-51 is c 1.40 metres above sea level, whereas the data corrections result in an average of c 0.40 metres above sea level; the average point-water head in HSH01 is c 0.50 metres above sea level. It was not possible to calculate environmental-water heads for HSH01. According to the field classification in Appendix 2, SSM000001 was classified as a "discharge well".

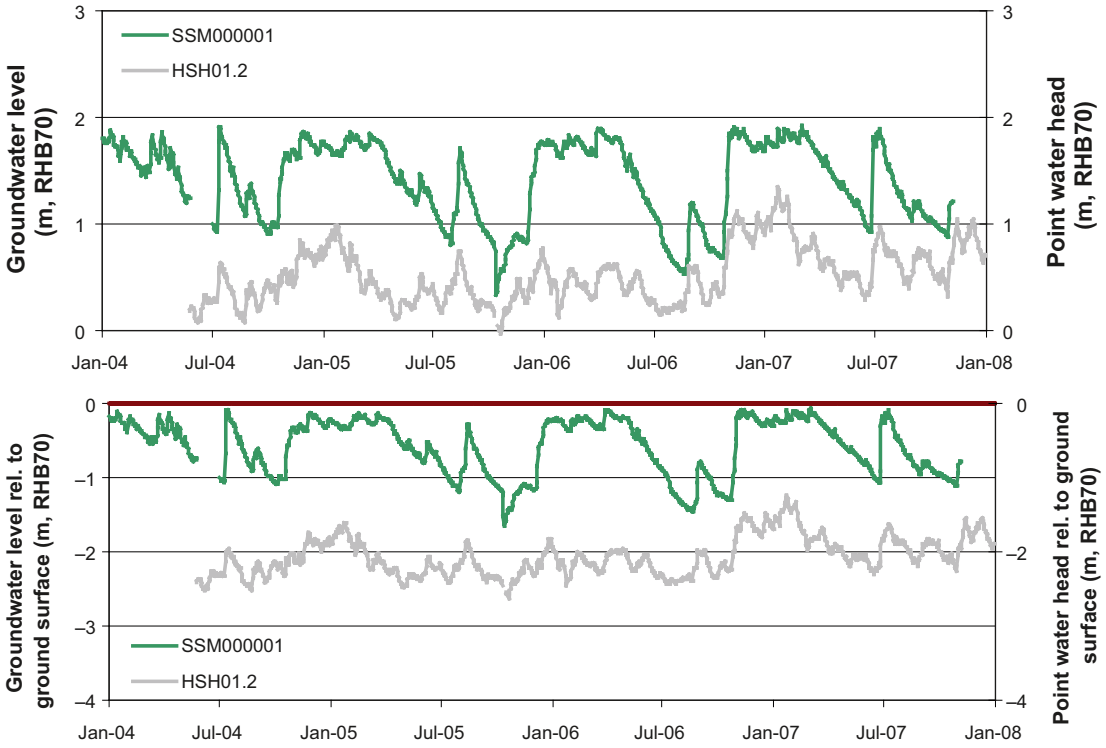

Figure 3-51. *Comparison of groundwater levels in SSM000001 and point-water heads in HSH01.*

SSM00004 and KSH02

Groundwater monitoring well SSM000004 (ground-surface elevation = 5.10 metres above sea level, rock-surface elevation = 2.60 metres above sea level) is installed c 25 m from core borehole KSH02 (ground-surface elevation = 5.38 metres above sea level, rock-surface elevation = 2.39 metres above sea level). The well-borehole pair is located on the Simpevarp peninsula, between the Clab facility and the Simpevarp power plant. The QD in this area are dominated by till and postglacial gravel at the surface, with a modest QD depth (2–4 m). Deformation zones ZSMNE930A and ZSMNE015A transect the area north and south, respectively, of SSM000004 and KSH02.

According to Figure 3-52, there is no period with simultaneous data from SSM000004 and KSH02. The available data may indicate that there is only a small hydraulic gradient between rock and QD in this area, but the lack of same-time data limits the possibilities to draw any conclusions. According to Appendix 1, vertical groundwater-density differences are small along the upper borehole sections of KSH02. Therefore, the use of point-water heads would likely give realistic indications of prevailing vertical gradients.

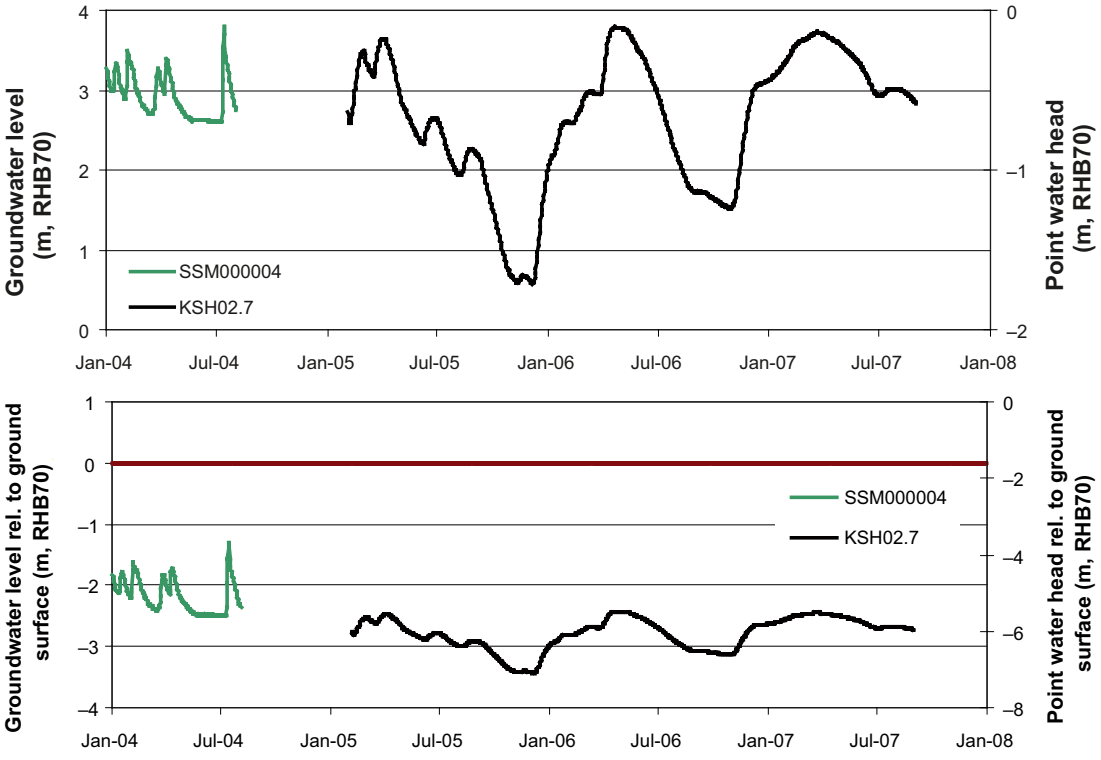

Figure 3-52. *Comparison of groundwater levels in SSM000004 and point-water heads in KSH02.*

4 Near-surface hydrogeological properties data

4.1 Conceptual model of regolith and near-surface rock

The conceptual model of the regolith and near-surface rock in Laxemar constitutes an underlying framework for interpretation of hydrogeological properties, and the associated development of a conceptual hydrogeological model of the site. Therefore, this chapter is initiated by summarising the conceptual model of regolith and near-surface rock /Sohlenius and Hedenström 2008/, before moving to the site data in the sections that follow.

/Sohlenius and Hedenström 2008/ define the term "regolith" as the loose deposits overlying the rock. All known regolith in Laxemar was deposited during the Quaternary period, which implies that the regolith may also be referred to as "Quaternary deposits" (abbreviated QD). The QD are divided into two main groups, glacial and postglacial. Glacial deposits (the oldest group present at the site) were deposited during the latest deglaciation (c. 12,000 years BC), either directly from the ice or by melt water, whereas postglacial deposits were deposited subsequent to deglaciation.

Due to the compression of the rock by the inland ice, the Laxemar area was covered with water after the deglaciation; the whole Laxemar area is located below the highest coastline. Figure 4-1 shows a typical QD stratigraphy for areas located below the highest coastline of Sweden, considered representative also for the Laxemar area /Sohlenius and Hedenström 2008/.

The geographical distribution of QD in Laxemar (including both terrestrial and marine areas) is shown in the QD map in Figure 4-2. Characteristic for the area is the large fraction of shallow or exposed rock; c 35% of the terrestrial part of the Laxemar-Simpevarp regional model area consists of rock outcrops. The dominant (and oldest) type of QD in Laxemar is glacial (sandy/gravelly) till, covering c 52% of the terrestrial part of the Laxemar-Simpevarp regional model area. The till was deposited directly from the melting ice. Particularly in the low-lying areas, glacial clay has been deposited above the till. The area also contains four glaciofluvial deposits (in the form of eskers), which also originate from melting ice. The glaciofluvial material in these eskers is well sorted and contain more rounded particles compared to the glacial till. Both till and glaciofluvial deposits rest directly on the rock.

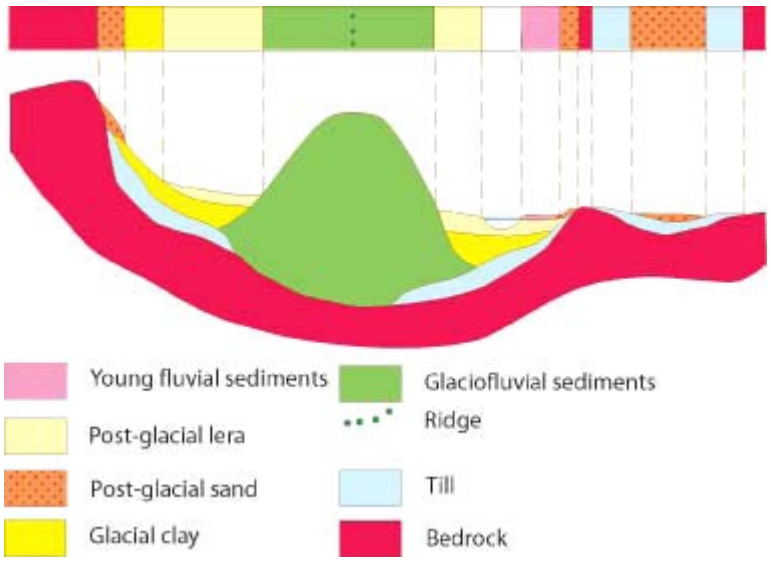

Figure 4-1. *Typical QD stratigraphy below the highest coastline /Sohlenius and Hedenström 2008/. "Post-glacial lera" is Swedish for postglacial clay.*

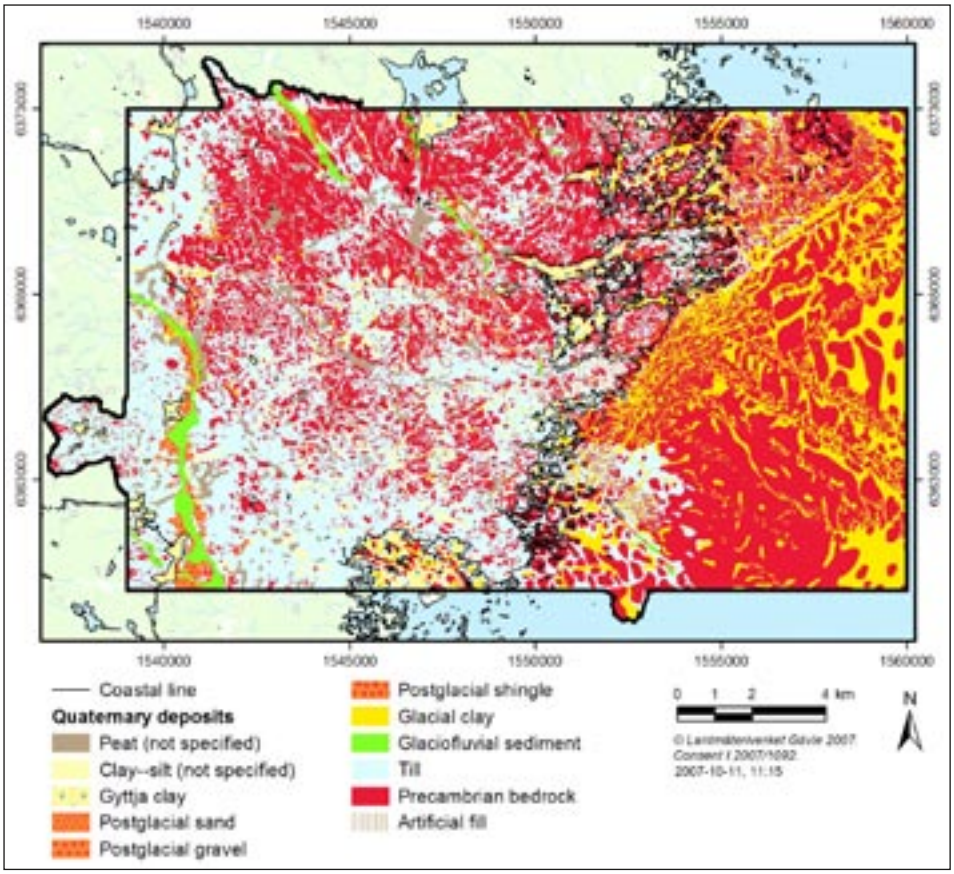

Figure 4-2. *Map of the QD in Laxemar, including both terrestrial and marine areas /Sohlenius and Hedenström 2008/.*

Subsequent to deglaciation, the area was subject to submarine waves and currents. Under these circumstances, postglacial sediments (gyttja/clay gyttja/gyttja clay and postglacial sand/gravel) were deposited above the glacial deposits in valleys and other sheltered positions. Gradually, the post-deglaciation land upheaval transformed sea bays to lakes, which subsequently were transformed to wetlands due to sedimentation and vegetation growth. Peat was accumulated in low-lying areas; many of these areas have during the last c 150 years been subject to land improvement and drainage operations.

/Nyman et al. 2008/ present a conceptual-geometrical model of the QD in Laxemar, here referred to as the Laxemar RDM (regolith depth and stratigraphy model). This model contains a 3D representation of the QD, including both the total QD thickness and the individual thicknesses of totally 6 QD layers (see Figures 4-3 and 4-4). The RDM is described and used further in section 5.2, including a preliminary hydrogeological parameterisation based on the properties data presented in section 4.3.

/Sohlenius and Hedenström 2008/ define 3 “regolith” type areas in Laxemar, based on the topography, the QD map and the RDM. These type areas can be summarised as follows:

Type area I – Topographically high areas: This type area is dominated by exposed/shallow rock and till, also including hummocky moraine areas (located in the south-western and central parts of Laxemar). The latter areas are characterised by thicker QD compared to the exposed/shallow rock areas.

Type area II – Valleys: This type area is characterised by relatively thick QD, including postglacial deposits (peat, clay gyttja, sand/gravel) overlying glacial deposits (glacial clay and till), as well as surface waters (lakes, wetlands, streams, and also sea bays). The till located in the terrestrial valley bottoms is likely more sorted compared to till in the other areas; the reason for this is unknown. The valleys generally coincide with lineaments (deformation zones) in the rock, and the upper rock is hence more densely fractured in this type area compared to the other type areas.

Type area III – Glaciofluvial eskers: The large esker (Tuna esker) and the 3 small eskers constitute their own type area. The QD in these eskers are dominated by well-sorted sand and gravel, assumed to rest directly on the rock.

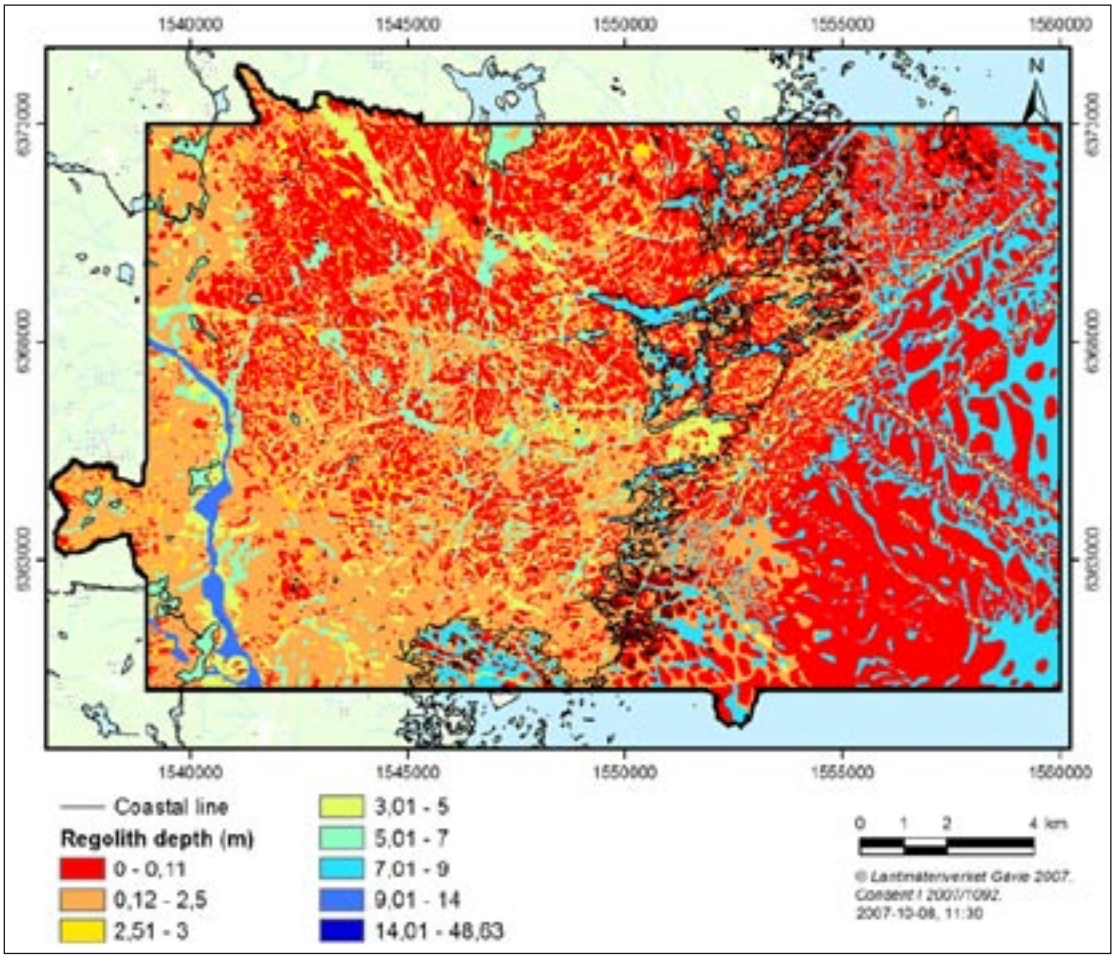

Figure 4-3. *Map of total regolith (QD) depths in the Laxemar area according to the RDM /Nyman et al. 2008/.*

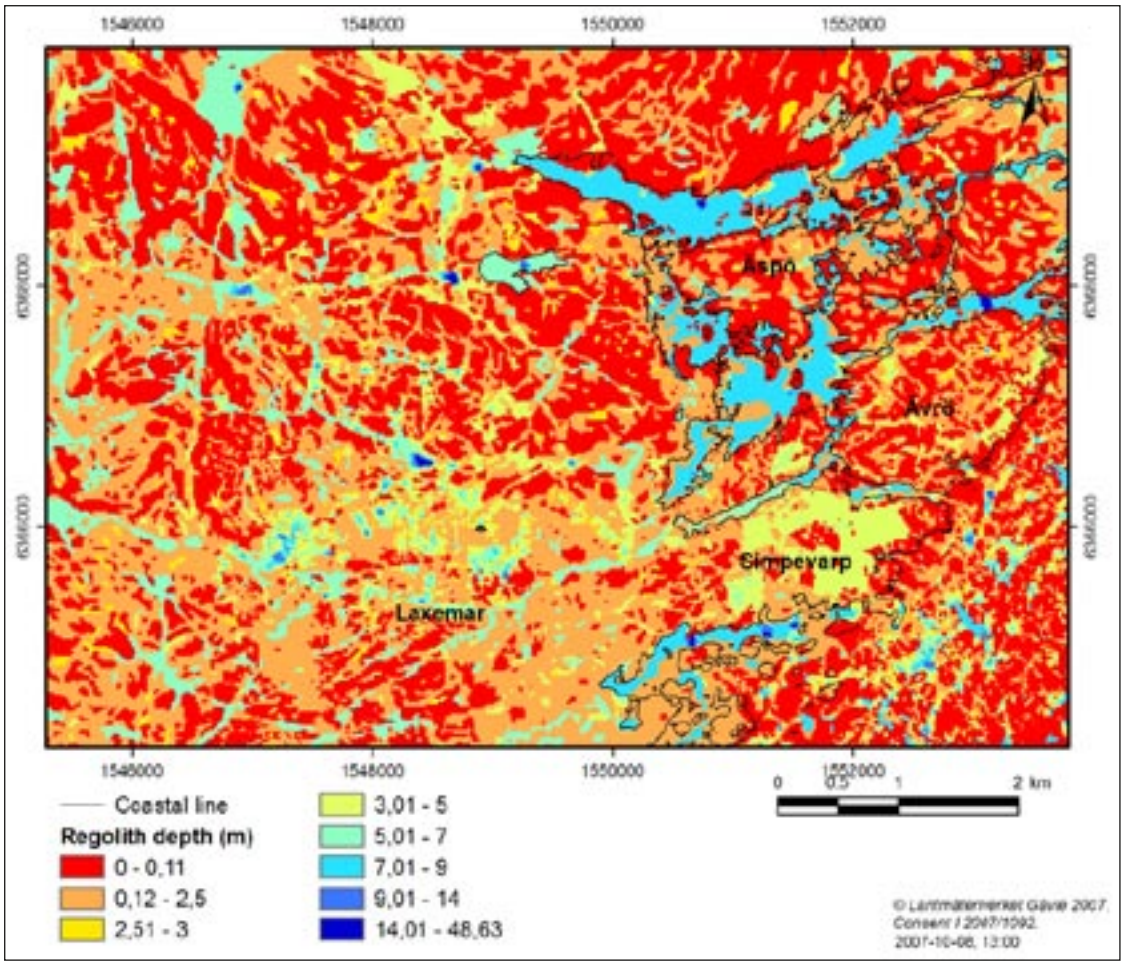

Figure 4-4. *Map of total regolith (QD) depths in the central part of Laxemar according to the RDM /Nyman et al. 2008/.*

4.2 Overview of near-surface hydrogeological properties data

Site-specific data on the hydrogeological properties of the QD in Laxemar originate from four types of laboratory- and field investigations, in this chapter presented in order of increasing (spatial) support scale: (1) Particle-size distribution (PSD) curves for QD samples, (2) laboratory permeameter tests on QD samples, (3) slug tests in groundwater monitoring wells, and (4) hydraulic single-hole and interference tests in groundwater monitoring wells. In addition, tracer dilution tests have been performed in groundwater monitoring wells, primarily providing estimates of groundwater flow velocities at well-screen depth; the latter type of data are available both for undisturbed and disturbed (i.e. during pumping) groundwater flow conditions. The hydraulic interaction between QD and rock have been investigated by means of hydraulic interference and tracer tests. In these tests, pumping was done from percussion boreholes in the rock, with simultaneous groundwater level- and tracer concentration measurements in nearby groundwater monitoring wells.

The hydrogeological properties data presented and analysed in this chapter are obtained from Sicada delivery #Sicada_07_334 (delivery Sep. 25, 2007). Table 4-1 provides an overview of the hydrogeological data set.

Table 4-1. Overview of near-surface hydrogeological properties data in the Laxemar 2.3 data set.

Data source	Parameter(s)	P-report /reference/
Particle-size distribution (PSD) curves	Laboratory-scale hydraulic conductivity (calculated) of QD samples	P-04-273 /Nilsson 2004/ P-05-47 /Bergman et al. 2005/ P-05-49 /Rudmark et al. 2005/ P-06-121 /Sohlenius et al. 2006/ P-07-91 /Morosini et al. 2007/
Permeameter tests	Laboratory-scale hydraulic conductivity of QD samples	P-06-121 /Sohlenius et al. 2006/
Slug tests	Small-scale hydraulic conductivity (and storativity) at well-screen depths	P-04-122 /Johansson and Adestam 2004a/ P-04-318 /Johansson and Adestam 2004c/ P-06-149 /Johansson and Göransson 2006/ P-06-150 /Svensson and Zetterlund 2006/ P-06-248 /Johansson et al. 2007/ P-07-91 /Morosini et al. 2007/
Hydraulic single-hole and interference tests in groundwater monitoring wells	Intermediate-scale hydraulic conductivity (single-hole tests)	P-07-173 /Gokall-Norman and Ludvigson 2007/
	Larger-scale hydraulic conductivity and storativity (interference tests)	
Tracer dilution tests in groundwater monitoring wells	Intermediate-scale groundwater flow velocities at well-screen depths	P-07-197 /Askling 2007/
Hydraulic interference- and tracer tests in percussion boreholes and groundwater monitoring wells	Hydraulic interaction between QD and rock	P-06-151 /Morosini and Wass 2007/ P-07-187 /Svensson et al. 2008/

4.3 Presentation of data

4.3.1 Hydraulic conductivity estimated from PSD curves

The PSD-based estimation of the hydraulic conductivity of QD samples is here performed using two alternative methods: the Hazen method and the Gustafson method /Andersson et al. 1984/. According to the Hazen method, the hydraulic conductivity K ($m \cdot s^{-1}$) is calculated by the expression

$$K = 0.01157 \cdot d_{10}^2 \tag{1}$$

where d_{10} (mm) is the particle (or grain) diameter for which 10% by weight of the material of the QD sample (by mass) is finer. The expression for K ($m \cdot s^{-1}$) according to the Gustafson method is

$$K = E(U) \cdot d_{10}^2 \tag{2a}$$

where d_{10} is in m and $U = d_{60}/d_{10}$, with d_{60} having a definition similar to that of d_{10} (i.e. the particle diameter for which 60% of the material of the QD sample is finer). The parameter E(U) in equation (2a) is given as

$$E(U) = 10.2 \cdot 10^6 \left(\frac{[e(U)]^3}{1 + e(U)} \right) \left(\frac{1}{[g(U)]^2} \right) \tag{2b}$$

in which the functions e(U) and g(U) are defined as

$$e(U) = 0.8 \left(\frac{1}{2 \cdot \ln(U)} - \frac{1}{U^2 - 1} \right) \tag{2c}$$

$$g(U) = \left(\frac{1.30}{\log(U)} \cdot \frac{U^2 - 1}{U^{1.8}} \right) \tag{2d}$$

Table 4-2. Summary of hydraulic conductivity data estimated from PSD curves.

Type of QD	Amount of PSD data	Arithmetic (geometric) average hydraulic conductivity, K ($m \cdot s^{-1}$)	
		Hazen method	Gustafson method
Sandy-gravelly till	43	$3.86 \cdot 10^{-5}$ ($1.49 \cdot 10^{-5}$)	$1.96 \cdot 10^{-5}$ ($4.34 \cdot 10^{-6}$)
Clayey till/silt, silty-clayey sand/gravel	7	$5.36 \cdot 10^{-7}$ ($4.64 \cdot 10^{-7}$)	$1.41 \cdot 10^{-7}$ ($1.07 \cdot 10^{-7}$)
Sand-gravel	20	$5.51 \cdot 10^{-4}$ ($2.89 \cdot 10^{-4}$)	$5.02 \cdot 10^{-4}$ ($2.34 \cdot 10^{-4}$)
Total	70		

Hence, both these methods require the d_{10}-value, which usually cannot be quantified for very fine-grained or clayey types of QD. Table 4-2 presents average values of the hydraulic conductivity for QD samples, classified into different types of QD, for which d_{10}-values are available.

As can be seen in Table 4-2, the Gustafson method yields slightly lower K-values compared to the Hazen method, with a Hazen/Gustafson ratio ranging from c 1.1 (sand-gravel samples) to 3.8 (clay-silt samples). The PSD estimation of K provides an average hydraulic conductivity of c $5 \cdot 10^{-4}$ $m \cdot s^{-1}$ for sand-gravel samples, and on the order of 10^{-5} and 10^{-7} $m \cdot s^{-1}$ for sandy-gravelly till and clay-silt samples, respectively. As known, the geometric averages of K are lower than the arithmetic averages. In connection to Table 4-2, it should be noted that the Hazen method strictly is considered valid only for well-sorted QD samples ($U = d_{60}/d_{10} \leq 5$), whereas most of the tested QD samples actually contain a rather wide range of particle sizes. Therefore, the K-values in Table 4-2 should be considered as indications rather than exact determinations of K. One should also note that the spread of K-values is relatively large within the individual QD classes defined for the purposes of this analysis. The coefficient of variation CV (= standard deviation/average) ranges between c 0.5 for the clay-silt class to c 1.5 for the sandy-gravelly till class.

In order to investigate any potential depth-dependence of K, Figure 4-5 shows Hazen-estimated hydraulic conductivity values ($m \cdot s^{-1}$) versus sampling depth (m below ground surface). The left plot in Figure 4-5 includes till samples only, whereas the right plot includes all frictional material (hence, also including sand and gravel samples). The left plot reveals the large spread of K for the till samples; the data do not demonstrate any obvious depth dependence. Note that most till samples are taken < 5 m below the ground surface. On the other hand, the incorporation of sand and gravel (the right plot) indicates that the frictional material has a high hydraulic conductivity both close to the ground surface and at larger depths.

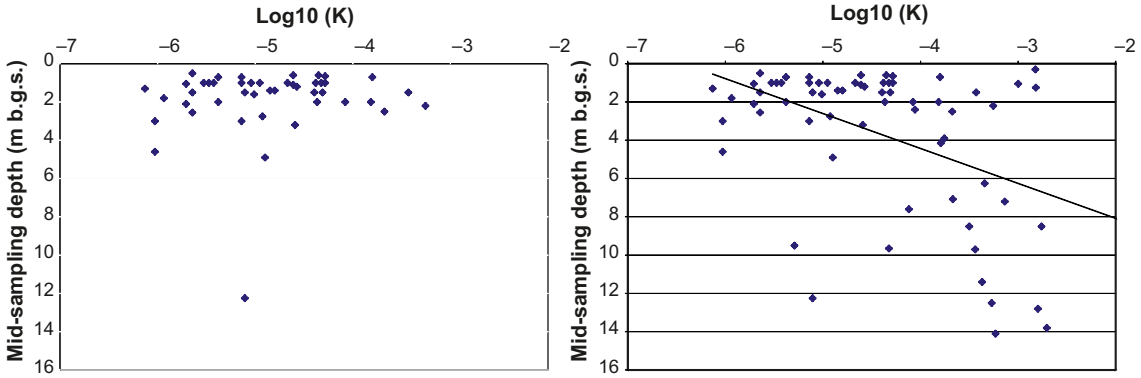

Figure 4-5. *Plots of the hydraulic conductivity K ($m \cdot s^{-1}$), estimated from PSD curves using the Hazen method, versus mid-sampling depth (m below ground surface). The left plot includes till samples only, whereas the right trend-line plot also includes sand and gravel. Note the log scale on the horisontal (K) axes.*

4.3.2 Hydraulic conductivity measured by permeameter tests

/Sohlenius et al. 2006/ present the results of so called constant-head permeameter tests, providing laboratory-scale hydraulic conductivity of QD sampled in dug trenches. The (undisturbed) QD samples were taken vertically using steel cylinders (Ø 0.072 m and length 0.05 m). The results of these tests are summarised in Table 4-3. In order to produce the table, the hydraulic conductivity data are grouped into different types of QD, classified according to /Sohlenius et al. 2006/. Most QD samples emanate from shallow depths (< 1 m below ground), which implies that the permeameter tests primarily provide data on near-surface, vertical hydraulic conductivity.

In general, the permeameter tests yield lower K-values for till compared to both PSD curves (section 4.2.1) and slug tests (see section 4.2.3 below). Hence, the permeameter tests indicate that the hydraulic conductivity of till is anisotropic, specifically that the vertical conductivity of the till is lower than the horisontal conductivity (which is assumed to be obtained from e.g. slug tests; see section 4.3.3). Comparing the arithmetic average of K for till obtained from PSD curves (Table 4-2) and slug tests (Table 4-4 below) to Table 4-3 yields an anisotropy ratio (K_h/K_v) in the interval 17–26. However, it should be noted that the spatial test scales of these methods are not the same, and also that the difference between the vertical and the horisontal hydraulic conductivity may be less pronounced in the upper part of the QD (say, the upper 1 m) due to the impact from soil-forming processes.

In Table 4-3 it is noted that the K-values for sand and gravel are unrealistically low, and that the K-values are notably high for "low-permeable" QD types such as clay gyttja, gyttja and glacial clay. There hence seem to be a limited use of the permeameter tests for estimation of K-values (note that no-flow tests, i.e. K = 0, were omitted from the calculations). Nevertheless, the tests indicate a rather high near-surface (vertical) hydraulic conductivity, including those of gyttja and clayey QD: Taking into account all K-data for QD sampled < 1 m below the ground surface, the arithmetic average of $K = 1.54 \cdot 10^{-5}$ m·s^{-1} (geometric mean = $7.52 \cdot 10^{-6}$ m·s^{-1}). The CV of the measured K-values ranges between c 0.5 (the postglacial gravel and stones class) and c 1.5 (the gyttja class).

Table 4-3. Hydraulic conductivity K (m·s^{-1}) measured by 24-h laboratory permeameter tests, classified according to /Sohlenius et al. 2006/. Note that tests with no flow are not considered in the calculation of averages.

Type of QD	Total number of K data (number of K = 0 data)	Arithm. average	Geom. average
Till	6 (3)	$1.47 \cdot 10^{-6}$	$9.52 \cdot 10^{-7}$
Clay gyttja	13 (1)	$1.08 \cdot 10^{-5}$	$5.64 \cdot 10^{-6}$
Gyttja	7 (0)	$2.31 \cdot 10^{-5}$	$1.08 \cdot 10^{-5}$
Glacial clay	8 (6)	$4.81 \cdot 10^{-5}$	$2.62 \cdot 10^{-5}$
Post-glacial sand	4 (2)	$1.53 \cdot 10^{-5}$	$6.89 \cdot 10^{-6}$
Post-glacial gravel and stones	8 (1)	$3.00 \cdot 10^{-6}$	$2.83 \cdot 10^{-6}$
Unknown QD (not described in /Sohlenius et al. 2006/)	1 (0)	$2.22 \cdot 10^{-8}$	$2.22 \cdot 10^{-8}$
Total	47 (13)		

4.3.3 Hydraulic conductivity measured by slug tests

The basic principle of slug tests is to initiate an instantaneous displacement of the water level in an observation (or groundwater monitoring) well, and to observe the subsequent recovery of the water level as function of time (see e.g. /Werner and Johansson 2003/). Table 4-4 summarises the results of the slug tests performed in groundwater monitoring wells in Laxemar. As for Tables 4-2 and 4-3, the hydraulic conductivity data are grouped in different types of QD, based on well-screen depth data versus stratigraphical interpretations available in the Sicada database.

As shown in Table 4-4, the slug tests provide an average hydraulic conductivity on the order of 10^{-4} m·s^{-1} for QD belonging to the boulder-gravel-sand class, 10^{-6} m·s^{-1} for the peat class, and 10^{-7} m·s^{-1} for the silty-clayey till class. As for both the method based on PSD curves and the permeameter tests, the slug tests show a spread of measured K-values within the individual QD classes; CV ranges between c 0.8 (the peat class) and c 1.2 (the till class 2, excluding QD-rock screens).

In Table 4-4, the K data for sandy-gravelly till is divided into two sub sets: one low-K data set (class 1) and one high-K data set (class 2). The reason for doing this is that the spread of K-values is notably high if all sandy-gravelly till data are treated as a single data set. Specifically, class 1 contains K-values in the approximate range 10^{-6}–10^{-5} m·s^{-1}, whereas class 2 is characterised by K-values on the order of 10^{-4}–10^{-3} m·s^{-1}. For both these classes, excluding data for wells with their screen across the QD-rock interface has only a minor effect on the calculated average hydraulic conductivity. This indicates that the hydraulic conductivity of the rock at the QD-rock interface has a hydraulic conductivity that is on the same order of magnitude or lower than the gravelly-sandy till; a substantially higher hydraulic conductivity of the upper rock would yield a lower average hydraulic conductivity for the data sets excluding wells with "QD-rock screens".

In order to further investigate any potential depth-dependence of K (cf. section 4.3.1), the K-values (m·s^{-1}) obtained from slug tests in wells with their screen installed in frictional material (including wells with their screen across the QD-rock interface) are plotted in Figure 4-6 versus the mid-screen depth (m below the ground surface). In the upper plot, one can note a trend with depth-increasing K-values down to a depth of approximately 10–15 m. The deepest screens are outliers from this trend (sand and till at 32 m depth, and clay and till at 17 m depth); these two outliers are not included when producing the trend line in the bottom plot.

Table 4-4. Hydraulic conductivity measured by slug tests, classified according to the (dominant) type of QD at the well-screen depth. Data excluding wells with their screen across the QD-rock interface are presented in a separate column. NC means "not calculated".

Type of QD	Amount of slug-test data	Arithm. average	Geom. average	Arithm. average (excl. "QD-rock screens")	Geom. average (excl. "QD-rock screens")
Till (class 1; low-K set)	31	$2.52 \cdot 10^{-5}$	$1.19 \cdot 10^{-5}$	$2.47 \cdot 10^{-5}$	$1.15 \cdot 10^{-5}$
Till (class 2; high-K set)	20	$8.57 \cdot 10^{-4}$	$3.37 \cdot 10^{-4}$	$8.94 \cdot 10^{-4}$	$3.07 \cdot 10^{-4}$
Till with silt and clay	2	$3.92 \cdot 10^{-7}$	$5.15 \cdot 10^{-8}$	NC	NC
Boulder-gravel-sand	10	$1.44 \cdot 10^{-4}$	$6.37 \cdot 10^{-5}$	NC	NC
Gyttja-gyttja clay	1	$1.00 \cdot 10^{-5}$	$1.00 \cdot 10^{-5}$	NC	NC
Peat	5	$2.44 \cdot 10^{-6}$	$2.03 \cdot 10^{-6}$	NC	NC
Total	71				

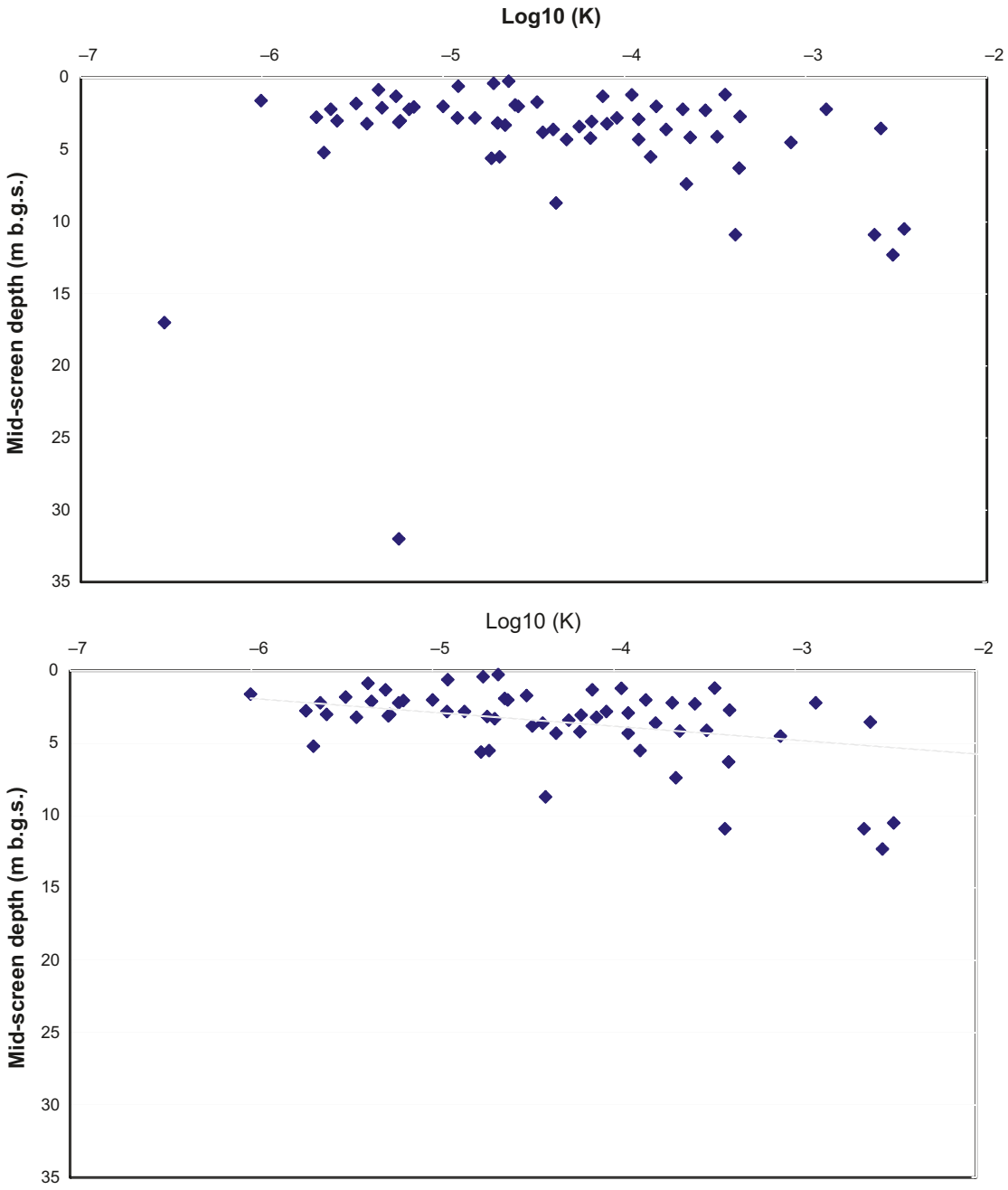

Figure 4-6. *Plots of hydraulic conductivity K ($m \cdot s^{-1}$) versus mid-screen depth (metres below ground surface). The top plot includes wells with their screen installed in till and gravel-sand (including wells with the screen installed across the QD-rock interface). The two deepest outliers are not considered in the trend-line plot (bottom). Note the log scale on the horisontal (K) axes.*

4.3.4 Hydraulic single-hole and interference tests in QD

/Gokall-Norman and Ludvigson 2007/ report hydraulic (pumping) tests in 8 groundwater monitoring wells installed in the QD. The wells were pumped for periods ranging from 10 hours to two days, with a discharge ranging from 0.2 to 130 $L \cdot min^{-1}$. Their investigation involved both single-hole tests (i.e. evaluation of pumping-well data only) and interference tests (evaluation of both pumping- and observation-well data), using totally 8 observation wells. A single-hole test was also planned for groundwater monitoring well SSM000217, but this test could not be performed due to the low water level in that well.

Drawdown and recovery data from the 8 pumping wells were used to estimate transmissivity T (= K·B), whereas data from the observation wells (located c 2–100 m from the pumping wells) were used to estimate both T and storativity $S = S_s \cdot B$; S_s denotes the so called specific storage coefficient (m^{-1}) and B is an assumed formation thickness (m). Parameters evaluated from the single-hole tests (here abbreviated ST) and the interference tests (abbreviated IT) are summarised in Table 4-5, whereas the overview map in Figure 4-7 for orientation shows the locations of the tested wells in terms of sites (Site 1-8).

Table 4-5. Hydraulic conductivity K ($m \cdot s^{-1}$) and specific storage coefficient S_s (m^{-1}), obtained from single-hole tests (ST) and interference tests (IT) in groundwater monitoring wells installed in QD / Gokall-Norman and Ludvigson 2007/. In the ST column, S_s estimates (S_s*) denote either (average) values of S_s obtained from the corresponding interference tests (IT), or assumed values of S_s, equal to $S_s = 5 \cdot 10^{-2}$ or $S_s = 1 \cdot 10^{-3}$ m^{-1}.

Pump. well ID	QD at well-screen depth	Eval. param. (ST) (K-value from slug test)		Obs. well ID (dist. to pump. well)	QD at well-screen depth	Eval. param. (IT) (K-value from slug test)	
		K	S_s*			K	S_s
SSM220	Sandy till (0.3 m), bouldery-gravelly sandy till (0.7 m)	$2.11 \cdot 10^{-4}$ ($1.30 \cdot 10^{-3}$)	$5.00 \cdot 10^{-2}$	SSM221 (53 m)	Boulder-bearing silty-sandy till	No response ($2.10 \cdot 10^{-4}$)	
SSM223	Blocky-sandy till	$1.72 \cdot 10^{-4}$ (too fast response to evaluate)	$5.00 \cdot 10^{-2}$				
SSM224	Gravelly sand	$1.03 \cdot 10^{-2}$ (too fast response to evaluate)	$3.81 \cdot 10^{-2}$	SSM225 (2.5 m)	Gravelly sand (0.1 m), stony-sandy gravel (0.9 m)	$6.30 \cdot 10^{-2}$ (too fast response to evaluate)	$3.81 \cdot 10^{-2}$
				SSM31 (112 m)	Silty-sandy till (0.1 m), gravelly-sandy till (0.9 m)	No response ($1.2 \cdot 10^{-4}$)	
SSM228	Sandy till (0.8 m), sandy-silty till (0.2 m)	$4.69 \cdot 10^{-5}$ (1.30·10–3)	$5.00 \cdot 10^{-2}$	SSM229 (28 m)	Gravelly sandy till	No response ($1.02 \cdot 10^{-5}$)	
SSM236	Clay (0.1 m), clayey sandy silt (0.3 m), sandy-silty till (0.6 m)	$1.05 \cdot 10^{-5}$ (slug tested but not evaluated)	$1.00 \cdot 10^{-3}$				
SSM261	Sand (medium to coarse)	$2.52 \cdot 10^{-4}$ ($4.20 \cdot 10^{-5}$)	$1.14 \cdot 10^{-3}$	SSM260 (83 m)	Coarse matrix, till (1.22 m), rock (0.78 m)	$3.15 \cdot 10^{-4}$ ($2.20 \cdot 10^{-4}$)	$7.00 \cdot 10^{-4}$
				SSM30 (84 m)	Gyttja (0.3 m), gravelly-sandy till (0.7 m)	$7.00 \cdot 10^{-4}$ ($2.20 \cdot 10^{-5}$)	$8.40 \cdot 10^{-4}$
SSM263	Till	$1.75 \cdot 10^{-4}$ ($4.30 \cdot 10^{-4}$)	$5.00 \cdot 10^{-4}$	SSM41 (70 m)	Sandy-clayey silt (1.8 m), sandy silty till (0.2 m)	No response ($6.50 \cdot 10^{-6}$)	
SSM265	Till (0.97 m), rock (1.03 m)	$4.31 \cdot 10^{-5}$ ($2.60 \cdot 10^{-3}$)	$1.19 \cdot 10^{-4}$	SSM266 (16 m)	Till (0.86 m), rock (0.14 m)	$6.00 \cdot 10^{-5}$ ($6.90 \cdot 10^{-6}$)	$2.40 \cdot 10^{-4}$

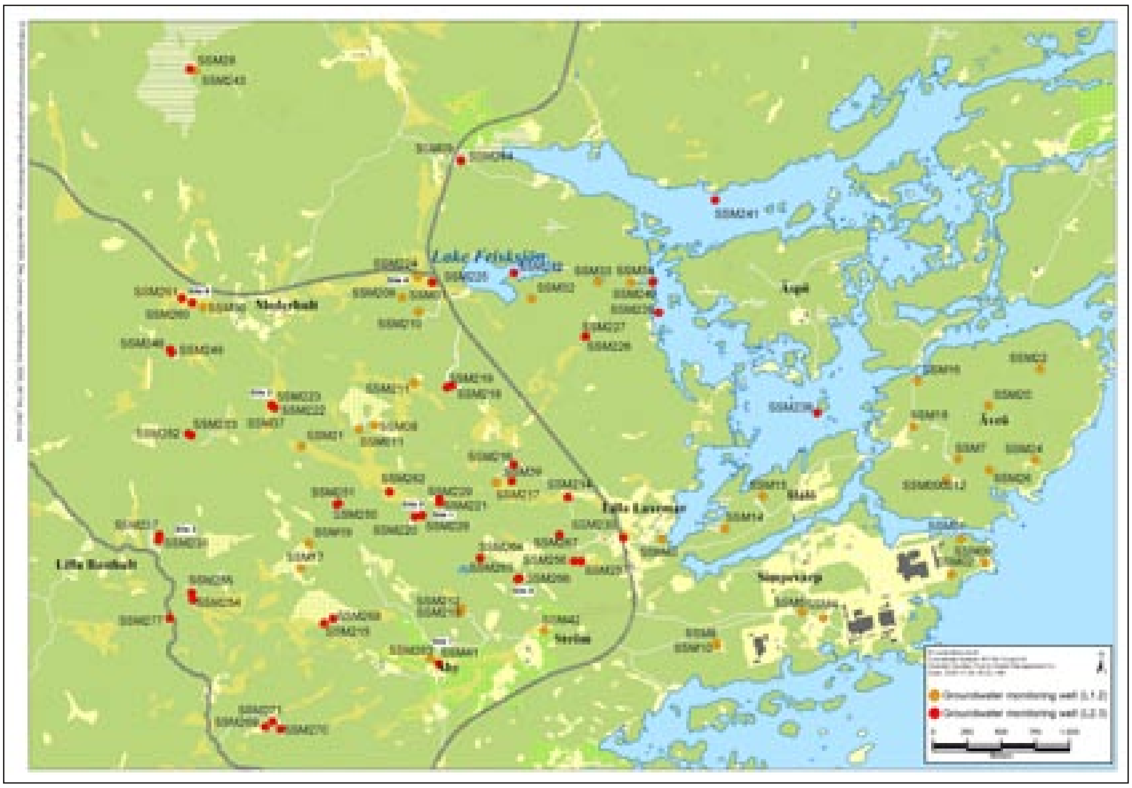

Figure 4-7. *Overview map of groundwater monitoring wells in Laxemar, showing the locations of the sites (Site 1-8) discussed in this section. The colour of the well symbols indicates wells installed up to DF L1.2 (orange) and up to DF L2.3 (red).*

Table 4-5 also shows corresponding hydraulic conductivity values (K), evaluated from slug tests in the same wells (see section 4.3.3). Following the Sicada notations (#Sicada_07_334), the K- and S_s-values in Table 4-5 assume that B is set equal to the screen length of the tested wells (B = 1 or 2 m). Note that well ID numbers here are written in short form (e.g. well SSM000220 is referred to as SSM220).

As shown in Table 4-5, the screens of the pumping wells are installed in medium to coarse sand and bouldery to silty till. The single-hole tests yield K-values on the order of 10^{-5}–10^{-4} $m \cdot s^{-1}$. Except from SSM261, the evaluated K-values are lower than those obtained from the corresponding slug tests. In the interference tests, there were no observed drawdown in 3 of the 8 observation wells; the tests in which SSM220, SSM228 and SSM263 were used as pumping wells. Moreover, the 10-hour pumping in well SSM224 did not yield any observable drawdown in observation well SSM31, but a weak hydraulic response in well SSM225.

As a general comment to the tests, it can be concluded that with two exceptions (SSM28 and SSM265), the K-values obtained from the single-hole tests generally correspond to those obtained from slug tests. However, the K-values obtained from observation wells in the interference tests are higher than those obtained by evaluation of the pumping wells; the observation well/pumping well "scale factor" is in the approximate interval 1.4–6. It should be noted that there is a small tested volume associated with slug tests, and to some extent also during single-hole tests. Generally, the K-values obtained from evaluation of observation-well data in interference tests are considered more appropriate for the large scale associated with numerical water flow models (see e.g. /Butler Jr and Healey 1998/).

The following general comments and interpretations can be made, based on the results of the individual single-hole and interference tests:

- Site 1: SSM220 (pumping well) and SSM221 (observation well) are installed in the Ekerumsån stream valley. Geological investigations, well installations and slug tests are described in /Ask et al. 2006, Svensson and Zetterlund 2006/. The top-down QD stratigraphy is silty clay-silty till-boulder bearing gravelly-sandy till at SSM220, and boulder/cobble bearing clayey gravelly sand-boulder bearing silty sandy till at SSM221. The 46-hour pumping (14 $L \cdot min^{-1}$) resulted in a drawdown of c 2.5 m in SSM220, corresponding to a specific capacity of c $9 \cdot 10^{-5}$ $m^2 \cdot s^{-1}$. There was no response in the observation well SSM221, located c 50 m from the pumping well. It can be concluded that both the single-hole test in SSM220 and the slug tests in SSM220 and SSM221 indicate a relatively high hydraulic conductivity of the till (on the order of 10^{-4}–10^{-3} $m \cdot s^{-1}$) in this valley.
- Site 2: SSM223 is installed in a valley north of the Ekerumsån stream valley. Geological investigations, well installation and slug test are described in /Johansson and Göransson 2006, Sohlenius et al. 2006/. The top-down QD stratigraphy is top soil-silty sand-clay-sandy till. The 12-hour pumping (124 $L \cdot min^{-1}$) in SSM223 resulted in a drawdown of c 3.5 m, corresponding to a specific capacity of c $6 \cdot 10^{-4}$ $m^2 \cdot s^{-1}$. The single-hole test indicate a relatively high hydraulic conductivity of the till (c. 10^{-4} $m \cdot s^{-1}$). Moreover, the slug-test recovery in SSM223 was too fast to evaluate /Johansson and Göransson 2006/.
- Site 3: SSM236 is installed in an area dominated by exposed or shallow rock, c 150 m from a tributary to the stream Laxemarån. Geological investigations, well installation and a slug test are described in /Ask et al. 2007a, Svensson and Zetterlund 2006/. The top-down QD stratigraphy at SSM236 is silt-clay-clayey sandy silt-sandy silty till. The 10-hour pumping (0.4 $L \cdot min^{-1}$) in SSM236 resulted in a drawdown of c 0.6 m, corresponding to a specific capacity of c $1 \cdot 10^{-5}$ $m^2 s^{-1}$. The single-hole test indicates a hydraulic conductivity typical for till in the area (c. 10^{-5} $m \cdot s^{-1}$).
- Site 4: SSM224 (pumping well) and SSM225 (observation well) are installed c 200 m west of Lake Frisksjön in a glaciofluvial deposit, whereas SSM31 (observation well) is installed in a fen peat area c 100 m northwest from SSM224 and 225. Geological investigations, well installations and slug tests are described in /Johansson and Adestam 2004b, Johansson and Göransson 2006, Sohlenius et al. 2006/. The top-down QD stratigraphy in this area is sand-clay-silt-gravel/sand, and peat-till at SSM31. The 10-hour pumping in SSM224 (140 $L \cdot min^{-1}$) resulted in drawdown of c 1 m in the pumping well, corresponding to a specific capacity of c $2 \cdot 10^{-3}$ $m^2 \cdot s^{-1}$. The drawdown was estimated to be c 0.05 m in observation well SSM225, located 2.5 m from SSM224, whereas there was no response in SSM31, 100 m from the pumping well. As expected, both the pumping test and the slug tests in these wells indicate a high conductivity for the glaciofluvial material, dominated by gravel and sand.
- Site 5: SSM228 (pumping well) and SSM229 (observation well) are installed c 10 m and 40 m, respectively, from the stream Ekerumsån. Geological investigations, well installations and slug tests are described in /Johansson and Göransson 2006, Sohlenius et al. 2006/. The general top-down QD stratigraphy in this area is sand-silt-till. The 2-day pumping (15 $L \cdot min^{-1}$) in SSM228 resulted in a drawdown of c 3 m, corresponding to a specific capacity of c $8 \cdot 10^{-5}$ $m^2 \cdot s^{-1}$. There was no response in SSM229. The hydraulic conductivity evaluated from the single-hole test in SSM228 (c. 10^{-5} $m \cdot s^{-1}$) is substantially lower than the conductivity evaluated from the corresponding slug test (c. 10^{-3} $m \cdot s^{-1}$), but similar to that evaluated from the slug test in SSM229.

- Site 6: SSM261 (pumping well), SSM30 and SSM260 (observation wells) are installed in the Mederhultsån stream valley. Geological investigations, well installations and slug tests in these wells are described in /Johansson and Adestam 2004b, Morosini et al. 2007/. The general top-down QD stratigraphy is peat-gyttja-till, with clay above the till at SSM260 and SSM261 but not at SSM30. The screen of the pumping well SSM261 is installed in a sand layer, above the clay. The QD overlying the rock at SSM260 is geologically interpreted as till, but as gravel/sand by grain-size analysis /Morosini et al. 2007/. Hence, the pumping was performed in a sand layer overlying clay (in turn overlying till) at SSM261, whereas the observation wells have their screens installed in till directly above the rock. The 45-hour pumping (8 $L \cdot min^{-1}$) in SSM261 resulted in a drawdown of c 5 m, corresponding to a specific capacity of c $3 \cdot 10^{-5}$ $m^2 \cdot s^{-1}$. There was a very small drawdown (estimated as 0.05 m) in the observation wells, which may be due to the presence of the low-permeable clay layer. The response occurred faster at SSM30 compared to SSM260, likely due to that the clay layer seems to be thinner in the vicinity of SSM30.
- Site 7: SSM263 (pumping well) and SSM41 (observation well) are installed in the Laxemarån stream valley. Geological investigations, well installations and slug tests are described in /Johansson and Adestam 2004b, Morosini et al. 2007/. The top-down QD stratigraphy at SSM263 is peat-clay-till, and sand-sandy clayey silt-till at SSM41. The 22-hour pumping in SSM263 (67 $L \cdot min^{-1}$) resulted in a drawdown of c 3.5 m, corresponding to a specific capacity of c $3 \cdot 10^{-4}$ $m^2 \cdot s^{-1}$. There was no hydraulic response in SSM41, located 70 m from SSM263. Both the single-hole test and the slug test in SSM263 indicate a relatively high hydraulic conductivity (c. 10^{-4} $m \cdot s^{-1}$) for the till in this valley.
- Site 8: SSM265 (pumping well) and SSM266 (observation well) are installed in a hummocky moraine area. Geological investigations, well installations and slug tests are described in /Morosini et al. 2007/. The general top-down QD stratigraphy in this area is clay-till. The screens of both wells are located across the till-rock interface. The 47-hour pumping (16 $L \cdot min^{-1}$) in SSM265 resulted in a drawdown of c 2 m in the pumping well, corresponding to a specific capacity of c $1 \cdot 10^{-4}$ $m^2 \cdot s^{-1}$. The drawdown in the observation well SSM266 was c 1 m. The hydraulic conductivity evaluated from the single-hole and interference test (c. 10^{-5} $m \cdot s^{-1}$) is substantially lower than the conductivity evaluated from the slug test in SSM265 (c. 10^{-3} $m \cdot s^{-1}$), but similar to that evaluated from the slug test in SSM266.

4.3.5 Tracer dilution tests in Quaternary deposits

/Askling 2007/ presents the results of tracer (Uranine) dilution tests in 5 groundwater monitoring wells, and use these results to calculate undisturbed groundwater flow across the screens of the tested wells. Based on the calculated groundwater flow (available in the Sicada database), the /Askling 2007/ report also provides rough estimates of the horisontal hydraulic head gradient across each of the well screens, based on the transmissivity (T) evaluated by slug tests in the same wells (cf. section 4.3.3). Note that geological investigations, well installations and slug tests in wells SSM243 and SSM244 are reported in /Johansson et al. 2007/, whereas /Morosini et al. 2007/ report the corresponding investigations and tests in SSM261–263. Table 4-6 summarises the results of the dilution tests. Note that well ID numbers are written in short form (e.g. well SSM000243 is referred to as SSM243).

The results in Table 4-6 show that with a couple of exceptions, the undisturbed horisontal groundwater flow (and the Darcy velocity) are relatively similar among the tested well screens. There a somewhat higher groundwater flow across the screen of well SSM243, installed in till below the Gäster wetland. Moreover, the Darcy velocity is comparatively higher across the screen of well SSM263; this screen is installed across the till-rock interface. It can be noted that the calculations based on the tracer dilution test in well SSM261 yield a notably high hydraulic head gradient ($i \approx 3$) in the sand layer in which the screen is installed.

Table 4-6. Summary of dilution tests in groundwater monitoring wells /Askling 2007/. Q_u = undisturbed groundwater flow, i = horisontal hydraulic head gradient.

Well ID	Location	QD at well-screen depth	K ($m \cdot s^{-1}$) evaluated by slug test	Q_u ($m^3 \cdot s^{-1}$)	Darcy velocity ($m \cdot s^{-1}$)	i (-)
SSM243	Wetland (Gästern)	Clay (0.6 m) + sandy till (0.4 m)	$1.97 \cdot 10^{-4}$	$4.17 \cdot 10^{-7}$	$3.3 \cdot 10^{-6}$	0.23
SSM244	Wetland (Kärrsvik)	Sandy till	$3.50 \cdot 10^{-3}$	$1.42 \cdot 10^{-6}$	$5.0 \cdot 10^{-6}$	No T data
SSM261	Mederhultsån stream valley	Sand	$4.06 \cdot 10^{-5}$	$1.92 \cdot 10^{-6}$	$1.9 \cdot 10^{-6}$	3.1
SSM262	Ekerumsån stream valley	Clay or silt or sand (0.5 m) + till (2.5 m) (sand and gravel acc. to /Morosini et al. 2007/)	$3.03 \cdot 10^{-3}$	$1.81 \cdot 10^{-6}$	$6.0 \cdot 10^{-6}$	0.0094
SSM263	Laxemarån stream valley	Till (1.02 m) + rock (0.98 m)	$1.71 \cdot 10^{-4}$	$2.56 \cdot 10^{-6}$	$1.3 \cdot 10^{-5}$	0.19

4.3.6 Hydraulic interference and tracer tests in QD and near-surface rock

Hydraulic interference and tracer tests in HLX34, HLX35, SSM37, SSM222 and SSM223

/Morosini and Wass 2007/ report hydraulic interference- and tracer tests, including percussion boreholes HLX34 and HLX35 and groundwater monitoring wells SSM37, SSM222, and SSM223, installed in a valley north of the Ekerumsån stream valley. The QD in the valley are dominated by clay gyttja, at some locations also with a thin peat cover, and the QD depth is c 3–6 m. Deformation zone ZSMNS059A coincides with the valley in this area. It can be noted that a single-hole test in well SSM223 is reported by /Gokall-Norman and Ludvigson 2007/ (cf. section 4.3.4). Specifically, the investigation by /Morosini and Wass 2007/ included the following tests:

(1) Pumping in percussion borehole HLX35, with simultaneous drawdown observations in HLX34, SSM37, SSM222, and SSM223.

(2) Tracer dilution tests in groundwater monitoring wells SSM37, SSM222, and SSM223, both prior to and during pumping in HLX35.

(3) Tracer injection in groundwater monitoring wells SSM222 and SSM223, with simultaneous pumping and tracer detection in HLX35.

The 1-month pumping (104 $L \cdot min^{-1}$) resulted in a drawdown of c 11 m in the pumping borehole HLX35. Further, there was a drawdown of c 4 m in the observation borehole HLX34 (located c 170 m from HLX35). However, there was no hydraulic response in the wells SSM37 and SSM222, installed c 50 m from HLX35. There was a clear response in well SSM223, installed c 80 m from HLX35. The evaluation of the drawdown in the wells was complicated by disturbances caused by precipitation during the pumping test. Prior to pumping, the point-water head in HLX35 and HLX34 was c 14 metres above sea level, whereas the pre-test groundwater level was c 10–11 metres above sea level in the groundwater monitoring wells. Note that the post data-freeze data corrections (section 2.4.2) imply that the groundwater level in SSM37 is increased c 0.7 m. Hence, the data prior to the test indicate groundwater discharge from the rock to the QD (cf. section 3.7.1). During the pumping test, the point-water head in HLX35 and HLX34 decreased to c 4 and 10 metres above sea level respectively, whereas the drawdown in well SSM223 was a few decimetres. This indicates a situation with groundwater recharge from the QD to the rock during pumping. The results of the hydraulic interference test are summarised in Table 4-7. Note that well ID numbers are written in short form (e.g. well SSM000037 is referred to as SSM37).

Table 4-7. Summary of the hydraulic interference test by /Morosini and Wass 2007/. K = hydraulic conductivity, T = transmissivity, and S = storativity (S* denotes an estimate based on the HLX34 interference-test data).

Pump. well ID	QD at well-screen depth	Eval. param. (D = drawdown, R = recovery) T ($m^2 \cdot s^{-1}$) K ($m \cdot s^{-1}$)	S*	Obs. well ID	QD at well-screen depth	Eval. param. T ($m^2 \cdot s^{-1}$) K ($m \cdot s^{-1}$)	S
HLX35	-	$T_D = 1.1 \cdot 10^{-4}$, $T_R = 1.2 \cdot 10^{-4}$ $K_D = 7.7 \cdot 10^{-7}$, $K_R = 8.2 \cdot 10^{-7}$	$1.5 \cdot 10^{-4}$	HLX34	-	$T = 1 \cdot 10^{-4}$ $K = 6.6 \cdot 10^{-7}$	$1.5–1.6 \cdot 10^{-4}$
				SSM37	Sandy-gravelly till	No response	
				SSM222	Sandy till (some boulders)	No response	
				SSM223	Blocky-sandy till	$T = 3.9 \cdot 10^{-3}$ $K = 2.0 \cdot 10^{-3}$	$8.1 \cdot 10^{-3}$

According to /Morosini and Wass 2007/, there are several plausible "hydraulic response paths" between borehole HLX35 and well SSM223: (1) Along the borehole and through the QD, (2) along the straight distance between the "points of application", and (3) along tortuous paths determined by fractures in the rock and the hydrogeological properties of the QD-rock interface; they considered hypothesis (3) to be the most likely. Specifically, percussion borehole HLX35 intersects deformation zone ZNMNS59A, which in turn is thought to outcrop in the vicinity of well SSM223, which could explain the drawdown in that well during pumping in HLX35 (see Figure 4-8).

Table 4-8 shows the results of the tracer (Uranine) dilution tests, based on which /Morosini and Wass 2007/ calculate both the undisturbed (i.e. prior to pumping in HLX35) and the disturbed (during pumping) groundwater flow through the well screen of wells SSM37, SSM222, and SSM223.

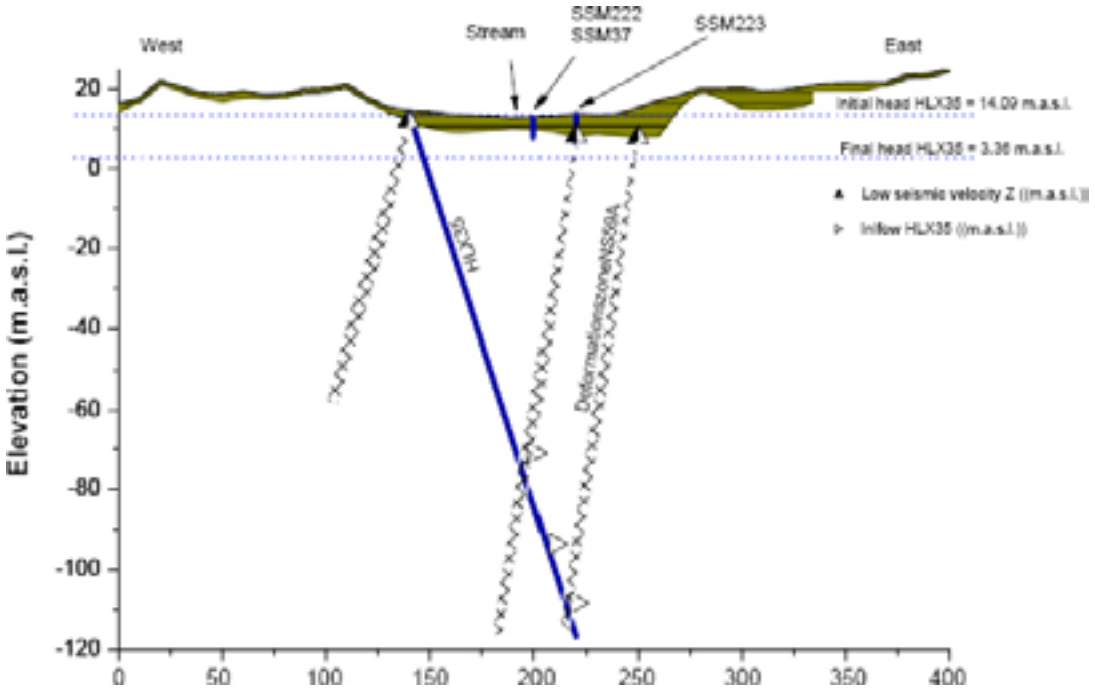

Figure 4-8. *Cross section illustrating the interpretation of the hydraulic response in SSM223 during pumping in HLX35 /Morosini and Wass 2007/.*

Table 4-8. Summary of tracer dilution tests in wells SSM37, SSM222, and SSM223 /Morosini and Wass 2007/. Q_u = undisturbed groundwater flow and Q_d = disturbed groundwater flow.

Well ID	QD at well-screen depth	K ($m \cdot s^{-1}$) evaluated by slug test	Q_u ($m^3 \cdot s^{-1}$)	Q_d ($m^3 \cdot s^{-1}$)	$Q_d \cdot Q_u^{-1}$
SSM37	Sandy-gravelly till	[1]$2 \cdot 10^{-5}$	$1.28 \cdot 10^{-8}$	$1.47 \cdot 10^{-8}$	1.15
SSM222	Sandy till (some boulders)	[2]$4.8 \cdot 10^{-5}$	$3.89 \cdot 10^{-9}$	$2.22 \cdot 10^{-9}$	0.57
SSM223	Blocky-sandy till	[3]$1.72\,10^{-4}$	$1.78 \cdot 10^{-6}$	[4]$2.75 \cdot 10^{-7}$	0.15

[1]/Johansson and Adestam 2004c/.
[2]/Johansson and Göransson 2006/.
[3]Obtained from the single-hole test performed by /Gokall-Norman and Ludvigson 2007/; during the slug test in SSM223, the water-level recovery was too fast for quantitative evaluation /Johansson and Göransson 2006/.
[4]Value missing in Sicada; here taken from the /Morosini and Wass 2007/ report.

Table 4-8 shows that both the undisturbed (Q_u) and the disturbed (Q_d) groundwater flow is larger across the well screen of well SSM223 compared to the flow across the screens of wells SSM37 and SSM222. This result is in accordance with the slug-and single-hole tests, which indicate a higher hydraulic conductivity at the screen of well SSM223. Compared to undisturbed flow conditions, there was a quicker tracer dilution in well SSM37 while pumping in HLX35, whereas the dilution was slower in SSM222 and SSM223; the flow reduction was largest across the screen of SSM223. According to /Morosini and Wass 2007/, this phenomenon may be interpreted by a reversed hydraulic head gradient during pumping. In addition, in SSM37 the measurements actually showed an increased tracer concentration after pump start in HLX35. This can also be explained by a reversed hydraulic head gradient during pumping; groundwater that had left the well screen of SSM37 returned to the well during pumping in HLX35.

As a last step of their tests /Morosini and Wass 2007/ injected tracers in well SSM222 (Uranine) and SSM223 (Rhodamine WT) while pumping in HLX35. Rhodamine WT was detected in HLX35, but there was no detection of the Uranine injected in well SSM222. Approximately 26 days after the Rhodamine WT injection, the tracer recovery in HLX35 was 7%.

Hydraulic interference- and tracer tests in HLX31, HLX33, SSM228 and SSM229

/Svensson et al. 2008/ performed (1) tracer (Uranine) dilution tests in SSM228 and SSM229, both prior to and during pumping in the nearby percussion borehole HLX33, and (2) Uranine injection in SSM228, with simultaneous pumping and tracer detection in HLX33. These boreholes and wells are located in the Ekerumsån stream valley. The QD are dominated by till and locally postglacial sand with a thin peat cover. The QD depth is very variable in this area (c 2–8 m). Deformation zone ZSMEW007A transects the area in the direct vicinity of HLX31 and -33. Note that single-hole and interference tests in SSM228 and SSM229 also are reported by /Gokall-Norman and Ludvigson 2007/ (cf. section 4.3.4).

The 5-week pumping (97 $L \cdot min^{-1}$) in HLX33 resulted in a drawdown of c 1 m in HLX31 (located c 500 m from HLX33). There was no hydraulic response in SSM228 and SSM229, located c 160 m from HLX33. Table 4-9 summarises the results of the tracer dilution tests. For each of the tested QD wells, the table shows the type of QD at the well-screen depth, the estimated undisturbed (Q_u) and disturbed (Q_d, i.e. during pumping) groundwater flow through each well screen, and the hydraulic conductivity K evaluated by slug tests /Johansson and Göransson 2006/ (see section 4.3.3). Note that well ID numbers are written in short form (e.g. well SSM000228 is referred to as SSM228).

Table 4-9. Results of dilution and tracer tests in SSM228 and SSM229 /Svensson et al. 2008/.

Well ID	QD at well screen	Q_u ($m^3 \cdot s^{-1}$)	Q_d ($m^3 \cdot s^{-1}$)	$Q_d \cdot Q_u^{-1}$	K ($m \cdot s^{-1}$), slug test
SSM228	Sandy till (0.8 m) + sandy-silty till (0.2 m)	$5.63 \cdot 10^{-7}$	$2.31 \cdot 10^{-7}$	0.41	$1.4 \cdot 10^{-4}$
SSM229	Gravelly sandy till	$7.50 \cdot 10^{-8}$	$2.03 \cdot 10^{-8}$	0.27	$8.2 \cdot 10^{-5}$

According to Table 4-9, the difference between the two tested wells in terms of undisturbed (Q_u) and disturbed (Q_d) groundwater flow, correlate well with the difference in hydraulic conductivity K as inferred from slug tests: Both Q_u, Q_d, (Table 4-9) and K (from the slug tests) are c one order of magnitude lower for SSM229 compared to SSM228. Compared to undisturbed flow conditions, there was a slower tracer dilution in SSM228 and SSM229 while pumping in HLX33 (as quantified by the ratio $Q_d \cdot Q_u^{-1}$). /Svensson et al. 2008/ interpreted this as a reversed hydraulic head gradient compared to undisturbed conditions.

Prior to pumping, the point-water head in HLX33 was c 11 metres above sea level whereas the pre-test groundwater level was c 10 metres above sea level in SSM228 and almost 12 metres above sea level in SSM229. Hence, under undisturbed conditions the groundwater level in SSM228 was slightly below the point-water head in HLX33 (indicating groundwater discharge from the rock to the QD), and vice versa for SSM229. During pumping, the point-water head in HLX33 was lowered c 1 m, creating conditions for groundwater recharge from the QD to the rock during the pumping. /Svensson et al. 2008/ injected another batch of Uranine in SSM228, while pumping was continued in HLX33. Approximately 32 days after the Uranine injection, the tracer recovery in HLX33 was 33%. Hence, the tracer test shows that there is a hydraulic contact between the QD and the underlying rock.

4.3.7 Porosity and hydrogeological properties of the unsaturated zone

Specific hydrogeological properties data are required for description and modelling of water flow in the unsaturated zone, including porosity, field capacity, residual water content, and wilting point. Further, such descriptions and modelling also need generic or experimental water-retention data, as well as data on the relationship between capillary pressure or tension head ψ and hydraulic conductivity. The field capacity, θ_{fc}, is defined as the remaining water content after free gravitational drainage of an initially saturated soil. θ_{fc} is commonly expressed as the water content at ψ = 1 m or pF 2 (pF = $\log_{10}(\psi)$ with ψ in centimetres). Moreover, at ψ values larger than the wilting point (commonly taken as ψ = 150 m or pF 4.2) roots of plants and trees cannot extract water. The residual water content can be defined as the asymptote of the pF curve; at the residual water content, the water content can only be decreased further by oven drying.

There are no site-specific data from Laxemar on the relationship between ψ and hydraulic conductivity. However, /Sohlenius et al. 2006/ present porosity- and water-retention data, obtained experimentally by applying increasing capillary pressure heads (0.10, 0.50, 1.00 and 5.00 m) on totally 34 QD samples obtained from trenches dug in the Laxemar area. The applied capillary pressure heads correspond to pF in the range 1–2.7, which means that the experiments provide values of field capacity (pF 2) but not wilting point (pF 4.2) or residual water content. The QD samples are obtained from rather shallow depths (< 3 m below the ground surface). The arithmetic average and the standard deviation of the resulting porosity and field capacity values are summarised in Table 4-10, whereas the corresponding water-retention curves (i.e. plots of water content versus ψ) are shown in Figures 4-9 to 4-13, presented by profile ID numbers in /Sohlenius et al. 2006/.

Some of the experimental water-retention curves show an expected drainage behaviour, i.e. easily-drained sand samples, a high water-retention capacity of samples of glacial clay and clay gyttja, and intermediate drainage characteristics of till samples. It can also be observed that in some cases, clay gyttja appear to be relatively easily drained (e.g. Figure 4-9).

Table 4-10. Summary of porosity and field capacity data reported in /Sohlenius et al. 2006/.

QD	Arithmetic mean porosity (%)	St. dev.	Arithmetic mean field capacity (%)	St. dev.
Sandy-gravelly till	45.8	18.2	42.5	19.0
Gyttja	80.3	7.1	70.1	11.6
Clay gyttja	65.1	11.8	53.8	17.9
Glacial clay	48.6	14.6	46.0	19.1
Post-glacial gravel	40.4	4.7	27.2	19.4
Post-glacial sand	45.3	9.1	23.6	12.9

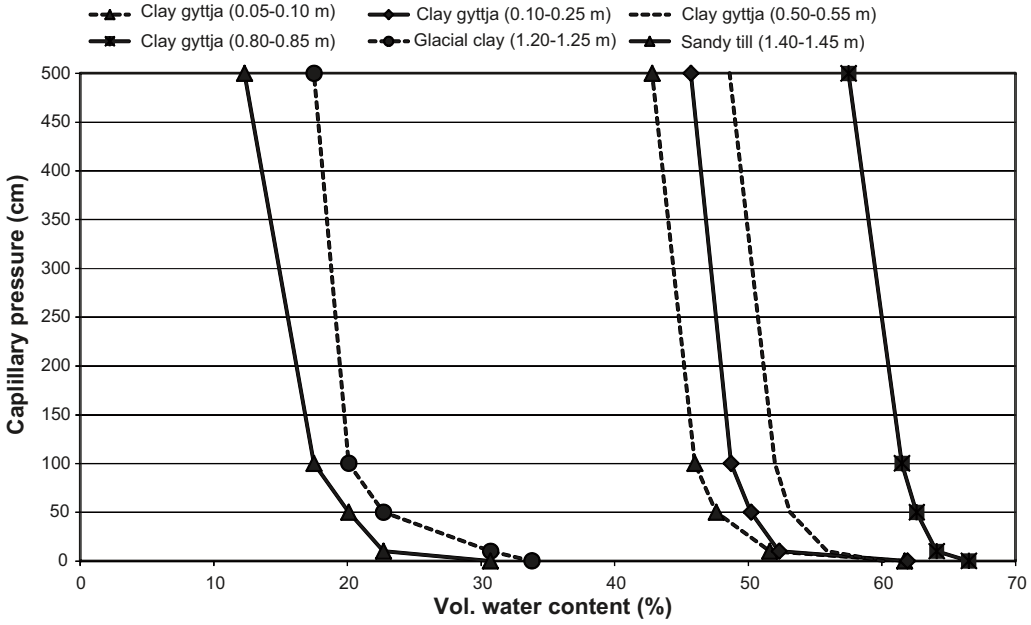

Figure 4-9. *Water-retention curves for QD samples at profile PSM007160 /Sohlenius et al. 2006/.*

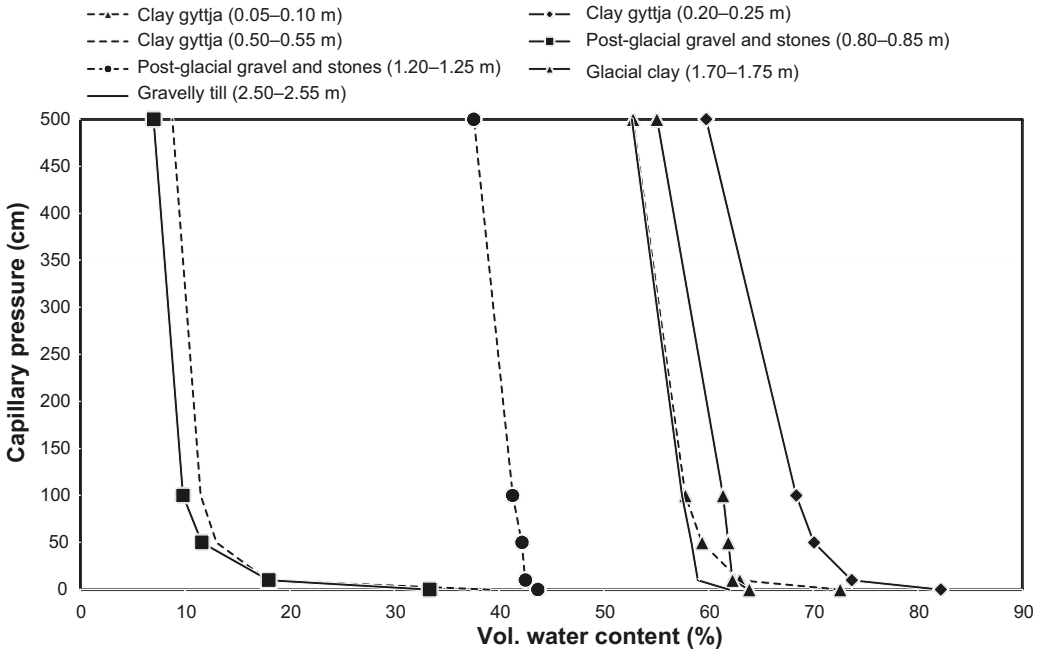

Figure 4-10. *Water-retention curves for QD samples at profile PSM007171A /Sohlenius et al. 2006/.*

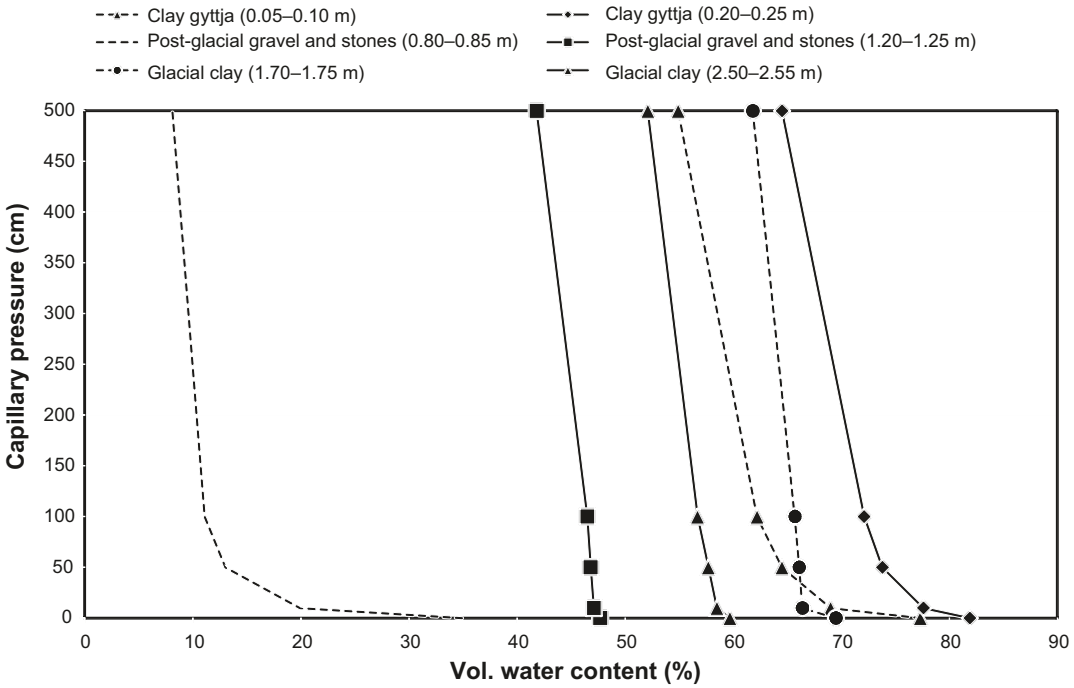

Figure 4-11. *Water-retention curves for QD samples at profile PSM007171B /Sohlenius et al. 2006/.*

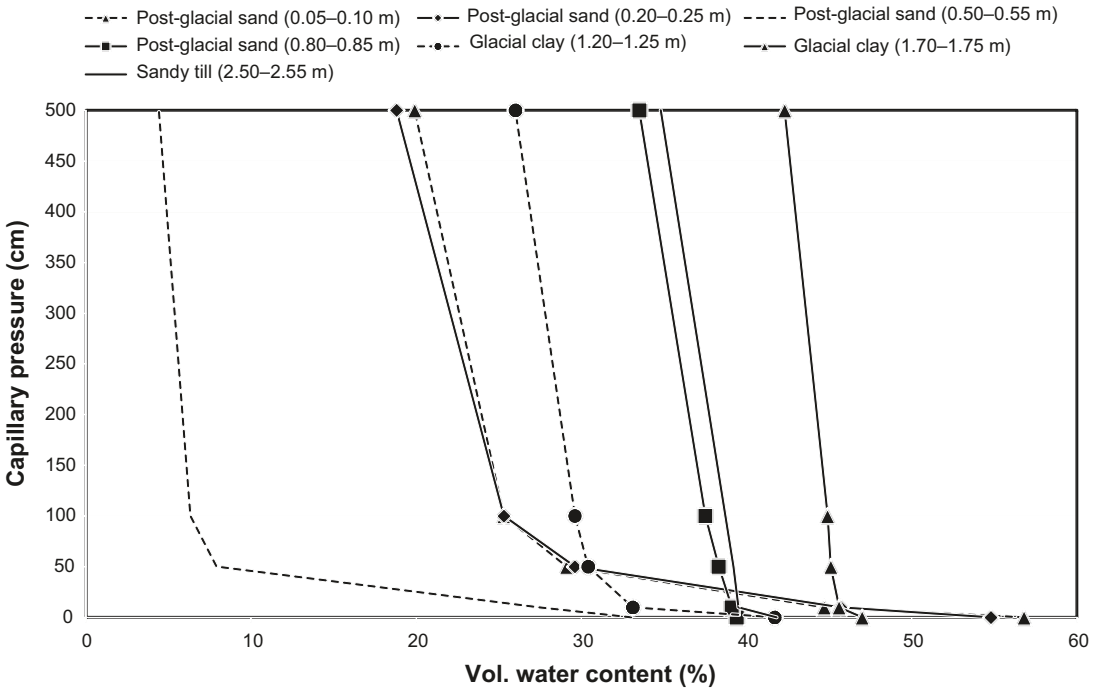

Figure 4-12. *Water-retention curves for QD samples at profile PSM007180A /Sohlenius et al. 2006/.*

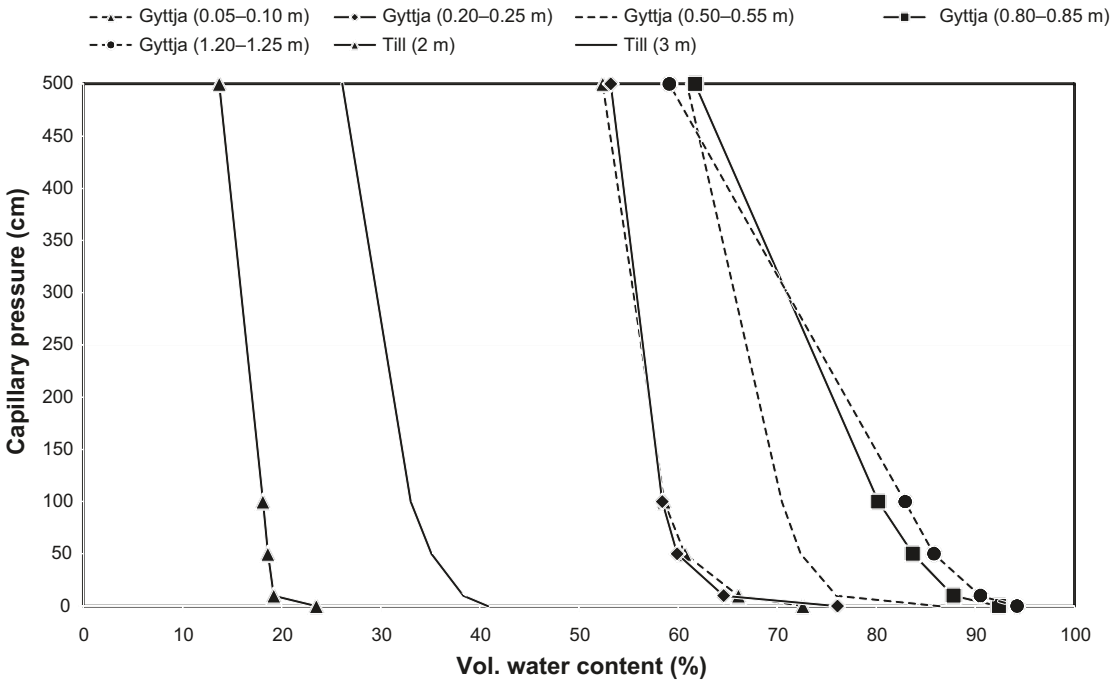

Figure 4-13. *Water-retention curves for QD samples at profile PSM007190A /Sohlenius et al. 2006/.*

The data in Table 4-10 can be compared with data from the literature, e.g. /Knutsson and Morfeldt 2002/ who report a typical porosity range of 40–55% for clay and till, and 30–40% for coarse sand and gravel. Based on other literature data, /Sohlenius and Hedenström 2008/ estimate the representative porosity ranges 10–25% for till and 15–50% for sand/gravel. Further, they estimate the average porosity of sand/gravel at the sea bottom to be 43±17%, based on submarine porosity data reported in /Fredriksson 2004/. It can therefore be concluded that the experimental porosity values in Table 4-10 seem reasonable for till, clay, sand and gravel.

Based on site-specific porosity data reported in /Nilsson 2004/ and /Fredriksson 2004/, /Sohlenius and Hedenström 2008/ estimate the mean porosity to be 90.0±3.4% for clay gyttja below lakes and peat lands, and 94.7±0.9% for clay gyttja located at the sea bottom. Further, they report the mean porosity of glacial clay to be 73.5±6.6%, using data from /Nilsson 2004/. It should be noted that /Nilsson 2004/ and /Fredriksson 2004/ sampled QD below lakes, peat areas and from the sea bottom, hence not from the unsaturated zone.

/Lundin et al. 2005/ also report porosity data, which (except from peat) were excluded from the summary by /Sohlenius and Hedenström 2008/ due to data uncertainties. They report a mean porosity of 92–93% for peat in Laxemar, using data from /Nilsson 2004/ (reported as water content by weight at full water saturation) and /Lundin et al. 2005/. From the latter investigation, they considered 10 out of totally 18 samples classified as peat by /Lundin et al. 2005/; it was considered uncertain whether some samples actually should be classified as peat. /Kellner 2003/ report 86–96% as a typical porosity range, representative for very dense to loose peat.

From the above, it can be concluded that porosity and other hydrogeological properties data relevant for flow in the unsaturated zone are associated with large uncertainty. The site-specific data as well as data from the literature demonstrate relatively wide ranges, which implies that the present data summary primarily serves as a guideline for assignment of reasonable values in descriptive and numerical flow modelling. Table 4-11 summarises the data on porosity and field capacity reported in /Sohlenius and Hedenström 2008/. For reference, the table also includes average values from Table 4-10, data used in previous water flow modelling of the Laxemar area /Aneljung et al. 2007/, data used in the descriptive modelling of Forsmark /Johansson 2008/, and data from a literature survey focused on the properties of peat /Kellner 2003/. In addition, the table provides values of specific yield (S_y), calculated according to the relation $S_y = \theta - \theta_{fc}$.

Table 4-11. Summary of porosity, field capacity and specific yield data reported in /Kellner 2003, Aneljung et al. 2007, Johansson 2008, Sohlenius and Hedenström 2008/.

QD	Porosity (%)	Field capacity (%)	Specific yield, $S_y = \theta - \theta_{fc}$
Sandy-gravelly till	10–25 /Sohlenius and Hedenström 2008/ 38 (47 for ”mid till”) /Aneljung et al. 2007/ 25–35 /Johansson 2008/	42.5 (Table 4-10) 30 /Aneljung et al. 2007/	3.3 (Table 4-10) 3–5 to 15 /Johansson 2008/
Gyttja	80.3 (Table 4-10) 50 /Johansson 2008/	70.1 (Table 4-10)	10.2 (Table 4-10) 3 /Johansson 2008/
Clay gyttja	65.1 (Table 4-10) 85–95 /Sohlenius and Hedenström 2008/ 50 /Johansson 2008/	53.8 (Table 4-10)	11.3 (Table 4-10) 3 /Johansson 2008/
Glacial clay	48.6 (Table 4-10) 65–80 /Sohlenius and Hedenström 2008/ 61.5 /Aneljung et al. 2007/ 45–55 /Johansson 2008/	46.0 (Table 4-10) 31 /Aneljung et al. 2007/	2.6 (Table 4-10) 3–5 /Johansson 2008
Post-glacial gravel	40.4 (Table 4-10) 15–50 /Sohlenius and Hedenström 2008/ 25–60 (sea bottom) /Sohlenius and Hedenström 2008/	27.2 (Table 4-10)	13.2 (Table 4-10)
Post-glacial sand	45.3 (Table 4-10) 15–50 /Sohlenius and Hedenström 2008/ 25–60 (sea bottom) /Sohlenius and Hedenström 2008/ 47 /Aneljung et al. 2007/ 35 /Johansson 2008/	23.6 (Table 4-10) 4 /Aneljung et al. 2007/	21.7 (Table 4-10) 20 /Johansson 2008/
Peat	92–93 /Sohlenius and Hedenström 2008/ 84 /Aneljung et al. 2007/ 40–60 /Johansson 2008/ 86–96 /Kellner 2003/	60 /Aneljung et al. 2007/	Aneljung et al. 2007/ 5–20 /Johansson 2008/ 24 /Kellner 2003/

5 Implications for conceptual and numerical water flow modelling

The development of an integrated hydrogeological-hydrological description of the Laxemar area is an iterative process, involving both the present type of data evaluations as well as the development of numerical models of water flow in rock and in the near-surface/surface system. The objective of this chapter is to summarise some findings and main conclusions from the data presentations and evaluations in this report, and to point out implications for the conceptual understanding and numerical water flow modelling of the Laxemar site.

5.1 Implications for the main components of the conceptual model

The description of the hydrological-hydrogeological conceptual model of the Laxemar area contains the following main components:

- Hydrological objects and hydrogeological flow domains: This component includes descriptions of properties and characteristics of the objects and flow domains that conceptually are thought to be of importance for water flow in the Laxemar area.
- Boundary conditions: This component includes a description of the upper (top) boundary, the boundary between terrestrial areas and the sea, and internal boundaries within the considered area (or domain).
- Infiltration and groundwater recharge: These processes are conceptually thought to be active in "source" areas, mainly in the high-altitude areas characterised by exposed or shallow rock, for which hydrogeological properties and flow processes need to be described.
- Sub-flow systems and discharge: The processes of groundwater discharge and formation of surface-water flow are conceptually thought to be active in "recipient" areas, mainly in valleys and other low-altitude areas, characterised by relatively thick QD and deformation zones in the rock, for which hydrogeological properties and flow processes need to be described.
- Water-flow processes in areas/domains between "source" and "recipient areas", and the hydrogeological properties associated to these areas/domains.

This section hence summarises some of the main findings from this study, in terms of the components listed above. It should be noted that the present summary focuses on the first four items in the list; processes taking place between groundwater recharge and discharge areas are implicitly discussed as part of the summaries of findings concerning infiltration and recharge, and sub-flow systems and discharge.

5.1.1 Hydrological objects

The hydrological objects in the Laxemar area are those typically encountered in Sweden, namely lakes, streams, wetlands and (along the coast) coastal sea basins. A brief conceptual description of such objects in Laxemar is given below, based on the findings in this report.

Lakes

The lakes in the area are relatively small and shallow. Lake level time series from four of the main lakes in the area (Jämsen, Plittorpsgöl, Frisksjön and Sörå; data period May/Jul. 2004–Dec. 2007) show that the lake-water levels are always above sea-water level, including

Lake Sörå at the coast. All lake-water levels demonstrate strong co-variation, with maxima during spring and minima during late summer and early autumn. The amplitude of the lake levels were relatively small during the considered period; Jämsen 25.36–25.97 (average 25.56), Plittorpsgöl 24.75–25.37 (average 24.99), Frisksjön 1.29–2.19 (average 1.57), and Sörå 1.51–2.05 (average 1.77) metres above sea level. The variability pattern of Lake Sörå deviates somewhat from the other three lakes, most likely because it is a man-made storage pond, with no surface in- or outlets.

There are no hydrogeological properties data available that directly can be used to characterise the bottom of the lakes or groundwater-lake interactions. Instead, this information needs to be obtained indirectly from geological observations of lake-bottom sediments. These observations indicate that, except for near-shore areas, the bottom of the lakes are dominated by low-permeable QD. Moreover, there is one groundwater monitoring installed below and at the shoreline, respectively, of Lake Frisksjön and Lake Jämsen. Both the geological observations as well as groundwater-level monitoring indicate that interaction between lake water and groundwater in the underlying QD is limited to near-shore areas. In particular, the monitoring data indicate that near-shore areas of Lake Jämsen act as groundwater recharge areas during dry summer periods, whereas there is almost no vertical hydraulic gradient between Lake Frisksjön and the underlying QD.

Streams

Monitoring data from 9 discharge-gauging stations show that stream flow in Laxemar is transient, characterised by long periods interrupted by flow peaks. In particular, small streams in the area seem to be dry during approximately half of the year, whereas there is some flow throughout the year in the larger streams in the area, mainly Laxemarån and Mederhultsån; the latter stream is however not included in the hydrological monitoring programme.

Transient stream flow implies that estimations of specific discharges and water balances based on gauging-station data from the area are influenced by the choice of period for which the estimate is to be made, specifically relative to the timings and sizes of discharge peaks. During a typical year, the main discharge peaks likely occur in connection to snowmelt, and foremost in connection to simultaneous snowmelt and rainfall.

As for the lakes (see above), there are no hydrogeological properties data available that directly can be used to characterise the bottom of the streams or groundwater-stream interactions. Investigations of the bottom characteristics of the streams indicate that bottom conditions are very variable. Further, the local conditions for surface water-groundwater interaction are also influenced by land improvement and drainage operations. For instance, stream water flows in subsurface pipes along some parts of the streams.

Joint evaluations of stream discharges and the electrical conductivity of the stream water indicate that most stream water seems to originate from surface (overland) water, near-surface groundwater (from the very upper parts of the QD) and water originating from snowmelt. The temperature of the stream water in Laxemar demonstrates small diurnal variations overlain by seasonal variations, and do not show any clear correlation to stream discharges.

Wetlands

As for lakes and streams (see above), there are no hydrogeological properties data available that directly can be used to characterise the bottom of the wetlands or groundwater-wetland interactions. Available geological information and data indicate that the bottom of the wetlands is dominated by low-permeable QD; this can be expected, since many wetlands are previous lakes.

Groundwater-level time series from 6 groundwater monitoring wells installed below three of the wetlands in the area (Klarebäcksmossen, Gäster, and Kärrsvik at the coast) indicate that there generally are small vertical hydraulic gradients between the wetlands and groundwater in the underlying QD.

Coastal sea basins

As for the other hydrological objects (see above), there are no hydrogeological properties data available that directly can be used to characterise the bottom of the sea bays or groundwater-sea interactions. Sea-water levels measured at three bays of the Baltic Sea show maximum and minimum daily average sea level during the considered period (May 2004–Dec. 2007) of –0.52 and 0.71 metres above sea level respectively, whereas the average sea-water level was 0.03 metres above sea level (RHB 70). The largest daily sea-level changes occurred on Nov. 1, 2006 (c +0.26 m) and Dec. 22, 2004 (c –0.23 m).

5.1.2 Hydrogeological flow domains

Quaternary deposits

Groundwater-level time series from groundwater monitoring wells installed in the QD show that groundwater levels generally are shallow, which implies that groundwater levels in Laxemar typically follow the ground-surface topography. Sandy-gravelly till is overlying the rock in the whole area, also in most areas with exposed/shallow rock (which may have a QD depth of up to c 0.5 m). The exceptions are some of the exposed/shallow rock areas, in which organic soil and a relatively thin vegetation layer is directly overlying the rock.

The sandy-gravelly till is characterised by a relatively high hydraulic conductivity (estimated as c $4 \cdot 10^{-5}$ m·s^{-1}). Furthermore, there are indications that the hydraulic conductivity of the QD overlying the rock in the deepest parts of the large valleys is about one order of magnitude higher compared to till in other parts of the area. Permeameter tests on till indicate an anisotropic hydraulic conductivity, with an anisotropy ratio (K_h/K_v) on the order of 15–30. However, this result should be used with caution since permeameter tests are conducted on relatively small QD samples. Generic data are used to support the estimates of the hydrogeological properties of QD types other than till.

Near-surface rock

Point-water head time series from percussion and core boreholes in the rock show that there is less correlation between point-water heads and ground-surface elevations, and no correlation between "point-water depths" and rock-surface depths. Estimations of so-called environmental-water heads, taking into account depth-dependent groundwater density, show that density differences likely have small impact on vertical hydraulic head gradients in the rock. Exceptions from this are some of the deep borehole sections near the coast, characterised by relatively high-density groundwater above less saline groundwater.

Note that explicit assessments of the hydrogeological properties of near-surface rock are outside the scope of this report. For such assessments, see e.g. /Rhén et al. 2008/.

5.1.3 Boundary conditions

The upper boundary

The precipitation demonstrates a near-coastal gradient, with less precipitation at the coast compared to areas further inland. The data evaluation shows that the "site-average" annual average precipitation can be estimated as 600 mm, with c 7% higher precipitation at the inland station Plittorp compared to the station on the island of Äspö at the coast. Moreover, the annual average potential evapotranspiration can be estimated to be c 530–540 mm·y^{-1}.

For hydrometeorological conditions typical for Sweden, snow accumulation during winter, snowmelt in spring and seasonally variable potential evapotranspiration imply that the actual "source term" for groundwater recharge and surface runoff demonstrate strong seasonal variations. This phenomenon is also demonstrated by the discharge-gauging data from the streams (cf. section 5.1.1).

The sea boundary

For a general overview of sea-water levels, see section 5.1.1. Joint evaluations of groundwater levels in the QD, point-water heads in the rock and sea-water levels show that there is a co-variation between the sea-water level and the groundwater levels in groundwater monitoring wells installed below Borholmsfjärden and a well (SSM000040) located close to the coast. Moreover, there is also some co-variation with point-water heads in percussion boreholes located at the coast of Laxemar.

Interestingly, there is some correlation between the sea-water level and point-water heads in some percussion boreholes located relatively far from the coast (on the order of one or a few km). In most cases, these boreholes are located to areas that coincide with deformation zones in the rock. This explanation is however complicated by that it is difficult to explain relatively large correlations for other boreholes (e.g. HLX40 and HLX41), located to areas that do not coincide with any identified deformation zone.

The internal boundaries

Average groundwater levels in the QD range from c –0.8 to 26 metres above sea level, whereas there is only a 4.5 m range in terms of groundwater levels below the ground surface. Conceptually, the 3D "groundwater surface" in the QD generally follows that of the ground surface, and it can be assumed that the identified surface-water divides /Brunberg et al. 2004/ coincide with the water divides for groundwater flow in the QD. The most pronounced outlier (SSM000230) is located in high-conductive glaciofluvial material, a material which normally is characterised by a large depth to the groundwater level.

5.1.4 Infiltration and groundwater recharge

According to the conceptual hydrogeological model, groundwater recharge primarily takes place in high-altitude areas, dominated by shallow/exposed rock. Groundwater recharge also takes place within so called hummocky moraine areas and also in areas with glaciofluvial deposits, characterised by smaller-scale topography and eskers, respectively. The high-altitude areas containing shallow/exposed rock are difficult to parameterise in conceptual models and also to represent properly in quantitative water flow models. There is generally a shortage of well installations and boreholes in the high-altitude areas, which implies that the development of the conceptual model of properties and processes in these areas needs to be based on qualitative reasoning rather than site data.

Precipitation and snowmelt are thought to be the dominant sources of groundwater recharge. The data evaluations show that the infiltration capacity of the QD in Laxemar generally exceeds the rainfall and snowmelt intensity. A rainfall/snowmelt time series, derived using a relatively simple model of snow accumulation and snowmelt, shows that even on an annual basis snow-melt represents an important source term, contributing with totally c 26% of the sum of rainfall plus snowmelt (R + S) during the herein considered data period. According to the model, the maximum snowmelt occurred on Dec. 5, 2004; 22 mm of snow melted in one day.

According to the data evaluation, a proper representation of the "source term" needs to take into account the temporal distribution of rainfall, snow accumulation and snowmelt. Specifically, snowmelt during parts of the winter but foremost during spring yields a large contribution to the surface runoff/infiltration/groundwater recharge source term, which is underestimated if repre-sented by precipitation only. Moreover, using precipitation as the source term overestimates the actual source term during cold winter periods, when precipitation is accumulated in the form of snow.

Analyses were performed on correlations between groundwater levels in the QD and point-water heads in percussion boreholes in the rock on the one hand, and the "net source term" (approximated as potential evapotranspiration minus the sum of rainfall and snowmelt) on the

other. These analyses show that there appears to be a "delay" in the system monitored by some of the groundwater monitoring wells and percussion boreholes; in some cases, the correlation is higher for the previous two months compared to the previous or current month. For some boreholes, the correlations to the net source term are of the same order of magnitude as the groundwater monitoring wells.

5.1.5 Sub-flow systems and discharge

Groundwater discharge is conceptually thought to take place in valleys and other low-altitude areas. Except for some minor wetlands, the surface waters (lakes, streams and wetlands) are located to the low-altitude areas. As mentioned in section 5.1.1, both geological observations and evaluation of groundwater-level monitoring data indicate that interaction between lake water and groundwater in the underlying QD is limited to near-shore areas. As also described in section 5.1.1, joint data evaluations indicate that most stream water mainly seems to originate from surface (overland) water, near-surface groundwater (from the very upper parts of the QD) and water originating from snowmelt.

At most streams, there appear to be "groundwater level thresholds" (in terms of the depth to the groundwater level), below which there is either no stream discharge or the discharge is very low. This threshold seems to be on the order of 0.5–2 m below the ground surface, which can be explained by the fact that the groundwater level at a stream may have to be above the stream bottom in order for stream discharge to occur. Confined conditions may prevail in those areas where streams pass relatively conductive postglacial sediments overlying less conductive sediments, and the groundwater level needs to be within the upper more conductive material (which interacts with the stream) for stream discharge to take place. In areas with relatively conductive types of QD throughout the QD profile, the condition for discharge to occur is simply that the groundwater level is above the stream bottom.

Joint evaluations of groundwater levels in the QD and point-water heads in boreholes in the rock indicate that groundwater discharge from the upper rock/QD part of the system to the surface (surface waters) is strongly influenced by the geometry and the hydrogeological properties of the QD overlying the till. Moreover, there is also an influence on this process by the horisontal extent and the hydrogeological properties of the upper rock (the deformation zones) and the high-conductive QD overlying the rock in the valleys. Locally, there is a fractionation into groundwater that discharges to the surface and groundwater that flows horisontally along the valley in the upper rock/QD system; groundwater discharge to the surface is facilitated in areas where there are no layers of glacial clay and postglacial sediments above the till.

5.2 Implications for quantitative water-flow modelling: Hydrogeological parameterisation of the Laxemar RDM

Quantitative water-flow modelling requires a parameterisation of the regolith, specifically assignment of hydrogeological properties to the QD. Based on the available hydrogeological properties data presented in this report, the assignment presented below follows the geometrical representation of the QD according to the RDM /Nyman et al. 2008/. It should be noted that the hydrogeological properties assignment below is preliminary, and it should be considered as a starting point for the quantitative water-flow modeling. Parameter values could be changed as a result of the quantitative modelling, e.g. for purposes of flow model calibration.

As introduced in section 4.1, /Nyman et al. 2008/ present an update of the previous regolith depth and stratigraphy model (here abbreviated RDM) of the Laxemar-Simpevarp area /Nyman 2005/. These models are based on the detailed digital elevation model of the area (with a horisontal resolution of 20 m by 20 m), the detailed QD map, and a large amount of geological and geophysical observation data. The RDM parameterised here takes into account site-investigation data available in the Laxemar 2.2 data freeze (Dec. 31, 2006).

The RDM developed by /Nyman et al. 2008/ contains six QD layers, denoted Z1–Z6; Z1 represents the upper QD layer. These layers, illustrated in the cross section in Figure 5-1, are defined and described as follows /Nyman et al. 2008, Sohlenius and Hedenström 2008/:

Layer Z1 represents a thin surface(-affected) layer. It is present both on land, below lakes and below the sea. The exception is areas with peat on the surface; in those areas, layer Z2 is the upper layer. In the RDM, the layer thickness is set to 0.10 m in areas with shallow/exposed rock (i.e. rock outcrops on the QD map), and to 0.60 m in other areas. If the total QD depth is less than 0.60 m, Z1 is the only layer (i.e. there are no Z2–Z6 layers). In the terrestrial areas, layer Z1 is assumed to be affected by soil-forming processes.

Layer Z2 represents (fen or bog) peat. This layer is only present in land areas where the QD map shows peat. Hence, layer Z2 is not present below lakes and the sea. The peat areas are further divided into "shallow" and "deep" peat areas. In the shallow peat areas, layer Z2 is directly underlain by layer Z6 (till; see below), which implies that there are no Z3–Z5 layers in those areas. In deep peat areas, Z2 is underlain by layers Z3–Z6. The thickness of Z2 is set equal to the calculated average thickness of peat in the area (0.85 m).

Layer Z3 represents postglacial clay, clay gyttja/gyttja clay, gyttja or recent fluvial sediments. The Z3 layer is only present in areas where clay gyttja is shown on the QD map, and where layer Z2 is present (i.e. in the "deep" peat areas). Layer Z3 is always underlain by layers Z4–Z6.

Layer Z4 represents postglacial sand/gravel, glaciofluvial sediments or artificial fill, and is hence only present in areas where these types of QD or peat (underlain by postglacial clay in layer Z3 and postglacial sand/gravel in layer Z3) are shown on the QD map. Note that glaciofluvial sediments and artificial fill rest directly on the rock (which is located below layer Z6), which means that there are no Z5 or Z6 layers in those areas. In areas with postglacial sand/gravel in layer Z4, this layer is underlain by glacial clay (layer Z5) and till (layer Z6).

Layer Z5 represents glacial clay. The Z5 layer is present where the QD map shows post-glacial sand/gravel, glacial clay or peat (in the "deep" peat areas).

Layer Z6 represents (glacial) till, which is directly underlain by rock. Layer Z6 has zero thickness is exposed/shallow rock areas (i.e. areas with a total QD depth less than 0.60 m), and in areas where layer Z4 directly overlies the rock. The lower level of layer Z6 in the RDM can hence be considered as a "digital elevation model" of the rock surface. The thickness of layer Z6 is estimated by the calculated average thickness of till in the area, except for areas in which till is shown on the QD map.

Except for layer Z1, the lower boundary of all layers is produced by kriging. The lower boundary of layer Z1 is calculated based on the DEM, the elevation of the rock surface and assigned rules for the layer thickness. In order to enable the construction of the RDM, /Nyman et al. 2008/ divided the area into 3 type areas (denoted I–III) and 9 domains. Table 5-1 summarises the QD layer structure of the RDM, including notations on which layers that are present "locally", given different types of QD on the QD map. In addition, the table presents average thicknesses of the individual layers. Table 5-2 below concludes this report, presenting a preliminary assignment of hydrogeological properties (hydraulic conductivity and storage parameters) to each layer defined in the RDM.

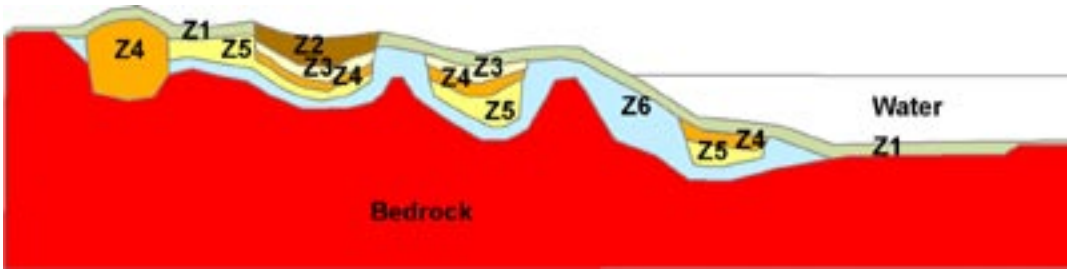

Figure 5-1. *Cross section illustrating the principles of the Laxemar RDM /Nyman et al. 2008/.*

Table 5-1. Summary of the layer definitions according to the regolith depth and stratigraphy model (adapted from /Sohlenius and Hedenström 2008/).

Domain no. (type area no.) and QD on QD map	Average total QD depth (m)	Z1 – Surface-affected layer (average layer depth, m)	Z2 – Peat	Z3 – Clay gyttja, gyttja or recent fluvial sediments	Z4 – Post-glacial sand/ gravel, glacio-fluvial sediments and/or artificial fill	Z5 – Glacial clay	Z6 – Till
1 (I)							
Rock outcrops	0.1	Surface-affected layer (0.1)	-	-	-	-	-
2 (I)							
Till	2.1	Surface-affected layer (0.6)	-	-	-	-	Till (2.0–2.3 m on land, 3.6 m in clay-covered valleys below the sea)
Till with a thin surface layer of peat	2.1	Surface-affected layer (0.6)	-	-	-	-	Till (2 m)
Postglacial shingle	2.1	Surface-affected layer (0.6)	-	-	-	-	Till (2 m)
Boulder deposit	2.1	Surface-affected layer (0.6)	-	-	-	-	Till (2 m)
3 (II)							
Gyttja clay/clay gyttja	5.7 (only terrestrial)	Surface-affected layer (0.6)	-	Gyttja clay/ clay gyttja (1.6 m land, 1.7 m sea)	Postglacial sand/gravel (0.7 m land, 0.8 m sea)	Glacial clay (1.3 m land, 2.6 m sea)	Till (2 m)
Gyttja	5.7 m (terrestrial) 8.7 m (sea)	Surface-affected layer (0.6)	-	Gyttja (1.6 m land, 1.7 m sea)	Postglacial sand/gravel (0.7 m land, 0.8 m sea)	Glacial clay (1.3 m land, 2.6 m sea)	Till (2 m)
Gyttja clay/clay gyttja with a thin surface layer of peat	5.7 m (only terrestrial)	Surface-affected layer (0.6)	-	Gyttja clay/ clay gyttja (1.6 m land, 1.7 m sea)	Postglacial sand/gravel (0.7 m land, 0.8 m sea)	Glacial clay (1.3 m land, 2.6 m sea)	Till (2 m)
Recent fluvial sediments	5.7 m (only terrestrial)	Surface-affected layer (0.6)	-	Gyttja clay/ clay gyttja (1.6 m land, 1.7 m sea)	Postglacial sand/gravel (0.7 m land, 0.8 m sea)	Glacial clay (1.3 m land, 2.6 m sea)	Till (2 m)
Gyttja clay with a thin surface layer of sand-gravel	8.7 (only below sea)	Surface-affected layer (medium sand-gravel)	-	Gyttja clay/ clay gyttja (1.6 m land, 1.7 m sea)	Postglacial sand/gravel (0.7 m land, 0.8 m sea)	Glacial clay (1.3 m land, 2.6 m sea)	Till (2 m)
4 (I)							
Peat, shallow (fen peat, bog peat, and unspecified peat)	3 m (only terrestrial)	-	Peat (0.85 m)	-	-	-	Till (2 m)
5 (II)							
Peat, deep (fen peat, bog peat, and unspecified peat)	6.6 m (only terrestrial)	-	Peat (0.85 m)	Gyttja clay/ clay gyttja (1.6 m land, 1.7 m sea)	Postglacial sand/gravel (0.7 m land, 0.8 m sea)	Glacial clay	Till (2 m)
6 (II)							
Glacial clay	4.1 (land) 7.1 (sea)	Surface-affected layer (0.6)	-	-	Postglacial sand/gravel (0.7 m land, 0.8 m sea)	Glacial clay	Till (2 m)
Glacial clay with a thin surface layer of post-glacial fine sand	4.1 (land) 7.1 (sea)	Surface-affected layer (0.6)	-	-	Postglacial sand/gravel (0.7 m land, 0.8 m sea)	Glacial clay	Till (2 m)

Domain no. (type area no.) and QD on QD map	Average total QD depth (m)	Z1 – Surface-affected layer (average layer depth, m)	Z2 – Peat	Z3 – Clay gyttja, gyttja or recent fluvial sedi-ments	Z4 – Post-glacial sand/ gravel, glacio-fluvial sediments and/or artificial fill	Z5 – Glacial clay	Z6 – Till
Glacial clay with a thin surface layer of post-glacial medium sand-gravel	4.1 (land) 7.1 (sea)	Surface-affected layer (0.6)	-	-	Postglacial sand/gravel (0.7 m land, 0.8 m sea)	Glacial clay	Till (2 m)
Clay-silt (unspecified)	4.1 (land) 7.1 (sea)	Surface-affected layer (0.6)	-	-	Postglacial sand/gravel (0.7 m land, 0.8 m sea)	Glacial clay	Till (2 m)
Postglacial fine sand	4.1 (land) 7.1 (sea)	Surface-affected layer (0.6)	-	-	Postglacial fine sand (0.7 m land, 0.8 m sea)	Glacial clay	Till (2 m)
Postglacial sand	4.1 (land) 7.1 (sea)	Surface-affected layer (0.6)	-	-	Postglacial sand (0.7 m land, 0.8 m sea)	Glacial clay	Till (2 m)
Postglacial sand with a thin surface layer of peat	4.1 (only land)	Surface-affected layer (0.6)	-	-	Postglacial sand (0.7 m land, 0.8 m sea)	Glacial clay	Till (2 m)
Postglacial medium sand-gravel	7.1 (only sea)	Surface-affected layer (0.6)	-	-	Postglacial medium sand-gravel (0.7 m land, 0.8 m sea)	Glacial clay	Till (2 m)
Postglacial gravel with a thin surface layer of peat	4.1 (only land)	Surface-affected layer (0.6)	-	-	Postglacial gravel (0.7 m land, 0.8 m sea)	Glacial clay	Till (2 m)
Postglacial gravel	4.1 (land) 7.1 (sea)	Surface-affected layer (0.6)	-	-	Postglacial gravel (0.7 m land, 0.8 m sea)	Glacial clay	Till (2 m)
Glacial clay with thin surface layer of peat	4.1 (only land)	Surface-affected layer (0.6)	-	-	Postglacial sand/gravel (0.7 m land, 0.8 m sea)	Glacial clay	Till (2 m)
Glacial silt	4.1 (land) 7.1 (sea)	Surface-affected layer (0.6)	-		Postglacial sand/gravel (0.7 m land, 0.8 m sea)	Glacial clay	Till (2 m)
7 (III)							
Glaciofluvial sediments, shallow	4.1	Surface-affected layer (0.6)	-	-	Glaciofluvial sediments (3.5)		
8 (III)							
Glaciofluvial sediments, deep (the Tuna esker)	13.8	Surface-affected layer (0.6)	-	-	Glaciofluvial sediments (13.2)	-	-
9 (no type area)							
Artificial fill	5	Surface-affected layer (0.6)	-	-	Artificial fill (4.4)	-	-

Table 5-2. Preliminary data-based assignment of hydrogeological properties to different types of QD, arranged in layers Z1–Z6 according to the regolith depth and stratigraphy model /Sohlenius and Hedenström 2008/. The assignment should be considered as a starting point for quantitative water-flow modeling. K_h = horisontal hydraulic conductivity ($m \cdot s^{-1}$), K_h/K_v = anisotropy ratio (-), S_y = specific yield (-), and S_s = specific storage coefficient (m^{-1}). SAL = surface-affected layer, PSG = postglacial sand/gravel, GS = glaciofluvial sediments, AF = artificial fill, GLC = glacial clay, and GC/CG = gyttja clay/clay gyttja. In the first column, (G) denotes that the properties are based on "generic" data and therefore are considered uncertain. (S) denotes that the properties are supported by site data and are considered more certain. (G/S) means that there is some site-data support. For layer Z6, the first set of parameter values tentatively applies to areas with a total QD depth less than 10 m, and the second set to areas with a total QD depth larger than 10 m.

Domain no. (type area no.) QD on QD map		Z1	Z2	Z3	Z4	Z5	Z6*
1 (I)							
Rock outcrops	QD	SAL (G)	-	-	-	-	-
	K_h	$4 \cdot 10^{-4}$					
	K_h/K_v	1					
	S_y	0.10					
	S_s	5·10–3					
2 (I)							
Till	QD	SAL (G)	-	-	-	-	Till (S)
	K_h	4·10–4					4·10–5 / 4·10–4
	K_h/K_v	1					1
	S_y	0.15					0.05 / 0.10
	S_s	1·10–3					1·10–3 / 5·10–3
Till with a thin surface layer of peat	QD	SAL (peat) (G/S)	-	-	-	-	Till (S)
	K_h	$3 \cdot 10^{-6}$					$4 \cdot 10^{-5}$ / $4 \cdot 10^{-4}$
	K_h/K_v	1					1
	S_y	0.24					0.05 / 0.10
	S_s	5·10–2					1·10–3 / 5·10–3
Postglacial shingle	QD	SAL (shingle) (G)	-	-	-	-	Till (S)
	K_h	1·10–2					4·10–5 / 4·10–4
	K_h/K_v	1					1
	S_y	0.25					0.05 / 0.10
	S_s	0.025					1·10–3 / 5·10–3
Boulder deposit	QD	SAL (G)	-	-	-	-	Till (S)
	K_h	4·10–4					4·10–5 / 4·10–4
	K_h/K_v	1					1
	S_y	0.15					0.05 / 0.10
	S_s	1·10–3					1·10–3 / 5·10–3

Domain no. (type area no.) QD on QD map		Z1	Z2	Z3	Z4	Z5	Z6*
3 (II)							
Gyttja clay/clay gyttja (GC/CG)	QD	SAL (G)	-	GC/CG (G)	PSG (G/S)	GLC (G)	Till (S)
	K_h	4·10–4		1·10–7	5·10–3	1·10–8	4·10–5 / 4·10–4
	K_h/K_v	1		1	1	1	1
	S_y	0.10		0.03	0.25	0.03	0.05 / 0.10
	S_s	$5·10^{-3}$		$6·10^{-3}$	0.025	$6·10^{-3}$	$1·10^{-3}$ / $5·10^{-3}$
Gyttja	QD	SAL (G)	-	Gyttja (G)	PSG (G/S)	GC	Till (S)
	K_h	$4·10^{-4}$		$1·10^{-8}$	$5·10^{-3}$	$1·10^{-8}$	$4·10^{-5}$ / $4·10^{-4}$
	K_h/K_v	1		1	1	1	1
	S_y	0.10		0.03	0.25	0.03	0.05 / 0.10
	S_s	5·10–3		6·10–3	0.025	6·10–3	1·10–3 / 5·10–3
Gyttja clay/ clay gyttja (GC/CG) with a thin surface layer of peat	QD	SAL (peat) (G/S)	-	GC/CG (G)	PSG (G/S)	GLC (G)	Till (S)
	K_h	$3·10^{-6}$		$1·10^{-7}$	$5·10^{-3}$	$1·10^{-8}$	$4·10^{-5}$ / $4·10^{-4}$
	K_h/K_v	1		1	1	1	1
	S_y	0.24		0.03	0.25	0.03	0.05 / 0.10
	S_s	5·10–2		6·10–3	0.025	6·10–3	1·10–3 / 5·10–3
Recent fluvial sediments	QD	SAL (G)	-	GC/CG (G)	PSG (G/S)	GLC (G)	Till (S)
	K_h	4·10–4		1·10–7	5·10–3	1·10–8	4·10–5 / 4·10–4
	K_h/K_v	1		1	1	1	1
	S_y	0.10		0.03	0.25	0.03	0.05 / 0.10
	S_s	5·10–3		6·10–3	0.025	6·10–3	1·10–3 / 5·10–3
Gyttja clay/ clay gyttja (GC/ CG) with a thin surface layer of sand-gravel	QD	SAL (sand-gravel) (G/S)	-	GC/CG(G)	PSG (G/S)	GLC (G)	Till (S)
	K_h	5·10–3		1·10–7	5·10–3	1·10–8	4·10–5 / 4·10–4
	K_h/K_v	1		1	1	1	1
	S_y	0.25		0.03	0.25	0.03	0.05 / 0.10
	S_s	0.025		$6·10^{-3}$	0.025	$6·10^{-3}$	$1·10^{-3}$ / $5·10^{-3}$
4 (I)							
Peat, shallow (fen peat, bog peat, and unspecified peat)	QD	-	Peat (G/S)	-	-	-	Till (S)
	K_h		3·10–6				4·10–5 / 4·10–4
	K_h/K_v		1				1
	S_y		0.24				0.05 / 0.10
	S_s		5·10–2				1·10–3 / 5·10–3

Domain no. (type area no.) QD on QD map		Z1	Z2	Z3	Z4	Z5	Z6*
5 (II)							
Peat, deep (fen peat, bog peat, and unspecified peat)	QD	-	Peat (G/S)	GC/CG (G)	PSG (G/S)	GLC (G)	Till (S)
	K_h		3·10–6	1·10–7	5·10–3	1·10–8	4·10–5 / 4·10–4
	K_h/K_v		1	1	1	1	1
	S_y		0.24	0.03	0.25	0.03	0.05 / 0.10
	S_s		5·10–2	6·10–3	0.025	6·10–3	1·10–3 / 5·10–3
6 (II)							
Glacial clay (GLC)	QD	SAL (G)	-	-	PSG (G/S)	GLC (G)	Till (S)
	K_h	4·10–4			5·10–3	1·10–8	4·10–5 / 4·10–4
	K_h/K_v	1			1	1	1
	S_y	0.10			0.25	0.03	0.05 / 0.10
	S_s	5·10–3			0.025	6·10–3	1·10–3 / 5·10–3
Glacial clay (GLC) with a thin surface layer of postglacial fine sand	QD	SAL (G)	-	-	PSG (G/S)	GLC	Till (S)
	K_h	5·10–4			5·10–3	1·10–8	4·10–5 / 4·10–4
	K_h/K_v	1			1	1	1
	S_y	0.25			0.25	0.03	0.05 / 0.10
	S_s	0.025			0.025	6·10–3	1·10–3 / 5·10–3
Glacial clay with a thin surface layer of post-glacial medium sand-gravel	QD	SAL (G)	-	-	PSG (G/S)	GLC (G)	Till (S)
	K_h	5·10–3			5·10–3	1·10–8	4·10–5 / 4·10–4
	K_h/K_v	1			1	1	1
	S_y	0.25			0.25	0.03	0.05 / 0.10
	S_s	0.025			0.025	6·10–3	1·10–3 / 5·10–3
Clay-silt (unspecified)	QD	SAL (G)	-	-	PSG (G/S)	GLC(G)	Till (S)
	K_h	4·10–4			5·10–3	1·10–8	4·10–5 / 4·10–4
	K_h/K_v	1			1	1	1
	S_y	0.10			0.25	0.03	0.05 / 0.10
	S_s	$5·10^{-3}$			0.025	$6·10^{-3}$	$1·10^{-3}$ / $5·10^{-3}$
Postglacial fine sand (PFS)	QD	SAL (G)	-	-	PFS (G/S)	GLC (G)	Till (S)
	K_h	$4·10^{-4}$			$5·10^{-4}$	$1·10^{-8}$	$4·10^{-5}$ / $4·10^{-4}$
	K_h/K_v	1			1	1	1
	S_y	0.10			0.25	0.03	0.05 / 0.10
	S_s	5·10–3			0.025	6·10–3	1·10–3 / 5·10–3
Postglacial sand (PS)	QD	SAL (G)	-	-	PS (G/S)	GC (G)	Till (S)
	K_h	$4·10^{-4}$			$1·10^{-3}$	$1·10^{-8}$	$4·10^{-5}$ / $4·10^{-4}$
	K_h/K_v	1			1	1	1
	S_y	0.10			0.25	0.03	0.05 / 0.10
	S_s	5·10–3			0.025	6·10–3	1·10–3 / 5·10–3
Postglacial sand (PS) with a thin surface layer of peat	QD	SAL (G)	-	-	PS	GLC (G)	Till (S)
	K_h	3·10–6			1·10–3	1·10–8	4·10–5 / 4·10–4
	K_h/K_v	1			1	1	1
	S_y	0.24			0.25	0.03	0.05 / 0.10
	S_s	5·10–2			0.025	6·10–3	1·10–3 / 5·10–3

Domain no. (type area no.) QD on QD map		Z1	Z2	Z3	Z4	Z5	Z6*
Postglacial medium sand-gravel	QD	SAL (G)	-	-	Postglacial medium sand-gravel (G/S)	GLC(G)	Till (S)
	K_h	4·10–4			5·10–3	1·10–8	4·10–5 / 4·10–4
	K_h/K_v	1			1	1	1
	S_y	0.10			0.25	0.03	0.05 / 0.10
	S_s	$5·10^{-3}$			0.025	$6·10^{-3}$	$1·10^{-3}$ / $5·10^{-3}$
Postglacial gravel (PG) with a thin surface layer of peat	QD	SAL (G)	-	-	PG (G/S)	GLC (G)	Till (S)
	K_h	$3·10^{-6}$			$1·10^{-2}$	$1·10^{-8}$	$4·10^{-5}$ / $4·10^{-4}$
	K_h/K_v	1			1	1	1
	S_y	0.24			0.25	0.03	0.05 / 0.10
	S_s	5·10–2			0.025	6□10–3	1·10–3 / 5·10–3
Postglacial gravel (PG)	QD	SAL (G)	-	-	PG (G/S)	GLC (G)	Till (S)
	K_h	4·10–4			1·10–2	1·10–8	4·10–5 / 4·10–4
	K_h/K_v	1			1	1	1
	S_y	0.10			0.25	0.03	0.05 / 0.10
	S_s	5·10–3			0.025	6·10–3	1·10–3 / 5·10–3
Glacial clay (GLC) with thin surface layer of peat	QD	SAL (G)	-	-	PSG (G/S)	GLC (G)	Till (S)
	K_h	3·10–6			5·10–3	1·10–8	4·10–5 / 4·10–4
	K_h/K_v	1			1	1	1
	S_y	0.24			0.25	0.03	0.05 / 0.10
	S_s	5·10–2			0.025	6·10–3	1·10–3 / 5·10–3
Glacial silt	QD	SAL (G)	-		PSG (G/S)	GLC (G)	Till (S)
	K_h	4·10–4			5·10–3	1·10–8	4·10–5 / 4·10–4
	K_h/K_v	1			1	1	1
	S_y	0.10			0.25	0.03	0.05 / 0.10
	S_s	5·10–3			0.025	6·10–3	1·10–3 / 5·10–3
7 (III)							
Glaciofluvial sediments (GS), shallow	QD	SAL (G)	-	-	GS (G/S)	-	-
	K_h	4·10–4			5·10–3		
	K_h/K_v	1			1		
	S_y	0.10			0.25		
	S_s	5·10–3			0.025		
8 (III)							
Glaciofluvial sediments (GS), deep (Tuna esker)	QD	SAL (G)	-	-	GS (G/S)	-	-
	K_h	4·10–4			5·10–3		
	K_h/K_v	1			1		
	S_y	0.10			0.25		
	S_s	5·10–3			0.025		
9 (no type area)	QD						
Artificial fill (AF)	QD	SAL (G)	-	-	AF (G)	-	-
	K_h	$4·10^{-4}$			$4·10^{-5}$		
	K_h/K_v	1			1		
	S_y	0.10			0.05		
	S_s	5·10–3			1·10–3		

References

Acworth R I, 2007. Measurement of vertical environmental-head profiles in unconfined sand aquifers using a multi-channel manometer board. Hydrogeol. J. 15, 1279–1289.

Alexandersson H, 2003. Korrektion av nederbörd enligt enkel klimatologisk metodik. SMHI Meteorologi 111. Swedish Meteorological and Hydrological Institute, Norrköping (in Swedish).

Andersson A-C, Andersson O, Gustafson G, 1984. Brunnar – undersökning – dimensionering – borrning – drift. Rapport R42:1984. Byggforskningsrådet (in Swedish).

Aneljung M, Gustafsson L-G, Sassner M, 2007. Sensitivity analysis and development of calibration methodology for near-surface hydrogeology model of Laxemar. SKB R-07-52, Svensk Kärnbränslehantering AB.

Ask H, Morosini M, Samuelsson L-E, Ekström L, Håkansson N, 2006. Oskarshamn site investigation. Drilling of cored borehole KLX10. SKB P-06-116. Svensk Kärnbränslehantering AB.

Ask H, Morosini M, Samuelsson L-E, Ekström L, Håkansson N, 2007a. Oskarshamn site investigation. Drilling of cored borehole KLX11A. SKB P-06-306.
Svensk Kärnbränslehantering AB.

Ask H, Tiberg L, Morosini M, 2007b. Oskarshamn site investigation. Summary of water pumping and release. Hydraulic disturbances from drilling and investigations during the site investigation in Oskarshamn, subareas Simpevarp and Laxemar, 2002–2007. SKB P-07-174, Svensk Kärnbränslehantering AB.

Askling P, 2007. Oskarshamn site investigation. Groundwater flow measurements in soil wells SSM000243, SSM000244, SSM000261, SSM000262 and SSM000263, spring 2007. Laxemar. Subarea Laxemar. SKB P-07-197, Svensk Kärnbränslehantering AB.

Bergman T, Malmberg-Persson K, Persson M, Albrecht J, 2005. Oskarshamn site investigation. Characterisation of Quaternary deposits from excavations in the southern part of Laxemar subarea. SKB P-05-47, Svensk Kärnbränslehantering AB.

Bosson E, 2006. Near-surface hydrogeological model of Laxemar. Open repository – Laxemar 1.2. SKB R-06-66, Svensk Kärnbränslehantering AB.

Bosson E, Sassner M, Gustafsson L-G, 2008. Numerical modelling of hydrology and near-surface hydrogeology at Laxemar-Simpevarp. Site descriptive modelling, SDM-Site Laxemar. SKB R-08-72, Svensk Kärnbränslehantering AB.

Brunberg A-K, Carlsson T, Brydsten L, Strömgren M, 2004. Identification of catchments, lake-related drainage parameters and lake habitats. Oskarshamn site investigation.
SKB P-04-242, Svensk Kärnbränslehantering AB.

Butler Jr J J, Healey J M, 1998. Relationship between pumping-test and slug-test parameters: Scale effect or artefact? Ground Water 36(2), 305–313.

Chow V T, Maidment D R, Mays L W, 1988. Applied Hydrology. McGraw-Hill, Inc. Singapore.

Eriksson B, 1981. Den potentiella avdunstningen i Sverige. SMHI Report RMK 28, Swedish Meteorological and Hydrological Institute, Norrköping (in Swedish).

Fredriksson R, 2004. Oskarshamn site investigation. Inventory of the soft-bottom macrozoobenthos community in the area around Simpevarp nuclear power plant. SKB P-04-17, Svensk Kärnbränslehantering AB.

Gokall-Norman K, Ludvigson J-E, 2007. Hydraulic pumping- and interference tests in soil monitoring wells on Laxemar, spring of 2007. SKB P-07-173, Svensk Kärnbränslehantering AB.

Hartley L, Hunter F, Jackson P, McCarthy R, Gylling B, Marsic N, 2006. Regional hydrogeological simulations using CONNECTFLOW. Preliminary site description Laxemar subarea – version 1.2. SKB R-06-23, Svensk Kärnbränslehantering AB.

Hartley L, Jackson P, Joyce S, Roberts D, Shevelan J, Swift B, Gylling B, Marsic N, Hermanson J, Öhman J, 2007. Hydrogeological pre-modelling exercises: Assessment of impact of the Äspö Hard Rock Laboratory. Sensitivities of palaeo-hydrogeology. Development of a local near-surface Hydro-DFN for KLX09B-F. Site descriptive modelling, SDM-Site Laxemar. SKB R-07-57, Svensk Kärnbränslehantering AB.

Johansson P-O, 2008. Description of surface hydrology and near-surface hydrogeology at Forsmark. Site descriptive modelling, SDM-Site Forsmark. SKB R-08-08, Svensk Kärnbränslehantering AB.

Johansson T, Adestam L, 2004a. Oskarshamn site investigation. Slug tests in groundwater monitoring wells in soil in the Simpevarp area. SKB P-04-122, Svensk Kärnbränslehantering AB.

Johansson T, Adestam L, 2004b. Oskarshamn site investigation. Drilling and sampling in soil. Installation of groundwater monitoring wells in the Laxemar area. SKB P-04-317, Svensk Kärnbränslehantering AB.

Johansson T, Adestam L, 2004c. Oskarshamn site investigation. Slug tests in groundwater monitoring wells in soil in the Laxemar area. SKB P-04-318, Svensk Kärnbränslehantering AB.

Johansson T, Göransson M, 2006. Oskarshamn site investigation. Slug tests in groundwater monitoring wells SSM000222–SSM000230 in soil – subarea Laxemar. SKB P-06-149, Svensk Kärnbränslehantering AB.

Johansson T, Göransson M, Zetterlund M, Jenkins C, Rönnback K, 2007. Oskarshamn site investigation. Hydrogeological characterization in bogs, lakes and sea bays. SKB P-06-248. Svensk Kärnbränslehantering AB.

Juston J, Johansson P-O, Levén J, Tröjbom M, Follin S, 2007. Analysis of meteorological, hydrological and hydrogeological monitoring data. Forsmark – stage 2.1. SKB R-06-49, Svensk Kärnbränslehantering AB.

Kellner E, 2003. Wetlands – different types, their properties and functions. SKB TR-04-08, Svensk Kärnbränslehantering AB.

Kellner E, 2007. Effects of variations in hydraulic conductivity and flow conditions on groundwater flow and solute transport in peatlands. SKB R-07-41, Svensk Kärnbränslehantering AB.

Knutsson G, Morfeldt C-O, 2002. Grundvatten – teori & tillämpning. Svensk Byggtjänst.

Larsson-McCann S, Karlsson A, Nord M, Sjögren J, Johansson L, Ivarsson M, Kindell S, 2002. Meteorological, hydrological and oceanographical information and data for the site investigation program in the community of Oskarshamn. SKB TR-02-03, Svensk Kärnbränslehantering AB.

Lundin L, Lode E, Stendahl J, Björkvald L, Hansson J, 2005. Soils and site types in the Oskarshamn area. Oskarshamn site investigation. SKB R-05-15, Svensk Kärnbränslehantering AB.

Lusczynski N J, 1961. Head and flow of ground water of variable density. J. Geophys. Res. 66(12), 4247–4256.

Lärke A, Hillgren R, 2003. Rekognocering av mätplatser för ythydrologiska mätningar i Simpevarpsområdet. SKB P-03-04, Svensk Kärnbränslehantering AB (in Swedish).

Lärke A, Hillgren R, Wern L, Jones J, Aquilonius K, 2005a. Oskarshamn site investigation. Meteorological and hydrological monitoring at Oskarshamn during 2003–2004. SKB P-05-227, Svensk Kärnbränslehantering AB.

Lärke A, Hillgren R, Wern L, Jones J, Aquilonius K, 2005b. Oskarshamn site investigation. Meteorological and hydrological monitoring at Oskarshamn, November 2004 until June 2005. SKB P-06-19, Svensk Kärnbränslehantering AB.

Morosini M, Wass E, 2007. Oskarshamn site investigation. Hydraulic interference and tracer testing of a soil-rock aquifer system between HLX35 and HLX34, SSM000037, SSM000222 and SSM000223. SKB P-06-151, Svensk Kärnbränslehantering AB.

Morosini M, Jenkins C, Simson S, Albrecht J, Zetterlund M, 2007. Oskarshamn site investigation. Hydrogeological characterization of deepest valley soil aquifers and soil-rock transition zone at Laxemar, 2006. SKB P-07-91, Svensk Kärnbränslehantering AB.

Nilsson G, 2004. Oskarshamn site investigation. Investigation of sediments, peat lands and wetlands. SKB P-04-273, Svensk Kärnbränslehantering AB.

Nord M, Jones J, Wern L, 2006. Känslighetsanalys – potentiell evapotranspiration Swedish Meteorological and Hydrological Institute, Norrköping (unpublished report).

Nyberg G, Wass E, 2005. Oskarshamn site investigation. Groundwater monitoring program. Report for November 2004–June 2005. SKB P-05-282, Svensk Kärnbränslehantering AB.

Nyberg G, Wass E, Askling P, 2005. Oskarshamn site investigation. Groundwater monitoring program. Report for December 2002–October 2004. SKB P-05-205, Svensk Kärnbränslehantering AB.

Nyberg G, Wass E, 2007a. Oskarshamn site investigation. Groundwater monitoring program. Report for July 2005–December 2006. SKB P-07-219, Svensk Kärnbränslehantering AB.

Nyberg G, Wass E, 2007b. Oskarshamn site investigation. Groundwater monitoring program. Report for January–August 2007. SKB P-08-28, Svensk Kärnbränslehantering AB.

Nyman H, 2005. Depth and stratigraphy of Quaternary deposits. Preliminary site description Laxemar subarea – version 1.2. SKB R-05-54, Svensk Kärnbränslehantering AB.

Nyman H, Sohlenius G, Strömgren M, Brydsten L, 2008. Depth and stratigraphy of regolith. Site descriptive modelling, SDM-Site Laxemar. SKB R-08-06, Svensk Kärnbränslehantering AB.

Penman H L, 1948. Natural evaporation from open water, bare soil, and grass. Proc R Soc London A193, 120–146.

Post V, Kooi H, Simmons C, 2007. Using hydraulic head measurements in variable-density ground water flow analyses. Ground Water 45(6), 664–671.

Rhén I (ed.), Gustafson G, Stanfors R, Wikberg P, 1997. Äspö HRL – Geoscientific evaluation 1997/5. Models based on site characterization 1986–1995. SKB TR-97-06, Svensk Kärnbränslehantering AB.

Rhén I, Forsmark T, Hartley L, Jackson P, Roberts D, Swan D, Gylling B, 2008. Hydrogeological conceptualisation and parameterisation. Site descriptive modelling, SDM-Site Laxemar. SKB R-08-78, Svensk Kärnbränslehantering AB.

Rudmark L, Malmberg-Persson K, Mikko H, 2005. Oskarshamn site investigation. Investigations of Quaternary deposits 2003–2004. SKB P-05-49, Svensk Kärnbränslehantering AB.

Sieck L C, Burges S J, Steiner M, 2007a. Challenges in obtaining reliable measurements of point rainfall. Water Resour Res, 43, W01420, doi: 10.1029/2005WR004519.

Sieck L C, Burges S J, Steiner M, 2007b. Correction to "Challenges in obtaining reliable measurements of point rainfall". Water Resour Res, 43, W06701, doi: 10.1029/2007WR005985.

Sjögren J, Hillgren R, Wern L, Jones J, Engdahl A, 2007a. Hydrological and meteorological monitoring at Oskarshamn, July 2005 until December 2006. SKB P-07-38, Svensk Kärnbränslehantering AB.

Sjögren J, Hillgren R, Wern L, Jones J, Engdahl A, 2007b. Hydrological and meteorological monitoring at Oskarshamn, January 2007 until August 2007. SKB P-07-172, Svensk Kärnbränslehantering AB.

SKB, 2001. Site investigations. Investigation methods and general execution programme. SKB TR-01-29, Svensk Kärnbränslehantering AB.

SKB, 2009. Site description of Laxemar-Simpevarp at completion of the site investigation phase. SKB TR-09-01, Svensk Kärnbränslehantering AB.

Sohlenius G, Bergman T, Snäll S, Lundin L, Lode E, Stendahl J, Riise A, Nilsson J, Johansson T, Göransson M, 2006. Oskarshamn site investigation. Soils, Quaternary deposits and bedrock in topographic lineaments situated in the Laxemar subarea. SKB P-06-121, Svensk Kärnbränslehantering AB.

Sohlenius G, Hedenström A, 2008. Description of regolith at Laxemar-Simpevarp. Site descriptive modelling, SDM-Site Laxemar. SKB R-08-05, Svensk Kärnbränslehantering AB.

Svensson J, Zetterlund M, 2006. Oskarshamn site investigation. Complementary slug tests in groundwater monitoring wells – February 2006. SKB P-06-150, Svensk Kärnbränslehantering AB.

Svensson T, Ludvigson J-E, Walger E, Thur P, Gokall-Norman K, Eva Wass E, Morosini M, 2008. Oskarshamn site investigation. Combined hydraulic interference and tracer test in HLX33, SSM000228 and SSM000229. SKB P-07-187, Svensk Kärnbränslehantering AB.

Söderbäck B, Lindborg T (ed.), 2009. Surface system Laxemar-Simpevarp. Site descriptive modelling, SDM-Site Laxemar. SKB R-09-01, Svensk Kärnbränslehantering AB.

Wern L, Jones J, 2006. Forsmark site investigation. Meteorological monitoring at Forsmark, June 2003 until July 2005. SKB P-05-221 (App. 2; in Swedish), Svensk Kärnbränslehantering AB.

Werner K, Johansson P-O, 2003. Forsmark site investigation. Slug tests in groundwater monitoring wells in soil. SKB P-03-65, Svensk Kärnbränslehantering AB.

Werner K, Bosson E, Berglund S, 2006. Description of climate, surface hydrology, and near-surface hydrogeology. Preliminary site description Laxemar subarea – version 1.2. SKB R-05-61, Svensk Kärnbränslehantering AB.

Werner K, Johansson P-O, Brydsten L, Bosson E, Tröjbom M, Nyman H, 2007. Recharge and discharge of near-surface groundwater in Forsmark – comparison of classification methods. SKB R-07-08, Svensk Kärnbränslehantering AB.

Werner K, Bosson E, Berglund S, Engqvist A, 2008. Description of hydrology and near-surface hydrogeology at Laxemar-Simpevarp. Site descriptive modelling, SDM-Site Laxemar. SKB R-08-71, Svensk Kärnbränslehantering AB.

Appendix 1

The influence of salinity on groundwater levels in rock

Point-water heads are measured in percussion and core boreholes. These boreholes are equipped with packers, dividing the borehole into sections numbered from the borehole bottom and upwards. Groundwater densities have been measured on water sampled from the borehole sections. For some boreholes or borehole sections, there are no density data. However, electrical conductivity (EC) data are in some cases available, which implies that an empirical relationship can be used to estimate the density (see section 2.4.4 in the report). When considered appropriate, calculated density values have been used to compensate for missing density data.

Data on point-water heads, water density and borehole geometry (secup and seclow) have been used to calculate fresh- and environmental water heads for each borehole section, according to the theory presented in section 2.4.4. Initially, the intension was to use groundwater-level data from nearby groundwater monitoring wells to represent the topmost (fresh) water column as reference for each percussion borehole. In the core boreholes, the point-water head in the topmost section (only having a lower packer and therefore being open from above) was used to represent the topmost water column. However, for the purposes of the present analysis, no groundwater monitoring wells are installed close enough to the considered percussion boreholes, which implies that the calculations had to be done in the same way as for the core boreholes.

The vertical hydraulic gradient along a borehole is calculated from the head differential between consecutive borehole sections. The tables on the following pages present differences in point-water heads (abbreviated PWH) and environmental-water heads (abbreviated EWH) between consecutive borehole sections. The tables also show the mean "compensation" per borehole section, defined as the difference between calculated environmental-water heads and measured point-water heads (i.e. EWH minus PWH).

Arrows and colours denote the following directions and magnitudes of the head differentials:

- Blue (↓) > 0.05 m difference: Indicates downward gradient.
- Yellow (↔) –0.05 m < difference < 0.05 m: Indicates small or no vertical gradient.
- Red (↑) –0.05 m < difference: Indicates upward gradient.

There are examples of boreholes (e.g. KLX09) in which there on average are small or no vertical gradients between all consecutive borehole sections, both in terms of PWH and EWH. Other examples can also be found (e.g. KLX05), with one direction of the hydraulic gradient in terms of PWH, and a reversed direction in terms of EWH. For all boreholes with sufficient data (point-water heads, water density and packer elevations), the plots on the following pages show time series of measured point-water heads (PWH) and calculated environmental-water heads (EWH). For reference, sea-water level data are also shown in each plot.

For quick reference, the corresponding data table is presented below each plot. In terms of both PWH and EWH, these borehole-specific tables show the average, minimum and maximum head differentials between consecutive borehole sections, and also the corresponding statistics for the "compensation", hence defined as the difference between calculated environmental-water heads and measured point-water heads (i.e. EWH minus PWH). In addition, the "temporal spread" of the head differentials are quantified in the table. "Percentil 0.02" means that 2% of the head differentials (in terms of PWH and EWH, respectively) are lower than the specified differential, whereas "Percentil 0.98" means that 2% are higher.

Note that time series (and the corresponding data evaluations in terms of PWH and EWH) are only shown up to data freeze Laxemar 2.3 (Aug. 31, 2007), i.e. for the time period for which data screening has been performed. "Const" denotes that the EWH calculations assume that the water density is constant within each borehole section. For convenience, the analysis is summarised in the table below in terms of averages of PWH and EWH for each of the considered borehole sections. "Antalv" denotes the number of available data days.

Medel	:1 PWH	antalv: 1 PWH	:1 EWH	antalv: 1 EWH	:2 PWH	antalv: 2 PWH	:2 EWH	antalv: 2 EWH	:3 PWH	antalv: 3 PWH	:3 EWH	antalv: 3 EWH	:4 PWH	antalv: 4 PWH	:4 EWH	antalv: 4 EWH	:5 PWH	antalv: 5 PWH	:5 EWH	antalv: 5 EWH	:6 PWH	antalv: 6 PWH	:6 EWH	antalv: 6 EWH	:7 PWH	antalv: 7 PWH	:7 EWH	antalv: 7 EWH	:8 PWH	antalv: 8 PWH	:8 EWH	antalv: 8 EWH	:9 PWH	antalv: 9 PWH	:9 EWH	antalv: 9 EWH	:10 PWH	antalv:10 PWH	:10 EWH	antalv:10 EWH
HLX21	6.51	491	6.52	491	6.43	491	6.43	491																																
KAV04A	2.79	786	7.95	786	-0.61	833	-0.45	833	1.58	833	1.57	833	3.72	835	3.72	835																								
KLX02	7.35	1111	7.38	819	5.88	1090	6.19	798	3.19	1111	2.77	819	5.38	831	5.35	773	6.19	1049	6.18	767	6.77	824	6.78	812	8.17	822	8.18	817	10.24	819	10.24	819								
KLX03	11.90	215	11.19	215	10.06	583	14.47	574	10.14	583	10.28	574	9.93	583	9.94	574	10.00	583	10.01	574	9.70	583	9.70	574	9.43	583	9.43	574	10.23	574	10.22	574	10.32	553	10.32	553	10.16	574	10.16	574
KLX05	9.57	661	10.23	460	9.94	450	10.22	447	9.07	554	9.43	420	9.12	583	9.39	444	9.97	460	10.01	460	9.85	460	9.99	460	9.84	458	10.01	458	9.96	460	9.98	460	9.94	460	9.95	460	10.03	460	10.03	460
KLX06	9.33	785	9.27	502	6.61	783	6.62	502	6.13	781	6.17	499	6.12	782	6.15	501	12.66	503	12.66	502	12.68	502	12.68	502	12.65	502	12.65	502	12.22	502	12.22	502								
KAV07A	4.69	441	4.90	291	4.37	423	4.60	284	4.28	439	4.48	289	7.64	330	7.60	320	7.87	330	7.92	320	8.92	330	8.93	320	9.20	320	9.20	320	10.02	320	10.02	320								
KAV07B	6.76	43	6.76	43	6.65	43	6.65	43	6.67	43	6.67	43																												
KLX08	9.40	75	9.17	75	10.59	73	10.36	73	10.74	72	10.51	72	10.89	75	10.66	75	12.66	75	13.44	75	11.79	75	11.92	75	12.59	75	12.61	75	13.12	75	13.12	75	13.10	75	13.10	75	13.18	75	13.18	75
KLX09	3.42	238	4.61	238	13.36	238	13.36	238	13.48	238	13.48	238	13.64	238	13.64	238	13.64	238	13.64	238																				
KLX10	6.96	320	8.04	318	6.83	318	8.12	318	10.35	373	11.64	373	12.02	373	12.86	373	12.32	355	12.95	355	12.40	372	12.81	372	12.83	372	12.83	372	12.82	373	12.82	373								
KLX12A	8.99	102	9.48	102	9.26	218	10.27	218	8.90	216	9.45	216	9.62	191	10.16	191	9.63	229	9.65	229	9.72	238	9.73	238	10.54	238	10.55	238	10.16	238	10.16	238	10.52	238	10.52	238				
KLX13A	12.00	21	12.28	20	11.99	21	12.04	20	14.30	20	14.30	20																												
KLX15A	5.21	2	6.23	2	5.90	2	6.82	2	6.20	2	6.20	2																												
KLX18A	12.42	197	12.42	197	12.34	197	12.34	197	12.32	181	12.32	181	12.25	197	12.25	197	12.55	197	12.55	197	13.29	197	13.29	197	13.63	197	13.63	197												
KSH01A	Missing	0	Missing	0	-0.83	1044	1.00	1025	-1.07	1037	0.77	1023	0.44	1035	1.35	1021	0.29	1019	0.68	1019	-0.46	1023	0.34	1022	0.40	1023	0.70	1023	0.16	1023	0.16	1022	0.51	1026	0.51	1026				
KSH02	-13.06	935	-7.97	935	-4.43	940	-0.61	940	-1.35	940	2.17	940	-1.01	935	-0.94	935	-2.18	772	-2.18	772	-0.16	940	-0.12	940	-0.68	940	-0.68	940												
KAV01	-1.64	698	-1.70	698	-1.97	654	-1.63	654	-1.60	699	-1.57	699	5.93	699	5.94	699	6.17	699	6.17	699																				
KLX19A	9.73	150	9.71	138	9.12	150	9.11	138	12.98	124	12.99	124	13.01	125	13.02	125	13.00	125	13.01	125	13.08	138	13.08	138	13.41	138	13.41	138	13.42	138	13.42	138								

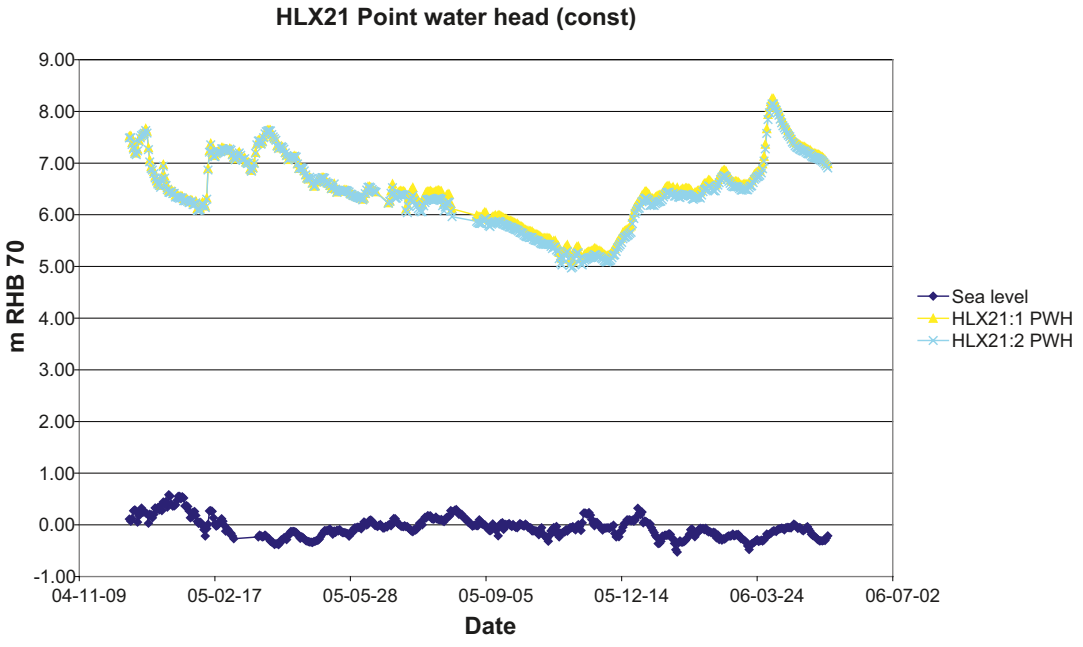

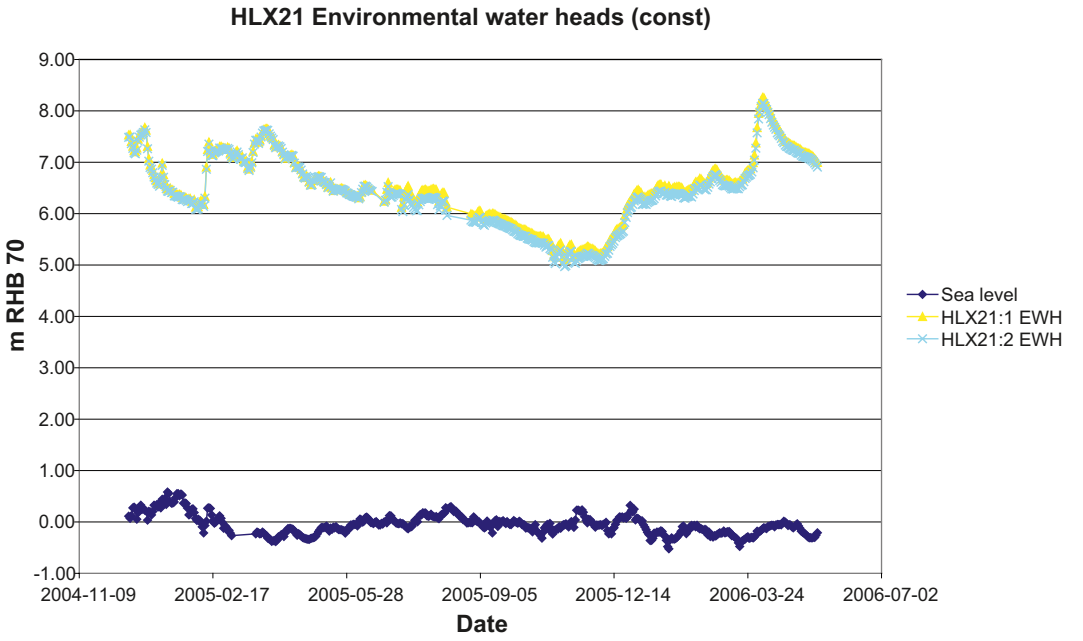

Figure A1. *Time-series plots of point-water heads end environmental-water heads in HLX21.*

HLX21 (Constant)

Section	Min		Percentil 0.02		Ave		Percentil 0.98		Max		Section	Compensation EWH-PWH min	mean	max
2	PWH2	EWH2	PWH2	EWH2	PWH2	EWH2	PWH2	EWH2	PWH2	EWH2	2	0.00	0.00	0.00
	0 ↔	0.01 ↔	0 ↔	0.01 ↔	0.08 ↑	0.09 ↑	0.16 ↑	0.17 ↑	0.16 ↑	0.17 ↑				
1	PWH1	EWH1	PWH1	EWH1	PWH1	EWH1	PWH1	EWH1	PWH1	EWH1	1	0.01	0.01	0.01

Specific comments for HLX21:

- As illustrated in the time-series plot below, the borehole packers have been moved several times in borehole HLX21.
- The point-water head time series obtained from the borehole section installed from the end of 2004 up to mid-2006 best corresponds to the borehole section from which density data are obtained. Point-water head data for section HLX21.1 are here represented by the time series from sections HLX21.1c and HLX21.1d, and data from section HLX21.2b for section HLX21.2 (even though the packers for section HLX21.1 were moved during this time).
- All measured densities in HLX21 are lower than freshwater density, whereas the calculated density is slightly higher than freshwater density. For calculation of environmental-water heads, calculated density values are used for both sections.
- The calculated environmental heads are uncertain due to that point-water heads may be associated to elevations along the borehole other than the density data.
- There is a possibility for misinterpretation of the statistics of the head time series, since the section-specific heads have been measured at different elevations.

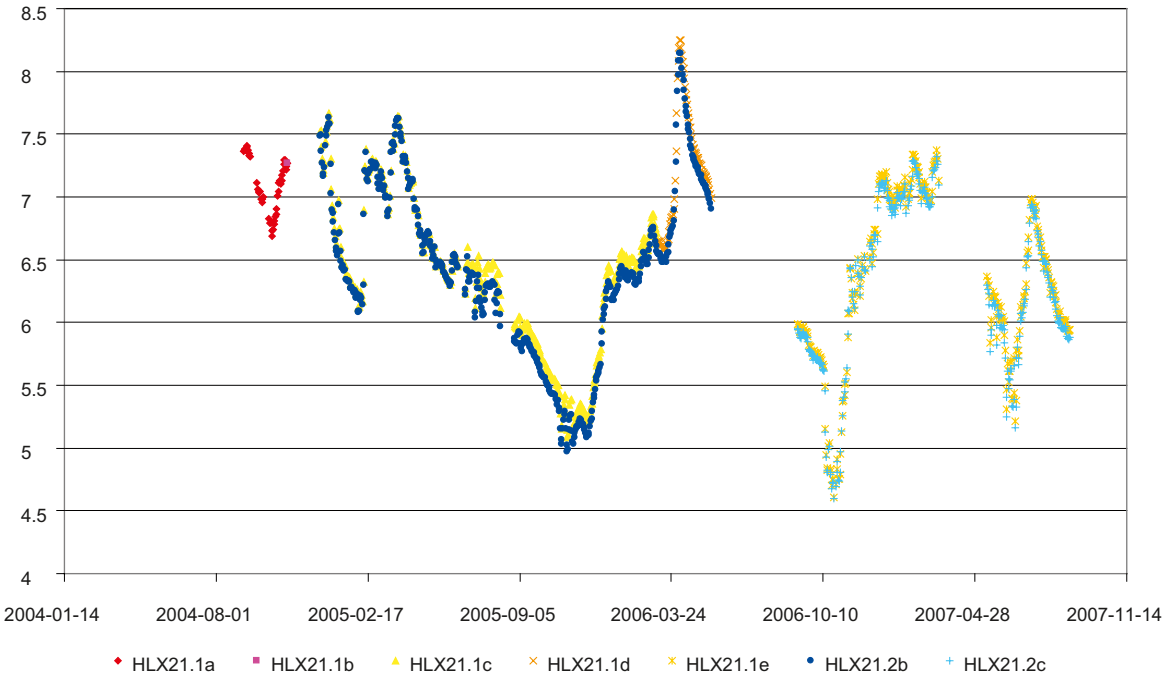

Figure A2. *Time-series plot of point-water heads in borehole sections HLX21.1 and HLX21.2.*

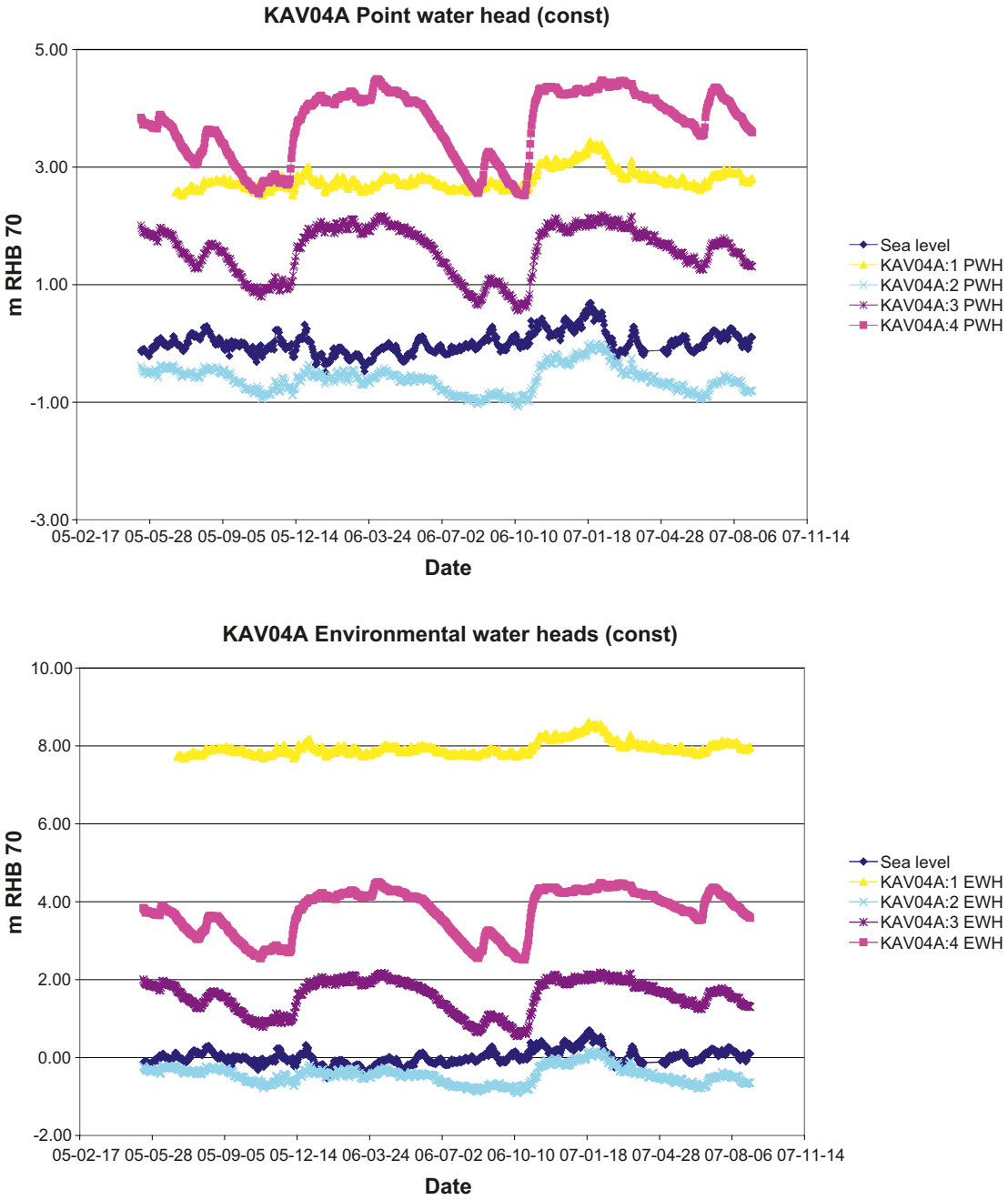

Figure A3. *Time-series plots of point-water heads end environmental-water heads in KAV04.*

KAV04A (Constant)

Section	Min		Percentil 0.02		Ave		Percentil 0.98		Max		Section	Compensation EWH-PWH		
												min	mean	max
4	PWH4	EWH4	PWH4	EWH4	PWH4	EWH4	PWH4	EWH4	PWH4	EWH4	4	0.00	0.00	0.00
	-2.68 ↓	-2.68 ↓	-2.59 ↓	-2.6 ↓	-2.14 ↓	-2.15 ↓	-1.73 ↓	-1.74 ↓	-1.65 ↓	-1.66 ↓				
3	PWH3	EWH3	PWH3	EWH3	PWH3	EWH3	PWH3	EWH3	PWH3	EWH3	3	-0.01	-0.01	-0.01
	-2.66 ↓	-2.49 ↓	-2.6 ↓	-2.43 ↓	-2.19 ↓	-2.02 ↓	-1.65 ↓	-1.48 ↓	-1.54 ↓	-1.37 ↓				
2	PWH2	EWH2	PWH2	EWH2	PWH2	EWH2	PWH2	EWH2	PWH2	EWH2	2	0.16	0.16	0.16
	3.03 ↑	8.02 ↑	3.12 ↑	8.12 ↑	3.41 ↑	8.41 ↑	3.61 ↑	8.61 ↑	3.64 ↑	8.64 ↑				
1	PWH1	EWH1	PWH1	EWH1	PWH1	EWH1	PWH1	EWH1	PWH1	EWH1	1	5.17	5.16	5.16

Specific comments for KAV04A:

- The measured density is higher than freshwater density in sections 1 and 2, but lower in sections 3 and 4.
- The calculated density is higher than freshwater density.
- The calculated density has been used for sections 3 and 4.

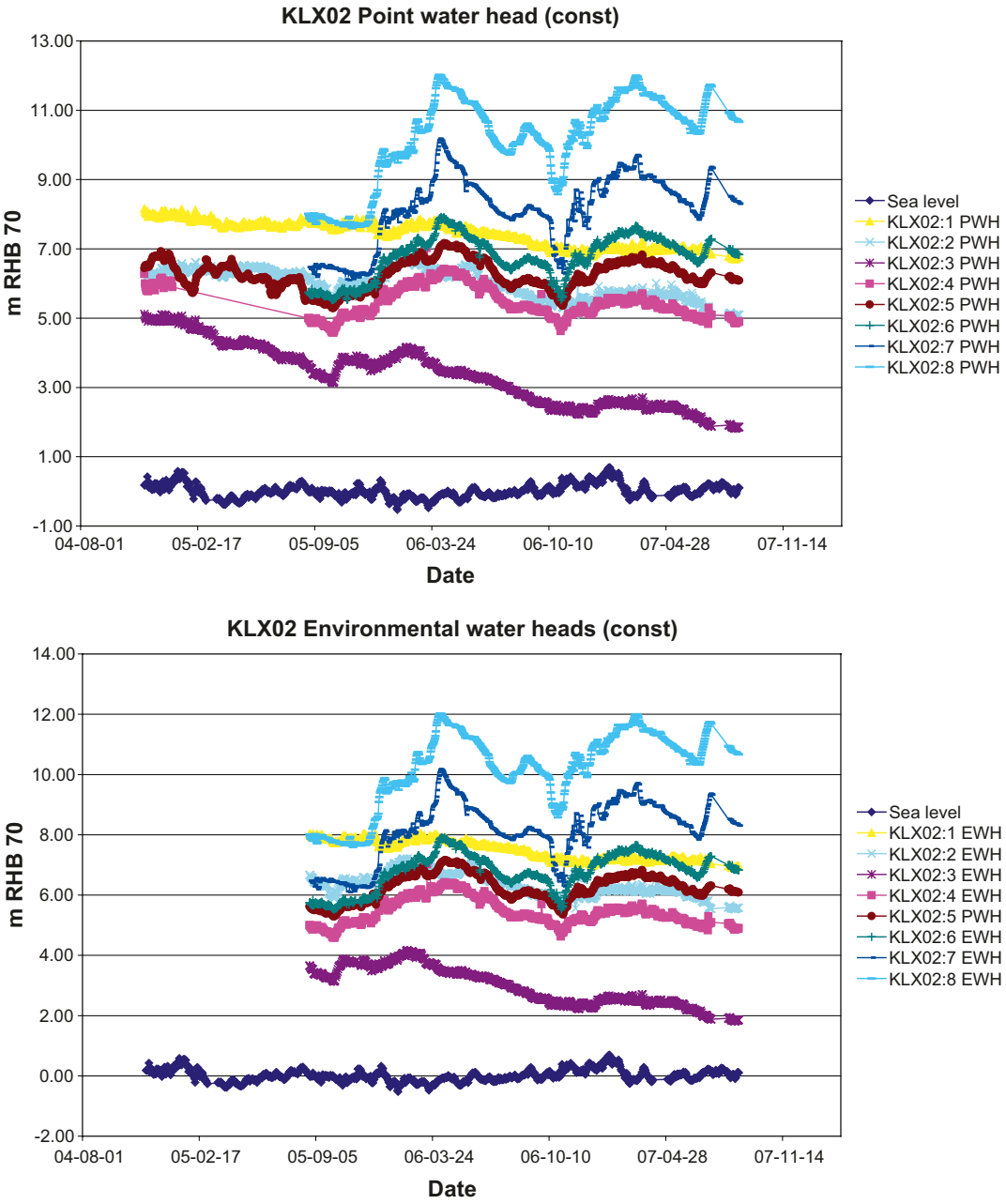

Figure A4. *Time-series plots of point-water heads end environmental-water heads in KLX02.*

KLX02 (Constant)

Section	Min		Percentil 0.02		Ave		Percentil 0.98		Max		Section	Compensation EWH-PWH		
												min	mean	max
8	PWH8	EWH8	PWH8	EWH8	PWH8	EWH8	PWH8	EWH8	PWH8	EWH8	8	0.00	0.00	0.00
	-2.63 ↓	-2.63 ↓	-2.53 ↓	-2.53 ↓	-2.05 ↓	-2.05 ↓	-1.34 ↓	-1.34 ↓	-1.32 ↓	-1.32 ↓				
7	PWH7	EWH7	PWH7	EWH7	PWH7	EWH7	PWH7	EWH7	PWH7	EWH7	7	0.00	0.00	0.00
	-2.36 ↓	-2.36 ↓	-2.08 ↓	-2.08 ↓	-1.37 ↓	-1.37 ↓	-1.37 ↓	-0.41 ↓	-0.36 ↓	-0.36 ↓				
6	PWH6	EWH6	PWH6	EWH6	PWH6	EWH6	PWH6	EWH6	PWH6	EWH6	6	0.00	0.00	0.00
	-0.98 ↓	-0.98 ↓	-0.92 ↓	-0.92 ↓	-0.53 ↓	-0.54 ↓	-0.53 ↓	-0.11 ↓	0.09 ↑	0.09 ↑				
5	PWH5	EWH5	PWH5	EWH5	PWH5	EWH5	PWH5	EWH5	PWH5	EWH5	5	0.00	0.00	0.00
	-1.38 ↓	-1.38 ↓	-1.24 ↓	-1.24 ↓	-0.82 ↓	-0.83 ↓	-0.82 ↓	-0.53 ↓	0.38 ↑	0.38 ↑				
4	PWH4	EWH4	PWH4	EWH4	PWH4	EWH4	PWH4	EWH4	PWH4	EWH4	4	0.00	0.00	0.00
	-3.38 ↓	-3.38 ↓	-3.11 ↓	-3.12 ↓	-2.36 ↓	-2.47 ↓	-2.36 ↓	-1.27 ↓	-0.8 ↓	-1.24 ↓				
3	PWH3	EWH3	PWH3	EWH3	PWH3	EWH3	PWH3	EWH3	PWH3	EWH3	3	0.00	0.00	0.00
	1.3 ↑	2.63 ↑	1.31 ↑	2.67 ↑	2.61 ↑	3.37 ↑	2.61 ↑	3.8 ↑	3.85 ↑	4.33 ↑				
2	PWH2	EWH2	PWH2	EWH2	PWH2	EWH2	PWH2	EWH2	PWH2	EWH2	2	0.48	0.48	0.48
	0.77 ↑	0.48 ↑	0.96 ↑	0.64 ↑	1.45 ↑	1.15 ↑	1.45 ↑	1.69 ↑	2.13 ↑	1.84 ↑				
1	PWH1	EWH1	PWH1	EWH1	PWH1	EWH1	PWH1	EWH1	PWH1	EWH1	1	0.19	0.19	0.19

Specific comments for KLX02:

- The measured density is lower than freshwater density for all sections at the time when all sections were measured (during another occasion when only two sections were measured, the density was slightly higher than freshwater density).
- The calculated density is slightly higher than freshwater density in sections 1 and 2.
- The calculated density has been used for sections 1 and 2, whereas freshwater density was used for the other sections.

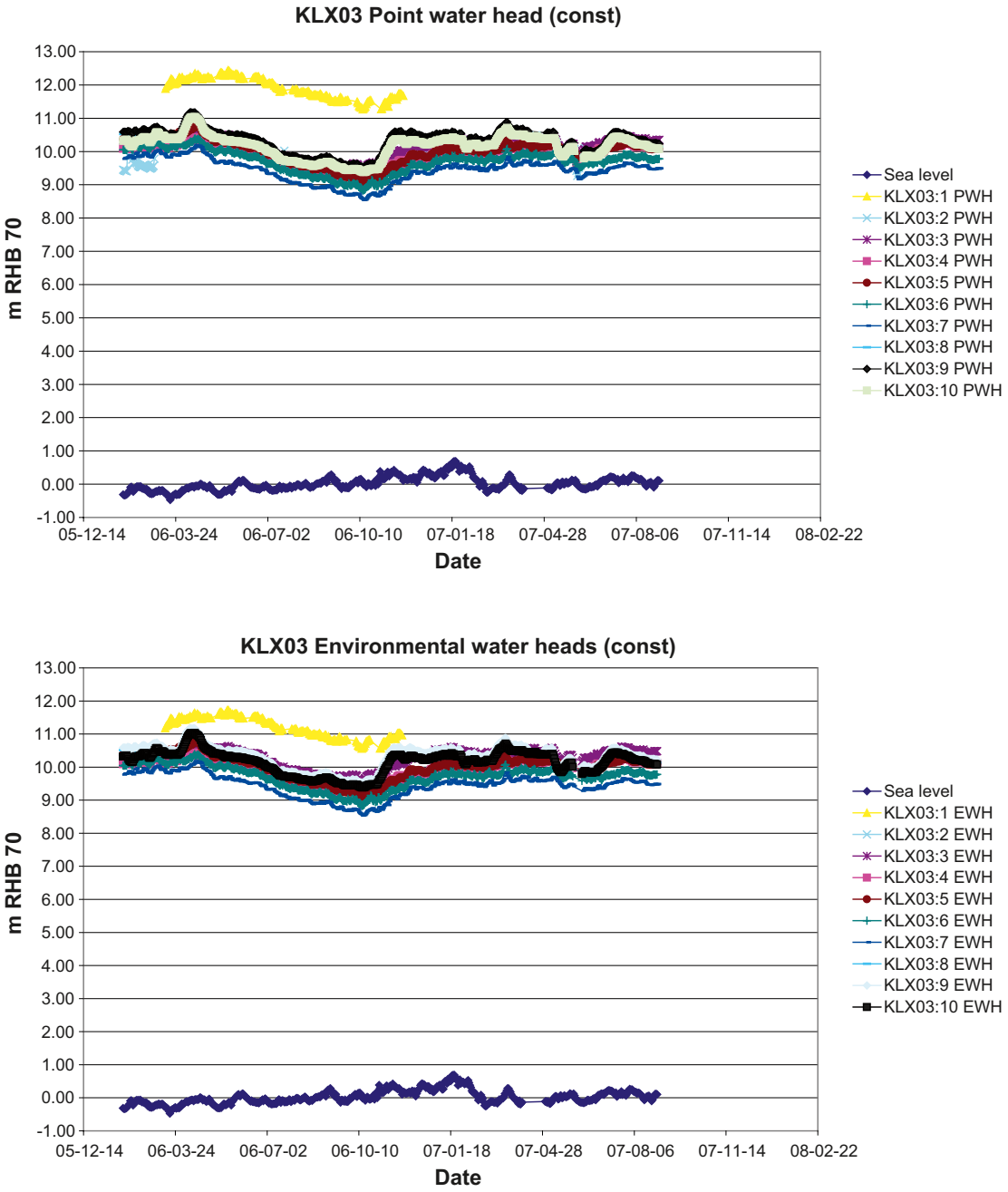

Figure A5. *Time-series plots of point-water heads end environmental-water heads in KLX03.*

KLX03 (Constant)

Section	Min		Percentil 0.02		Ave		Percentil 0.98		Max		Section	Compensation EWH-PWH min	mean	max
10	PWH10	EWH10	PWH10	EWH10	PWH10	EWH10	PWH10	EWH10	PWH10	EWH10	10	0.00	0.00	0.00
	-0.05 ↔	-0.05 ↓	0.11 ↑	0.11 ↑	0.18 ↑	0.17 ↑	0.31 ↑	0.31 ↑	0.4 ↑	0.4 ↑				
9	PWH9	EWH9	PWH9	EWH9	PWH9	EWH9	PWH9	EWH9	PWH9	EWH9	9	0.00	-0.01	-0.01
	-0.19 ↓	-0.2 ↓	-0.16 ↓	-0.16 ↓	-0.1 ↓	-0.11 ↓	-0.05 ↔	-0.05 ↓	0.1 ↑	0.1 ↑				
8	PWH8	EWH8	PWH8	EWH8	PWH8	EWH8	PWH8	EWH8	PWH8	EWH8	8	-0.01	-0.01	-0.01
	-1.39 ↓	-1.39 ↓	-1.26 ↓	-1.25 ↓	-0.79 ↓	-0.79 ↓	-0.53 ↓	-0.52 ↓	-0.43 ↓	-0.43 ↓				
7	PWH7	EWH7	PWH7	EWH7	PWH7	EWH7	PWH7	EWH7	PWH7	EWH7	7	0.00	0.00	0.00
	0.15 ↑	0.15 ↑	0.2 ↑	0.2 ↑	0.27 ↑	0.27 ↑	0.35 ↑	0.35 ↑	0.45 ↑	0.45 ↑				
6	PWH6	EWH6	PWH6	EWH6	PWH6	EWH6	PWH6	EWH6	PWH6	EWH6	6	0.00	0.00	0.00
	0.14 ↑	0.15 ↑	0.25 ↑	0.26 ↑	0.3 ↑	0.31 ↑	0.37 ↑	0.38 ↑	0.39 ↑	0.4 ↑				
5	PWH5	EWH5	PWH5	EWH5	PWH5	EWH5	PWH5	EWH5	PWH5	EWH5	5	0.01	0.01	0.01
	-0.37 ↓	-0.37 ↓	-0.33 ↓	-0.33 ↓	-0.08 ↓	-0.07 ↓	0.06 ↑	0.06 ↑	0.12 ↑	0.12 ↑				
4	PWH4	EWH4	PWH4	EWH4	PWH4	EWH4	PWH4	EWH4	PWH4	EWH4	4	0.01	0.01	0.01
	0.03 ↔	0.15 ↑	0.03 ↔	0.16 ↑	0.21 ↑	0.34 ↑	0.35 ↑	0.47 ↑	0.48 ↑	0.6 ↑				
3	PWH3	EWH3	PWH3	EWH3	PWH3	EWH3	PWH3	EWH3	PWH3	EWH3	3	0.13	0.13	0.13
	-0.74 ↓	3.52 ↑	-0.67 ↓	3.6 ↑	-0.08 ↓	4.19 ↑	0.31 ↑	4.59 ↑	0.43 ↑	4.71 ↑				
2	PWH2	EWH2	PWH2	EWH2	PWH2	EWH2	PWH2	EWH2	PWH2	EWH2	2	4.41	4.41	4.40
	1.26 ↑	-3.86 ↓	1.33 ↑	-3.79 ↓	1.92 ↑	-3.2 ↓	2.14 ↑	-2.97 ↓	2.16 ↑	-2.95 ↓				
1	PWH1	EWH1	PWH1	EWH1	PWH1	EWH1	PWH1	EWH1	PWH1	EWH1	1	-0.71	-0.71	-0.71

Specific comments for KLX03:

- The secup elevation in the packer data file are registered from Jan. 2006 and differs some decimetres from the secup elevation according to the chemistry data file, reported to Sicada both prior to and after the packer data.
- Density values are available for several dates, but never the same date for all sections.
- The density data used originate from water sampling Jan. 2006.
- The measured density is higher than freshwater density for sections 1 and 2, but lower than freshwater density for the other sections.
- The calculated density is slightly higher than freshwater density.
- The measured density has been used for sections 1 and 2, whereas the calculated density has been used for the other sections.
- There is no obvious risk that density values are referring to other section elevations than those applicable for the head data, considering that the section discrepancy is small.
- There is no obvious risk that different parts of the head time series refer to different section elevations, considering that the section discrepancy is small.

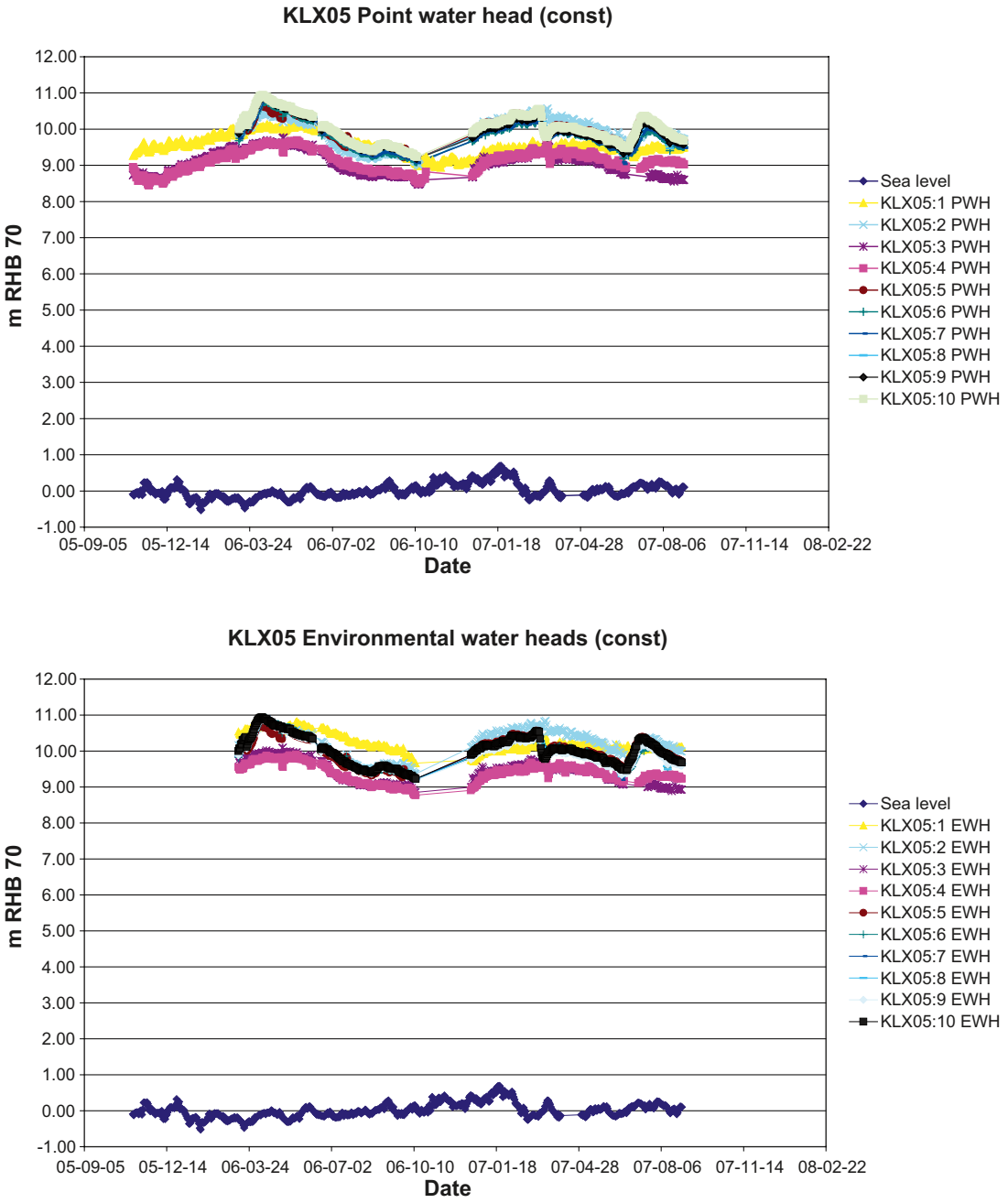

Figure A6. *Time-series plots of point-water heads end environmental-water heads in KLX05.*

KLX05 (Constant)

Section	Min		Percentil 0.02		Ave		Percentil 0.98		Max		Section	Compensation EWH-PWH min	mean	max
10	PWH10	EWH10	PWH10	EWH10	PWH10	EWH10	PWH10	EWH10	PWH10	EWH10	10	0.00	0.00	0.00
	-0.24 ↓	-0.23 ↓	-0.2 ↓	-0.19 ↓	-0.08 ↓	-0.08 ↓	-0.02 ↔	-0.01 ↔	0 ↔	0.01 ↔				
9	PWH9	EWH9	PWH9	EWH9	PWH9	EWH9	PWH9	EWH9	PWH9	EWH9	9	0.00	0.00	0.00
	-0.15 ↓	-0.13 ↓	-0.05 ↔	-0.03 ↔	0.02 ↔	0.03 ↔	0.07 ↑	0.09 ↑	0.16 ↑	0.18 ↑				
8	PWH8	EWH8	PWH8	EWH8	PWH8	EWH8	PWH8	EWH8	PWH8	EWH8	8	0.02	0.02	0.02
	-0.28 ↓	-0.14 ↓	-0.16 ↓	-0.02 ↔	-0.12 ↓	0.02 ↔	-0.1 ↓	0.04 ↔	-0.1 ↓	0.05 ↔				
7	PWH7	EWH7	PWH7	EWH7	PWH7	EWH7	PWH7	EWH7	PWH7	EWH7	7	0.17	0.16	0.16
	-0.17 ↓	-0.19 ↓	-0.07 ↓	-0.09 ↓	0.01 ↔	-0.01 ↔	0.09 ↑	0.07 ↑	0.24 ↑	0.21 ↑				
6	PWH6	EWH6	PWH6	EWH6	PWH6	EWH6	PWH6	EWH6	PWH6	EWH6	6	0.14	0.14	0.14
	-0.27 ↓	-0.37 ↓	-0.17 ↓	-0.27 ↓	0.11 ↑	0.02 ↔	0.44 ↑	0.34 ↑	0.48 ↑	0.38 ↑				
5	PWH5	EWH5	PWH5	EWH5	PWH5	EWH5	PWH5	EWH5	PWH5	EWH5	5	0.04	0.04	0.04
	-1.42 ↓	-1.25 ↓	-1.26 ↓	-1.09 ↓	-0.79 ↓	-0.62 ↓	-0.47 ↓	-0.31 ↓	-0.23 ↓	-0.06 ↓				
4	PWH4	EWH4	PWH4	EWH4	PWH4	EWH4	PWH4	EWH4	PWH4	EWH4	4	0.21	0.21	0.21
	-0.51 ↓	-0.39 ↓	-0.45 ↓	-0.33 ↓	-0.05 ↓	0.03 ↔	0.13 ↑	0.24 ↑	0.45 ↑	0.57 ↑				
3	PWH3	EWH3	PWH3	EWH3	PWH3	EWH3	PWH3	EWH3	PWH3	EWH3	3	0.33	0.33	0.33
	0.43 ↑	0.37 ↑	0.5 ↑	0.44 ↑	0.84 ↑	0.79 ↑	1.31 ↑	1.26 ↑	1.36 ↑	1.3 ↑				
2	PWH2	EWH2	PWH2	EWH2	PWH2	EWH2	PWH2	EWH2	PWH2	EWH2	2	0.28	0.27	0.27
	-0.93 ↓	-0.58 ↓	-0.89 ↓	-0.54 ↓	-0.33 ↓	0.02 ↔	0.35 ↑	0.7 ↑	0.41 ↑	0.76 ↑				
1	PWH1	EWH1	PWH1	EWH1	PWH1	EWH1	PWH1	EWH1	PWH1	EWH1	1	0.63	0.63	0.62

Specific comments for KLX05:

- The measured density is lower than freshwater density for all sections.
- The calculated density is slightly higher than freshwater density for all sections, except for the uppermost section.
- The calculated density has been used for all sections, except for the uppermost section.
- Freshwater density is used for the uppermost section.

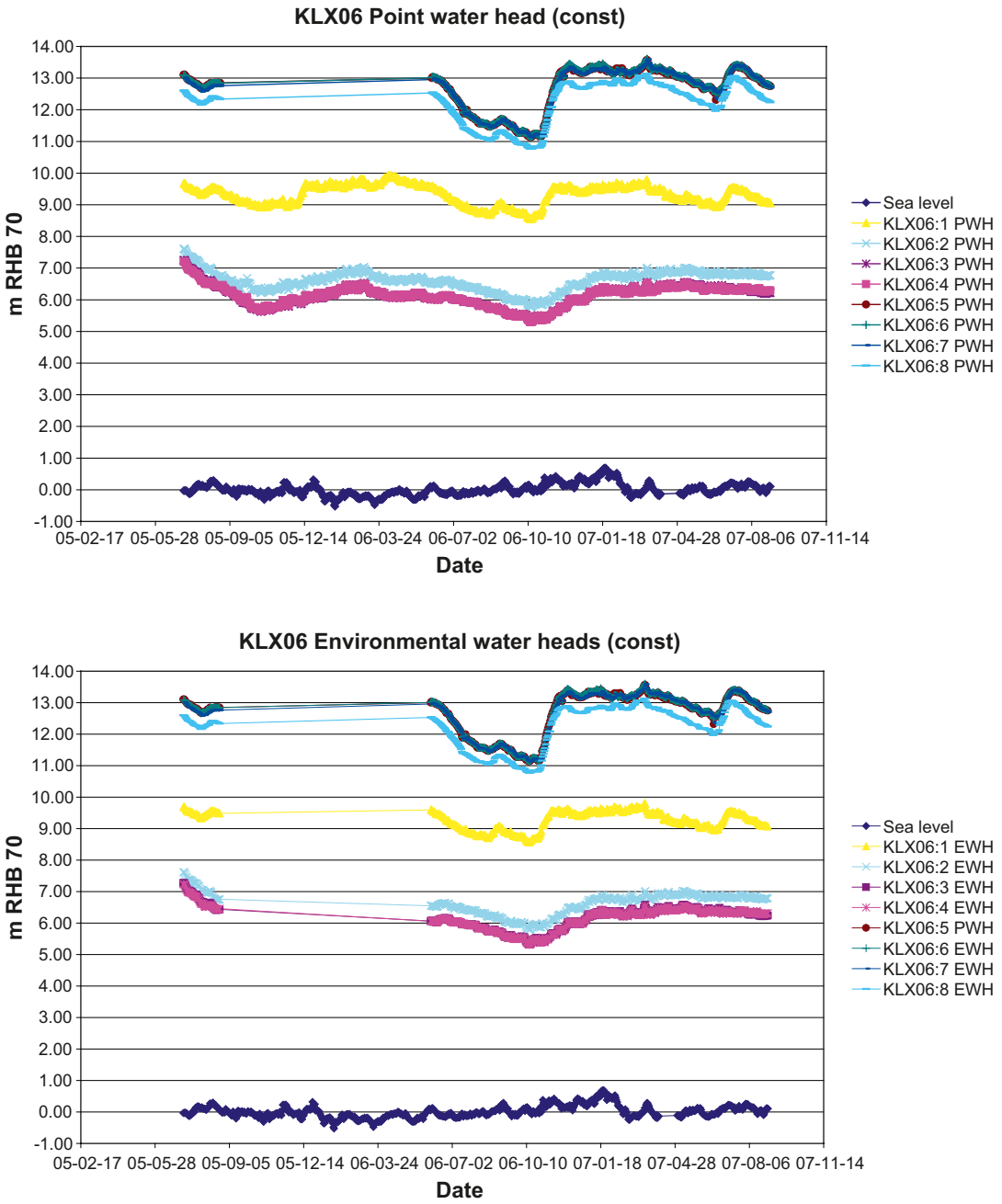

Figure A7. *Time-series plots of point-water heads end environmental-water heads in KLX06.*

KLX06 (Constant)

Section	Min		Percentil 0.02		Ave		Percentil 0.98		Max		Section	Compensation EWH-PWH min	mean	max
8	PWH8	EWH8	PWH8	EWH8	PWH8	EWH8	PWH8	EWH8	PWH8	EWH8	8	0.00	0.00	0.00
	0.19 ↑	0.19 ↑	0.25 ↑	0.25 ↑	0.42 ↑	0.42 ↑	0.53 ↑	0.53 ↑	0.55 ↑	0.55 ↑				
7	PWH7	EWH7	PWH7	EWH7	PWH7	EWH7	PWH7	EWH7	PWH7	EWH7	7	0.00	0.00	0.00
	-0.06 ↓	-0.06 ↓	-0.02 ↔	-0.02 ↔	0.03 ↔	0.03 ↔	0.03 ↑	0.1 ↑	0.15 ↑	0.15 ↑				
6	PWH6	EWH6	PWH6	EWH6	PWH6	EWH6	PWH6	EWH6	PWH6	EWH6	6	0.00	0.00	0.00
	-0.18 ↓	-0.18 ↓	-0.05 ↔	-0.05 ↔	-0.01 ↔	-0.01 ↔	-0.01 ↔	0.04 ↔	0.09 ↑	0.09 ↑				
5	PWH5	EWH5	PWH5	EWH5	PWH5	EWH5	PWH5	EWH5	PWH5	EWH5	5	0.00	0.00	0.00
	-7.51 ↓	-7.5 ↓	-7.42 ↓	-7.4 ↓	-6.53 ↓	-6.51 ↓	-6.53 ↓	-5.73 ↓	-5.73 ↓	-5.71 ↓				
4	PWH4	EWH4	PWH4	EWH4	PWH4	EWH4	PWH4	EWH4	PWH4	EWH4	4	0.02	0.02	0.02
	-0.08 ↓	-0.07 ↓	-0.05 ↔	-0.06 ↓	0.01 ↔	0.01 ↔	0.01 ↑	0.06 ↑	0.06 ↑	0.06 ↑				
3	PWH3	EWH3	PWH3	EWH3	PWH3	EWH3	PWH3	EWH3	PWH3	EWH3	3	0.02	0.02	0.02
	0.32 ↑	0.32 ↑	0.33 ↑	0.32 ↑	0.48 ↑	0.45 ↑	0.48 ↑	0.54 ↑	0.68 ↑	0.55 ↑				
2	PWH2	EWH2	PWH2	EWH2	PWH2	EWH2	PWH2	EWH2	PWH2	EWH2	2	0.02	0.02	0.02
	2.07 ↑	2.07 ↑	2.16 ↑	2.15 ↑	2.72 ↑	2.65 ↑	2.72 ↑	3.4 ↑	3.46 ↑	3.46 ↑				
1	PWH1	EWH1	PWH1	EWH1	PWH1	EWH1	PWH1	EWH1	PWH1	EWH1	1	0.02	0.02	0.02

Specific comments for KLX06:

- The measured density is lower than freshwater density.
- The calculated density is slightly higher than freshwater density for sections 1 to 4.
- Calculated density has been used for sections 1 to 4.
- Freshwater density has been used for the uppermost sections.
- All density data from the chemistry data file are available from dates earlier than the dates specified in the packer data file. However, the latest date specified in the chemistry data file are the same as those specified in the packer data file. These density data have therefore been used.

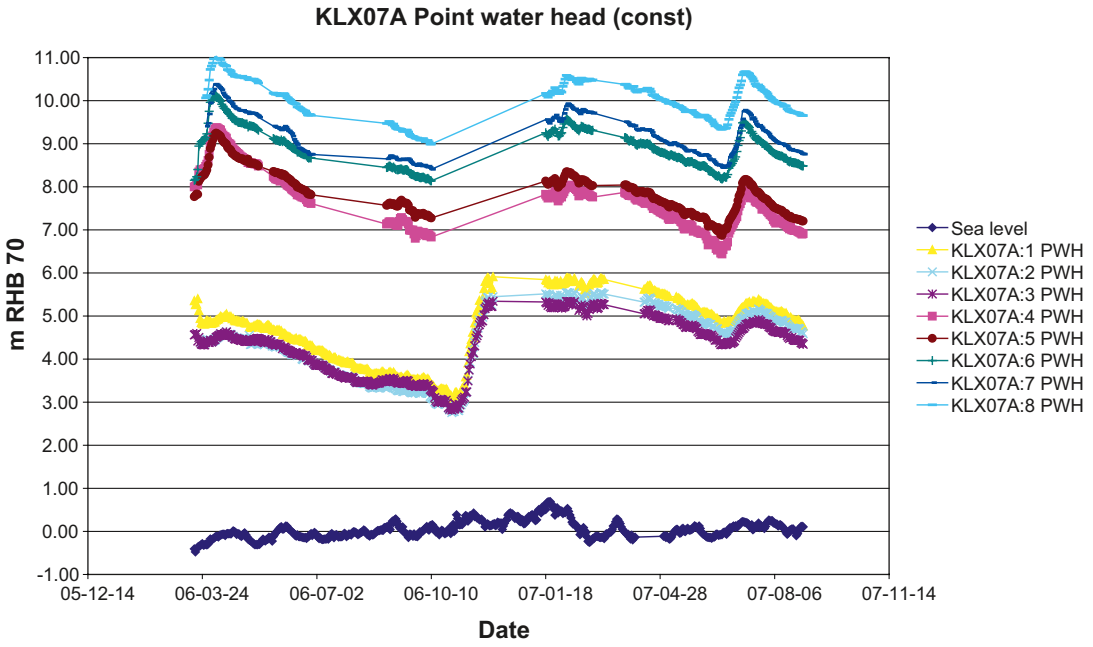

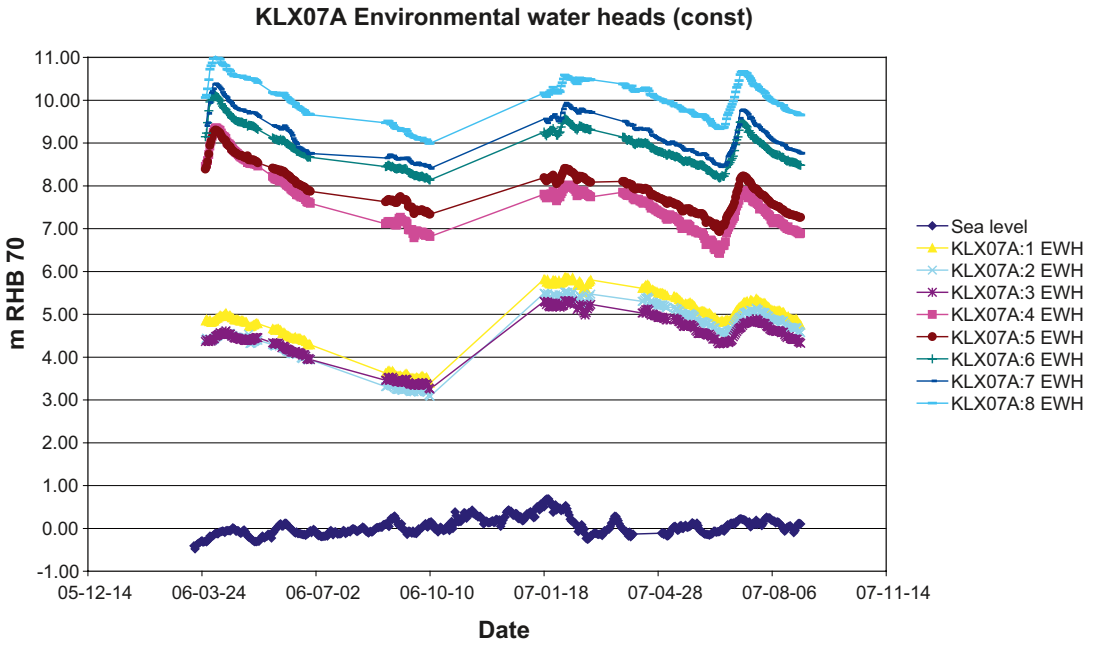

Figure A8. *Time-series plots of point-water heads end environmental-water heads in KLX07A.*

KLX07A (Constant)

Section	Min		Percentil 0.02		Ave		Percentil 0.98		Max		Section	Compensation EWH-PWH min	mean	max
8	PWH8	EWH8	PWH8	EWH8	PWH8	EWH8	PWH8	EWH8	PWH8	EWH8	8	0.00	0.00	0.00
	-1 ↓	-1 ↓	-0.97 ↓	-0.97 ↓	-0.82 ↓	-0.82 ↓	-0.59 ↓	-0.59 ↓	-0.53 ↓	-0.53 ↓				
7	PWH7	EWH7	PWH7	EWH7	PWH7	EWH7	PWH7	EWH7	PWH7	EWH7	7	0.00	0.00	0.00
	-0.41 ↓	-0.41 ↓	-0.39 ↓	-0.39 ↓	-0.28 ↓	-0.28 ↓	-0.28 ↓	-0.08 ↓	-0.07 ↓	-0.07 ↓				
6	PWH6	EWH6	PWH6	EWH6	PWH6	EWH6	PWH6	EWH6	PWH6	EWH6	6	0.00	0.00	0.00
	-1.4 ↓	-1.34 ↓	-1.3 ↓	-1.24 ↓	-1.05 ↓	-1.01 ↓	-1.05 ↓	-0.7 ↓	-0.38 ↓	-0.67 ↓				
5	PWH5	EWH5	PWH5	EWH5	PWH5	EWH5	PWH5	EWH5	PWH5	EWH5	5	0.06	0.06	0.06
	-0.49 ↓	-0.57 ↓	-0.45 ↓	-0.53 ↓	-0.22 ↓	-0.31 ↓	-0.22 ↑	0.06 ↑	0.22 ↑	0.06 ↑				
4	PWH4	EWH4	PWH4	EWH4	PWH4	EWH4	PWH4	EWH4	PWH4	EWH4	4	-0.02	-0.02	-0.02
	-4.87 ↓	-4.87 ↓	-4.76 ↓	-4.76 ↓	-3.15 ↓	-3.12 ↓	-3.15 ↓	-2.17 ↓	-2.08 ↓	-2.08 ↓				
3	PWH3	EWH3	PWH3	EWH3	PWH3	EWH3	PWH3	EWH3	PWH3	EWH3	3	-0.02	-0.02	-0.02
	-0.19 ↓	-0.19 ↓	-0.18 ↓	-0.18 ↓	0.08 ↑	0.12 ↑	0.08 ↑	0.29 ↑	0.29 ↑	0.29 ↑				
2	PWH2	EWH2	PWH2	EWH2	PWH2	EWH2	PWH2	EWH2	PWH2	EWH2	2	-0.02	-0.02	-0.02
	0.18 ↑	0.18 ↑	0.2 ↑	0.2 ↑	0.32 ↑	0.31 ↑	0.32 ↑	0.43 ↑	0.48 ↑	0.44 ↑				
1	PWH1	EWH1	PWH1	EWH1	PWH1	EWH1	PWH1	EWH1	PWH1	EWH1	1	-0.02	-0.02	-0.02

Specific comments for KLX07A:

- The measured density is lower than freshwater density.
- The calculated density is higher than freshwater density only for section 5.
- Calculated density has been used for section 5.
- Several density data are available in the chemistry data file from dates prior to the dates specified in the packer data file, and the sections in the chemistry data file differ from those specified in the packer data file. However, the latest date specified in the chemistry data file is later than the specification in the packer data file, and it specifies sections that are the same as those in the packer data file. These density readings have therefore been used.

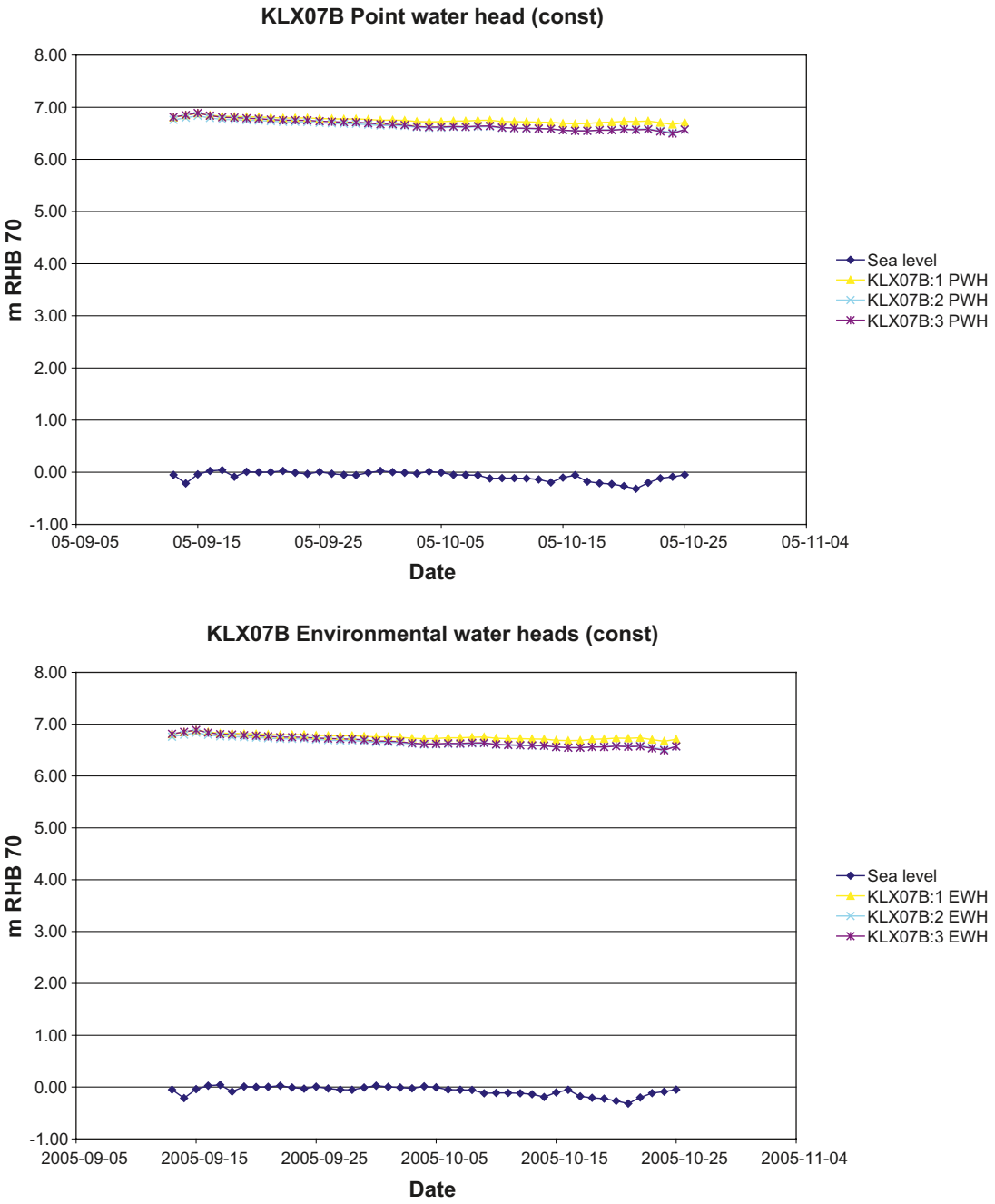

Figure A9. *Time-series plots of point-water heads end environmental-water heads in KLX07B.*

KLX07B (Constant)

Section	Min		Percentil 0.02		Ave		Percentil 0.98		Max		Section	Compensation EWH-PWH min	mean	max
3	PWH3	EWH3	PWH3	EWH3	PWH3	EWH3	PWH3	EWH3	PWH3	EWH3	3	0.00	0.00	0.00
	-0.05 ↓	-0.05 ↓	-0.05 ↓	-0.05 ↓	-0.02 ↔	-0.02 ↔	0.02 ↔	0.02 ↔	0.02 ↔	0.02 ↔				
2	PWH2	EWH2	PWH2	EWH2	PWH2	EWH2	PWH2	EWH2	PWH2	EWH2	2	0.00	0.00	0.00
	0.05 ↔	0.05 ↔	0.05 ↔	0.05 ↔	0.11 ↑	0.11 ↑	0.15 ↑	0.15 ↑	0.16 ↑	0.16 ↑				
1	PWH1	EWH1	PWH1	EWH1	PWH1	EWH1	PWH1	EWH1	PWH1	EWH1	1	0.00	0.00	0.00

Specific comments for KLX07B:

- Section elevations differ between the packer data file and the chemistry data file.
- The data screening (see the main report) indicates the dates when borehole sections were shifted in KLX07B, see below.
- Early time series have been selected, from a point in time when data from all three sections are available (see time-series plot below).
- The measured density is lower than freshwater density.
- The calculated density is lower than freshwater density.
- Freshwater densities have been used for all sections.
- Due to that densities are low and freshwater density is used for all sections, there is no risk for misinterpretation of EWH.

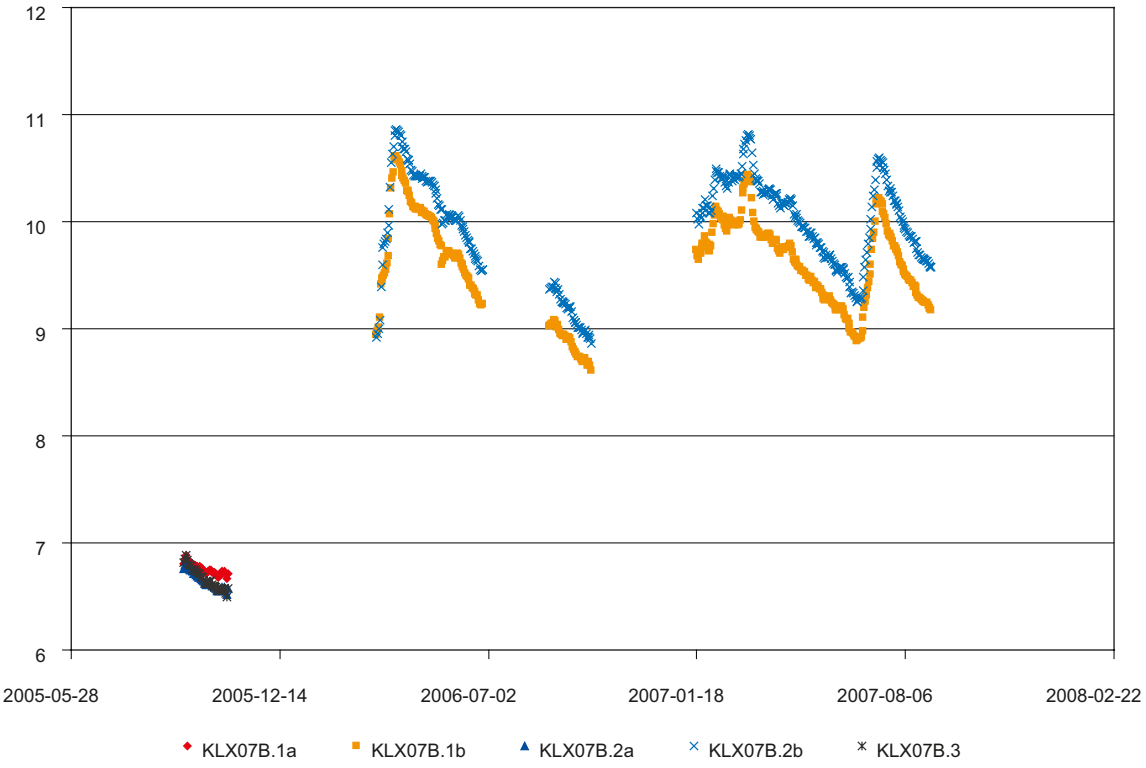

Figure A10. *Time-series plots of point-water heads in borehole sections KLX07B.1, KLX07B.2 and KLX07B.3.*

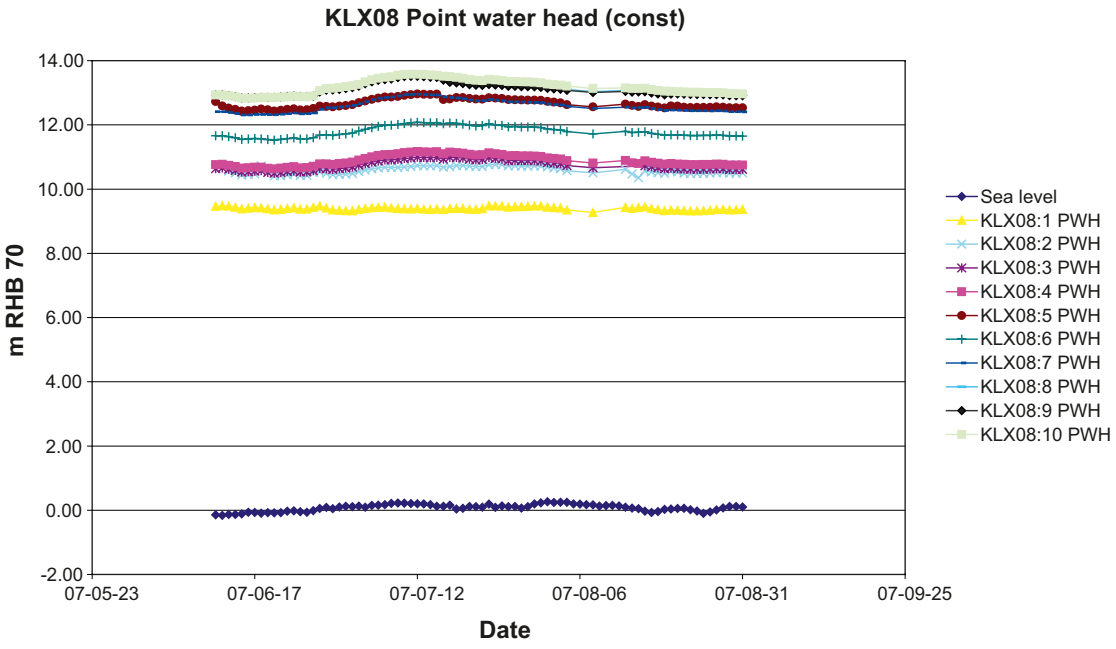

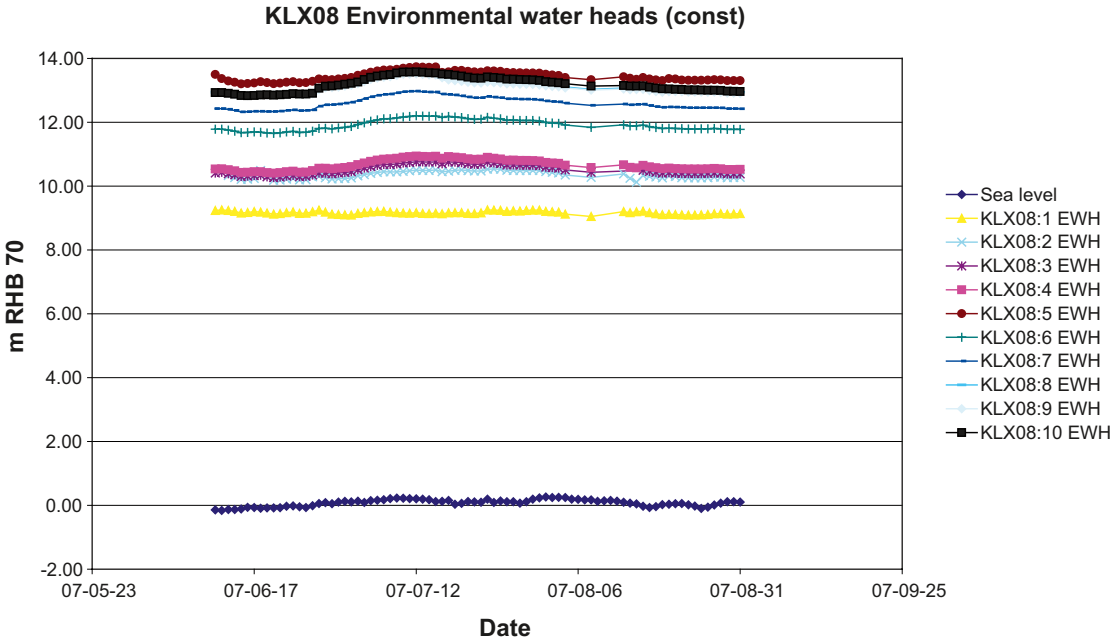

Figure A11. *Time-series plots of point-water heads end environmental-water heads in KLX08.*

KLX08 (Constant)

Section	Min		Percentil 0.02		Ave		Percentil 0.98		Max		Section	Compensation EWH-PWH min	mean	max
10	PWH10	EWH10	PWH10	EWH10	PWH10	EWH10	PWH10	EWH10	PWH10	EWH10	10	0.00	0.00	0.00
	-0.17 ↓	-0.17 ↓	-0.17 ↓	-0.17 ↓	-0.08 ↓	-0.08 ↓	0.01 ↔	0.01 ↔	0.01 ↔	0.01 ↔				
9	PWH9	EWH9	PWH9	EWH9	PWH9	EWH9	PWH9	EWH9	PWH9	EWH9	9	0.00	0.00	0.00
	0 ↔	0 ↔	0 ↔	0 ↔	0.02 ↔	0.02 ↔	0.03 ↔	0.03 ↔	0.03 ↔	0.03 ↔				
8	PWH8	EWH8	PWH8	EWH8	PWH8	EWH8	PWH8	EWH8	PWH8	EWH8	8	0.00	0.00	0.00
	-0.57 ↓	-0.55 ↓	-0.56 ↓	-0.55 ↓	-0.53 ↓	-0.51 ↓	-0.5 ↓	-0.49 ↓	-0.5 ↓	-0.49 ↓				
7	PWH7	EWH7	PWH7	EWH7	PWH7	EWH7	PWH7	EWH7	PWH7	EWH7	7	0.02	0.02	0.02
	-0.9 ↓	-0.79 ↓	-0.89 ↓	-0.79 ↓	-0.79 ↓	-0.69 ↓	-0.75 ↓	-0.64 ↓	-0.75 ↓	-0.64 ↓				
6	PWH6	EWH6	PWH6	EWH6	PWH6	EWH6	PWH6	EWH6	PWH6	EWH6	6	0.12	0.12	0.12
	0.75 ↑	1.4 ↑	0.78 ↑	1.43 ↑	0.87 ↑	1.52 ↑	0.93 ↑	1.58 ↑	1.06 ↑	1.71 ↑				
5	PWH5	EWH5	PWH5	EWH5	PWH5	EWH5	PWH5	EWH5	PWH5	EWH5	5	0.77	0.77	0.77
	-1.96 ↓	-2.96 ↓	-1.82 ↓	-2.82 ↓	-1.77 ↓	-2.78 ↓	-1.7 ↓	-2.7 ↓	-1.66 ↓	-2.66 ↓				
4	PWH4	EWH4	PWH4	EWH4	PWH4	EWH4	PWH4	EWH4	PWH4	EWH4	4	-0.23	-0.23	-0.23
	-0.18 ↓	-0.18 ↓	-0.18 ↓	-0.18 ↓	-0.15 ↓	-0.15 ↓	-0.12 ↓	-0.12 ↓	-0.11 ↓	-0.11 ↓				
3	PWH3	EWH3	PWH3	EWH3	PWH3	EWH3	PWH3	EWH3	PWH3	EWH3	3	-0.23	-0.23	-0.23
	-0.29 ↓	-0.29 ↓	-0.27 ↓	-0.27 ↓	-0.16 ↓	-0.16 ↓	0.03 ↔	0.03 ↔	0.15 ↑	0.15 ↑				
2	PWH2	EWH2	PWH2	EWH2	PWH2	EWH2	PWH2	EWH2	PWH2	EWH2	2	-0.23	-0.23	-0.23
	-1.36 ↓	-1.36 ↓	-1.35 ↓	-1.35 ↓	-1.19 ↓	-1.19 ↓	-1.04 ↓	-1.04 ↓	-0.93 ↓	-0.93 ↓				
1	PWH1	EWH1	PWH1	EWH1	PWH1	EWH1	PWH1	EWH1	PWH1	EWH1	1	-0.23	-0.23	-0.23

Specific comments for KLX08:

- Section elevations in the packer data file are registered from Jun. 2007 and differ from the sections according to the chemistry data file, registered prior to 2007.
- Density data are only available for sections 5 to 8.
- The measured density is lower than freshwater density for all but one section.
- The calculated density is slightly higher than freshwater density for sections 6 and 7.
- The measured density has been used for section 5, calculated density has been used for sections 6 and 7, and freshwater density has been used for section 8.
- There is a risk that head data refer to other section elevations than the density data.
- Due to that densities are low and freshwater density is used for all sections, there is no risk for misinterpretation of EWH.

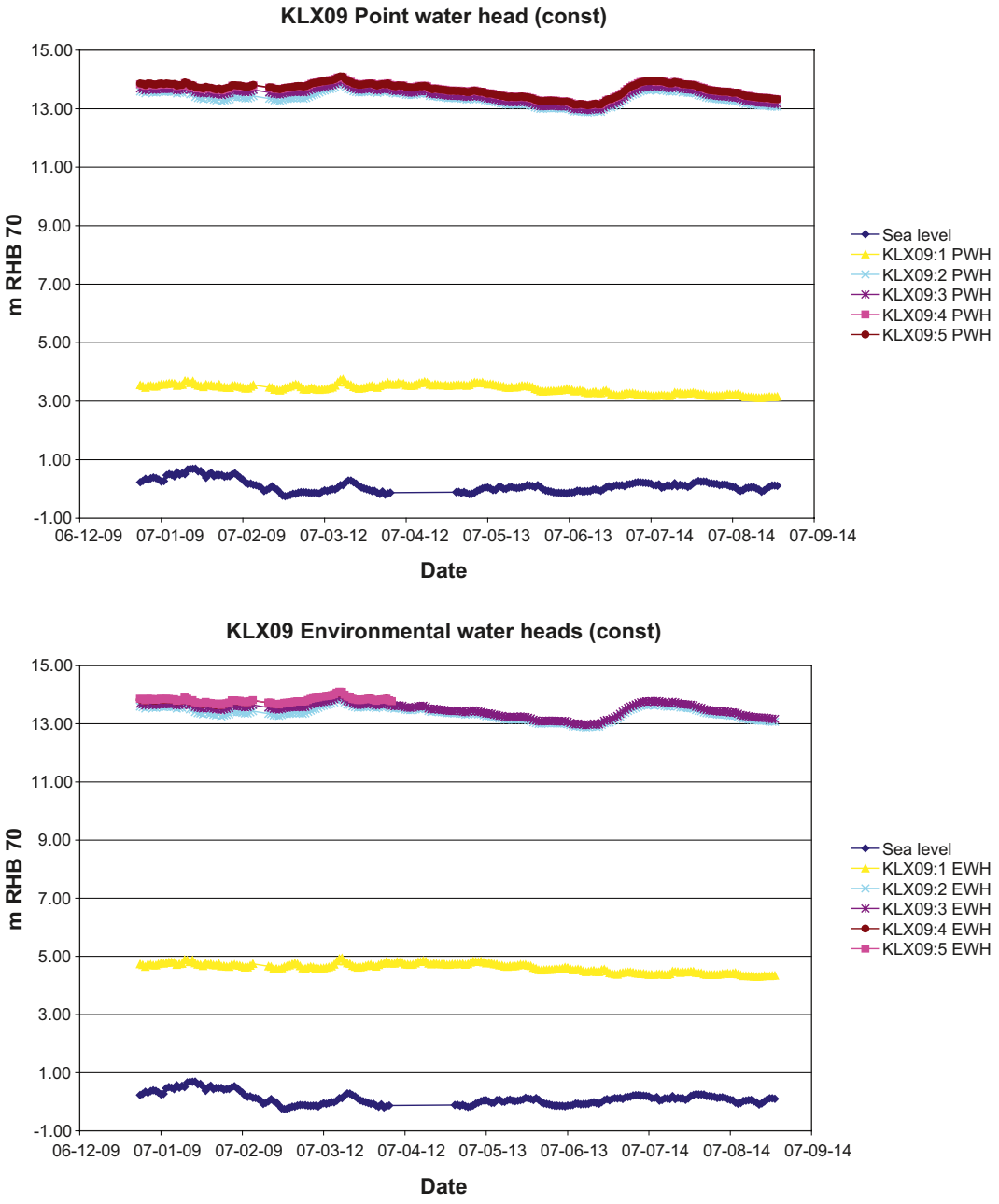

Figure A12. *Time-series plots of point-water heads end environmental-water heads in KLX09.*

KLX09 (Constant)

Section	Min		Percentil 0.02		Ave		Percentil 0.98		Max		Section	Compensation EWH-PWH min	mean	max
5	PWH5	EWH5	PWH5	EWH5	PWH5	EWH5	PWH5	EWH5	PWH5	EWH5	5	0.00	0.00	0.00
	-0.04 ↔	-0.04 ↔	-0.02 ↔	-0.02 ↔	0 ↔	0 ↔	0.01 ↔	0.01 ↔	0.02 ↔	0.02 ↔				
4	PWH4	EWH4	PWH4	EWH4	PWH4	EWH4	PWH4	EWH4	PWH4	EWH4	4	0.00	0.00	0.00
	-0.2 ↓	-0.2 ↓	-0.19 ↓	-0.19 ↓	-0.16 ↓	-0.16 ↓	-0.13 ↓	-0.13 ↓	-0.11 ↓	-0.11 ↓				
3	PWH3	EWH3	PWH3	EWH3	PWH3	EWH3	PWH3	EWH3	PWH3	EWH3	3	0.00	0.00	0.00
	-0.22 ↓	-0.22 ↓	-0.22 ↓	-0.22 ↓	-0.12 ↓	-0.12 ↓	-0.08 ↓	-0.08 ↓	-0.07 ↓	-0.07 ↓				
2	PWH2	EWH2	PWH2	EWH2	PWH2	EWH2	PWH2	EWH2	PWH2	EWH2	2	0.00	0.00	0.00
	-10.47 ↓	-9.28 ↓	-10.44 ↓	-9.25 ↓	-9.94 ↓	-8.75 ↓	-9.58 ↓	-8.39 ↓	-9.55 ↓	-8.36 ↓				
1	PWH1	EWH1	PWH1	EWH1	PWH1	EWH1	PWH1	EWH1	PWH1	EWH1	1	1.19	1.19	1.19

Specific comments for KLX09:

- Section elevations in the packer data file are available from Dec. 2006, and the same elevations are available in the chemistry data file, however registered from Nov. 2007.
- The measured density is lower than freshwater density.
- The calculated density is slightly higher than freshwater density only for section 1.
- Calculated density has been used for section 1, whereas freshwater density has been used for the other sections.

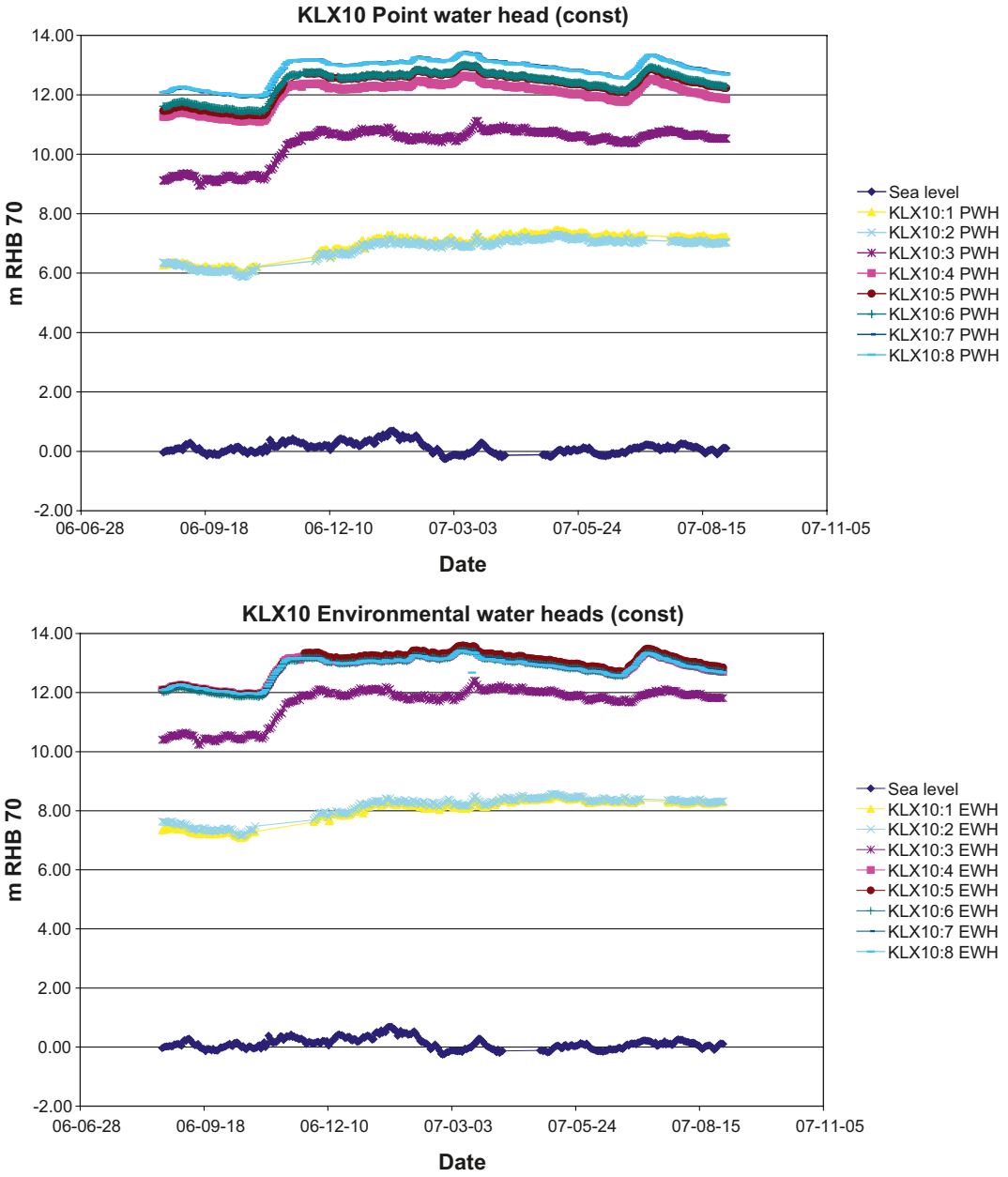

Figure A13. *Time-series plots of point-water heads end environmental-water heads in KLX10.*

KLX10 (Constant)

Section	Min		Percentil 0.02		Ave		Percentil 0.98		Max		Section	Compensation EWH-PWH min	mean	max
8	PWH8	EWH8	PWH8	EWH8	PWH8	EWH8	PWH8	EWH8	PWH8	EWH8	8	0.00	0.00	0.00
	-0.03 ↔	-0.03 ↔	-0.03 ↔	-0.02 ↔	0 ↔	0.01 ↔	0.02 ↔	0.03 ↔	0.03 ↔	0.04 ↔				
7	PWH7	EWH7	PWH7	EWH7	PWH7	EWH7	PWH7	EWH7	PWH7	EWH7	7	0.01	0.01	0.01
	-0.49 ↓	-0.07 ↓	-0.48 ↓	-0.07 ↓	-0.43 ↓	-0.02 ↔	-0.43 ↓	0.02 ↔	-0.39 ↓	0.02 ↔				
6	PWH6	EWH6	PWH6	EWH6	PWH6	EWH6	PWH6	EWH6	PWH6	EWH6	6	0.42	0.42	0.42
	-0.16 ↓	0.04 ↔	-0.15 ↓	0.05 ↑	-0.07 ↓	0.14 ↑	-0.07 ↔	0.17 ↑	-0.03 ↔	0.17 ↑				
5	PWH5	EWH5	PWH5	EWH5	PWH5	EWH5	PWH5	EWH5	PWH5	EWH5	5	0.62	0.62	0.62
	-0.37 ↓	-0.16 ↓	-0.37 ↓	-0.15 ↓	-0.31 ↓	-0.09 ↓	-0.31 ↓	0.02 ↔	-0.19 ↓	0.02 ↔				
4	PWH4	EWH4	PWH4	EWH4	PWH4	EWH4	PWH4	EWH4	PWH4	EWH4	4	0.84	0.84	0.84
	-2.32 ↓	-1.87 ↓	-2.14 ↓	-1.7 ↓	-1.67 ↓	-1.22 ↓	-1.67 ↓	-0.89 ↓	-1.32 ↓	-0.87 ↓				
3	PWH3	EWH3	PWH3	EWH3	PWH3	EWH3	PWH3	EWH3	PWH3	EWH3	3	1.29	1.29	1.29
	-4.26 ↓	-4.26 ↓	-4.15 ↓	-4.16 ↓	-3.53 ↓	-3.54 ↓	-3.53 ↓	-2.9 ↓	-2.77 ↓	-2.77 ↓				
2	PWH2	EWH2	PWH2	EWH2	PWH2	EWH2	PWH2	EWH2	PWH2	EWH2	2	1.29	1.28	1.28
	-0.09 ↓	-0.3 ↓	-0.01 ↔	-0.21 ↓	0.13 ↑	-0.08 ↓	0.13 ↑	-0.03 ↔	0.19 ↑	-0.02 ↔				
1	PWH1	EWH1	PWH1	EWH1	PWH1	EWH1	PWH1	EWH1	PWH1	EWH1	1	1.08	1.08	1.07

Specific comments for KLX10:

- Section elevations are registered in the packer data file from Jul. 2006.
- Density data are available from several dates in the chemistry data file.
- The most recent date after packer installation has been selected.
- The measured density is lower than freshwater density for sections 7 and 8.
- The calculated density is higher than freshwater density for all sections except section 8.
- The measured density has been used for sections 1 to 6, the calculated density has been used for section 7 and freshwater density has been used for section 8.

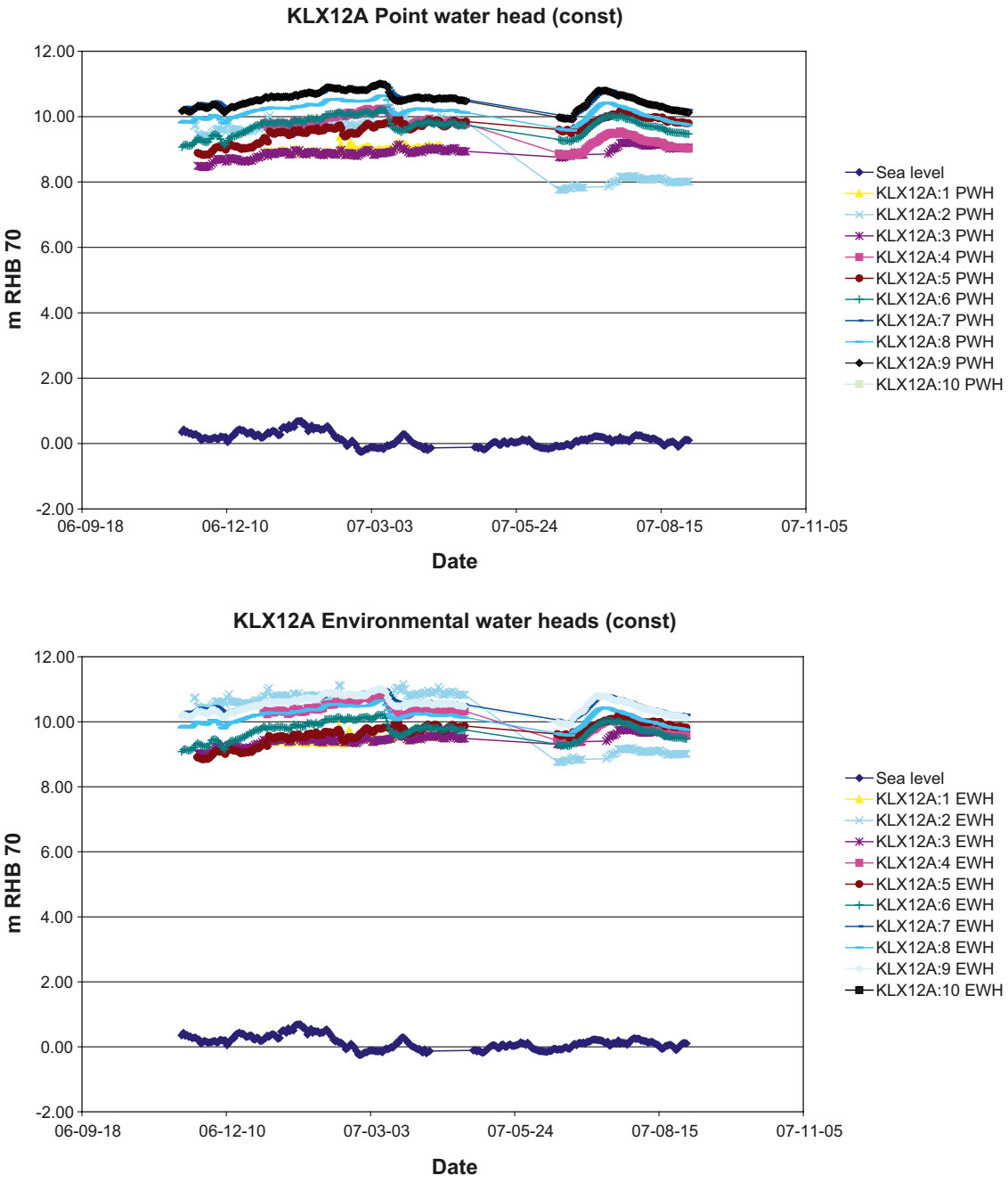

Figure A14. *Time-series plots of point-water heads end environmental-water heads in KLX12A.*

KLX12A (Constant)

Section	Min		Percentil 0.02		Ave		Percentil 0.98		Max		Section	Compensation EWH-PWH min	mean	max
9	PWH9	EWH9	PWH9	EWH9	PWH9	EWH9	PWH9	EWH9	PWH9	EWH9	9	0.00	0.00	0.00
	-0.5 ↓	-0.49 ↓	-0.48 ↓	-0.47 ↓	-0.36 ↓	-0.35 ↓	-0.3 ↓	-0.3 ↓	-0.3 ↓	-0.29 ↓				
8	PWH8	EWH8	PWH8	EWH8	PWH8	EWH8	PWH8	EWH8	PWH8	EWH8	8	0.01	0.01	0.01
	0.33 ↑	0.33 ↑	0.33 ↑	0.33 ↑	0.39 ↑	0.39 ↑	0.54 ↑	0.54 ↑	0.57 ↑	0.57 ↑				
7	PWH7	EWH7	PWH7	EWH7	PWH7	EWH7	PWH7	EWH7	PWH7	EWH7	7	0.01	0.01	0.01
	-1.18 ↓	-1.18 ↓	-1.16 ↓	-1.16 ↓	-0.83 ↓	-0.83 ↓	-0.69 ↓	-0.69 ↓	-0.69 ↓	-0.69 ↓				
6	PWH6	EWH6	PWH6	EWH6	PWH6	EWH6	PWH6	EWH6	PWH6	EWH6	6	0.01	0.01	0.01
	-0.65 ↓	-0.64 ↓	-0.6 ↓	-0.58 ↓	-0.11 ↓	-0.1 ↓	0.33 ↑	0.34 ↑	0.38 ↑	0.39 ↑				
5	PWH5	EWH5	PWH5	EWH5	PWH5	EWH5	PWH5	EWH5	PWH5	EWH5	5	0.02	0.02	0.02
	-0.8 ↓	-0.28 ↓	-0.78 ↓	-0.25 ↓	-0.13 ↓	0.4 ↑	0.6 ↑	1.12 ↑	0.63 ↑	1.16 ↑				
4	PWH4	EWH4	PWH4	EWH4	PWH4	EWH4	PWH4	EWH4	PWH4	EWH4	4	0.55	0.55	0.55
	-1.35 ↓	-1.35 ↓	-1.34 ↓	-1.34 ↓	-0.68 ↓	-0.68 ↓	0.02 ↔	0.02 ↔	0.04 ↔	0.04 ↔				
3	PWH3	EWH3	PWH3	EWH3	PWH3	EWH3	PWH3	EWH3	PWH3	EWH3	3	0.55	0.55	0.55
	-1.05 ↓	-0.59 ↓	-1.05 ↓	-0.59 ↓	0.35 ↑	0.81 ↑	1.12 ↑	1.58 ↑	1.18 ↑	1.63 ↑				
2	PWH2	EWH2	PWH2	EWH2	PWH2	EWH2	PWH2	EWH2	PWH2	EWH2	2	1.01	1.00	1.00
	-1.11 ↓	-1.63 ↓	-0.99 ↓	-1.51 ↓	-0.83 ↓	-1.34 ↓	-0.64 ↓	-1.15 ↓	-0.51 ↓	-1.03 ↓				
1	PWH1	EWH1	PWH1	EWH1	PWH1	EWH1	PWH1	EWH1	PWH1	EWH1	1	0.49	0.49	0.49

Specific comments for KLX12A:

- The measured density is lower than freshwater density for sections 5 to 9.
- The calculated density is slightly higher than freshwater density, except for section 9.
- The measured density has been used for sections 1 to 4, the calculated density has been used for sections 5 to 8 and freshwater density has been used for section 9.

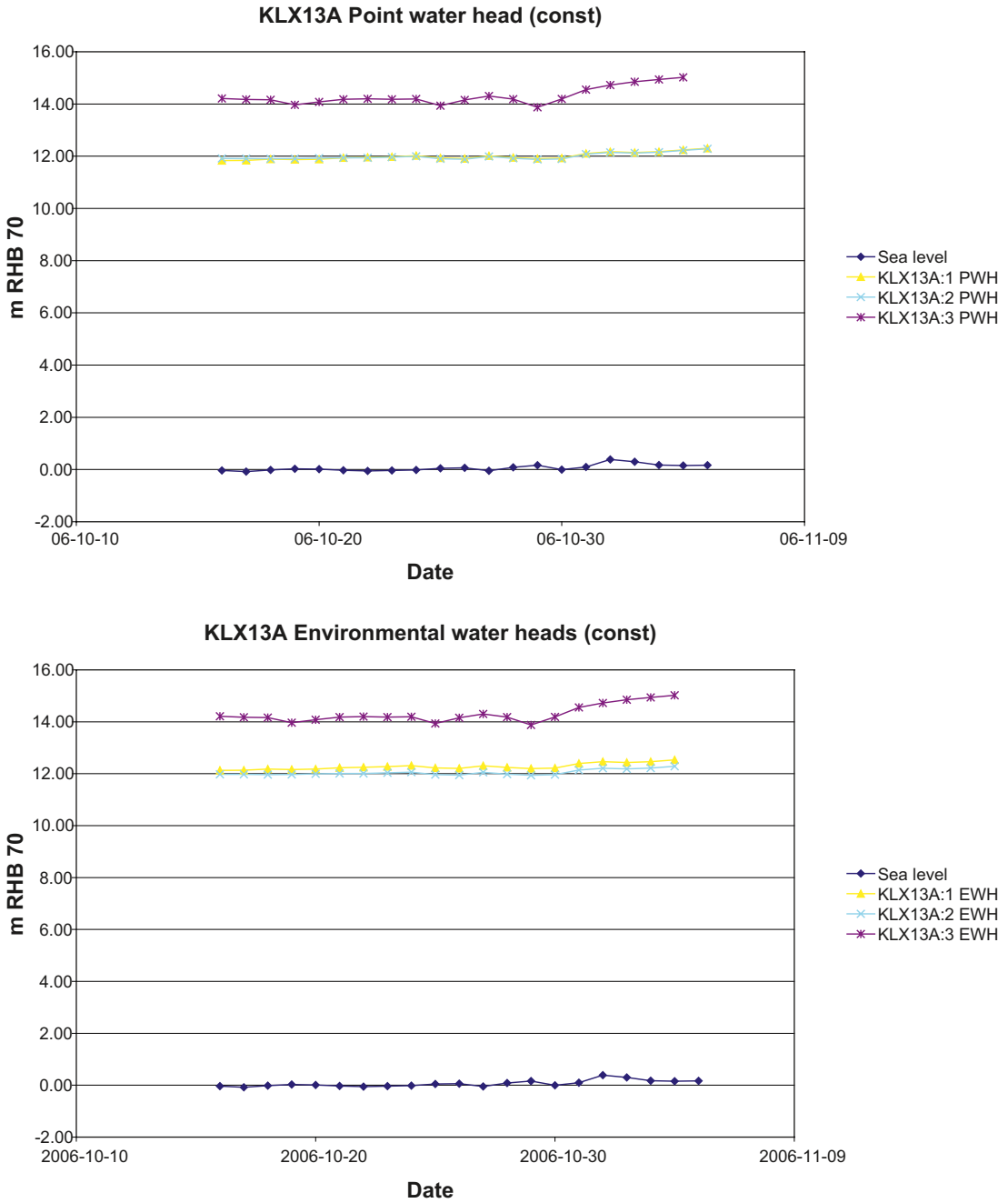

Figure A15. *Time-series plots of point-water heads end environmental-water heads in KLX13A.*

KLX13A (Constant)

Section	Min		Percentil 0.02		Ave		Percentil 0.98		Max		Section	Compensation EWH-PWH min	mean	max
3	PWH3	EWH3	PWH3	EWH3	PWH3	EWH3	PWH3	EWH3	PWH3	EWH3	3	0.00	0.00	0.00
	-2.8 ↓	-2.74 ↓	-2.8 ↓	-2.73 ↓	-2.32 ↓	-2.26 ↓	-2.01 ↓	-1.95 ↓	-2 ↓	-1.94 ↓				
2	PWH2	EWH2	PWH2	EWH2	PWH2	EWH2	PWH2	EWH2	PWH2	EWH2	2	0.07	0.07	0.07
	-0.08 ↓	0.15 ↑	-0.07 ↓	0.15 ↑	0.01 ↔	0.23 ↑	0.03 ↔	0.26 ↑	0.03 ↔	0.26 ↑				
1	PWH1	EWH1	PWH1	EWH1	PWH1	EWH1	PWH1	EWH1	PWH1	EWH1	1	0.29	0.29	0.29

Specific comments for KLX13A:

- The measured density is higher than freshwater density for sections 1 and 2, but lower for section 3.
- The calculated density is also lower than freshwater density for section 3.
- The measured density has been used for sections 1 and 2, whereas freshwater density has been used for section 3.
- Density data from the chemistry data file are available from several occasions, but have been selected form late 2006, when data are available from 3 sections.
- Section elevations in the packer data file (from late 2006) do not correspond to the section elevations in the chemistry data file.
- There is a risk that head values refer to other section elevations than the density data.
- The available PWH time series is very short.

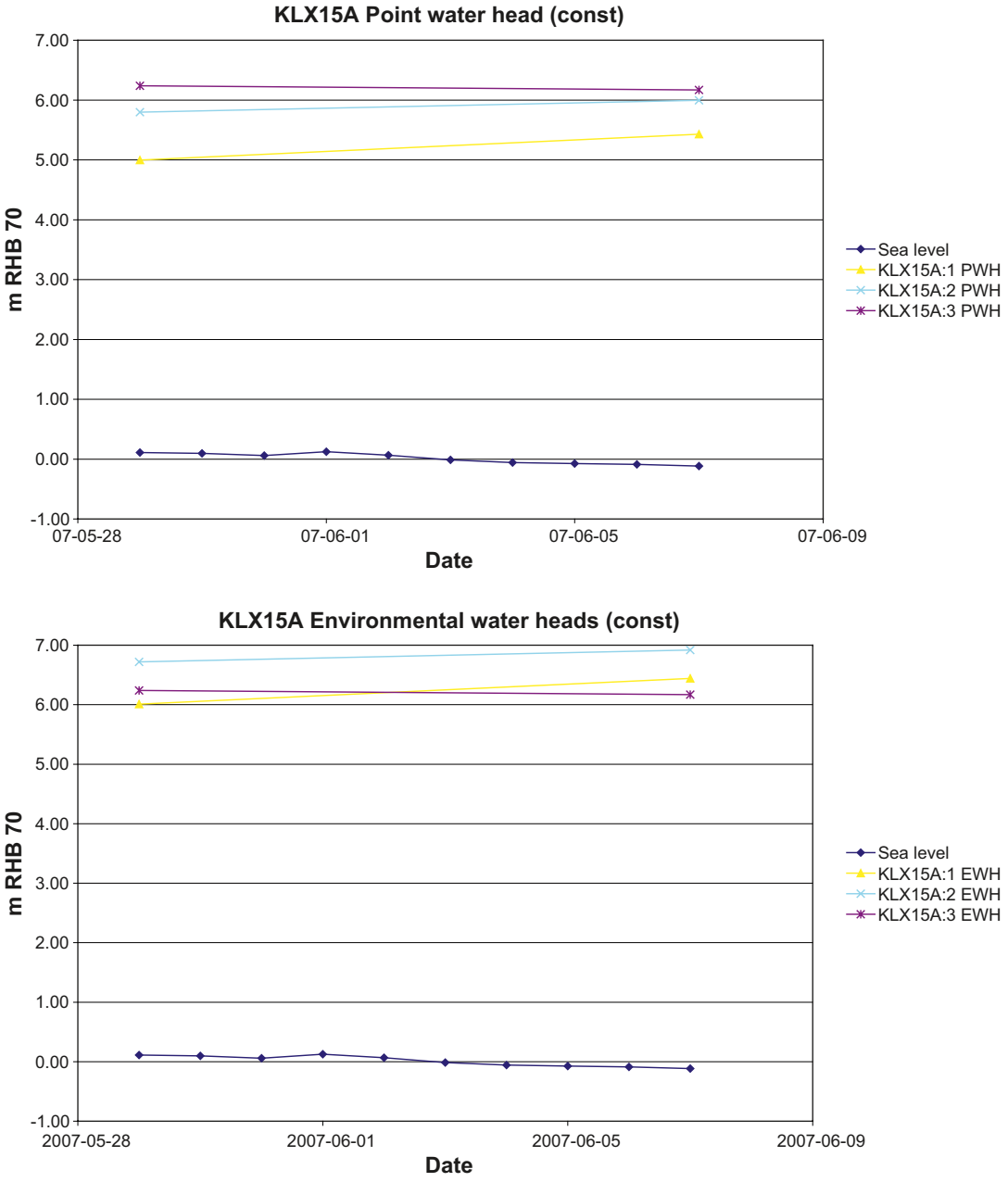

Figure A16. *Time-series plots of point-water heads end environmental-water heads in KLX15A.*

KLX15A (Constant)

Section	Min		Percentil 0.02		Ave		Percentil 0.98		Max		Section	Compensation PWH-EWH min	mean	max
3	PWH3	EWH3	PWH3	EWH3	PWH3	EWH3	PWH3	EWH3	PWH3	EWH3	3	0.00	0.00	0.00
	-0.44 ↓	0.48 ↑	-0.43 ↓	0.49 ↑	-0.31 ↓	0.62 ↑	-0.18 ↓	0.75 ↑	-0.17 ↓	0.75 ↑				
2	PWH2	EWH2	PWH2	EWH2	PWH2	EWH2	PWH2	EWH2	PWH2	EWH2	2	0.92	0.92	0.92
	-0.8 ↓	-0.71 ↓	-0.8 ↓	-0.71 ↓	-0.68 ↓	-0.59 ↓	-0.57 ↓	-0.48 ↓	-0.57 ↓	-0.48 ↓				
1	PWH1	EWH1	PWH1	EWH1	PWH1	EWH1	PWH1	EWH1	PWH1	EWH1	1	1.01	1.01	1.01

Specific comments for KLX15A:

- The section definitions in the packer data file are ambiguous; three section elevations are available, but the numbering end at 8. Only two section elevations are available in the chemistry data file. There is no correspondence between the elevations registered in the two files.
- The data screening overrules this problem, three sections with short PWH time series are available, and only two registrations are available.
- Density data are available from three different dates.
- The measured density is higher than freshwater density.
- The calculated density is higher than freshwater density.
- The measured density has been used for all sections.
- Due to the many uncertainties, the three density readings have been interpreted as relevant for three different borehole sections, sorted with the highest density in the lowermost section.
- There is an obvious risk that head values refer to other section elevations than the density data.
- The available PWH time series is very short.

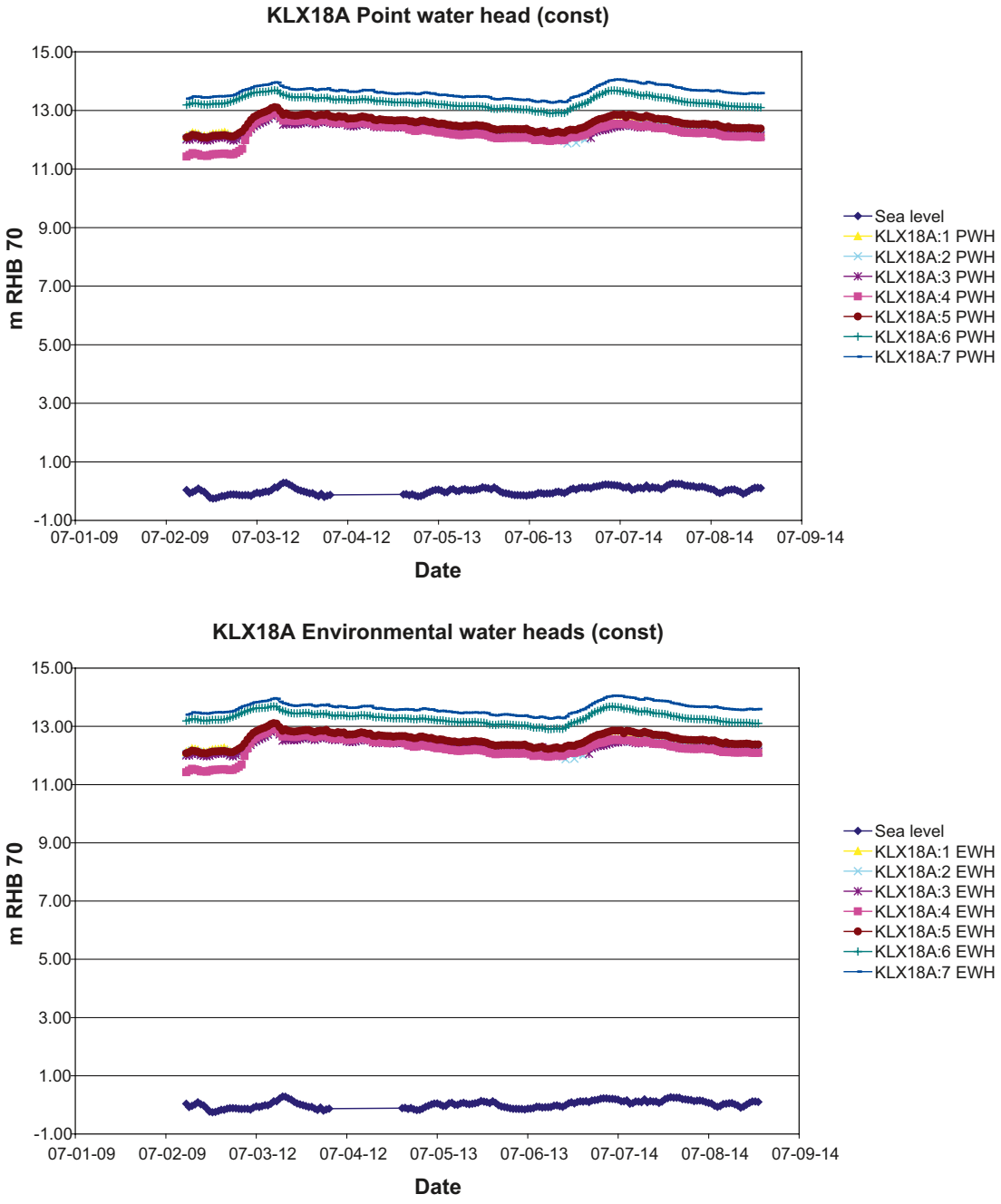

Figure A17. *Time-series plots of point-water heads end environmental-water heads in KLX18A.*

KLX18A (Constant)

Section	Min		Percentil 0.02		Ave		Percentil 0.98		Max		Section	Compensation EWH-PWH min	mean	max
7	PWH7	EWH7	PWH7	EWH7	PWH7	EWH7	PWH7	EWH7	PWH7	EWH7	7	0.00	0.00	0.00
	-0.49 ↓	-0.49 ↓	-0.46 ↓	-0.46 ↓	-0.34 ↓	-0.34 ↓	-0.21 ↓	-0.21 ↓	-0.2 ↓	-0.2 ↓				
6	PWH6	EWH6	PWH6	EWH6	PWH6	EWH6	PWH6	EWH6	PWH6	EWH6	6	0.00	0.00	0.00
	-1.22 ↓	-1.22 ↓	-1.17 ↓	-1.17 ↓	-0.74 ↓	-0.74 ↓	-0.58 ↓	-0.58 ↓	-0.56 ↓	-0.56 ↓				
5	PWH5	EWH5	PWH5	EWH5	PWH5	EWH5	PWH5	EWH5	PWH5	EWH5	5	0.00	0.00	0.00
	-0.65 ↓	-0.65 ↓	-0.63 ↓	-0.63 ↓	-0.3 ↓	-0.3 ↓	-0.18 ↓	-0.18 ↓	-0.18 ↓	-0.18 ↓				
4	PWH4	EWH4	PWH4	EWH4	PWH4	EWH4	PWH4	EWH4	PWH4	EWH4	4	0.00	0.00	0.00
	-0.23 ↓	-0.23 ↓	-0.12 ↓	-0.12 ↓	0.06 ↑	0.06 ↑	0.56 ↑	0.56 ↑	0.58 ↑	0.58 ↑				
3	PWH3	EWH3	PWH3	EWH3	PWH3	EWH3	PWH3	EWH3	PWH3	EWH3	3	0.00	0.00	0.00
	-0.19 ↓	-0.19 ↓	0.01 ↔	0.01 ↔	0.04 ↔	0.04 ↔	0.1 ↑	0.1 ↑	0.19 ↑	0.19 ↑				
2	PWH2	EWH2	PWH2	EWH2	PWH2	EWH2	PWH2	EWH2	PWH2	EWH2	2	0.00	0.00	0.00
	0.06 ↑	0.06 ↑	0.06 ↑	0.06 ↑	0.08 ↑	0.08 ↑	0.15 ↑	0.15 ↑	0.26 ↑	0.26 ↑				
1	PWH1	EWH1	PWH1	EWH1	PWH1	EWH1	PWH1	EWH1	PWH1	EWH1	1	0.00	0.00	0.00

Specific comments for KLX18A:

- The measured density is lower than freshwater density.
- The calculated density is lower than freshwater density.
- Freshwater density has been used for all sections.

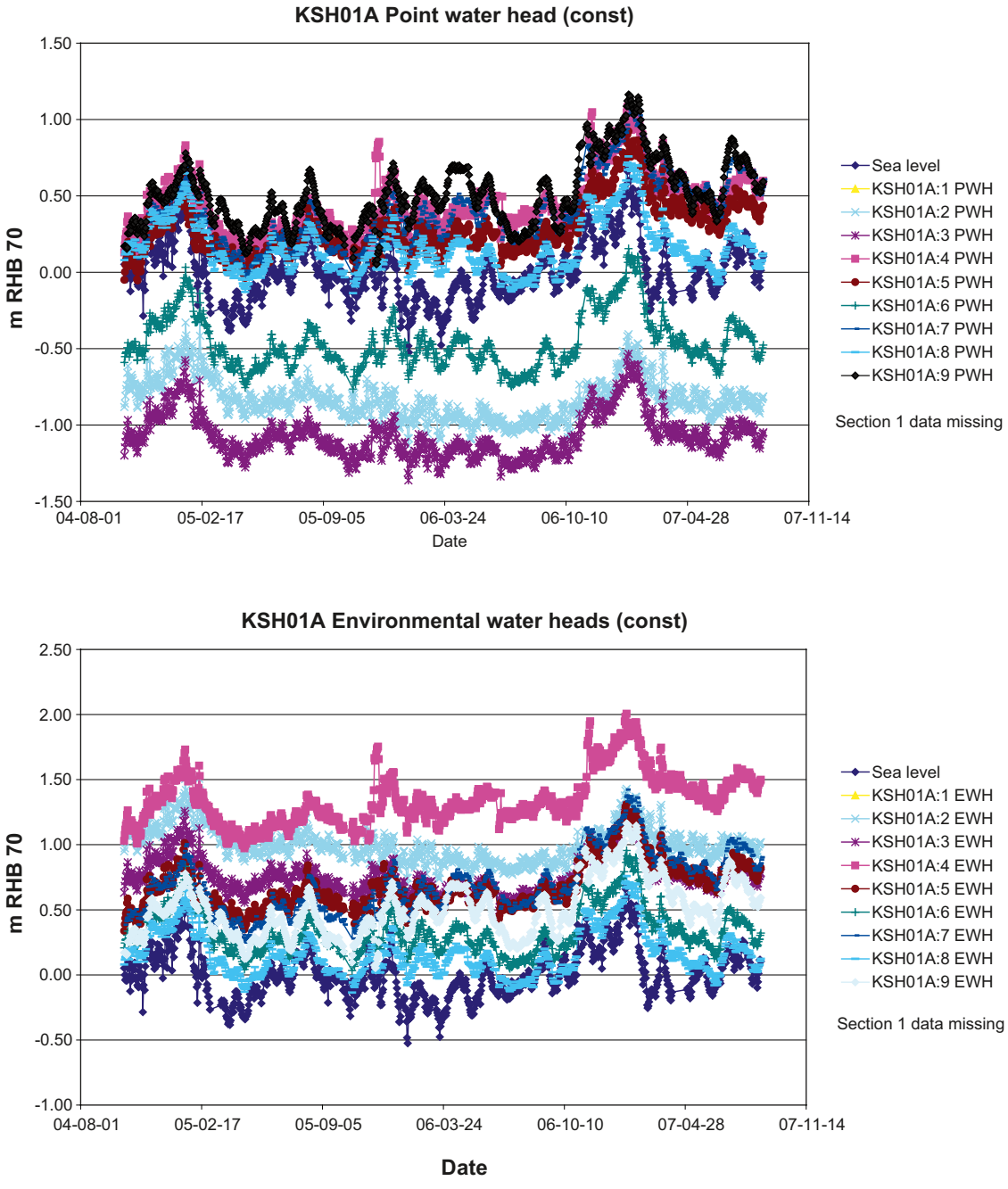

Figure A18. *Time-series plots of point-water heads end environmental-water heads in KSH01A.*

KSH01A (Constant)

Section	Min		Percentil 0.02		Ave		Percentil 0.98		Max		Section	Compensation EWH-PWH min	mean	max
9	PWH9	EWH9	PWH9	EWH9	PWH9	EWH9	PWH9	EWH9	PWH9	EWH9	9	0.00	0.00	0.00
	-0.59 ↓	-0.59 ↓	-0.56 ↓	-0.56 ↓	-0.35 ↓	-0.35 ↓	-0.1 ↓	-0.1 ↓	0 ↔	0 ↔				
8	PWH8	EWH8	PWH8	EWH8	PWH8	EWH8	PWH8	EWH8	PWH8	EWH8	8	0.00	0.00	0.00
	-0.01 ↔	0.28 ↑	0 ↔	0.3 ↑	0.24 ↑	0.54 ↑	0.48 ↑	0.78 ↑	0.51 ↑	0.81 ↑				
7	PWH7	EWH7	PWH7	EWH7	PWH7	EWH7	PWH7	EWH7	PWH7	EWH7	7	0.30	0.30	0.29
	-1.1 ↓	-0.6 ↓	-1.07 ↓	-0.57 ↓	-0.86 ↓	-0.36 ↓	-0.66 ↓	-0.16 ↓	-0.65 ↓	-0.15 ↓				
6	PWH6	EWH6	PWH6	EWH6	PWH6	EWH6	PWH6	EWH6	PWH6	EWH6	6	0.80	0.80	0.80
	0.41 ↑	0 ↔	0.5 ↑	0.09 ↑	0.75 ↑	0.34 ↑	0.93 ↑	0.52 ↑	0.97 ↑	0.56 ↑				
5	PWH5	EWH5	PWH5	EWH5	PWH5	EWH5	PWH5	EWH5	PWH5	EWH5	5	0.39	0.39	0.39
	0.02 ↔	0.53 ↑	0.06 ↑	0.57 ↑	0.16 ↑	0.67 ↑	0.27 ↑	0.79 ↑	0.52 ↑	1.03 ↑				
4	PWH4	EWH4	PWH4	EWH4	PWH4	EWH4	PWH4	EWH4	PWH4	EWH4	4	0.90	0.90	0.90
	-1.87 ↓	-0.94 ↓	-1.69 ↓	-0.76 ↓	-1.51 ↓	-0.58 ↓	-1.31 ↓	-0.38 ↓	-1.27 ↓	-0.33 ↓				
3	PWH3	EWH3	PWH3	EWH3	PWH3	EWH3	PWH3	EWH3	PWH3	EWH3	3	1.83	1.83	1.83
	0.02 ↔	0.02 ↔	0.09 ↑	0.08 ↑	0.24 ↑	0.24 ↑	0.36 ↑	0.36 ↑	0.46 ↑	0.46 ↑				
2	PWH2	EWH2	PWH2	EWH2	PWH2	EWH2	PWH2	EWH2	PWH2	EWH2	2	1.83	1.83	1.83
	Missing	Missing	Missing	Missing	Missing	Missing	Missing	Missing	Missing	Missing				
1	PWH1	EWH1	PWH1	EWH1	PWH1	EWH1	PWH1	EWH1	PWH1	EWH1	1	Missing data	Missing data	Missing data

Specific comments for KSH01A:

- The measured density is higher than freshwater density.
- The measured density has been used for all sections.
- The secup elevations in the packer data file coincides with the elevations in the chemistry data file.
- After screening, data from section 1 are removed.

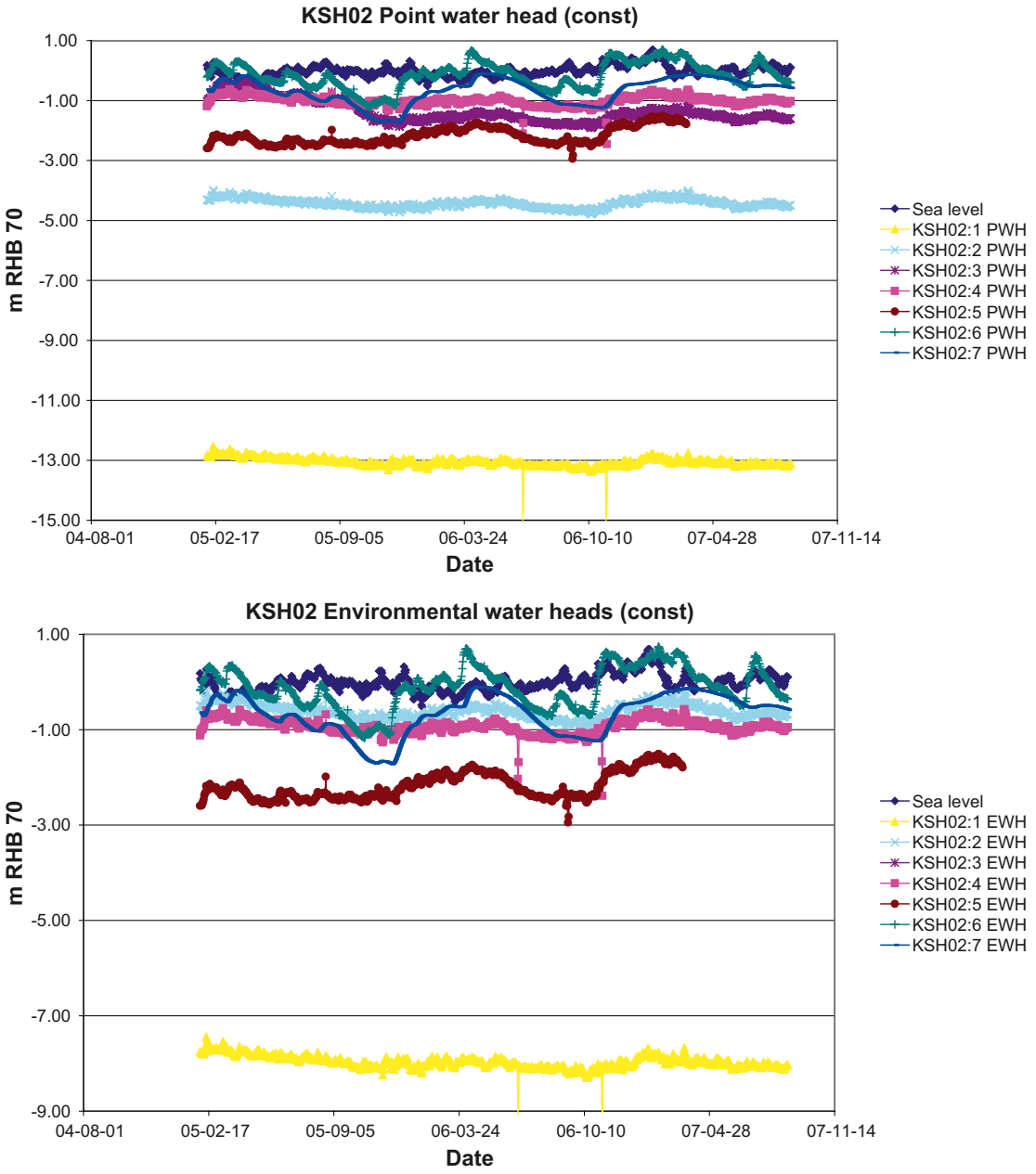

Figure A19. *Time-series plots of point-water heads end environmental-water heads in KSH02.*

KSH02 (Constant)

Section	Min		Percentil 0.02		Ave		Percentil 0.98		Max		Section	Compensation EWH-PWH min	mean	max
7	PWH7	EWH7	PWH7	EWH7	PWH7	EWH7	PWH7	EWH7	PWH7	EWH7	7	0.00	0.00	0.00
	-0.09 ↓	-0.05 ↓	-0.01 ↔	0.03 ↔	0.51 ↑	0.55 ↑	1.3 ↑	1.34 ↑	1.59 ↑	1.63 ↑				
6	PWH6	EWH6	PWH6	EWH6	PWH6	EWH6	PWH6	EWH6	PWH6	EWH6	6	0.04	0.04	0.04
	-2.58 ↓	-2.62 ↓	-2.48 ↓	-2.53 ↓	-2 ↓	-2.04 ↓	-1.27 ↓	-1.31 ↓	-1.2 ↓	-1.24 ↓				
5	PWH5	EWH5	PWH5	EWH5	PWH5	EWH5	PWH5	EWH5	PWH5	EWH5	5	0.00	0.00	0.00
	-0.35 ↓	-0.27 ↓	0.79 ↑	0.86 ↑	1.17 ↑	1.24 ↑	1.63 ↑	1.7 ↑	1.7 ↑	1.77 ↑				
4	PWH4	EWH4	PWH4	EWH4	PWH4	EWH4	PWH4	EWH4	PWH4	EWH4	4	0.07	0.07	0.07
	-0.67 ↓	2.78 ↑	-0.59 ↓	2.86 ↑	-0.34 ↓	3.11 ↑	0.4 ↑	3.86 ↑	0.82 ↑	4.26 ↑				
3	PWH3	EWH3	PWH3	EWH3	PWH3	EWH3	PWH3	EWH3	PWH3	EWH3	3	3.53	3.52	3.52
	-3.85 ↓	-3.56 ↓	-3.81 ↓	-3.52 ↓	-3.08 ↓	-2.78 ↓	-2.84 ↓	-2.55 ↓	-2.83 ↓	-2.53 ↓				
2	PWH2	EWH2	PWH2	EWH2	PWH2	EWH2	PWH2	EWH2	PWH2	EWH2	2	3.82	3.82	3.81
	-12.27 ↓	-11.02 ↓	-8.78 ↓	-7.51 ↓	-8.63 ↓	-7.36 ↓	-8.49 ↓	-7.22 ↓	-8.44 ↓	-7.17 ↓				
1	PWH1	EWH1	PWH1	EWH1	PWH1	EWH1	PWH1	EWH1	PWH1	EWH1	1	5.09	5.09	5.06

Specific comments for KSH02:

- The secup elevations for sections 1 to 6 in the packer data file are registered from Dec. 2004 and coincide with the secup elevations in the chemistry data file, registered from the same period.
- Secup elevation is missing for section 7 in the chemistry data file.
- There is a section in the chemistry data file that is below secup for section 1 in the packer data file; it is even below the bottom of the borehole. Density data from this section have therefore not been used.
- The measured densities are higher than freshwater density for sections 1 to 3.
- The calculated densities are higher than freshwater density.
- The measured density has been used for sections 1 to 3, calculated densities have been used for sections 4 to 6, and freshwater density has been used for the "missing" section 7.
- There is a risk that head data refer to other section elevations than the density data.
- There is a risk that the numbering of "density sections" is wrong, leading to the unnecessary offset of one section and replacement with freshwater density data in section 1.
- However, if there is an error in the section numbering, the density trend would be the same in the borehole, but starting and ending with higher densities.

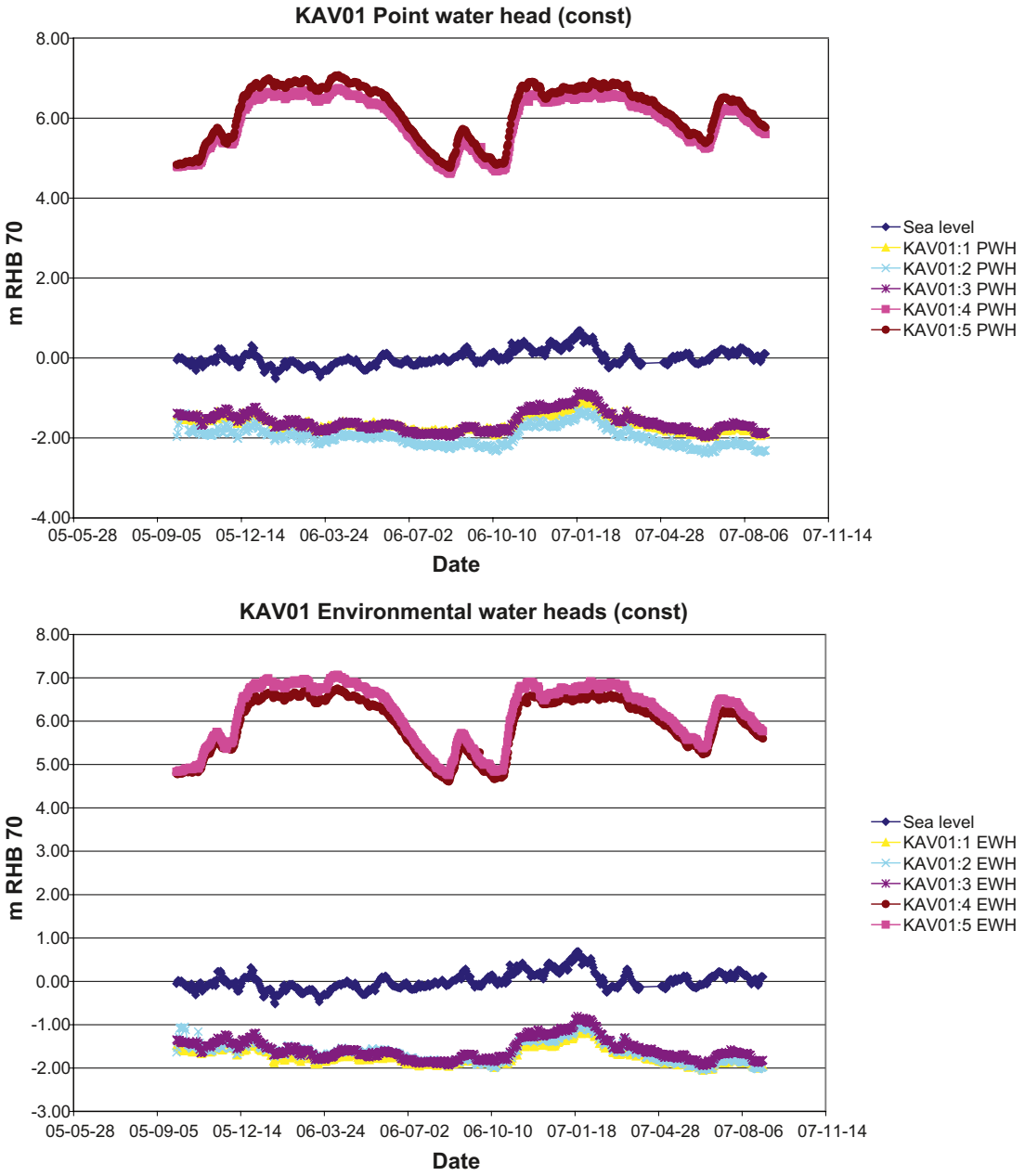

Figure A20. *Time-series plots of point-water heads end environmental-water heads in KAV01.*

KAV01 (Constant)

Section	Min		Percentil 0.02		Ave		Percentil 0.98		Max		Section	Compensation EWH-PWH		
												min	mean	max
5	PWH5	EWH5	PWH5	EWH5	PWH5	EWH5	PWH5	EWH5	PWH5	EWH5	5	0.00	0.00	0.00
	-0.49 ↓	-0.49 ↓	-0.35 ↓	-0.35 ↓	-0.23 ↓	-0.23 ↓	-0.06 ↓	-0.06 ↓	0.18 ↑	0.18 ↑				
4	PWH4	EWH4	PWH4	EWH4	PWH4	EWH4	PWH4	EWH4	PWH4	EWH4	4	0.00	0.00	0.00
	-8.45 ↓	-8.42 ↓	-8.34 ↓	-8.31 ↓	-7.54 ↓	-7.51 ↓	-6.28 ↓	-6.25 ↓	-6.17 ↓	-6.14 ↓				
3	PWH3	EWH3	PWH3	EWH3	PWH3	EWH3	PWH3	EWH3	PWH3	EWH3	3	0.03	0.03	0.03
	-0.6 ↓	-0.3 ↓	-0.48 ↓	-0.18 ↓	-0.36 ↓	-0.06 ↓	-0.22 ↓	0.08 ↑	0.05 ↔	0.35 ↑				
2	PWH2	EWH2	PWH2	EWH2	PWH2	EWH2	PWH2	EWH2	PWH2	EWH2	2	0.33	0.33	0.33
	-0.14 ↓	-0.53 ↓	0.24 ↑	-0.16 ↓	0.33 ↑	-0.06 ↓	0.42 ↑	0.02 ↔	0.55 ↑	0.15 ↑				
1	PWH1	EWH1	PWH1	EWH1	PWH1	EWH1	PWH1	EWH1	PWH1	EWH1	1	-0.06	-0.06	-0.06

Specific comments for KAV01:

- Secup elevations in the packer data file are registered from Sep. 2005.
- Density data are selected from the chemistry data file with simultaneous registrations as in the packer data file.
- The measured density is lower than freshwater density.
- The calculated density is slightly higher than freshwater density for sections 1 to 4, but lower than freshwater density for section 5.
- The calculated density has been used for section 1 to 4, and freshwater density has been used for section 5.

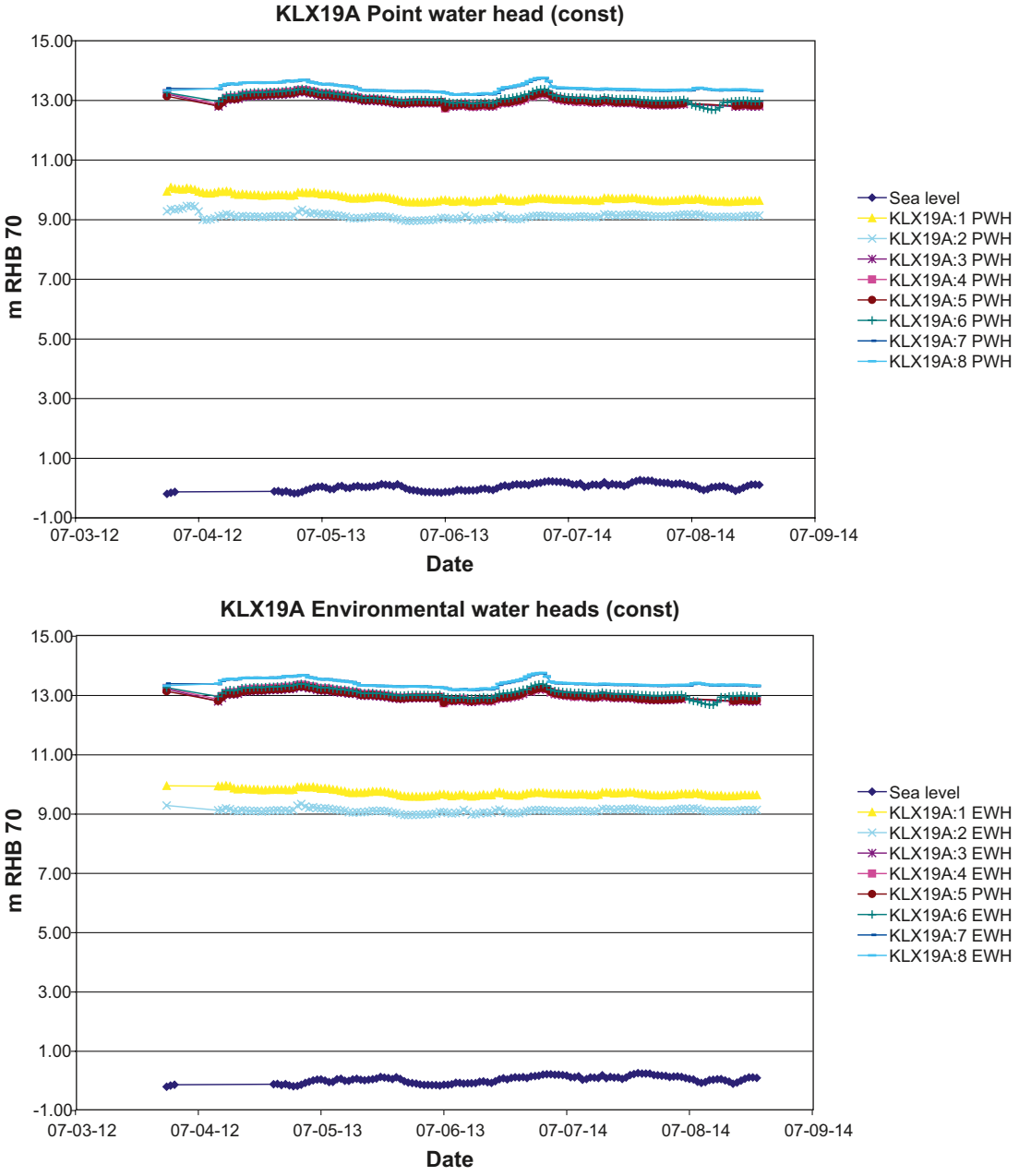

Figure A21. *Time-series plots of point-water heads end environmental-water heads in KLX19A.*

KLX19A (Constant)

Section	Min		Percentil 0.02		Ave		Percentil 0.98		Max		Section	Compensation EWH-PWH min	mean	max
8	PWH8	EWH8	PWH8	EWH8	PWH8	EWH8	PWH8	EWH8	PWH8	EWH8	8	0.00	0.00	0.00
	-0.03 ↔	-0.03 ↔	-0.02 ↔	-0.02 ↔	-0.01 ↔	-0.01 ↔	0 ↔	0 ↔	0.07 ↑	0.07 ↑				
7	PWH7	EWH7	PWH7	EWH7	PWH7	EWH7	PWH7	EWH7	PWH7	EWH7	7	0.00	0.00	0.00
	-0.66 ↓	-0.66 ↓	-0.64 ↓	-0.64 ↓	-0.33 ↓	-0.32 ↓	-0.33 ↓	-0.25 ↓	-0.14 ↓	-0.14 ↓				
6	PWH6	EWH6	PWH6	EWH6	PWH6	EWH6	PWH6	EWH6	PWH6	EWH6	6	0.01	0.01	0.01
	-0.21 ↓	-0.21 ↓	-0.15 ↓	-0.14 ↓	-0.1 ↓	-0.1 ↓	-0.1 ↓	-0.06 ↓	-0.06 ↓	-0.06 ↓				
5	PWH5	EWH5	PWH5	EWH5	PWH5	EWH5	PWH5	EWH5	PWH5	EWH5	5	0.01	0.01	0.01
	-0.03 ↔	-0.02 ↔	-0.01 ↔	-0.01 ↔	0.01 ↔	0.01 ↔	0.01 ↔	0.04 ↔	0.11 ↑	0.11 ↑				
4	PWH4	EWH4	PWH4	EWH4	PWH4	EWH4	PWH4	EWH4	PWH4	EWH4	4	0.01	0.01	0.01
	-0.06 ↓	-0.07 ↓	-0.06 ↓	-0.07 ↓	-0.03 ↔	-0.04 ↔	-0.03 ↔	-0.02 ↔	-0.01 ↔	-0.01 ↔				
3	PWH3	EWH3	PWH3	EWH3	PWH3	EWH3	PWH3	EWH3	PWH3	EWH3	3	0.00	0.00	0.00
	-4.11 ↓	-4.11 ↓	-4.09 ↓	-4.09 ↓	-3.88 ↓	-3.88 ↓	-3.88 ↓	-3.67 ↓	-3.66 ↓	-3.66 ↓				
2	PWH2	EWH2	PWH2	EWH2	PWH2	EWH2	PWH2	EWH2	PWH2	EWH2	2	0.01	0.01	0.01
	0.5 ↑	0.5 ↑	0.5 ↑	0.5 ↑	0.62 ↑	0.6 ↑	0.62 ↑	0.77 ↑	0.91 ↑	0.82 ↑				
1	PWH1	EWH1	PWH1	EWH1	PWH1	EWH1	PWH1	EWH1	PWH1	EWH1	1	0.01	0.01	0.01

Specific comments for KLX19A:

- Secup elevations in the packer data file are registered from Apr. 2007, whereas secup elevations in the chemistry data file are registered from Mar. 2007 and earlier.
- The latest density data have been used, with secup elevations corresponding to those in the packer data file.
- The measured density is lower than freshwater density for all section, except for section 3.
- The calculated density is slightly higher than freshwater density.
- The calculated density has been used for sections 1 to 2 and sections 4 to 6. The measured density has been used for section 3.

Appendix 2

Field classification of groundwater monitoring wells

Totally 64 groundwater monitoring wells have been recharge-discharge classified. For a description of classification parameters, see the reference /Werner et al. 2007/ in the main report.

Table A2. Recharge-discharge classification made in the field. R = recharge, PR = probable recharge, I = intermediate/varying, PD = probable discharge, and D = discharge.

Well ID	Recharge-discharge classification
SSM000001	D
SSM000007	D
SSM000009	R
SSM000011	D
SSM000016	PD
SSM000018	D
SSM000020	PD
SSM000021	D
SSM000022	D
SSM000024	D
SSM000026	PD
SSM000028	D
SSM000029	D
SSM000030	D
SSM000031	D
SSM000032	D
SSM000033	D
SSM000034	D
SSM000037	D
SSM000039	R
SSM000040	D
SSM000041	D
SSM000042	D
SSM000211	D
SSM000212	PD
SSM000213	PD
SSM000214	PD
SSM000215	D
SSM000216	PD
SSM000217	I
SSM000218	R
SSM000219	D
SSM000220	D
SSM000221	D
SSM000222	D
SSM000223	PD
SSM000224	PR
SSM000225	PR
SSM000226	D

Well ID	Recharge-discharge classification
SSM000227	D
SSM000228	PD
SSM000229	PR
SSM000230	R
SSM000236	D
SSM000237	D
SSM000244	D
SSM000248	D
SSM000249	D
SSM000250	PR
SSM000251	D
SSM000252	D
SSM000253	D
SSM000254	PR
SSM000255	D
SSM000256	D
SSM000257	D
SSM000260	D
SSM000261	D
SSM000262	D
SSM000263	D
SSM000264	R
SSM000265	D
SSM000267	R
SSM000268	D